Foodyplast, food plastic packaging with naturals additives and recyclable

Antonio Garcia Contreras

THÈSE

Pour obtenir le grade de

Docteur

Délivré par

UNIVERSITE DE PERPIGNAN VIA DOMITIA

Préparée au sein de l'école doctorale
Et de l'unité de recherche

Spécialité : Chimie

Présentée par
Antonio García Contreras

TITRE DE LA THESE

Foodyplast, Des emballages plastiques alimentaires avec des additifs naturels et recyclables

Soutenue le XX juin 2019 devant le jury composé de

Mme. Valérie NASSIET, Professeur, Ecole Nationale d'Ingenieurs de Tarbes	Rapporteur
Mme. Cristina NERIN, Professeur, Universidad de Zaragoza	Rapporteur
Mme. Gaelle CATANANTE, Maître de Conférences, Université de Perpignan Via Domitia	Examinateur
M. Nicolas INGUIMBERT, Professeur, Université de Perpignan Via Domitia	Examinateur
M. Frédéric LEONARDI, Maître de Conférences, Université de Pau et des Pays de l'Adour	Examinateur
M. Thierry NOGUER, Professeur, Université de Perpignan Via Domitia	Directeur de Thèse
Ahmed ALLAL , Professeur Université de Pau et des Pays de l'Adour	Co-Directeur de Thèse
Jean Louis MARTY, Professeur honoraire	Invité

Acknowledgements

This project thesis was funded by the Mexican Government through the Secretaría de Energía and CONACyT (scholarship no. 539811). Foodyplast project was part of PhD programs offered in México via Campus France. I would like to thank the strong bilateral relations between France and México that opened the possibility to students pursuing graduate degrees.

The experimental research work was performed at L'Université de Perpignan Via Domitia (UPVD) and L'Université de Pau et des Pays de l'Adour (UPPA). I would like to thank to the BAE-lab at the UPVD for their entire support way before my arrival to France. Many thanks to Prof. Gaelle Catanante for her mentorship and scientific support as well as Prof. Thierry Noguer and Prof. Carol Calas-Blanchard for their constructive scientific support, all encouraging me to deepen my research work. Further thanks to Prof. Georges Istamboulié and Virginie Casadei for all their kind support. Also, I would like to thank to my lab mates: Yugi, Moemen, Elise, Nadin, Mian, and Akthar, the hours spent at lab were minutes while sharing with you all.

I would like to thank to the IPREM-lab at UPPA. Many thanks to Anthony Laffore who guided me into equipment specifications and standard operating procedures (besides the training session with pétanque along with Xavier Cailles). I also would like to thank to M. Bernard, responsible of the Halle Matériaux, for all his support. Special thanks to Prof. Frédéric Leonardi for his scientific cooperation and support during the experimental work.

Special thanks to my co-director Prof. Ahmed Allal to give me the opportunity of being part of Foodyplast project and sponsored my stay during the experimental work in IPREM-lab at UPPA. Thanks for all your support, cooperation, and scientific orientation. Also, I would like to thank Ambre and Christelle as part of the UPPA team and all the Foodyplast partners. Further thanks to my lab mates: Tiki, Mam, Hussein, Wissem, Geo Mojado, Jordana, and Laura to share a part of you with my family.

I would like to thank Prof. Cristina Nerin and Prof. Valérie Nassiet to accept being the rapporteurs of this thesis dissertation and Prof. Nicolas Inguimbert, Prof. Frédéric Leonardi, and Prof. Gaelle Catanante for being members of the jury.

Special thanks to Prof. Jean Louis Marty, my Thesis Director. As a foreign student, I must have to say that I felt entirely integrated in all aspects in France because of you. Being you Prof. Marty, the responsible for international affairs at UPVD, I must have to say that, you are a well-known person in México and I thank you for your guidance and advices. Muchas gracias por permitirme ser su tesista, he aprendido mucho de Usted.

Also, I would like to thank to Dr. Luis Antonio Rodríguez Guadarrama, Dr. Nicholas Schiller, Dr. Hugo De Alva Salazar, Eng. Jorge Barrón de la Rosa, and Eng. Ricardo Orozco Cejudo to trust in me and extended the recommendation letters to pursue, now defend, this thesis dissertation.

Finally, I would like to thank my wife Mariana, my sons Ana Lourdes and Mateo, and my family for all your love and support and being part of this landed dream, which is becoming true.

Dedications

To God, St. Jude, my parents, our families, and with all my love to Mariana, Ana, and Mateo.

RESUME

Les matières plastiques ont désormais envahi notre quotidien. Elles sont le symbole de la société de consommation, car elles sont considérées comme un matériau non noble: les consommateurs l'assimilent à un produit jetable après usage. N'étant pas dégradables, les plastiques représentent donc un réel danger pour l'environnement, la faune et la flore.

L'objectif de ce travail de thèse a été de développer en collaboration avec l'Institut des Sciences Analytiques et de Physico-Chimie pour l'Environnement et les Matériaux (Université de Pau) de nouvelles formulations avec des additifs naturels pour obtenir des plastiques résistants et recyclables. Deux types de résines ont été utilisées: le polypropylène isotactique (i-PP) et le polyéthylène à basse densité (LDPE). Des antioxydants naturels tels que l'acide ascorbique, l'alpha-tocophérol et l'huile de lin ont été testés et leur encapsulation a permis d'améliorer leur résistance à la dégradation. Les caractérisations thermique et rhéologique des résines ont montré des qualités supérieures aux résines commerciales actuelles. Nous avons pu démontrer que les plastiques obtenus pouvaient être recyclés 9 fois sans perte de leurs caractéristiques. Des essais avec des barquettes fabriquées avec les produits élaborés sont en cours pour valider les modèles développés.

Directeurs de thèse:

Jean Louis MARTY, Laboratoire de Biodiversité et Biotechnologies Microbiennes, Université de Perpignan Via Domitia

Thierry NOGUER, Laboratoire de Biodiversité et Biotechnologies Microbiennes, Université de Perpignan Via Domitia

Ahmed ALLAL, Institut des Sciences Analytiques et de Physico-Chimie pour l'Environnement et les Matériaux, Université de Pau et des Pays de l'Adour

INDEX

List of Figures

Chapter I: State of the art

Chapter II: Antioxidants

Chapter III: Polymers

Chapter IV: Polymer Formulation:

Incorporation of natural antioxidant molecules

List of Tables

Chapter I: State of the art

Chapter II: Antioxidants

Chapter III: Polymers

Chapter IV: Polymer Formulation:

Incorporation of natural antioxidant molecules

Thesis Project

FOODYPLAST, Eco-friendly and recyclable materials for food packaging applications

Scope

The objective of the thesis research project is to deliver a formulation, with natural additives, that provides thermal stability to olefin polymers during industrial transformation via free radical scavenging. Two food grade resins were evaluated: isotactic polypropylene (i-PP) and low-density polyethylene (LDPE) with potential food packaging applications.

Hypothesis

Natural antioxidant molecules act as a radical scavenger providing stability against thermal oxidation to i-PP induced by thermo-mechanical stresses during polymer industrial transformation,

Natural antioxidant molecules act as a radical scavenger providing stability against thermal oxidation to LDPE induced by thermo-mechanical stresses during polymer industrial transformation.

General Objective

To develop a formulation based on natural molecules with antioxidant activity for i-PP and LDPE stabilization against thermal degradation during polymer industrial transformation.

General Introduction

The need of food preservation for troops during war was placed in context and a solution emerged in France. The first conception of tin can was developed by Nicholas Appert who further published a book: The Art of Preserving Animal and Vegetable Substances for Many Years (Baldesi et al., 2019). Since then, packaging systems have evolved, not only considering a package based on its primary functions: containment, protection, and communication but also considering consumers demands for safety and freshness and food industry seeking toward extended shelf life for food products without any quality loss (Nerin, Vera, & Canellas, 2017).

Research groups have explored the potential use of natural sources such as bioactive compounds, as the case of essential oils which are incorporated as an alternative to traditional chemical preservatives (Gherardi, Becerril, Nerin, & Bosetti, 2016), bio-resource materials for food packaging applications (Gherardi et al., 2016), active packaging films with antimicrobial (Gherardi et al., 2016) or antioxidant activities (Carrizo, Gullo, Bosetti, & Nerín, 2014; Moudache, Nerín, Colon, & Zaidi, 2017; Tovar, Salafranca, Sánchez, & Nerín, 2005; Wrona, Nerín, Alfonso, & Caballero, 2017) among others.

Nowadays, the global food system needs to be driven by sustainability to fulfill environmental and societal challenges merged in a fast paced and highly interconnected industrial environment with a world plastic consumption per capita in 2015 of 45 kg ("Per capita consumption of plastic materials worldwide in 2015 by region (in kilograms)," 2015) and a growing urban population reported in 2017 of 4.128 billion ("Population growth (annual %)," 2017).

In Europe, the demand of plastic converters for 2016 represented 49.9 million tons. Out of those, the thermoplastic resins led the volume consumption, and only two resins comprised almost half of the total demand: polypropylene and polyethylene diversified into different grades (LDPE, LLDPE, MDPE, HDPE). Moreover, 39.9% of this consumption is related to the food packaging sector ("Plastics – the Facts 2017 An analysis of European plastics production, demand and waste data," 2018).

In the light of this information, the perception of consumption by society has evolved towards healthier food consumption habits and environmental ethics awareness (Reisch, Eberle, & Lorek, 2013). One case of study, in the wine industry in New Zealand, concluded that the implementation of environmentally sustainable practices derived in the consumer preference. Hence, product diversification resulted as a competitive advantage in the marketplace (Forbes, Cohen, Cullen, Wratten, & Fountain, 2009).

Furthermore, in the food packaging industry, a research study presented the consumer demands for 2018 comprised into 8 megatrends. Concluding that, “healthy living” is the megatrend that drives innovation (Euromonitor International, 2018).

Align to “healthy living”, the food Industry is being directed towards nutrition and natural wellbeing, i.e., raw and cold products (uncooked or unprocessed), clean label (fewer and natural ingredients), no sugar (sugar alternatives products), and functional foods such as: fermented food, ancient grains and probiotics, and healthy fats (oils) (Euromonitor International, 2018). Among all the processes involved in a food system, the present project research is focused on: processing (polymer industrial transformation), packaging (formulation), and disposal of food-related items (recyclability) processes.

Chapter two presents the methodology of the analytical method (spectrophotometry) on the evaluation of the antioxidant capacity of natural molecules and foodstuff with potential application in polymer packaging formulation. The chapter covers the analytical method assessment (machine, method, materials, measurement, and environment) to determine the overall effect of variables on the antioxidant capacity thus, resulting in the test-method standardization.

Chapter three presents mainly two analytical methods, thermal and rheological characterization of the resins: un-stabilized polypropylene (i-PP), un-stabilized low-density polyethylene (LDPE), and commercial LDPE. The chapter deepens on the methodology to characterize the effect of thermo-oxidative and mechanical stresses, during polymer

industrial transformation, on the resulting product (extrudate) and continues with an analysis and discussion of the resins prior to formulation with antioxidant molecules.

Chapter four is subject to polymer formulation and recyclability analysis by multi-extrusion cycles. After an introductory chapter three, where it was presented the test methods to assess the effect of processing on the polymer stability, the discussion now relies in polymer formulation with natural antioxidants such as α-Tocopherol, ascorbic acid, and flaxseed oil. Furthermore, the encapsulation of ascorbic acid into a food grade carrier, and the incorporation into isotactic polypropylene (i-PP) as a solution for i-PP stabilization is assessed.

Bibliography

Baldesi, P., Feber, D., Santhanam, N., Spranzi, P., Tewari, A., & Varanasi, S. (2019). *Packaging Solutions: Poised to take off?* Retrieved from https://www.mckinsey.com/industries/advanced-electronics/our-insights/packaging-solutions-poised-to-take-off

Carrizo, D., Gullo, G., Bosetti, O., & Nerín, C. (2014). Development of an active food packaging system with antioxidant properties based on green tea extract. *Food Additives and Contaminants - Part A Chemistry, Analysis, Control, Exposure and Risk Assessment*, *31*(3), 364–373. https://doi.org/10.1080/19440049.2013.869361

Euromonitor International. (2018). *PACKAGE FOOD: 8 FOOD TRENDS FOR 2018*.

Forbes, S. L., Cohen, D. A., Cullen, R., Wratten, S. D., & Fountain, J. (2009). Consumer attitudes regarding environmentally sustainable wine: an exploratory study of the New Zealand marketplace. *Journal of Cleaner Production*, *17*(13), 1195–1199. https://doi.org/10.1016/j.jclepro.2009.04.008

Gherardi, R., Becerril, R., Nerin, C., & Bosetti, O. (2016). Development of a multilayer antimicrobial packaging material for tomato puree using an innovative technology. *LWT - Food Science and Technology*, *72*, 361–367. https://doi.org/10.1016/j.lwt.2016.04.063

Moudache, M., Nerín, C., Colon, M., & Zaidi, F. (2017). Antioxidant effect of an innovative active plastic film containing olive leaves extract on fresh pork meat and its evaluation by Raman spectroscopy. *Food Chemistry*, *229*, 98–103. https://doi.org/10.1016/j.foodchem.2017.02.023

Nerin, C., Vera, P., & Canellas, E. (2017). Active and Intelligent Food Packaging. In V. Rai Ravishankar & J. A Bai (Eds.), *Food Safety and Protection* (p. 700). CRC Press.

Per capita consumption of plastic materials worldwide in 2015 by region (in kilograms). (2015). Retrieved from https://www.statista.com/statistics/270312/consumption-of-plastic-materials-per-capita-since-1980/

Plastics – the Facts 2017 An analysis of European plastics production, demand and waste data. (2018). Retrieved from https://www.plasticseurope.org/application/files/5715/1717/4180/Plastics_the_facts_2017_FINAL_for_website_one_page.pdf

Population growth (annual %). (2017). Retrieved from https://data.worldbank.org/indicator/SP.POP.GROW?end=2017&start=1960&view=chart

Reisch, L., Eberle, U., & Lorek, S. (2013). Sustainable food consumption: an overview of contemporary issues and policies. *Sustainability: Science, Practice and Policy*, *9*(2), 7–25. https://doi.org/10.1080/15487733.2013.11908111

Tovar, L., Salafranca, J., Sánchez, C., & Nerín, C. (2005). Migration studies to assess the safety in use of a new antioxidant active packaging. *Journal of Agricultural and Food Chemistry*, *53*(13), 5270–5275. https://doi.org/10.1021/jf050076k

Wrona, M., Nerín, C., Alfonso, M. J., & Caballero, M. Á. (2017). Antioxidant packaging with encapsulated green tea for fresh minced meat. *Innovative Food Science and Emerging Technologies*, *41*, 307–313. https://doi.org/10.1016/j.ifset.2017.04.001

CHAPTER I

STATE OF THE ART

Polymers are shaped into plastic products, with innumerable end-user applications, by industrial operations such as extrusion, injection molding, thermoforming, among others. In the case of thermoplastic resins, processing conditions may lead molecular damage associated to specific degradation mechanisms. Therefore, the need to incorporate antioxidants as thermal stabilizers.

In this chapter, it is presented a review of the degradation mechanisms involved for two thermoplastic resins: un-stabilized isotactic polypropylene (i-PP) and un-stabilized low-density polyethylene (LDPE). Also, it covers a review of synthetic antioxidants and classification, and presents natural antioxidants as potential thermal stabilizers. This chapter, also addresses the need for a more sustainable economy model based on recycling and supported by regulatory outlines particularly, for food contact plastic materials.

1.1 Polymer and classification

A polymer is a large molecule derived from the chemical reaction (polymerization) of n-repetitive monomer(s) units. One general classification is based on their origin divided into natural, half synthetic, and synthetic polymers.

Natural polymers are those present in nature in vegetable and animal tissues, mainly in the form of cellulose and proteins. Half synthetic polymers are partly natural polymers with chemical modifications and finally, synthetic polymers those who are synthesized from one or more monomer units via polymerization.

Another important classification is based on the end-use performance (physical properties) particularly, the elastic modulus and the degree of elongation. Based on this, polymer materials can be classified into elastomers, plastics, and fibers. Elastomers or rubbers are characterized by a long-range extensibility which is highly reversible at room temperature. On the other hand, plastics have a partial reversible extensibility while fibers present a high tensile strength but a reduced extensibility. Plastics are further divided into thermoplastics,

where deformation at elevated temperatures (but below its degradation temperature) is reversible and thermosets which undergo irreversible changes when heated (Beyler & Hirschler, 2002).

1.2 Thermal degradation and Thermal decomposition

The effect of heat on polymeric based materials leads to undesirable properties due to physical and chemical changes derived from the thermal exposure of the material. Industrial processors for economical reasons, operate in an oxidative atmosphere (air) and in this case, the decomposition temperature is decreased. This consideration is important for the determination of physical and chemical changes. Furthermore, in the calculation of kinetic parameters.

According to the American Society for Testing and Materials, thermal decomposition is defined as “a process of extensive chemical species change caused by heat” whereas thermal degradation is “a process whereby the action of heat or elevated temperature on material, product, or assembly causes a loss on physical, mechanical, or electrical properties” (Beyler & Hirschler, 2002).

1.3 Physical Processes on Polymers as a function of Temperature

The physical processes involve during thermal decomposition can depend on the nature of the material. In the case of thermosetting polymers, these are infusible and insoluble once they are shaped thus, physical changes upon heating are not present. On the other hand, thermoplastic polymers can be softened while heating without irreversible changes to the material below the decomposition temperature. In view of this, thermoplastics provide the characteristic and feasibility of being molded or thermoformed (Beyler & Hirschler, 2002).

The physical effect of thermoplastics while heating is dependent on the degree of crystallinity (the degree of order in molecular packing). For crystalline materials there is a defined melting temperature. Contrarily, materials that do not present an internal ordered packing are defined as amorphous (Beyler & Hirschler, 2002).

Most olefin resins are semicrystalline, consisting of two or more solid phases and, in at least one, molecular chain segments are organized into a three-dimensional array (crystalline region) whereas the other phase(s) chains are disordered (amorphous or noncrystalline region) (Beyler & Hirschler, 2002).

1.4 Chemical Processes on Polymers as a function of Temperature

Thermal degradation in polymers may proceed either by oxidative processes or simple by heat input. There are general chemical mechanisms of thermal decomposition in polymers:

1. **Random-chain scission.** A chemical reaction where chain scission results at random locations in the polymer chain,

2. **End-chain scission.** Individual sequentially monomer units are removed at the chain end,

3. **Chain-stripping.** Atoms or groups independent of the polymer chain are cleaved,

4. **Cross-linking.** Bonds are formed between polymer chains.

The interaction of both processes is defined, in the case of Thermoplastics, as the action of heat to induce melt and form a viscous state (without chemical reaction but with an initial thermal decomposition before melting), the polymer melt can then be decomposed in liquid or gaseous fragments. Finally, remaining liquid will further decomposed up to depletion (volatilization) (Beyler & Hirschler, 2002).

1.5 Reactive Oxygen Species (ROS)

The main source of degradation in olefin resins are oxidative processes where a free radical atom or molecule with at least one unpaired electron reacts on the weakest bond dissociation energy of the polymer backbone. Any radical including oxygen is referred to as ROS which includes different species, some of them not in radical form such as singlet oxygen and hydrogen peroxide and radical species among the principal, triplet oxygen, superoxide anion, peroxide, and hydroxyl radical (Kolakowska & Bartosz, 2014).

1.6 General mechanism of oxidative degradation

Polymers in presence of oxygen, undergo into three main reactions.

1. Separately occurring molecule reactions,
2. Radical chain mechanism,

3. Products of thermal decomposition and oxidation of polymers catalyze further decomposition of the polymer.

Thermal oxidation of polyolefins followed a radical chain mechanism process, where alkyd (R*), alkoxide (RO*), and peroxide (ROO*) macroradicals along with low molecular weight radicals (r*) are predominant in the oxidative degradation of polymers. This process includes parallel reactions in the propagation step either inside or between two macromolecules. Figure 1.1 describes the mechanism (Shibryaeva, 2012).

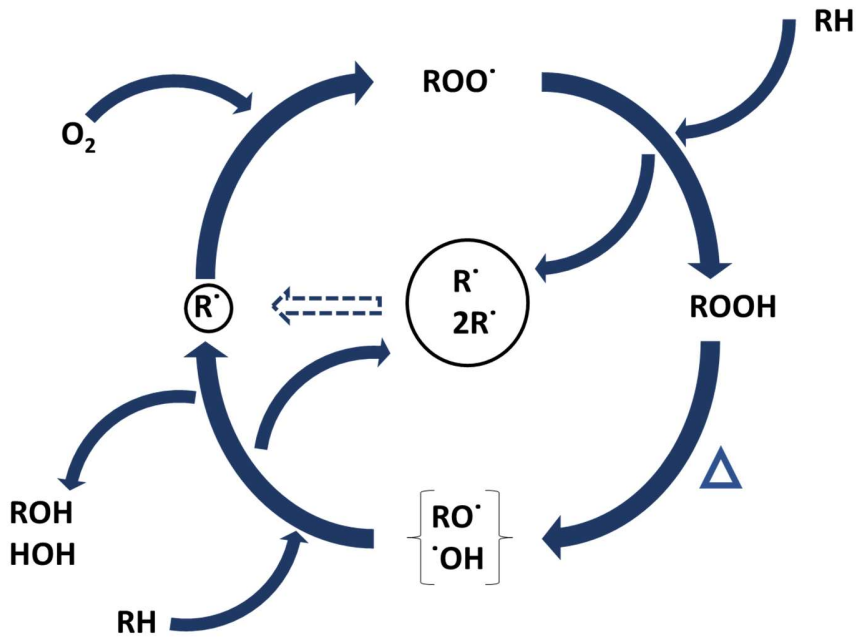

Figure 1.1. General degradation mechanism for polyolefins (Hinsken, Moss, Pauquet, & Zweifel, 1991).

1.7 Polypropylene (PP)

An olefin resin derived from the polymerization of propylene. Nowadays new generation catalysts are capable to produce commercially stereoregular PP. Stereoregularity is controlled by three factors:

1. Linearity. The consecutive monomer unit is added at the end of the growing chain,

2. Pendant methyl group (Regiospecific). The consecutive monomer unit in the growing chain is added in the same manner (heat to head, heat to tail, tail to tail),

3. Right or left hand (Stereospecific). The monomer unit always is added in the same stereo arrangement in the growing chain.

Based on above factors, PP is divided into isotactic PP when obeys all three considerations allowing PP to crystallize. Syndiotactic PP when the n^{th}-consecutive monomer unit is added at the end of the growing chain in the opposite hand and atactic PP when there is a deviation in any of the above factors mentioned. Among these three categories, Isotactic PP is the most relevant in the industry (Becker, Burton, & Amos, 1996).

1.7.1 Degradation mechanism of PP

The oxidative processes of PP are intricate where products formed are dependent on a variety of factors as such as oxygen availability, impurities, residual catalyst, physical form (melt state or solid), crystallinity, storage temperature, air pollutants, radiation, chemical, and metal exposure, part thickness, stress in the part, co-monomer content and other additives present.

It is reported the formation of aldehydes groups in the polymer matrix as end groups during chain braking along with ketones groups in the zone of the brake. These are middle products of oxidation of relaxed through-pass chains. The four general steps of oxidation and degradation of PP are initiation, propagation, branching, and termination (Becker et al., 1996).

1.7.1.1 Initiation

Initiation is induced by means of an energy source to yield an alkyl radical and a hydrogen atom. Below reaction does not consider the reaction between molecular oxygen and hydrocarbons (Becker et al., 1996).

$$RH + Energy \rightarrow R^{\cdot} + H^{\cdot} \quad (1.1)$$

The effect of oxidation in hydrocarbons during initiation step is given by equation 1.2.

$$RH + O_2 \rightarrow R^{\bullet} + {}^{\bullet}OOH \quad (1.2)$$

The oxidation reaction is prone to recombination within the polymer cage to produce either hydroperoxide (equation 1.3) or remain as an alkyl radical and hydroperoxy radical (equation 1.2).

$$R^{\bullet} + {}^{\bullet}OOH \rightarrow ROOH \quad (1.3)$$

The effect of viscosity during the initiation reactions step makes highly probable the reaction from equation 1.3 (in a high viscosity media) leading a recombination to produce hydroperoxides thus, the propagation step is delayed until sufficient energy is achieved to induce an homolytic cleavage of the hydroperoxide proceeding with the propagation step (Becker et al., 1996).

1.7.1.2 Propagation

In this step, delocalization of the radical site is present without an overall increase in the number of radicals of the following reactions:

$$R^{\bullet} + O_2 \rightarrow ROO^{\bullet} \quad (1.4)$$

$$ROO^{\bullet} + RH \rightarrow ROOH + R^{\bullet} \quad (1.5)$$

$$RH + H^{\bullet} \rightarrow H_2 + R^{\bullet} \quad (1.6)$$

$$R^{\bullet} + R'H \rightarrow RH + R'^{\bullet} \quad (1.7)$$

Additional reactions derived from the small free radical fragments:

$$OOH^{\bullet} + RH \rightarrow R^{\bullet} + H_2O_2 \quad (1.8)$$

$$OH^{\bullet} + RH \rightarrow R^{\bullet} + H_2O \quad (1.9)$$

$$H^{\bullet} + RH \rightarrow R^{\bullet} + H_2 \quad (1.10)$$

If the alkyl and hydroperoxy radicals formed (equation 1.1 and 1.2) during the initiation step remained separate, the path of propagation is represented by equations 1.5 to 1.8. Further propagation reactions are followed from the carbon-based radical formation (equations 1.5 to 1.10) via:

1. Alkyl peroxy radical formation (equation 1.4) followed by intramolecular abstraction of hydrogen (equation 1.5), or

2. Intramolecular reaction, hydrogen abstraction (equation 1.7).

The resulting effect of intramolecular reactions cause the radical site to migrate down the polymer chain with a possible interaction with other radical thus, finalizing the chain reaction (Becker et al., 1996).

1.7.1.3 Branching

These propagation reactions cause an increment in the number of radicals.

$$ROOH \rightarrow RO^{\bullet} + {}^{\bullet}OH \quad (1.11)$$

Hydroperoxides can be formed either in the propagation step (equation 1.5) or in the initiation step product of the recombination of the radical species as in equation 1.3. The homolytic cleavage of hydroperoxides plays a key role toward increasing the concentration of radicals in the polymer. This reaction is considered also a secondary initiation (Becker et al., 1996).

1.7.1.4 Termination

This step comprises the reactions involved in the formation of nonradical products where the number of radicals is reduced by combinations of two radical sites enabling the polymer to stabilize.

$$RO^{\bullet} + H^{\bullet} \rightarrow ROH \quad (1.12)$$

$$ROO^{\bullet} + H^{\bullet} \rightarrow ROOH \quad (1.13)$$

$$R^{\bullet} + R'^{\bullet} \rightarrow R\text{-}R' \quad (1.14)$$

$$RO^{\bullet} + R^{\bullet} \rightarrow ROR \quad (1.15)$$

$$2ROO^{\bullet} \rightarrow ROOR + O_2 \quad (1.16)$$

$$2\ RO^{\bullet} \rightarrow ROOR \quad (1.17)$$

$$2\ R^{\bullet} \rightarrow -HC{=}R + -H_2C\text{-}R \quad (1.18)$$

It is important to remark that unsaturated products are more susceptible to oxidation. Equation 1.18 represents the bimolecular disproportionation reaction for carbon centered radicals where intramolecular reaction is assumed. This reaction can remove two radicals from either propagation or branching reactions (Becker et al., 1996).

1.7.1.5 Chain scission

The tertiary sterically hindered radical carbon present in Polypropylene reduces the probability of cross-linking. Loss of molar mass is a severe result of degradation, the most common paths of chain scission in PP followed by the reaction of an alkyl radical (Becker et al., 1996) (equation 1.19) are:

(1.19)

1. Unimolecular β-scission of carbon

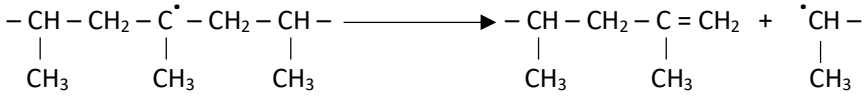

(1.20)

2. Oxygen radicals (aldehyde and ketone groups) (Hinsken et al., 1991)

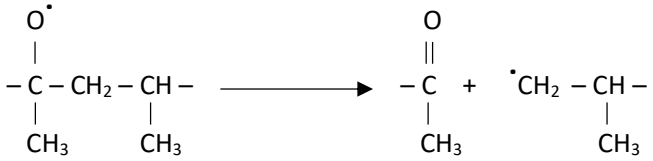

(1.21a)

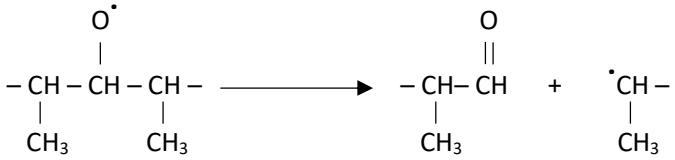

(1.21b)

1.8 Polyethylene (PE)

Polyethylene is the polymerized n^{th}-repetitive unit of ethylene monomer with chain ends terminated by methyl groups. The main classification of polyethylene is (Peacock, 2000b):

1. High Density Polyethylene (HDPE). A high degree of crystallinity Polyethylene composed of unbranched molecules with few defects of organization. Due to this characteristic, HDPE presents the highest stiffness and lowest permeability among all PE grades. HDPE is appropriate for liquid containment applications (i.e. milk and detergent bottles, drums, pails, and chemical storage tanks) or in film applications where good tensile strength is required such as grocery sacks and trash can liners.

2. Low Density Polyethylene (LDPE). Polyethylene backbone with considerable concentrations of branches mainly of ethyl and butyl groups along with some long-chain branches. Long-chain branches provide ease of processability conferring high melt strengths with relative low viscosity, suitable for film-blowing process. Major applications comprise low load commercial and retail packaging applications and trash bags. Additionally, LDPE can be laminated onto cardboard to provide waterproof and heat-sealable properties for fruit juice and milk cartons.

3. Linear Low Density Polyethylene (LLDPE). A Polyethylene resin comprising linear backbones with alkyl groups attached at random intervals. Commonly branches, but not limited, are ethyl, butyl, or hexyl groups. Applications relies on the field of LDPE distinguishing by its superior toughness. On a larger scale, LLDPE is used for food processing containers, storage tanks, and highway construction barriers.

4. Very Low Density Polyethylene (VLDPE). A specialized resin that has a higher concentration of short-chain branches than LLDPE, resulting in a predominantly amorphous material. Depending upon the co-monomer content, VLDPE is used by its clarity, softness, strain recovery, and toughness in applications such as medical tubing, meat packaging, and diaper backing.

1.8.1 Degradation mechanism of PE

Polyethylene resin by its nature is relatively inert. The saturated carbon to carbon covalent bonds limit the reactions that PE undergo. It is when the introduction of unsaturation or the incorporation of other atoms rises the probability of a chemical reaction. The principal reactions are chain degradation, cross-linking, oxidation, surface modification, and grafting. In a molecular level, degradation of PE follows different ways, including chain scission, cross-linking, and the insertion of chemical moieties. Degradation reactions lead to changes in the molecular weight affecting rheological characteristics and the mechanical properties of the end-product (Peacock, 2000b).

In the case of chain scission reaction, the average molecular weight is reduced with a drop in the mechanical properties of the end-product i.e. a reduction in the tear strength and the onset of embrittlement. Furthermore, the introduction of new groups derived from the oxidation reaction, affect the optical properties (Peacock, 2000b).

In a cross-linking reaction, the glass transition temperature (Tg) is increased as the degree of cross-linking increases. On the other hand, the cross-linking agent can be considered as a type of copolymerizing unit thus, the copolymer effect can either increase or decrease Tg depending on its chemical composition (Nielsen, 1969).

Furthermore, above the glass transition temperature, the modulus is dependent upon the extent of crosslinking. Also, it is reported for several polymers that elongation to break decreases as cross-linking increases, whereas tensile strength first increases with cross-linking, goes through a maximum at low degrees of cross-linking, and then progressively decreases (Nielsen, 1969).

The main oxidative degradation of PE comprises four reactions: initiation, propagation, branching, and termination.

1.8.1.1 Initiation

Radical species are formed by the effect of energy or heat as shown previously in equation 1.1 via hydrogen abstraction from PE backbone or by backbone cleavage to produce terminal radicals generated from severe thermo-mechanical stresses either in the molten state or solid (end-product). Another radical source, that is possibly present, is an oxyradical radical generated from the homolytic cleavage of a peroxide molecule thus, leading to an alkyl radical and an alcohol (Peacock, 2000a).

1.8.1.2 Propagation

A two sequential reaction steps, first the alkyl radicals formed during initiation rapidly reacts with molecular oxygen to form alkyl peroxy radicals followed by its stabilization via hydrogen atom abstraction from an adjacent PE molecule to generate hydroperoxide and another alkyl radical (autocatalytic reaction) (Peacock, 2000a).

Propagation step and further reactions are limited to the amorphous regions where molecular oxygen absorbed is free to migrate. In the absence of oxygen, alkyl radicals migrate until they encountered and react with another radical. The rate-limiting reaction for the entire autoxidation process is the alkyl peroxy reaction with an adjacent PE molecule that yields hydroperoxide (Peacock, 2000a).

1.8.1.3 Branching

Hydroperoxide concentration dependent reactions that involve in one way, the homolytic cleavage to form alkoxy and hydroxy radicals which both, further reacts through hydrogen abstraction from the contiguous PE molecule generating an alcohol, water, and additional alkyl radicals leading from the latter, the continuing of the propagation reaction step.

Another path involves more complex reactions, through six-membered transition state (Gugumus, 2002), where the hydroperoxide group reacts with a neighboring chain segment either from the same or another macromolecule yielding vinylene unsaturation, water, and alcohol. The overall result of branching is the increase in concentration of the alkyl radicals thus, accelerating the oxidation process (Peacock, 2000a).

1.8.1.4 Termination

This step comprises quenching reactions from alkyl and alkoxy radicals with one another or with atomic hydrogen. Cross-linking reactions are present when alkyl radicals from contiguous chains quench one another.

β-chain scission reactions are also present and occur when isolated alkyl peroxy or alkoxy radicals decompose. In the case of alkyl peroxy radicals, decomposition leads terminal aldehydes, terminal unsaturation, and hydroxy radicals. On the other hand, the isolated reactions of alkoxy radicals yield terminal aldehydes and terminal alkoxy radicals. β-chain scission reactions lead to a reduction in the average molecular weight. The following scheme (Figure 1.2) depicts the overall oxidation mechanism along with the corresponding termination reactions (Peacock, 2000a):

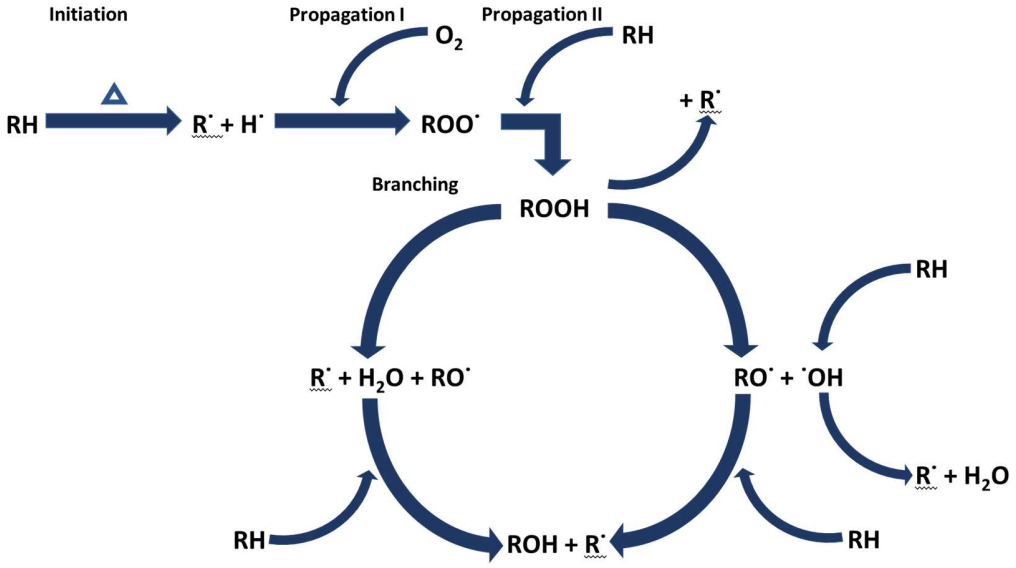

Figure 1.2. PE degradation mechanism. The formation of radical species derived from thermo-mechanical stresses followed by the reaction against molecular oxygen and the consequently stabilization with an adjacent hydrogen from a contiguous PE molecule thus, yielding hydroperoxide and alkyl radical R· formation that leads two reaction pathways (R· denotes the available alkyl radical species formed to further react with molecular oxygen).

1.8.1.5 Termination Step reactions

$$ROO^{\cdot} + ROO^{\cdot} \rightarrow ROOR + O_2 \quad (1.22)$$

$$R^{\cdot} + R^{\cdot} \rightarrow R\text{-}R \text{ (cross-linking)} \quad (1.23)$$

$$RO^{\cdot} + H^{\cdot} \rightarrow ROH \quad (1.24)$$

$$R^{\cdot} + H^{\cdot} \rightarrow RH \quad (1.25)$$

1.9 Polymer Processing

Is defined as the industrial transformation of raw materials (polymer based) into finished plastic products involving operations that provide defined shapes and properties oriented to specific customer applications. Polymer processing involves different operation steps, from the manufacturing of the polymer resin up to the finished plastic processor including (Tadmor & Gogos, 2006):

1.9.1 Post-reactor polymer processing operations

Also called finishing operations. In a broad sense, the product coming from a polymerization reactor is exposed to separation and drying steps to obtain the polymer resin (powder). Subsequently, polymer resin follows a dry mixing step where additives are charged (i.e. stabilizers and processing aids). The first thermomechanical event is presented when material is fed into a Co-rotating Twin Screw Extruder or a Continuous Melter. Material is then melted, mixed, homogenized, and conveyed (through a gear pump) into an underwater pelletizer to obtain the final pellet shape and dried.

1.9.2 Polymer compounding operations

This operation constitutes the compounding (mixing) of different additives into the manufacturer virgin pellets to provide add-value and desirable end-properties. In general, the processing equipment used is Co-rotating and Counterrotating Twin Screw Extruder and, in less demand, Single-Screw Extruder. This operation exposes the virgin pellet to a second thermomechanical event and the end-product goes directly to finished plastic products processors.

1.9.3 Reactive polymer processing operations

In this operation, the post-reactor resin is modified or functionalized. Resin in powder, is fed along with reactive additives (i.e. peroxides and functional groups compounds) into a Co- or counterrotating Twin Extruder or Continuous Melter which are favored by an efficient distributive mixing. An additional elementary operation is added before melt is conveyed, a devolatilization process, where side products derived from reaction are removed. Reactive processing can then be the first or second thermomechanical event of reactor polymers.

1.9.4 Polymer blending operations

Industrial operation oriented to produce polymer blends and alloys that provide added value to product applications. Processing operation involves the feed of two or more polymers along with a compatibilizer into a Co- or counterrotating Twin Screw Extruder. Final product is a customized (micro-structured) polymer system. The polymer blend flow stream is exposed to the same elementary steps. Finally, polymer blending expose reactor polymers to their second or third thermomechanical event.

1.9.5 Plastic products operations

The operations comprise the processing of post-reactor, compounded, reactive, or blended resins to shape finished plastic products. The equipment generally used by processors are Single Screw Extruder and Injection molding machines. The polymer melt is flowed through a die or into a cold mold to form the final product shape. In some applications, a post-shaping operation, uniaxial or biaxial orientation is performed.

1.9.6 Shaping operation methods

The selection of the shaping operation is defined by product geometries and in some instances, when there are alternative shaping methods, by its economical impact. The shaping methods are classified into four general groups:

1. **Calendring and coating.** A steady and continuous process used in the rubber and plastic industry.

2. **Die forming.** The most important industrial operation which entails forcing a melt through a die. Applications include fiber spinning, film and sheet forming, pipe, tube, profile forming, and wire and cable coating.

3. **Mold coating.** A cyclic process that involves the formation of a thick coating at the surface of the mold. Used in applications as dip coating, slush molding, powder coating, and rotational molding.

4. **Molding and casting.** A cyclic process of filling molds with either thermoplastic or thermosetting resins. Involves operations such as injection molding, transfer molding, and compression molding.

5. **Stretch shaping.** Shaping of preformed polymers by stretching. Applications includes thermoforming, blown molding, stretch blow molding, and cold forming.

1.10 Polymer Stabilization

Polypropylene and Polyethylene, as virgin olefin resins, are susceptible to deterioration i.e. atmospheric attack leads to oxidation varying its intrinsic properties such as optical and mechanical properties. Storage conditions, temperature, and available oxygen are important factors to consider in the development of detrimental properties. The incorporation of additives to stabilize these resins, and or to provide additional features to the end-use application (i.e. color, static buildup modifications, surface modifications, and stabilizers among others) are of vital importance.

1.11 Antioxidants

Antioxidants are molecules that retard the effect of degradation in the polymer backbone caused by the presence of radical species. The mechanism involved is through the inactivation of free radical species either in the propagation or branching step, where the antioxidant at least, is capable of scavenging two radicals. First, an inactivation of an alkyl, alkoxyl, or alkyl peroxy radical and secondly, when the oxidized antioxidant reacts with another radical to form a nonradical specie in a termination reaction (Peacock, 2000a).

Some antioxidants can scavenge more than two radicals, particularly when the oxidized form of the antioxidant still possess an available hydrogen to inactivate an additional radical specie. Furthermore, an antioxidant can be reduced by another molecule to regenerate and reactivate to its original form.

1.11.1 Primary antioxidants

Also called radical scavengers, chain-breaking agents, or termination agents. A Branch of organic molecules containing a hydrogen able to be abstracted from a radical specie. The radicals involved in the polymer degradation mechanism are represented from Eq. 1.2 to 1.11. Among the principal primary antioxidants are Hindered Phenols (HP) and Hindered Amines (HA) (Peacock, 2000a).

1.11.1.1 Hindered Phenols

Hindered phenols provide good protection against degradation (physical properties deterioration) and it is of great industrial importance. Among its applications, there is a high consumption demand in polyolefins particularly, for PP (Pospíšil, 1988). The general mechanism of HP involves the scavenging of radical species as depicted in below equations.

$R^{\cdot} + AH \rightarrow RH + A^{\cdot}$ (1.26)

$RO^{\cdot} + AH \rightarrow ROH + A^{\cdot}$ (1.27)

$ROO^{\cdot} + AH \rightarrow ROOH + A^{\cdot}$ (1.28)

The hydrogen abstraction from a HP results in reaction products that are stable as in eq. 1.26 and 1.27 avoiding effectively radical reactions in the propagation steps. Depending on the nature of the initial radical specie, as in eq. 1.28, a new hydroperoxide can be formed which further undergoes homolytic cleavage, leading the formation of two additional radical species (Becker et al., 1996). Figure 1.3 depicts the radical scavenging mechanism of a typical HP.

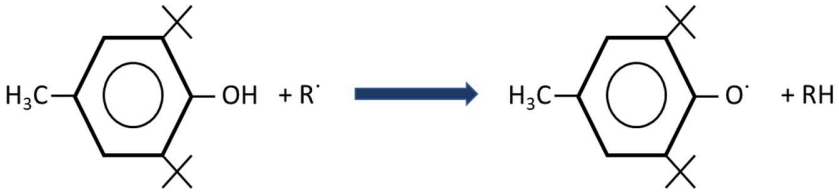

Figure 1.3. Scavenging activity of Hindered Phenol against an alkyl radical.

HP terminates autoxidation chains by trapping oxygen centered radicals such as alkoxy and alkyl peroxy, and alkyl radicals (eq. 1.26 – 1.28). Figure 1.4 represents the scavenging activity action of a single HP on two alkoxy radicals (Becker et al., 1996).

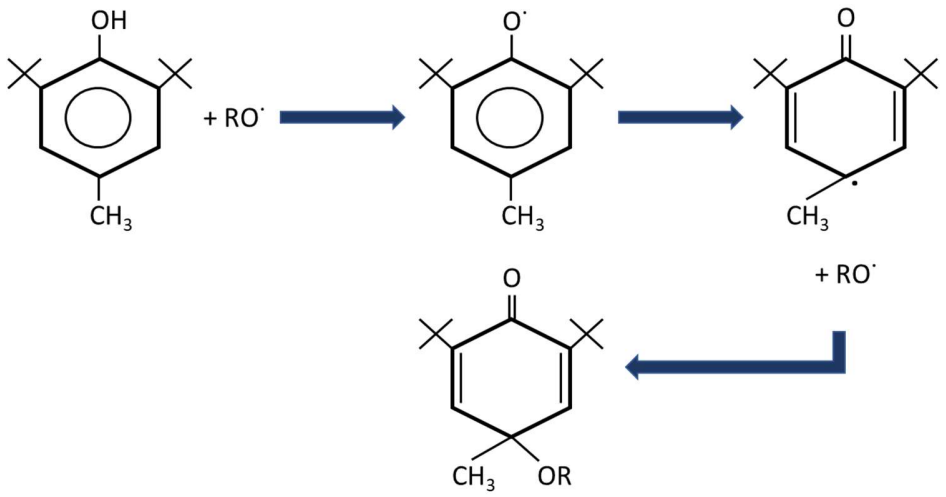

Figure 1.4. Delocalization of phenoxy radical to scavenge two alkoxy radicals.

Polar and steric substituent play a key role on the reactivity of the hydroxyl group in phenols (Leopoldini, Russo, & Toscano, 2011; Pospíšil, 1988). The most efficient phenols are 2,4,6-trisubstituted (sterically hindered phenols) followed by 2,4,5-trisubstituted and 2,4-disubstituted phenols. The steric hindrance of the hydroxyl group by bulky substituents in positions 2 and 6 is optimal to control the phenoxyl radical formation (Pospíšil, 1988; Wypych, 2015). The industrial application substitution is a combination of two tert-butyl groups or one methyl and one tert-butyl group. Furthermore, the chemical character of the substituent in position 4 is of relevant importance on the reactivity of the hydroxyl group in phenols and often contributes to the stabilizing mechanism (Pospíšil, 1988).

Some Industrial and efficient HP used in polyolefins stabilization are: butylated ester type phenols (such as Irganox 1010 and Hostanox) and Butylated hydroxytoluene (BHT) as shown in Figure 1.5.

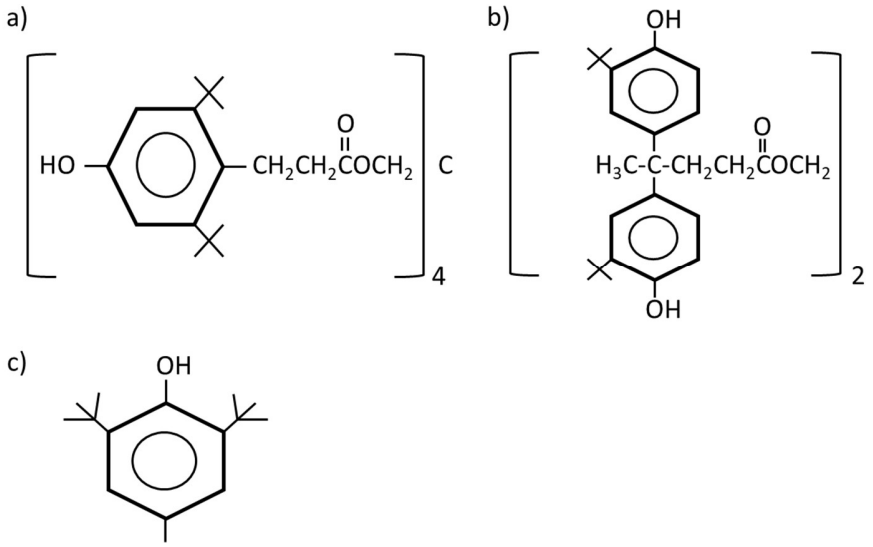

Figure 1.5. Commercial hindered phenols. a) Irganox 1010, b) Hostanox, c) BHT.

1.11.1.2 Hindered Amines

Hindered Amines or Hindered Amine Stabilizers (HAs) act as a radical scavenger where the active specie is the oxidized form of the amine group, the nitroxyl radical. One important feature is that the radical formed, can be regenerated until some extent. The most important application in volume of HA, is as light stabilizers and plays a significant role in PP industrial applications (Becker et al., 1996).

1.11.2 Secondary Antioxidants

Defined as peroxide decomposers. Only acts synergistically with primary antioxidants providing a control of hydroperoxides (ROOH). Secondary antioxidants reduced hydroperoxides to alcohols, a stable product. Thus, eliminating the possibility of new radical sites formation caused by the homolytic cleave of additional hydroperoxides. The two most common classes of secondary antioxidants are phosphites (a) and thio compounds (b). Figure 1.6 represents the general mechanism of reaction (Becker et al., 1996).

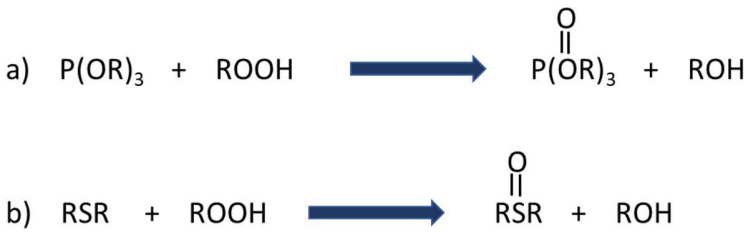

Figure 1.6. Scavenging activity of phosphites (a) and thio compounds (b) on hydroperoxides.

1.11.3 Natural Antioxidants

The interest of antioxidants in the food industry has evolved and deepened, starting from the original product-oriented purpose of prevention or retardation of lipid oxidation in foods, to the conceptualization of biological oxidative stress, and the consequent research on the contribution of dietary antioxidants to enhance the mechanism of defense of human body (Nenadis & Tsimidou, 2010).

Furthermore, research is now being oriented to health concerns derived from the use of synthetic molecules and their possible mutagenic activity in food as well as the migration of those molecules from food contact materials (FCM). Align with customer demand for a natural source of ingredients both Industries must align efforts to produce healthier foods, and to preserve and ensure food freshness and healthiness through a package.

1.12 Food stability and the role of antioxidants

The incorporation of polyunsaturated fatty acids in foods provides health benefits as the case of omega-3 fatty acid. In an increasing customer demand for healthier products rises the challenge for food preservation against the free radical oxidative deterioration (Vercellotti, St. Angelo, & Spanier, 1992).

Lipids are present in almost all foodstuff, the two most important factors in lipid oxidation are unsaturation of fatty acids and oxygen thus, the need to assess the oxidative degradation mechanism and the effect of either endogenous system of antioxidants or exogenous antioxidants in formulation.

Oxidative degradation is initiated by a ROS and external agents such as UV, ionization radiation, temperature, enzymes, and metals. In a broad sense, the oxidation of lipids involves the generation of hydroperoxides which undergo either further oxidation or decomposition into secondary oxidation products leading a loss in food quality (sensory characteristics and nutritional aspects).

1.13 Lipid oxidation mechanism

Oxidation of lipids relies on three different oxygen reaction pathways (Skibsted, 2010a). Figure 1.7 represents schematically the different reactions:

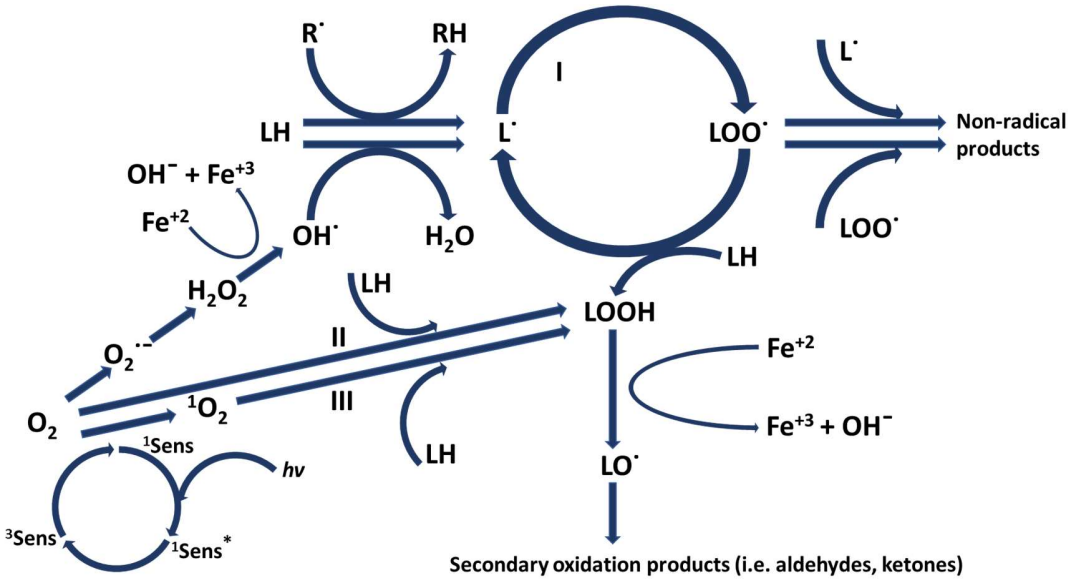

Figure 1.7. Lipid Oxidation mechanism (Skibsted, 2010a).

1. **Reaction I or autoxidation process**. Alkyl lipid radical formation (L˙) at the initiation step, where free radical chain reaction with lipid molecules (LH) is either initiated by oxygen activation to produce hydroxyl radicals (OH˙) or induced by temperature, irradiation, and the action of oxidants (R˙). In fats and oils, the presence of traces of transition metal compounds can accelerate this step. Process further involves a propagation step, where an alkyl lipid radical reacts with oxygen to form a peroxy lipid radical (LOO˙). The subsequent hydrogen atom abstraction from the new peroxy lipid radical causes an autocatalytic chain reaction. The reaction between two radicals terminates the autoxidation process.

2. **Reaction II or lipoxygenase**. An iron-containing enzyme present in plants and animals, that catalyze the oxidation of polyunsaturated fatty acids producing lipid hydroperoxides which further decompose and form secondary oxidation products.

3. **Reaction III or photosensitized oxidation.** Hydroperoxide formation induced by the presence of oxygen, light energy, and a photosensitizer. Where a singlet sensitizer (^{1}Sens) absorbs light and converts into triplet sensitizer (^{3}Sens) thus, initiating photooxidation (Frankel, 2005).

1.14 Secondary oxidation products

Lipid hydroperoxides (LOOH) can undergo β-scission reactions due to temperature, irradiation, and the presence of prooxidants. Products formed may include aldehydes, ketones, lactones, alcohols, keto acids, hydroxy acids, epidioxides, and other volatile compounds (VOC) leading a loss in the nutritional value of the food, causing odor, and for some components, toxicity in humans such as malondialdehyde (MDA) and trans-4-hydroxy-2-nonenal (HNE) (Kolakowska & Bartosz, 2014).

1.15 Antioxidant performance

The activity of an antioxidant system in food depends on factors such as physical location, interaction with other food components, and environmental conditions such as pH, besides the inherent chemical reactivity of the antioxidant (either free scavenger or chelator). One of the major implications on antioxidant activity is their behavior in the media or solvent (in lipids, organic media or aqueous) (Decker, Warner, Richards, & Shahidi, 2005).

In food systems, the antioxidant activity is directly correlated to the partitioning behavior. Thus, polar antioxidants are more effective in bulk oils as being positioned and accumulated at the air-oil interface where lipid oxidation reactions are the highest due to a direct oxygen and prooxidant interaction (Decker et al., 2005)

On the other hand, nonpolar antioxidants are more effective in emulsions as being retained in the oil droplets or accumulate at the oil-water interface with a direct interaction with hydroperoxides and prooxidants. In this case, polar antioxidants are less effective since they will remain in the aqueous phase with a less effective antioxidant activity (Decker et al., 2005), a term defined as the antioxidant paradox (Porter, 1993).

1.16 Polyphenols

Organic compounds abundant in plants and mainly composed by multiple phenol unit structures (conformed of one or more hydroxy groups attached to an aromatic ring). Polyphenols impart protection against UV-irradiation, in high concentrations in young fruits prevents the attack of insects, form the basis for colorants in flowers and fruits. Furthermore, participates in a repair mechanism from plants through oxidative polymerization by enzymes following mechanical damage (Skibsted, 2010b).

The main antioxidant activity of phenolic compounds is via free-radical. The mechanism involves hydrogen abstraction from peroxy radicals yielding phenolic radicals which either

further react each other to form phenolic dimers or phenolic quinones or react with peroxy radicals producing phenolic peroxy species adducts that may undergo in further degradation (Brewer, 2011; Shingai, Fujimoto, Nakamura, & Masuda, 2011). The position of the hydroxy group on the phenyl group plays an important role; substitution at either ortho or para position lowers the oxygen-hydrogen bond energy thus, increasing its reactivity to free radicals (Pokorný, 2001).

One classification is based on the number of carbons in the molecule (Harborne and Simmonds, 1964) (Vermerris & Nicholson, 2008), and further detailed (Gliszczyńska-Świgło & Oszmiański, 2014). Table 1.1 shows the main categories of phenol compounds present in food.

Chemical Structure	Class	Source	Main compounds
C6-C1 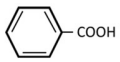	Benzoic acids and Benzaldehydes	Berries, cereals, herbs, and spices	4-Hydroxybenzoic, gallic, protocatechuick salicylic, vanillic, gentisic, and ellagic acids; vanillin
C6-C3 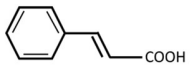	Cinnamic acids	Apple, cherry, plum, berries, tomato, asparagus, white grape, and herbs	*p* -Coumaric, caffeic, ferulic, sinapic, and chlorogenic acids
C15 (C6-C3-C6)	Flavonoids		
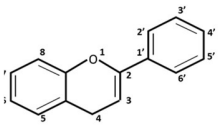	Flavonols	Onion, tomato, apple, brocoli, red wine	Kaempferol, Quercitin, Myricetin, Rutin
	Flavones	Herbs, celery, parsley, fruit skins	Luteolin, Apigenin, Chrysin
	Flavan-3-ols	Tea, cacao	(+)-Catechin, (-)-EC, (-)-ECG, (-)-EGC, (-)-EGCG
	Flavanones	Citrus fruits and juices	Hesperetin, Hesperidin, Naringenin, Naringin, Eriodictyol
	Isoflavones	Soybean	Genistein, Genistin, Daidzein, Daidzin
	Anthocyanins	Apple, pear, tomato	Pelargonidin, Cyanidin, Delphinidin, Malvidin
C6-C2-C6 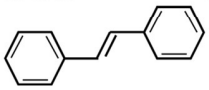	Stilbenes	Grapes and wine	Resveratrol
C18	Betacyanins	Red beet and opuntia	Betanin and isobetanin
Dimers or oligomers	Lignans	Flaxseed, sesame seed, cereals, legumes, berries, and vegetables	Secoisolariciresinol, secoisolariciresinol diglucoside, isolariciresinol, pinoresinol, and matairesinol
Oligomers or polymers	Tannins	Apples, berries, grapes, and red wine	Procyanidins B1, B2, B3, B4, C, gallotannins, and ellagitannins

Table 1.1. Phenolic compounds classification.

1.17 Ascorbic Acid

Also known as L-ascorbic acid, a low molar mass water-soluble natural antioxidant abundant in fresh fruits. Ascorbic acid cannot be synthesized by humans thus, solely rely upon a dietary source (Davey et al., 2000; Jomova, Lawson, & Valko, 2014). The molecular structure presents two hydroxyl groups hence being a diacid ($AscH_2$) with a high reductive potential able to scavenge superoxide anion radicals, singlet oxygen, hydrogen peroxide, and hydroxyl radicals (Bennette, Logan, Shiferaw-Terefe, Singh, & Robin, 2014; Jomova et al., 2014). The hydroxyl groups on adjacent carbon atoms can chelate metal ions and quench singlet oxygen (Brewer, 2011). Figure 1.8 represents the chemical structure.

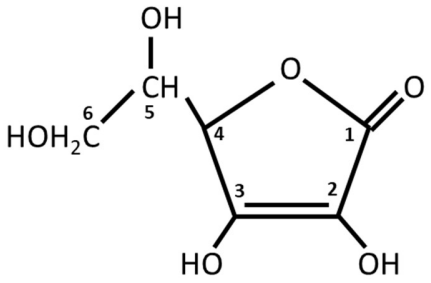

Figure 1.8. Ascorbic Acid structure.

Ascorbic acid ($AscH^2$) contains an enediol group (C2-C3), a conjugated system that stabilizes the molecule and causes the hydrogen of the C3 hydroxyl group to dissociate with a pKa of 4.13. Consequently, at physiological pH, ascorbic acid exists as a monovalent anion (L-ascorbate, $AscH^-$). Dissociation of the second hydroxyl (Asc^{2-}) takes place at a pH of 11.6 (Davey et al., 2000).

The first oxidation product of ascorbic acid is the radical monodehydroascorbate (MDHA) or semidehydroascorbate, a low reactivity radical (Davey et al., 2000; Jomova et al., 2014). Tough, two MDHA radicals may disproportionate to form ascorbic acid and dehydroascorbic acid (DHA) (Washko, Welch, Dhariwal, Wang, & Levine, 2004) where the latter, is characterized with no antioxidant activity (Nimse & Pal, 2015). In cell metabolism, reductants

convert DHA into Ascorbic Acid (Wilson, 2002) or it may undergo an irreversible hydrolytic ring rupture to form 2,3-diketogulonic acid (Washko et al., 2004).

Figure 1.9 presents the different forms of ascorbic acid in redox reactions and the scavenging activity against ROS to yield an ascorbyl radical considered as a terminal radical due to its low reactivity (Jomova et al., 2014; Nimse & Pal, 2015).

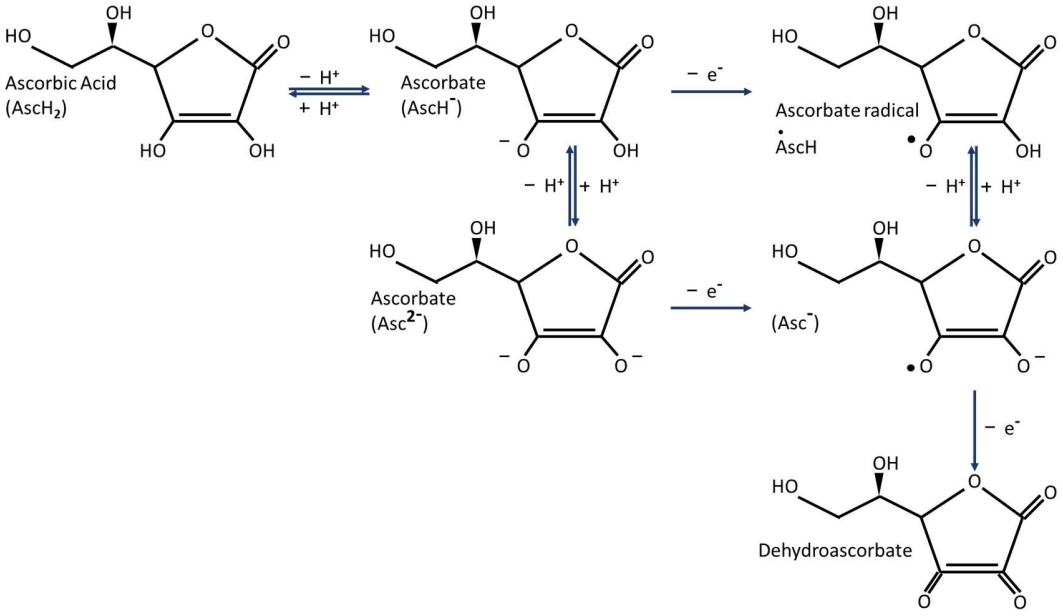

Figure 1.9. Ascorbic acid radical scavenging activity (Nimse & Pal, 2015).

Ascorbic acid is widely used in the food industry for nutraceutical applications such as vitamin/antioxidant supplement; in food processing as additive to replenish ascorbic acid during processing and used as an antioxidant either as ascorbic acid and its salts or as a fatty acid ester (ascorbyl palmitate) (Gliszczynska-Swigło & Oszmianski, 2014).

1.18 Vitamin E

A lipid-soluble antioxidant abundant in vegetable oils and green vegetables. Vitamin E comprises 8 different derivatives of the monophenolic chromanol ring substituted by an aliphatic side chain grouped as tocopherols and tocotrienols. Figure 1.10 embodies the chemical structures (Gliszczynska-Swigło & Oszmianski, 2014; Jomova et al., 2014; Shahidi & Ambigaipalan, 2015).

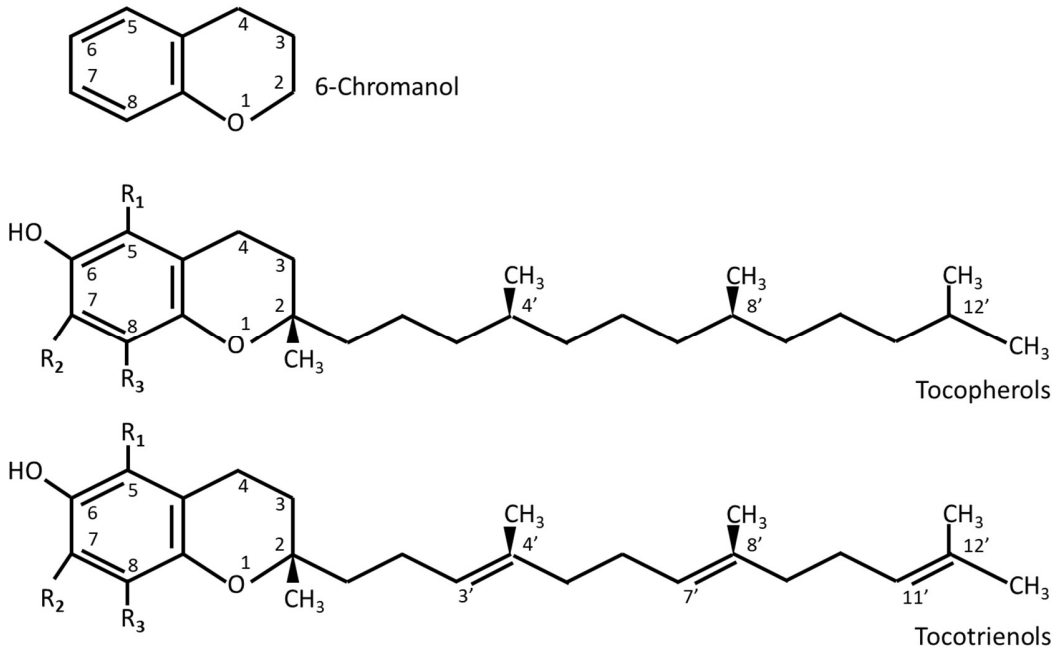

Vitamin E compounds	R_1	R_2	R_3
5,7,8-Trimethyl Tocopherol (α-tocopherol) 5,7,8-Trimethyl Tocotrienol (α-tocotrienol)	CH_3	CH_3	CH_3
7,8-Dimethyl Tocopherol (β-tocopherol) 7,8-Dimethyl Tocotrienol (β-tocotrienol)	H	CH_3	CH_3
5,8-Dimethyl Tocopherol (ϒ-tocopherol) 5,8-Dimethyl Tocotrierol (ϒ-tocotrienol)	CH_3	H	CH_3
8-Methyl Tocopherol (δ-tocopherol) 8-Methyl Tocotrienol (δ-tocotrienol)	H	H	CH_3

Figure 1.10. Vitamin E chemical structures (Gliszczynska-Swigło & Oszmianski, 2014; Shahidi & Ambigaipalan, 2015).

The family of tocopherols comprise 4 structure-related phenolic compounds, varying only in the position and number of the methyl group on the aromatic ring. Being α-tocopherol (α-Toc-OH) fully methylated and the most biologically active compound among tocopherols (Burton & Ingold, 1986; Kiokias, Varzakas, & Oreopoulou, 2008). Whereas in the family of tocotrienols contrasted the grade of unsaturation in the side chain at position 3', 7, and 11' (Kiokias et al., 2008; Seppanen, Song, & Saari Csallany, 2010).

α-tocopherol is considered the most effective lipid-soluble chain-breaking antioxidant in biological activities. It is known in metabolism that α-Toc-OH inhibits lipid autoxidation via hydrogen transfer to lipid peroxy radicals. The radical scavenge activity leads the formation of a stable tocopheroxyl radical which further undergo termination reactions to yield nonradical products (Al-Malaika, Ashley, & Issenhuth, 1994). Furthermore, an α-tocopherol radical can be reduced to the original form by ascorbic acid (AscA) (Kiokias et al., 2008; Kojo, 2004; Mukai, Nishimura, & Kikuchi, 1991; Packer, Slater, & Willson, 1979) under the following general mechanism scheme described in equation 1.29 and 1.30.

$$\alpha\text{-Toc-OH} + R^{\cdot} \rightarrow \alpha\text{-Toc-O}^{\cdot} + RH \quad (1.29)$$

$$\alpha\text{-Toc-O}^{\cdot} + \text{AscA-OH} \rightarrow \alpha\text{-Toc-OH} + \text{AscA-O}^{\cdot} \quad (1.30)$$

1.19 Flax

An annual blue flower herb (Linum usitassimum L.) within the family Linaceae (Rubilar, Gutiérrez, Verdugo, Shene, & Sineiro, 2010). The plant seed varies in color from light yellow to brown and is known as Flaxseed or Linseed. Both terms are used interchangeably though, flaxseed is commonly used when consumed by humans whereas linseed is used for industrial applications (Morris, 2007).

Flaxseed is recognized as a functional food, a term defined as a food or food ingredients (either natural or formulated) that provide physiological benefits beyond the traditional

nutrients it contains (Al-Okbi, 2005). Flaxseed is rich in fatty acids such as alpha-linoleic acid, the parent fatty acid of the omega-3 series (ALA, 18:3n-3), and linoleic acid, the parent fatty acid of the omega-6 series (LA, 18:2n-6), in phytochemicals such as lignans (Touré & Xueming, 2010), proteins (content varies from 20 to 30% including arginine, glutamic acid and lysine), dietary fiber, and phenolic compounds such as phenolic acids (ferulic acid, chlorogenic acid, gallic acid and traces of 4-hidroxybenzoic acid), tocopherols, and flavonoids (flavone C- and O- glycosides) (Singh, Mridula, Rehal, & Barnwal, 2011).

1.19.1 Flaxseed Oil

A polyunsaturated oil derived from the seed of the flax plant; it is one of the most unsaturated common oils. Among the total fatty acids content, around 50% corresponds to ALA, 18% to Oleic acid, and 14% to LA (Daun, Barthet, Chornick, & Duguid, 2003) (figure 1.11 represents the chemical structures).

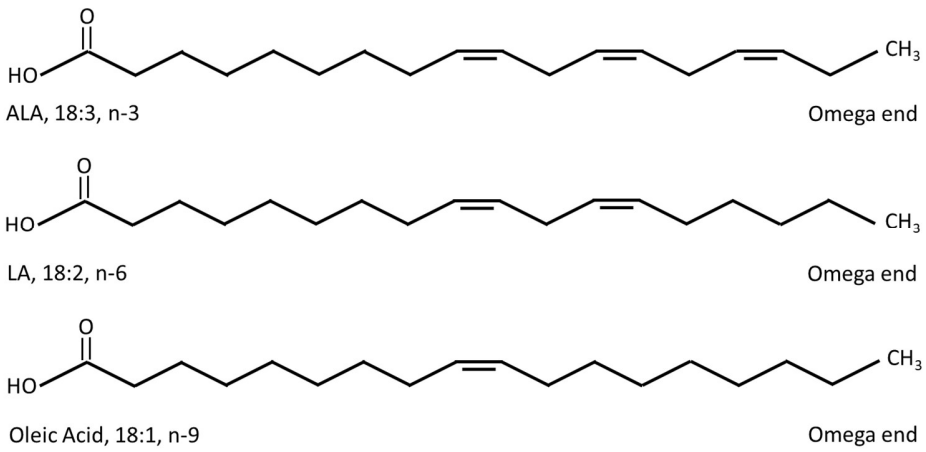

Figure 1.11. Fatty acids structures.

α-Linolenic acid (ALA) undergoes metabolic pathways to produce long chain omega-3 polyunsaturated fatty acids (n-3 PUFA), such as eicosapentaenoic acid (EPA, 20:5n-3),

docosapentaenoic acid (DPA, 22:5n-3), and docosahexaenoic acid (DHA, 22:6n-3) (Li, Attar-Bashi, & Sinclair, 2003; Morris, 2007). A broad research has been done around omega-3 fatty acids: researchers have evaluated the intake of n-3 PUFA during infant development and the relationship in brain and eye development (Carlson & Neuringer, 1999; Gibson, Chen, & Makrides, 2001; Willatts, Forsyth, DiModugno, Varma, & Colvin, 1998); the effect of n-3 PUFA treatment in behavior disorders in adults such as depression (Wani, Bhat, & Ara, 2015), the study of ALA in neurological disorders such as stroke (Blondeau, 2016; Blondeau et al., 2015; Blondeau & Tauskela, 2013), and the incidence of a n-3 PUFFA dietary intake in heart diseases (Ascherio et al., 1996; Willett et al., 2018) and breast cancer (Franceschi et al., 1996; Voorrips et al., 2018) among others.

1.20 Recycling

The increasing global demand on plastic consumption arises the concern of society towards waste disposal and environmental impact. Businesses and governments are incorporating these problems into a sustainable growth, where efficiency is maximized throughout the value chain of goods from production to waste disposals (Sari, Sharika, Bicy, & Thomas, 2016).

Polyolefins are the most used polymer resins where, polyethylene (PE) and polypropylene (PP), account 45% of the global market share (Abdel-Bary, 2003). Starting from 2015, approximately 6500 million metric tons (Mt) of plastic waste had been generated globally. Out of which 9% had been recycled, 12% incinerated, and 79% accumulated in landfills or elsewhere. Based on production forecast and current waste management policies, it is expected that approximately 12000 Mt of plastic waste will be generated by 2050 (Geyer, Jambeck, & Law, 2017).

The food packaging industry plays an important challenge in polymer sustainability in two ways: First, it is a continuous growing business where a higher demand for food consumption leads to a higher demand for a package that protects and preserves the freshness of food content. Secondly, the growth of recycled plastics for food contact

applications is driven by two key parameters: domestic and/or international regulations and the economical behavior of the fossil-fuel industry (i.e. the higher the fossil-fuel price the higher the attractiveness of recycled plastics) (Lally, 2011).

1.21 Regulatory Outline in Food Packaging

Most of the food is sold within a package that provides protection and prolong the shelf life of the food product. Chemical components present in a plastic package such as additives (i.e. antioxidants, stabilizers, slip agents or fillers among others) or any other compound with a molar mass lower than 1000 Da can migrate from the plastic container to the food product and pose a health risk (Cristina Nerin, Vera, & Canellas, 2017). Furthermore, non intentionally added substances (NIAS) such as products derived from a degradation process may also migrate to food and finally expose to a potential health risk (C Nerin, Alfaro, Aznar, & Domeño, 2013).

In light of this information, the food packaging legislation is of major concern and, in a broad sense, regulations are addressed to ensure the safety contact between food and the plastic packaging where, the latter, must be inert and protects the food in the following aspects (Lally, 2011):

- Migration of substance shall not compromise human health,
- Migration cannot lead unacceptable changes in food composition,
- Migration cannot affect organoleptic properties of foodstuff.

1.21.1 US Food Regulations in Post-Consumer Recycled (PCR) materials

In United States, the US Food and Drug Administration (FDA) regulates the use of PCR materials in food-contact articles and points the following safety concerns (Lally, 2011):

1. Contaminants from PCR materials may appear in the final food-contact product made from the recycled material,

2. PCR materials not regulated for food-contact use may be incorporated into food-contact packaging,

3. Additives in the recycled plastic may not comply with the regulations for food-contact use.

FDA issued the *Guidance for Industry – Use of Recycled Plastics in Food Packaging: Chemistry considerations* that assists manufacturers of food packaging in evaluating processes for recycling plastics into food packaging.

1.21.2 European regulations

In 2004, the European Commission established the Regulation: (EC) 1935/2004 (L338/4) for materials and articles intended for food contact. The Framework Regulation sets up general requirements for all food contact materials and states (Lally, 2011):

1. Food contact materials shall be safe,

2. Food contact materials shall not transfer their components into the food in quantities that could endanger human health,

3. Food contact materials cannot change the composition of the food in an unacceptable way or deteriorate the taste and odor of foodstuffs.

In 2008, European regulation on recycled plastic materials in contact with foods aligned with the European Food Safety Authority (EFSA). EFSA is now the foundation of Europe risk

assessment regarding food and feed safety and most of the national entities serve as adjunct committees (Lally, 2011).

Commission Regulation (EC) No. 282/2008 applies to recycled plastic materials and articles intended for food contact including PCR plastics. States that recycled plastics must be obtained from an EC authorized process.

1.22 Recycling operations

Conceptually, recycling is the process where waste is converted into an end-product. Recycling technologies of polymers are divided as follows:

1. Primary Recycling or Re-extrusion. A simple and economical process to recycle. The industrial scrap is re-processed in-plant during the manufacture of food-contact materials where, controlled history scrap of a single type resin, is cleaned, uncontaminated, and is not expected to pose a hazard to the consumer (Sari et al., 2016).

2. Secondary Recycling or Physical Reprocessing. Processes involving grinding, melting, and shaping plastic packaging material. Plastics must be separated by color or resin type as well as effectively washed to remove contaminants before melting. In some cases, the reprocessed material may be blended with virgin polymer. According to regulations, processors must be capable to demonstrate that contaminant levels in the PCR material have been reduced to ensure safety in its end-use. Furthermore, in the case that processors utilize stabilizers, processing aids, and other additives in the recycled polymer, the type and total amount of these additives must comply with existing authorizations and ensure that any additional additive in the plastic may not react during the recycling process to form substances whose safety has not been evaluated by regulatory agencies.

3. Tertiary Recycling or Chemical. Chemical processes (may involve depolymerization) where polymers are converted into their constitutive monomers. Resulting products are used for petrochemical or plastic production.

4. Quaternary. Utilizes the energy (gas) of plastic waste generated by a Pyrolysis process. Important applications are electricity generation, gas engine, and heating generation (Sari et al., 2016).

Primary recycling is defined as a closed loop cycle, where reclaim material can be reground and re-processed as many times as the main properties of the end-use product are not compromised. Experiments can be performed along with specific characterization methods to assess the effect of cycles on properties (i.e. closed loop cycle with regrind only and blending with virgin material for a single product component).

Physical reprocessing is the most used recycling method for post-consumer plastics (Goodship, 2007; Pfaendner, 2015). Important considerations must be addressed since the original polymer properties can vary due to the presence of contaminants and the exposure to thermal, mechanical or shear, oxidative, and photochemical degradation processes. Figure 1.12 depicts the process flow in recycled materials (Primary and Secondary processes).

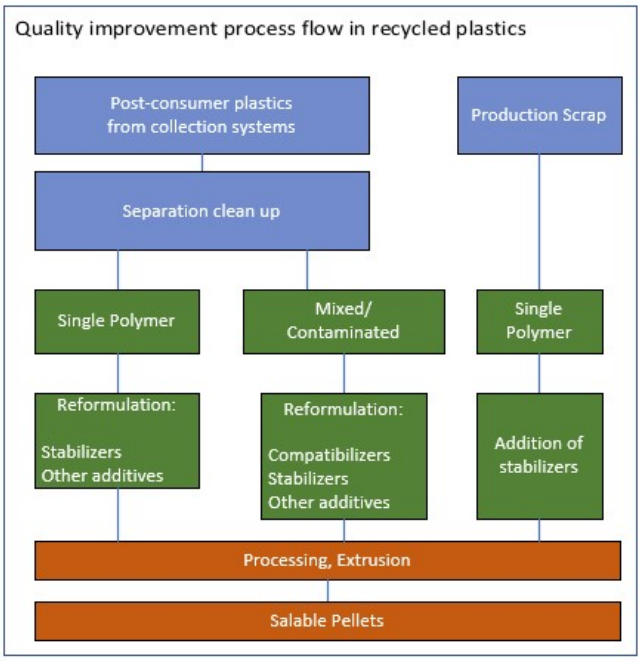

Figure 1.12. Quality assessment layout (Pfaendner, 2015).

The repeated operation cycles in polymer recycling undergo thermo-mechanical and thermo-oxidative degradation along with periods of aging thus, the importance to assess the polymer end-use performance throughout the life-cycle. Polypropylene follows a β scission degradation mechanism whereas Polyethylene, undergoes simultaneously competitive reactions: chain scission and chain branching, leading to crosslinking (Dostál, Kašpárková, Zatloukal, Muras, & Šimek, 2008; Goodship, 2007). Furthermore, authors have evaluated the effect of reprocessing in polyolefins (Jin, Gonzalez-Gutierrez, Oblak, Zupančič, & Emri, 2012; Luzuriaga, Kovářová, & Fortelný, 2006; Teteris, 1999) and the effect of stabilizers in PCR materials against degradation (Boldizar, Jansson, Gevert, & Möller, 2000; Kartalis, Papaspyrides, & Pfaendner, 2000; Martins & De Paoli, 2001, 2002).

Bibliography

Abdel-Bary, E. M. (2003). Recycling of Plastic Waste. In E. M. Abdel-Bary (Ed.), *Handbook of Plastic Films* (pp. 357–380). Rapra Technology Limited.

Al-Okbi, S. Y. (2005). Highlights on Functional Foods, with Special Reference to Flaxseed. *Journal of Natural Fibers*, *2*(3), 63–68. https://doi.org/10.1300/J395v02n03

Al-Malaika, S., Ashley, H., & Issenhuth, S. (1994). The antioxidant role of α-tocopherol in polymers. I. The nature of transformation products of α-tocopherol formed during melt processing of LDPE. *Journal of Polymer Science Part A: Polymer Chemistry*, *32*(16), 3099–3113. https://doi.org/10.1002/pola.1994.080321610

Ascherio, A., Rimm, E. B., Giovannucci, E. L., Spiegelman, D., Stampfer, M., & Willett, W. C. (1996). Dietary fat and risk of coronary heart disease in men: cohort follow up study in the United States. *BMJ*, *313*(7049), 84–90. https://doi.org/10.1136/bmj.313.7049.84

Becker, R. F., Burton, L. P. J., & Amos, S. E. (1996). Additives. In E. P. Moore (Ed.), *Polypropylene Handbook: Polymerization, Characterization, Properties, Processing, Applications* (pp. 177–210). Hanser Publishers.

Bennette, L., Logan, A., Shiferaw-Terefe, N., Singh, T., & Robin, W. (2014). Measuring the Oxidation Potential in Foods. In G. Bartosz (Ed.), *Food Oxidants and Antioxidants Chemical, Biological, and Functional Properties* (pp. 47–79). CRC Press.

Beyler, C. L., & Hirschler, M. M. (2002). Thermal Decomposition of Polymers. In P. J. DiNenno, D. Drysdale, C. L. Bayler, D. W. Walton, R. L. P. Custer, J. R. Hall, & J. M. Watts (Eds.), *SFPE Handbook of Fire Protection Engineering* (3rd ed., pp. 110–131). National Fire Protection Association. https://doi.org/10.1021/cm200949v

Blondeau, N. (2016). The nutraceutical potential of omega-3 alpha-linolenic acid in reducing the consequences of stroke. *Biochimie*, *120*, 49–55. https://doi.org/10.1016/j.biochi.2015.06.005Review

Blondeau, N., Lipsky, R. H., Bourourou, M., Duncan, M. W., Gorelick, P. B., & Marini, A. M. (2015). Alpha-Linolenic Acid: An Omega-3 Fatty Acid with Neuroprotective Properties—Ready for Use in the Stroke Clinic? *BioMed Research International*, *2015*(Figure 1), 1–8. https://doi.org/10.1155/2015/519830

Blondeau, N., & Tauskela, J. S. (2013). New Future in Brain Preconditioning Based on Nutraceuticals: A Focus on alpha-Linolenic Omega-3 Fatty Acid for Stroke Protection. In J. M. Gidday, M. A. Perez-Pinzon, & J. H. Zhang (Eds.), *Innate Tolerance in the CNS. Translational Neuroprotection by Pre- and Post-Conditioning.* (pp. 133–163). Springer.

Boldizar, A., Jansson, A., Gevert, T., & Möller, K. (2000). Simulated recycling of post-consumer high density polyethylene material. *Polymer Degradation and Stability*, *68*(3), 317–319. https://doi.org/10.1016/S0141-3910(00)00012-4

Brewer, M. S. (2011). Natural Antioxidants: Sources, Compounds, Mechanisms of Action, and Potential Applications. *Comprehensive Reviews in Food Science and Food Safety*, *10*(4), 221–247. https://doi.org/10.1111/j.1541-4337.2011.00156.x

Burton, G. W., & Ingold, K. U. (1986). Vitamin E: Application. *Acc .Chem. Res.*, *19*(7), 194–201.

Carlson, S. E., & Neuringer, M. (1999). Polyunsaturated fatty acid status and neurodevelopment: A summary and critical analysis of the literature. *Lipids*, *34*(2), 171–178. https://doi.org/10.1007/s11745-999-0351-2

Daun, J. K., Barthet, V. J., Chornick, T. L., & Duguid, S. (2003). Structure, Composition, and Variety Development of Flaxseed. In L. U. Thompson & S. C. Cunnane (Eds.), *Flaxseed in Human Nutrition* (2nd ed., pp. 1–40). AOCS Press.

Davey, M. W., Van Montagu, M., Inzé, D., Sanmartin, M., Kanellis, A., Smirnoff, N., … Fletcher, J. (2000). Plant L-ascorbic acid: chemistry, function, metabolism, bioavailability and effects of processing. *Journal of the Science of Food and Agriculture*, *80*(7), 825–860. https://doi.org/10.1002/(SICI)1097-0010(20000515)80:7<825::AID-JSFA598>3.0.CO;2-6

Decker, E. A., Warner, K., Richards, M. P., & Shahidi, F. (2005). Measurment Antioxidant Effectiveness. *Journal of Agricultural and Food Chemistry*, *53*, 4303–4310.

Dostál, J., Kašpárková, V., Zatloukal, M., Muras, J., & Šimek, L. (2008). Influence of the repeated extrusion on the degradation of polyethylene. Structural changes in low density polyethylene. *European Polymer Journal*, *44*(8), 2652–2658. https://doi.org/10.1016/j.eurpolymj.2008.05.028

Franceschi, S., Favero, A., Decarli, A., Negri, E., La Vecchia, C., Ferraroni, M., … Giacosa, A. (1996). Intake of macronutrients and risk of breast cancer. *Lancet*, *347*(9012), 1351–1356. https://doi.org/10.1016/S0140-6736(96)91008-9

Frankel, E. N. (2005). Photooxidation of unsaturated fats. In *Lipid Oxidation* (2nd ed., pp. 50–66). Woodhead Publishing Limited.

Geyer, R., Jambeck, J. R., & Law, K. L. (2017). Production, Use, And Fate Of All Plastics Ever Made. *Science Advances*, *3*(7), 25–29.

Gibson, R. A., Chen, W., & Makrides, M. (2001). Randomized trials with polyunsaturated fatty acid interventions in preterm and term infants: Functional and clinical outcomes. *Lipids*, *36*(9), 873–883. https://doi.org/10.1007/s11745-001-0797-2

Gliszczynska-Swigło, A., & Oszmianski, J. (2014). Antioxidant and Prooxidant Activity of Food Components. In G. Bartosz (Ed.), *Food Oxidants and Antioxidants Chemical, Biological, and Functional Properties* (pp. 375–431). CRC Press.

Gliszczyńska-Świgło, A., & Oszmiański, J. (2014). Antioxidant and Prooxidant Activity of Food Components. In G. Bartosz (Ed.), *Food Oxidants and Antioxidants Chemical, Biological, and Functional Properties* (pp. 375–431). CRC Press.

Goodship, V. (2007). Reprocessing of Thermoplastic Recyclates. In V. Goodship (Ed.), *Introduction to Plastic Recycling* (2nd ed., p. 174). Smithers Rapra Technology Limited.

Gugumus, F. (2002). Physico-chemical aspects of polyethylene processing in an open mixer. *Polymer Degradation and Stability*, *75*(1), 55–71. https://doi.org/10.1016/s0141-3910(01)00204-x

Hinsken, H., Moss, S., Pauquet, J.-R., & Zweifel, H. (1991). Degradation of Polyolefins during Melt Processing. *Polymer Degradation and Stability*, *34*(March 1990), 279–293.

Jin, H., Gonzalez-Gutierrez, J., Oblak, P., Zupančič, B., & Emri, I. (2012). The effect of extensive mechanical recycling on the properties of low density polyethylene. *Polymer Degradation and Stability*, *97*(11), 2262–2272. https://doi.org/10.1016/j.polymdegradstab.2012.07.039

Jomova, K., Lawson, M., & Valko, M. (2014). Mechanisms of Antioxidant Activity. In G. Bartosz (Ed.), *Food Oxidants and Antioxidants Chemical, Biological, and Functional Properties* (pp. 325–342). CRC Press.

Kartalis, C. N., Papaspyrides, C. D., & Pfaendner, R. (2000). Recycling of post-used PE packaging film using the restabilization technique. *Polymer Degradation and Stability*, *70*(2), 189–197. https://doi.org/10.1016/S0141-3910(00)00106-3

Kiokias, S., Varzakas, T., & Oreopoulou, V. (2008). In vitro activity of vitamins, flavonoids, and natural phenolic antioxidants against the oxidative deterioration of oil-based systems. *Critical Reviews in Food Science and Nutrition*, *48*(1), 78–93. https://doi.org/10.1080/10408390601079975

Kojo, S. (2004). Vitamin C: Basic Metabolism and Its Function as an Index of Oxidative Stress. *Current Medicinal Chemistry*, *11*(8), 1041–1064. https://doi.org/10.2174/0929867043455567

Kolakowska, A., & Bartosz, G. (2014). Oxidation on Food Components An Introduction. In G. Bartosz (Ed.), *Food Oxidants and Antioxidants. Chemical, Biological, and Functional Properties* (1st ed., pp. 1–17). CRC Press.

Lally, R. (2011). *Recycled Plastics for Food Contact Applications*. (A. Page, Ed.). Pira International Ltd.

Leopoldini, M., Russo, N., & Toscano, M. (2011). The molecular basis of working mechanism of natural polyphenolic antioxidants. *Food Chemistry*, *125*(2), 288–306. https://doi.org/10.1016/j.foodchem.2010.08.012

Li, D., Attar-Bashi, N., & Sinclair, A. J. (2003). α-Linolenic Acid and Heart Disease. In L. U. Thompson & S. C. Cunnane (Eds.), *Flaxseed in Human Nutrition* (2nd ed., pp. 244–259). AOCS Press.

Luzuriaga, S., Kovářová, J., & Fortelný, I. (2006). Degradation of pre-aged polymers exposed to simulated recycling: Properties and thermal stability. *Polymer Degradation and Stability*, *91*(6), 1226–1232. https://doi.org/10.1016/j.polymdegradstab.2005.09.004

Martins, M. H., & De Paoli, M.-A. (2001). Polypropylene compounding with recycled material I. Statistical response surface analysis. Polymer Degradation and Stability, *71*, 293–298.

Martins, M. H., & De Paoli, M. A. (2002). Polypropylene compounding with post-consumer material: II. Reprocessing. *Polymer Degradation and Stability*, *78*(3), 491–495.

https://doi.org/10.1016/S0141-3910(02)00195-7

Morris, D. H. (2007). *Flax – A Health and Nutrition Primer* (4th ed.). FLAX COUNCIL OF CANADA.

Mukai, K., Nishimura, M., & Kikuchi, S. (1991). Stopped-flow investigation of the reaction of vitamin C with tocopheroxyl radical in aqueous Triton X-100 micellar solutions. The structure-activity relationship of the regeneration reaction of tocopherol by vitamin C. *Journal of Biological Chemistry*, *266*(1), 274–278.

Nenadis, N., & Tsimidou, M. Z. (2010). Assessing the activity of natural food antioxidants. In E. A. Decker, R. J. Elias, & J. D. McClements (Eds.), *Oxidation in Foods and Beverages and Antioxidant Applications. Volume 1: Understanding mechanisms of oxidation and antioxidant activity* (pp. 332–367). Woodhead Publishing Limited.

Nerin, C, Alfaro, P., Aznar, M., & Domeño, C. (2013). The challenge of identifying non-intentionally added substances from food packaging materials : A review. *Analytica Chimica Acta*, *775*, 14–24. https://doi.org/10.1016/j.aca.2013.02.028

Nerin, Cristina, Vera, P., & Canellas, E. (2017). Active and Intelligent Food Packaging. In V. Rai Ravishankar & J. A Bai (Eds.), *Food Safety and Protection* (p. 700). CRC Press.

Nielsen, L. E. (1969). Cross-Linking–Effect on Physical Properties of Polymers. *Journal of Macromolecular Science, Part C: Polymer Reviews*, *3*(1), 69–103.

Nimse, S. B., & Pal, D. (2015). Free radicals, natural antioxidants, and their reaction mechanisms. *RSC Advances*, *5*(35), 27986–28006. https://doi.org/10.1039/c4ra13315c

Packer, J. E., Slater, T. F., & Willson, R. L. (1979). Direct observation of a free radical interaction between vitamin E and vitamin C. *Nature*. https://doi.org/10.1038/278737a0

Peacock, A. J. (2000a). The Chemistry of Polyethylene. In A. J. Peacock (Ed.), *Handbook of Polyethylene: Structures, Properties, and Applications* (pp. 375–414). Marcel Dekker.

Peacock, A. J. (2000b). The Essence of Polyethylene. In A. J. Peacock (Ed.), *Handbook of Polyethylene: Structures, Properties, and Applications* (pp. 1–25). Marcel Dekker.

Pfaendner, R. (2015). Improving the quality of recycled materials. *Kunststoffe International*,

105(12), 41–44.

Pokorný, J. (2001). Antioxidants and food stability. In J. Pokorný, N. Yanishlieva, & M. Gordon (Eds.), *Antioxidants in Food. Practical Applications* (pp. 7–84). Woodhead Publishing Limited.

Porter, W. L. (1993). Paradoxical behavior of antioxidants in food and biological systems. *Toxicology and Industrial Health*, *9*(1–2), 93–122.

Pospíšil, J. (1988). Mechanistic Action of Phenolic antioxidants in Polymers-A review. *Polymer Degradation and Stability*, *20*(3–4), 181–202. https://doi.org/10.1016/0141-3910(88)90069-9

Rubilar, M., Gutiérrez, C., Verdugo, M., Shene, C., & Sineiro, J. (2010). Flaxseed As a Source of Functional Ingredients. *Journal of Soil Science and Plant Nutrition*, *10*(3), 373–377. https://doi.org/10.4067/S0718-95162010000100010

Sari, P. S., Sharika, T., Bicy, K., & Thomas, S. (2016). Recycling of Polyolefin Materials. In M. A.-A. AlMa'adeed (Ed.), *Polyolefin Compounds and Materials. Fundamentals and Industrial Applications.* (pp. 315–339). Springer.

Seppanen, C. M., Song, Q., & Saari Csallany, A. (2010). The antioxidant functions of tocopherol and tocotrienol homologues in oils, fats, and food systems. *JAOCS, Journal of the American Oil Chemists' Society*, *87*(5), 469–481. https://doi.org/10.1007/s11746-009-1526-9

Shahidi, F., & Ambigaipalan, P. (2015). Phenolics and polyphenolics in foods, beverages and spices: Antioxidant activity and health effects - A review. *Journal of Functional Foods*, *18*, 820–897. https://doi.org/10.1016/j.jff.2015.06.018

Shibryaeva, L. (2012). *Thermal Oxidation of Polypropylene and Modified Polypropylene – Structure Effects*. INTECH Open access.

Shingai, Y., Fujimoto, A., Nakamura, M., & Masuda, T. (2011). Structure and Function of the Oxidation Products of Polyphenols and Identification of Potent Lipoxygenase Inhibitors from fe-Catalyzed Oxidation of Resveratrol. *Journal of Agricultural and Food Chemistry*, *59*(15), 8180–8186. https://doi.org/10.1021/jf202561p

Singh, K. K., Mridula, D., Rehal, J., & Barnwal, P. (2011). Flaxseed: A potential source of food, feed and fiber. *Critical Reviews in Food Science and Nutrition*, *51*(3), 210–222.

https://doi.org/10.1080/10408390903537241

Skibsted, L. H. (2010a). Understanding oxidation processes in foods. In E. A. Decker, R. J. Elias, & J. G. McClements (Eds.), *Oxidation in foods and beverages and antioxidant applications Volume 1: Understanding mechanisms of oxidation and antioxidant activity* (pp. 3–35). Woodhead Publishing Limited.

Skibsted, L. H. (2010b). Understanding oxidation processes in foods. In E. A. Decker, R. J. Elias, & J. D. McClements (Eds.), *Oxidation in foods and beverages and antioxidant applications Volume 1: Understanding mechanisms of oxidation and antioxidant activity* (pp. 3–35). Woodhead Publishing Limited.

Tadmor, Z., & Gogos, C. G. (2006). *Principles of Polymer Processing*. (2, Ed.). WILEY.

Teteris, G. (1999). Degradation of polyolefines during various recovery processes. *Macromolecular Symposia*, *144*, 471–479. https://doi.org/10.1002/masy.19991440143

Touré, A., & Xueming, X. (2010). Flaxseed lignans: Source, biosynthesis, metabolism, antioxidant activity, Bio-active components, and health benefits. *Comprehensive Reviews in Food Science and Food Safety*, *9*(3), 261–269. https://doi.org/10.1111/j.1541-4337.2009.00105.x

Vercellotti, J. R., St. Angelo, A. J., & Spanier, A. M. (1992). Lipid Oxidation in Foods. An Overview. In A. J. St. Angelo (Ed.), *Lipid Oxidation in Food* (pp. 1–11). ACS Symposium Series.

Vermerris, W., & Nicholson, R. (2008). Families of Phenolic Compounds and Means of Classification. In *Phenolic Compound Biochemistry* (pp. 1–34). Springer.

Voorrips, L. E., Brants, H. A., Kardinaal, A. F., Hiddink, G. J., van den Brandt, P. A., & Goldbohm, R. A. (2018). Intake of conjugated linoleic acid, fat, and other fatty acids in relation to postmenopausal breast cancer: the Netherlands Cohort Study on Diet and Cancer. *The American Journal of Clinical Nutrition*, *76*(4), 873–882. https://doi.org/10.1093/ajcn/76.4.873

Wani, A. L., Bhat, S. A., & Ara, A. (2015). Integrative Medicine Research Omega-3 fatty acids and the treatment of depression: a review of scientific evidence. *Integrative Medicine Research*, *4*(2), 132–141. https://doi.org/10.1016/j.imr.2015.07.003

Washko, P. W., Welch, R. W., Dhariwal, K. R., Wang, Y., & Levine, M. (2004). Ascorbic acid

and dehydroascorbic acid analyses in biological samples. *Analytical Biochemistry*, *204*(1), 1–14. https://doi.org/10.1016/0003-2697(92)90131-p

Willatts, P., Forsyth, J. S., DiModugno, M. K., Varma, S., & Colvin, M. (1998). Influence of long-chain polyunsaturated fatty acids on infant cognitive function. *Lipids*, *33*(10), 973–980. https://doi.org/10.1007/s11745-998-0294-7

Willett, W. C., Manson, J. E., Stampfer, M. J., Hennekens, C. H., Colditz, G. A., Wolk, A., … Hu, F. B. (2018). Dietary intake of Alpha-linolenic acid and risk of fatal ischemic heart disease among women. *The American Journal of Clinical Nutrition*, *69*(5), 890–897. https://doi.org/10.1093/ajcn/69.5.890

Wilson, J. X. (2002). The physiological role of dehydroascorbic acid. *FEBS Letters*, *527*(1–3), 5–9. https://doi.org/10.1016/S0014-5793(02)03167-8

Wypych, G. (2015). Mechanisms of UV Stabilization. In *Handbook of UV Degradation and Stabilization* (2nd ed., p. 419). ChemTec Publishing.

CHAPTER II

ANTIOXIDANTS

2.1 Introduction

In previous chapter it was emphasized the importance of antioxidants and its role to suppress food degradation and to provide thermal stability to polymers acting as radical scavengers.

The aim of this chapter is to address the need of standardizing an analytical protocol to assess the antioxidant capacity of natural molecules such as ascorbic acid, α-tocopherol, gallic acid, quercetin, rosmarinic acid, and trolox.

Foodstuff is also a potential source of antioxidants such as flavonoids (flavonols, flavones, flavanones, and flavan-3-ols), proanthocyanidin, and isoflavone (Bhagwat & Haytowitz, 2015; Haytowitz, Wu, & Bhagwat, 2018b, 2018a). In light of this information, a biological source is included to assess the effect of a real sample preparation on the antioxidant capacity determination. For this, a design of experiments was proposed to validate the best practices for a fresh sample preparation validated by standardized antioxidant capacity assays.

The need to frame a methodology and standardize the analytical method is of importance for future work and comparison analysis. Several research groups use different protocols and nomenclatures to estimate the antioxidant capacity of specific molecules or foodstuff such as antioxidant power, antioxidant potential, or antioxidant performance among others (Sun, Yang, & Tsao, 2018). This chapter proposes a structured methodology and analysis to assess the antioxidant capacity of antioxidant molecules and foodstuff for potential incorporation into a polymer matrix for food packaging applications.

Selected samples were assessed by UV/Visible spectrophotometric analysis to evaluate the antioxidant capacity against two synthetic radicals and one biological radical source and evaluate their potential incorporation as additives into un-stabilized isotactic polypropylene (i-PP) and un-stabilized low-density polyethylene (LDPE). The methodology proposed is

presented in the fishbone diagram shown in Figure 2.1. Thus, the robustness of the analysis will corroborate the test-method standardization.

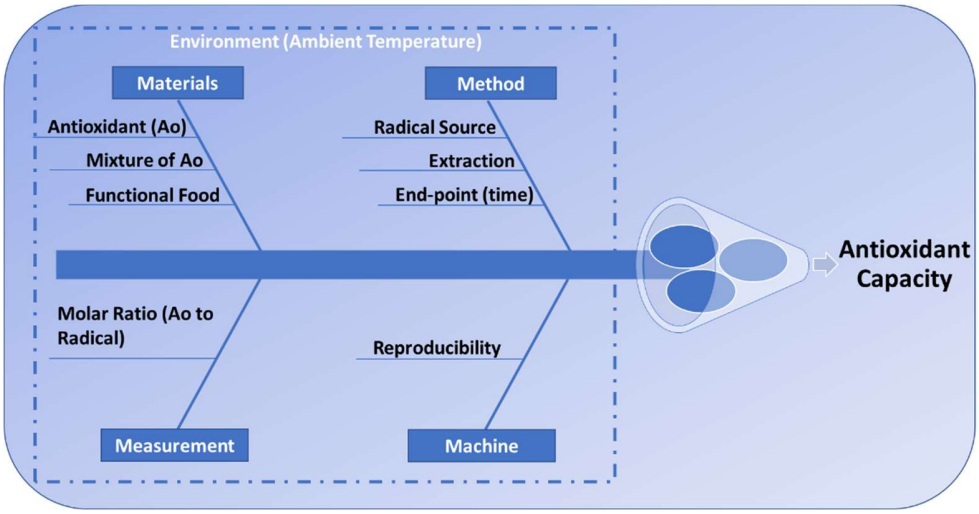

Figure 2.1. 6M Methodology to evaluate the effect of different factors on the antioxidant capacity determination.

2.2 Specific Objectives

- To assess the antioxidant capacity of natural molecules and extracts by spectrophotometric analysis: $DPPH^{\bullet}$, $ABTS^{\bullet+}$, and Superoxide anion test-methods.

2.3 Radical Scavenging Assays

Antioxidant capacity assays, followed by UV/ Visible spectrophotometry, measure the scavenging activity of an antioxidant system against free radicals. The chemical reaction involves two mechanisms: single electron transfer reaction (SET) and hydrogen atom transfer reaction (HAT), which both may occur in parallel. Table 2.1 depicts the main experimental conditions of the test-methods.

DPPH$^{\cdot}$				
λ [nm]	**t [min]**	**R$^{\cdot}$ [μM]$_{Final}$**	**Solvent**	**References**
517	30	20	Methanol	a
515	60	22.5	Methanol	b
517	20 and 60	50	Ethanol	c
516	60	~59	Methanol	d
515	5 up to 90	80	Methanol	e
517	30	100	Ethanol	f
517	30	250	Methanol	g
517	30	250	Methanol	h
ABTS$^{\cdot+}$				
λ [nm]	**t [min]**	**R$^{\cdot}$ [μM]$_{Final}$**	**Solvent-pH**	**References**
744	60	~42	Methanol	i
734	1, 4, and 6	Abs 0.7	Semi-aqueous, pH 7.4	j
734	6	Abs 0.7	0.01M PBS, pH 7.4	k
734	10	Abs 0.65	0.1M PBS, pH 7.4	l
734	10	Abs 0.65	0.01M PBS, pH 7.4	m
734	6	Abs 0.35-0.4	0.1M PBS, pH 7.4	n
Super Oxide Anion assay $O_2^{\cdot-}$ (SOA)				
λ [nm]	**t [min]**	**Catalyst**	**Solvent-pH**	**References**
560	20	0.05 U/mL	0.05M PPB, pH 7.4	o
560	10	0.07 U/mL	0.1M PB, pH 7.8	p
560	20	0.049 U/mL	0.1M PB, pH 8	q
295	10	0.04 U/mL	0.1M PB, pH 7.8	r
292	kinetic	0.024 U/mL	0.05 PB, pH 7.4	s
560	20	0.049 U/mL	0.1M PB, pH 8	t

Table 2.1. Antioxidant Capacity assays. λ: wavelength; t: end-point in time; R$^{\cdot}$: radical; PBS: Potassium phosphate saline; PPB: Potassium phosphate buffer; PB: Phosphate buffer. **a** (Chien, Sheu, Huang, & Su, 2007) **b** (Bozin, Mimica-Dukic, Simin, & Anackov, 2004) **c** (Skaltsa, Hadjipavlou-Litina, Fleischer, Karioti, & Mensah, 2004) **d** (Olszowy & Dawidowicz, 2018) **e** (Eklund et al., 2005) **f** (TAKAYANAGI, KANO, HARADA, ISHIKAWA, & MAKINO, 2005) **g** (Kim et al., 2004) **h** (Digrak, Yildirim, Mavi, Alma, & Hirata, 2003) **i** (Olszowy & Dawidowicz, 2018) **j** (Re et al., 1999) **k** (Chien et al., 2007) **l** (Chun, Kim, & Lee, 2003) **m** (Floegel, Kim, Chung, Koo, & Chun, 2011) **n** (Van Den Berg, Haenen, Van Den Berg, & Bast, 1999) **o** (Chun et al., 2003) **p** (Robak & Gryglewski, 1988) **q** (Lu & Yeap Foo, 2000) **r** (Montoro, Braca, Pizza, & De Tommasi, 2005) **s** (Russo, Longo, & Vanella, 2002) **t** (Lu & Foo, 2001)

As observed in Table 2.1 research groups utilized different test-conditions to assess antioxidant capacity under the same analytical method. Though these assays are well known and reproducible it is necessary to standardize a methodology and build reproducible results that can be further exploited and compared. Variables such as kinetic end-point, radical concentration, environmental conditions, and standard references such as trolox and ascorbic acid were assessed to monitor the antioxidant activity of molecules and real samples.

The standardization of an analytical method ensures product reliability and safety, in the case of antioxidant capacity determination, the nutraceutical industry demands agreement on standards for quantities and units in terms of safety and innovation (Prior, Wu, & Schaich, 2005).

Furthermore, the standardization of a test-method allows: best practices implementation of assays, product commercialization and marketing, and quality assessment and product regulation (regulatory issues by government or regional agencies such as the Federal Drug Administration (FDA) agency and the European Commission (EU) agency) (Prior et al., 2005).

2.4 DPPH$^{\cdot}$ radical

A method developed by Blois in 1958, a stable free radical α, α-diphenyl-β-picrylhydrazyl (DPPH$^{\cdot}$; C18H12N5O6, M = 394.33) soluble in organic solvents commonly used as an indicator for antioxidant chemistry (Hicks, 2010). The odd electron of nitrogen atom in DPPH$^{\cdot}$ has the possibility to accept a hydrogen atom from an antioxidant source and transformed into hydrazine (Kedare & Singh, 2011).

The reaction is monitored spectrophotometrically, upon hydrazyl radical reduction, as a discoloration from violet to light yellow (the hydrazine reduced form). The commonly

accepted absorption band is 520 nm (Yordanov, 1996). The DPPH˙ radical may interact with other radicals in different ratios of antioxidant to DPPH˙ which in turn, the time-response curve deviates from linearity (Kedare & Singh, 2011).

2.4.1 General Mechanism

Briefly, the mechanism represents the scavenging reaction between DPPH˙ and an antioxidant (AH) as illustrated in equation (2.1) (Boly, Lamkami, Lompo, Dubois, & Guissou, 2016).

$$[DPPH^{\cdot}] + [AH] \Leftrightarrow DPPH{-}H + [A^{\cdot}] \quad (2.1)$$

Secondary reactions are present but limited due to the stability of the antioxidant in its radical form. Equation (2.2) and (2.3) depicts the possible reactions (Mishra, Ojha, & Chaudhury, 2012).

$$[DPPH^{\cdot}] + [A^{\cdot}] \rightarrow DPPH - A \quad (2.2)$$

$$[A^{\cdot}] + [A^{\cdot}] \rightarrow A - A \quad (2.3)$$

2.4.2 Materials

2,2-Diphenyl-1-picrylhydrazyl (DPPH˙) was purchased from Sigma-Aldrich (France). Antioxidants tested: ascorbic acid, gallic acid, quercetin, rosmarinic acid, α-tocopherol, and ®-(+)-6-Hydroxy-2,5,7,8-tetramethylchroman-2-carboxylic acid (trolox) were purchased from Sigma-Aldrich (France). Cherries (burlat variety), as a biological source, were supplied from a local market (southeast of France).

2.4.3 Methods

Antioxidant capacity was assessed using a Hewlett Packard 8452A Diode-Array Spectrophotometer and an UV-Vis 2450 Shimadzu for single cuvette analysis (VWR PMMA disposable cuvettes), and a Thermo Scientific Multiskan EX Spectrophotometer adapted for 96-wells microplates.

Several authors refer a strong band width in the region of 515 nm to 517 nm. The followed methodology in the experimental section was performed based on the results of a wavelength scan (250 nm – 800 nm) from a $DPPH^{\cdot}$ radical in solution for single cuvette measurement and considering the specific filters adapted in the Thermo Scientific Multiskan Ex spectrophotometer for microplate measurements.

A 2 mM $DPPH^{\cdot}$ stock solution and 2 mM antioxidant stock solution were daily prepared in ethanol. The solutions were vortexed for 2 minutes at room temperature and sonicated for additional 10 minutes. Test solutions were further diluted in ethanol to represent a percentage of $DPPH^{\cdot}$ scavenged ranging between 20% and 80% approximately. The volume reaction mixture for the assay was 10% v/v antioxidant solution and 90% v/v $DPPH^{\cdot}$ solution.

2.4.4 Results

For comparison analysis between a single-cuvette and multi-channel spectrophotometer system array, an experimental screening for a fixed absorbance value was assessed at different wavelengths based on the individual filters available in the multiskan spectrophotometer: 405 nm, 490 nm, and 560 nm.

A full wavelength scan was performed in the region between 250 nm and 800 nm for a 128 μM $DPPH^{\cdot}$ radical ethanolic solution as shown in Figure 2.2. As reported in literature, it is observed a maximum bandwidth in the region between 515 nm and 520 nm. The radical

concentration was fixed for an absorbance value λ = 490 nm of 1 representing 10% of the incident light.

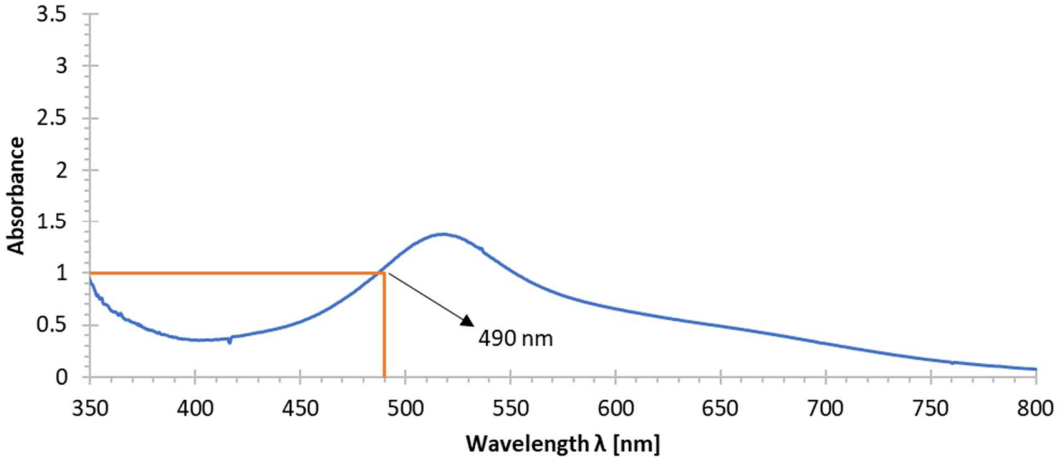

Figure 2.2. UV-VIS Spectrophotometry wavelength scan for a DPPH˙ radical solution.

A DPPH˙ calibration curve was performed considering the absorbance readout specification limits of the spectrophotometer and validating the absorbance value at a wavelength of 490 nm. Figure 2.3 shows the linear domain for the DPPH˙ radical solution.

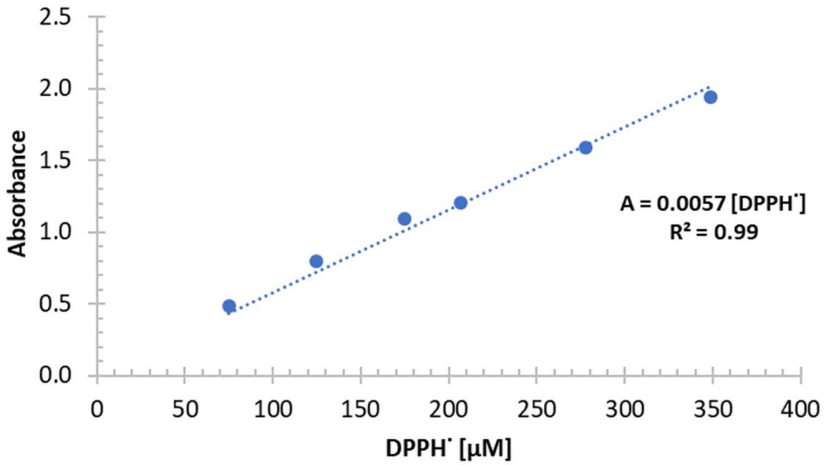

Figure 2.3. DPPH˙ calibration curve.

2.4.4.1 Effect of temperature and incubation time

Antioxidant capacity determination of foodstuff or real samples involves different groups of molecules with antioxidant activity. Thus, for comparison purpose, researchers often express the resultant antioxidant capacity in terms of equivalents of trolox or ascorbic acid, two antioxidants used as standard references (Aruoma, Ramful, Bahorun, Tarnus, & Bourdon, 2011; de Sousa et al., 2011; Floegel et al., 2011; Gil, Tomas-Barberan, Hess-Pierce, Holcroft, & Kader, 2000; Proteggente et al., 2002).

It is reported in literature different end-points in time to represent the EC_{50} defined as the efficient concentration of an antioxidant source (substrate) needed to reduce 50% of a radical activity. Furthermore, the antioxidant activity reaction against $DPPH^{\cdot}$ is reported as fast, medium, and slow while most of the $DPPH^{\cdot}$ assays are carried out at room temperature. Hence, the reaction rate from equation 2.1 must be assessed as a function of time (end-point), temperature, and trolox and ascorbic acid as standard references. Figure 2.4 and Figure 2.5 represent the correlation among the above conditions in the percentage of $DPPH^{\cdot}$ radical reduced.

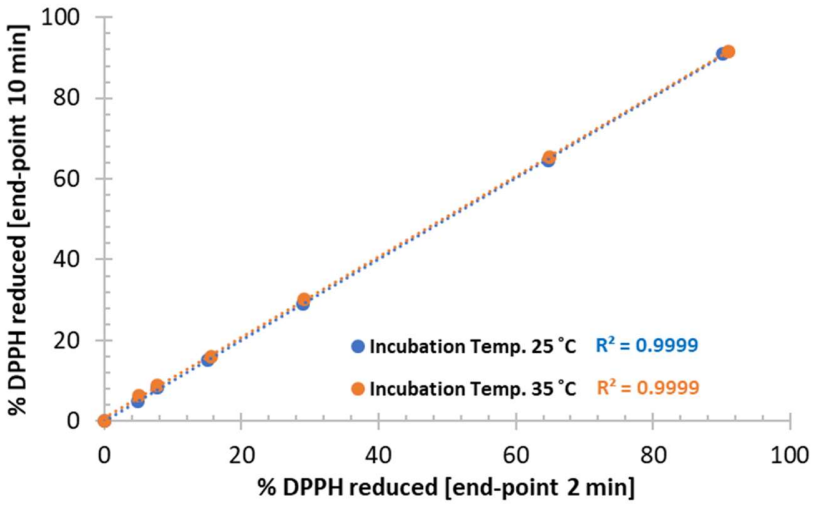

Figure 2.4. Effect of temperature and time on the scavenging activity of trolox.

From Figure 2.4 it is observed no significant difference in the percentage of DPPH˙ reduced of trolox, as the standard reference, within the time interval of 2 and 10 minutes and the incubation temperature of 25°C and 35°C. Table 2.2 represents the EC_{50} value and it is observed no significant difference on EC_{50} and a fast reaction (within 2 minutes).

Antioxidant	End-point [min]	Temp. [°C]	EC_{50} [µM]	r^2
Trolox	2	25	41.29	0.997
	5	25	41.26	0.998
	10	25	41.12	0.998
	2	35	40.98	0.998
	5	35	40.93	0.998
	10	35	40.49	0.998

Table 2.2. Effect of temperature and incubation time on DPPH˙ assay based on EC_{50}.

Figure 2.5 illustrates the resulting percentage of DPPH˙ reduced of ascorbic acid as the antioxidant reference. Experimental conditions evaluated in terms of incubation temperature and time were the same as for the trolox antioxidant system.

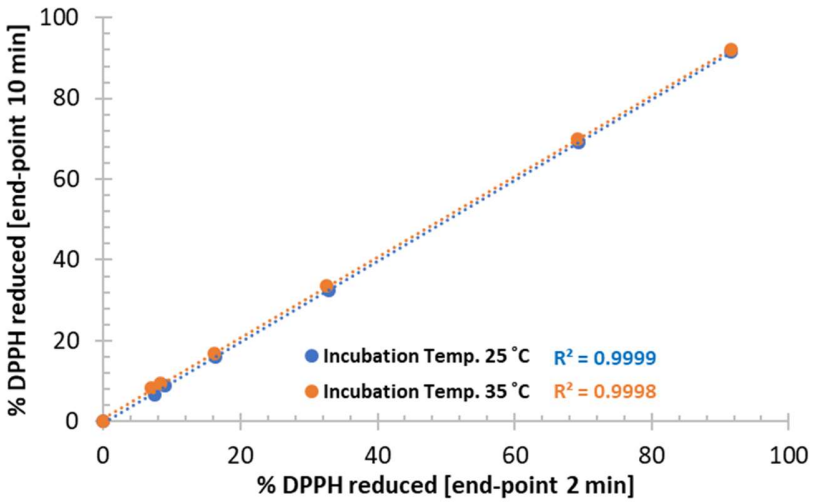

Figure 2.5. Effect of temperature and time on the scavenging activity of Ascorbic acid.

No significant difference in the percentage of DPPH$^{\cdot}$ reduced is observed. Furthermore, Table 2.3 presents the results in terms of EC_{50} value. It is observed a fast reaction rate (within 2 minutes) and no significant difference in EC_{50}.

Antioxidant	End-point [min]	Temp. [°C]	EC_{50} [μM]	r^2
Ascorbic Acid	2	25	40.94	0.993
	5	25	41.01	0.994
	10	25	40.89	0.994
	2	35	40.95	0.994
	5	35	40.94	0.994
	10	35	40.51	0.993

Table 2.3. Effect of temperature and incubation time on DPPH$^{\cdot}$ assay based on EC_{50}.

Both antioxidants presented a fast reaction rate against DPPH$^{\cdot}$ radical. It may be concluded that there is no effect of environmental conditions such as temperature and kinetic point on the antioxidant activity of trolox and ascorbic acid toward DPPH$^{\cdot}$ radical.

Furthermore, Figure 2.6 and Figure 2.7 illustrate a regression analysis for trolox and ascorbic acid on DPPH$^{\cdot}$ assay (trolox r^2 = 0.9947 and ascorbic acid r^2 = 0.9962). The experimental conditions fixed were 25°C and different end-points: 2 min, 5 min, 10 min, and 25 min.

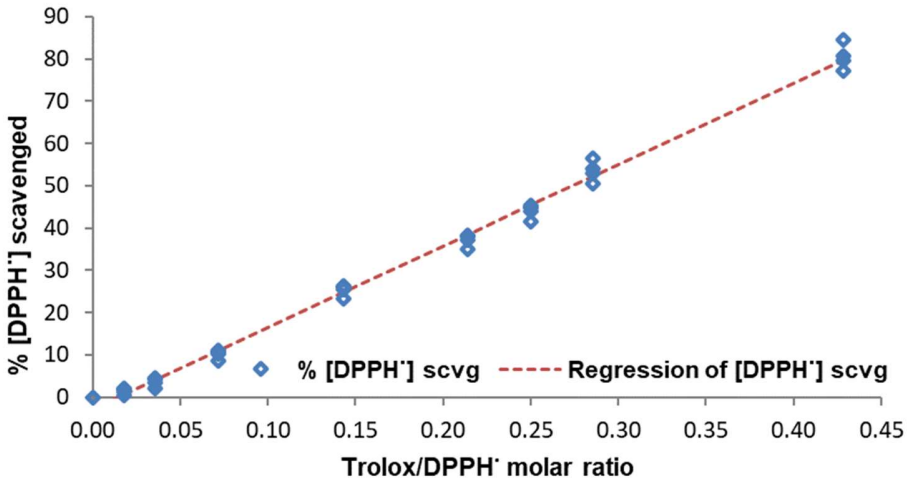

Figure 2.6. Trolox scavenging activity as a function of the molar ratio: Trolox to DPPH˙ radical. Trolox kinetic scavenging activity was monitored spectrophotometrically at a wavelength of 490 nm.

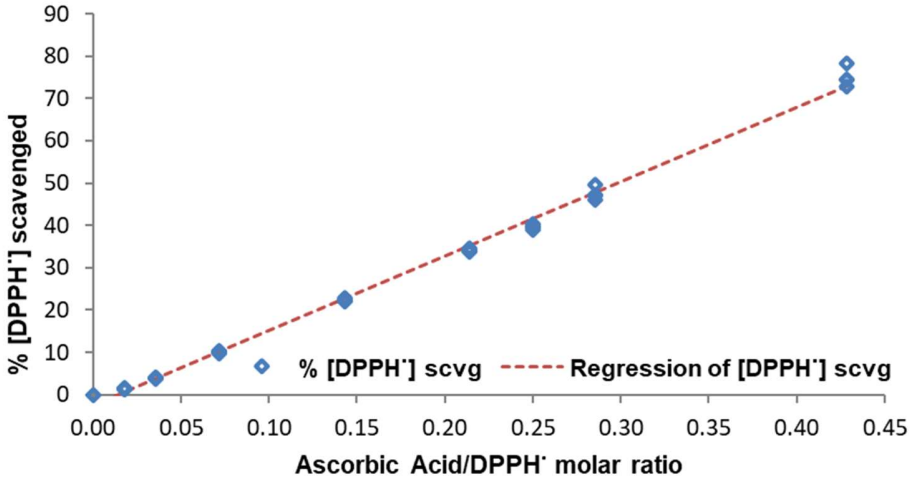

Figure 2.7. Ascorbic acid scavenging activity as a function of the molar ratio: Ascorbic acid to DPPH˙ radical. Ascorbic acid kinetic scavenging activity was monitored spectrophotometrically at a wavelength of 490 nm.

The resulting EC_{50} value for both antioxidants (47.94 μM and 52.14 μM; trolox and ascorbic acid respectively) indicates no significant difference in the scavenging activity of DPPH˙. Hence, under the experimental conditions evaluated, the rate of reaction of either trolox or ascorbic acid may provide a reference value for comparison analysis of antioxidant capacity determination of single molecules and foodstuff.

2.4.4.2 Antioxidant capacity of α-Tocopherol (vitamin E) a comparison with the analog water-soluble Trolox

Vitamin E or α-Tocopherol is a natural antioxidant of industrial importance as a food ingredient, thermal stabilizer for polymers, and odor suppressor (Brody, Strupinsky, & Kline, 2001; Ho, Yam, Young, & Zambetti, 1994; López-Rubio et al., 2004). The main difference in the chemical structure when compared to the analogous water-soluble trolox is the linear side chain present in Vitamin E which provides a lipophilic character.

Figure 2.8 depicts the antioxidant capacity determination for both antioxidants evaluated at ambient temperature (25°C) and 5 minutes as the end-point. Results are expressed as the percentage of DPPH˙ radical scavenged at different antioxidant concentrations.

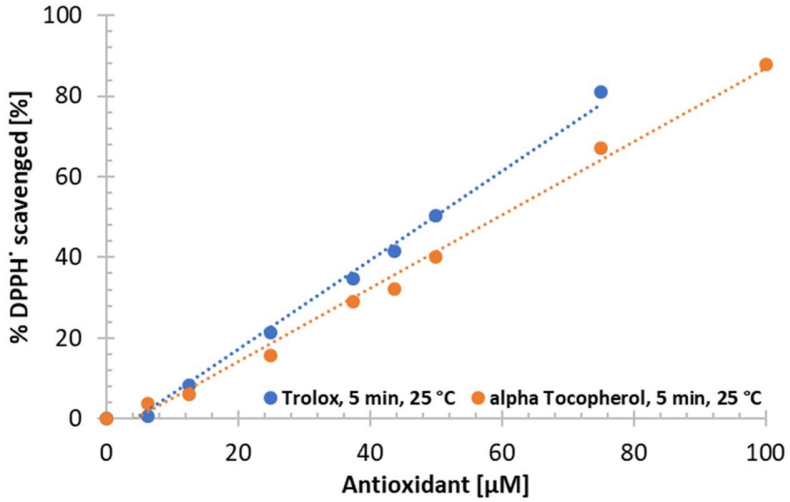

Figure 2.8. Antioxidant activity of trolox and α-tocopherol.

From Figure 2.8 it is observed that trolox presented the steepest slope thus, indicating a faster radical scavenged effect on DPPH˙. Resulting equation 2.4 and equation 2.5 are derived from the linear regression of the individual antioxidants.

$$\% \text{ DPPH}^{\cdot} \text{ scavenged} = 1.1065 \times [\text{Trolox}, \mu M] - 4.8542 \quad (2.4)$$

$$\% \text{ DPPH}^{\cdot} \text{ scavenged} = 0.9083 \times [\alpha\text{-Tocopherol}, \mu M] - 4.0086 \quad (2.5)$$

Table 2.4 shows the EC_{50} values for both antioxidants within an end-point from 2 minutes and 25 minutes.

Antioxidant	End-point [min]	EC_{50} [μM]	r^2
Trolox	2	50.68	0.993
	5	51.51	0.992
	10	49.69	0.992
	25	49.63	0.999
α-Tocopherol	2	61.20	0.994
	5	59.57	0.994
	10	60.47	0.996
	25	60.16	0.996

Table 2.4. Effect of incubation time on DPPH˙ assay based on EC_{50}.

From above results, it is observed a lower EC_{50} value for trolox thus, representing a higher antioxidant capacity against DPPH˙ radical. It is important to remark that, in the case of α-Tocopherol the antioxidant capacity is influenced by the solvent media as observed by K. Mishra (Mishra et al., 2012) who reported different EC_{50} values for methanol and semi-aqueous media (methanol and phosphate buffer). Also, it is important to mention that a new lot of trolox was utilized (Table 2.4) representing a variation from data obtained in Table 2.2 of 50.4 +/- 0.8 and 41 +/- 0.3 respectively.

2.4.4.3 Antioxidant to DPPH˙ radical molar ratio

Expressing the percentage of DPPH˙ radical scavenged as a function of the molar ratio of antioxidant to radical for EC_{50} calculation provides independency on the DPPH˙ final concentration used in the assay (standardization). However, steric effects may affect the real antioxidant capacity in the reduction of the DPPH˙ radical (Nenadis & Tsimidou, 2018).

Other factors such as polarity and the affinity to form hydrogen bonds from the medium, the pH, contaminants present in the solvent, and the structural characteristics of antioxidants may influence the antioxidant capacity (Foti, 2015; Xie & Schaich, 2014). Thus, it is important to evaluate the rate of reaction under different antioxidant to radical concentrations as shown in Figure 2.9.

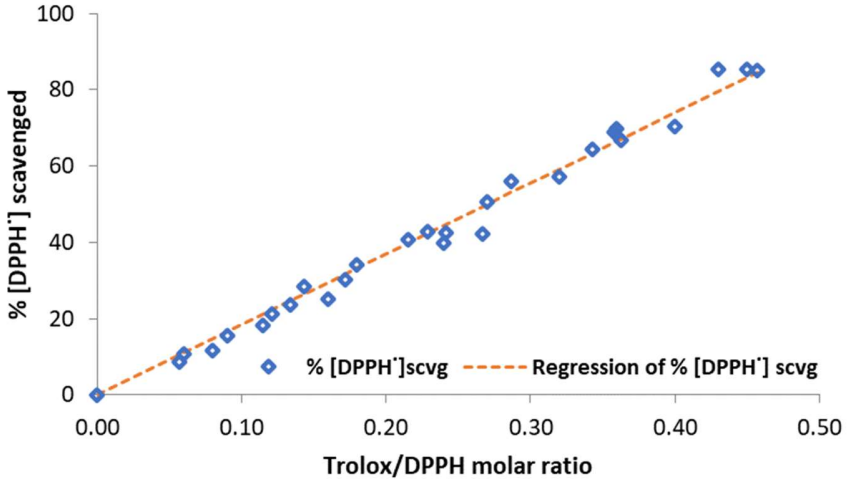

Figure 2.9. Trolox scavenging activity as a function of the molar ratio: Trolox to DPPH˙ radical. Kinetic scavenging activity followed spectrophotometrically at a wavelength of 490 nm and 5 minutes (end-point).

From the kinetic analysis, the resulting EC_{50} value showed no significant difference with respect to the DPPH˙ radical concentration as illustrated in Figure 2.10.

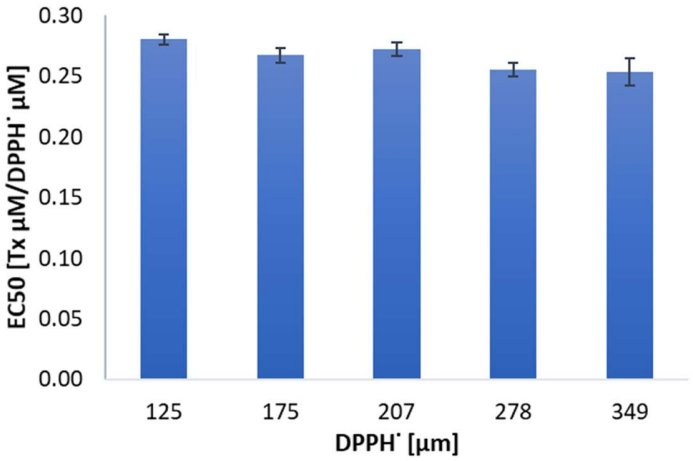

Figure 2.10. EC_{50} values of trolox on DPPH˙ assay at different molar ratios.

Therefore, we may conclude that there is no steric restriction in the scavenging activity of trolox on DPPH˙ radical under the experimental conditions evaluated.

2.4.4.4 Reproducibility

Ascorbic acid was assessed experimentally at two different DPPH˙ radical concentrations. The resulting EC_{50} values shown in Table 2.5 varies as a function of the DPPH˙ radical concentration (175 µM and 200 µM respectively).

Expressing the results as the molar ratio of ascorbic acid to DPPH˙, the EC_{50} value presents no significant difference (0.341 +/- 0.002 and 0.349 +/- 0.002 respectively). Hence, it may represent a via to standardize the test-method.

			EC_{50} [µM]							
Antioxidant	Replicate	DPPH· [µM]	t=2 min	r^2	t= 5 min	r^2	t = 10 min	r^2	t = 20 min	r^2
Ascorbic Acid	1	175	57.51	0.994	57.30	0.995	57.48	0.995	58.25	0.993
	2		57.84	0.993	57.83	0.993	58.26	0.991	58.55	0.990
	3		63.42	0.989	63.35	0.990	63.42	0.989	63.50	0.989
	1	200	75.29	0.993	75.17	0.993	75.26	0.993	76.03	0.992
	2		69.10	0.993	69.35	0.992	69.97	0.991	70.08	0.991
	3		64.04	0.998	63.96	0.997	64.29	0.996	65.15	0.994

Table 2.5. Reproducibility analysis of Ascorbic Acid on DPPH· assay.

2.4.4.5 Antioxidant capacity determination of natural antioxidants

Based on these findings, the antioxidant capacity of 5 selected antioxidants: ascorbic acid, gallic acid, quercetin, rosmarinic acid, α-tocopherol, and trolox were evaluated by DPPH· method. Figure 2.11 presents the kinetic activity by means of the molar ratio of antioxidant to DPPH· radical.

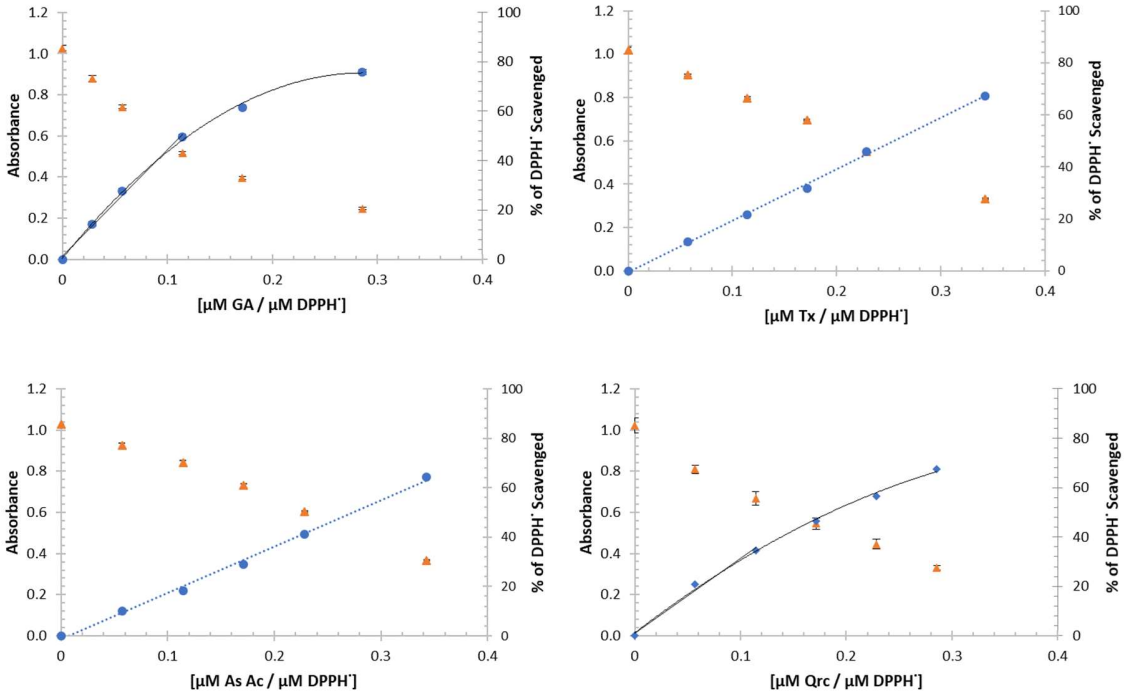

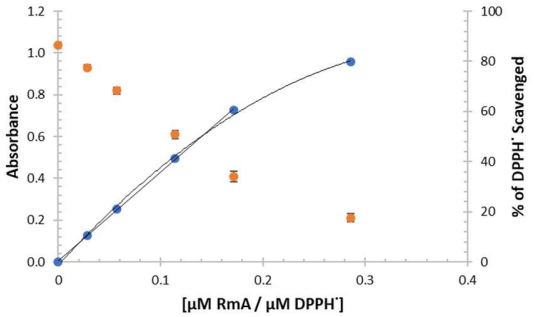

Figure 2.11. DPPH˙ antioxidant activity followed spectrophotometrically at a wavelength of 490 nm and 5 minutes (end-point).

The observed rate of reaction of the radical scavenging mechanism were fast, achieving the EC_{50} value within the endpoint of 5 minutes. Ascorbic acid (As. Ac.) and trolox (Tx), presented a linear kinetic behavior ($r^2 = 0.99$).

Furthermore, in the case of quercetin (Qrc), rosmarinic acid (RmA), and gallic acid (GA) linearity deviated at an initial percentage of DPPH˙ inhibition. Some authors have reported nonlinear kinetic behavior for pure compounds in the antioxidant activity determination (Brand-Williams, Cuvelier, & Berset, 1995).

The resultant EC_{50} value may rank the antioxidants assessed by means of their activity to scavenged the DPPH radical. The ranked order of DPPH˙ scavenging activity is as follows: GA > RmA > Qrc > Tx > As. Ac.

Gallic acid represented the highest DPPH˙ scavenging activity with an EC_{50} value expressed as the molar ratio of antioxidant to DPPH˙ radical of 0.11 (the equivalent in GA concentration of ~20 µM to scavenged 50% of the DPPH˙ radical concentration in solution); followed by RMA and Qrc with calculated EC_{50} values of 0.14 and 0.16 respectively (the equivalent in

antioxidant concentration of 25 μM and 28 μM). Trolox and ascorbic acid showed a similar antioxidant activity toward $DPPH^{\cdot}$ radical with EC_{50} values of 45 μM and 48 μM respectively.

2.5 $ABTS^{\cdot+}$ radical

Initially, the original assay proceeded with the generation of ferryl myoglobin radical from the reaction of metmyoglobin and hydroperoxide (N. J. Miller & Rice-Evans, 1997; N. J. Miller, Rice-Evans, Davies, Gopinathan, & Milner, 1993). The formed radical oxidized the $ABTS^{\cdot+}$ in solution to generate the $ABTS^{\cdot+}$ cation radical.

One major constraint of this method is that, the antioxidant is placed in parallel to the generation of the $ABTS^{\cdot+}$ cation radical, leading a noise in the antioxidant capacity determination since antioxidants may react either via two mechanisms: a scavenging effect over the formed $ABTS^{\cdot+}$ cation radical or a decrease in the rate of $ABTS^{\cdot+}$ cation radical formation (Strljbe, Haenen, Van Den Berg, & Bast, 1997).

A modified method was proposed where the $ABTS^{\cdot+}$ cation radical is formed before the antioxidant capacity test-method using an oxidizing agent i.e. potassium persulfate. Thus, the antioxidant only reacts with the $ABTS^{\cdot+}$ cation radical formed (Re et al., 1999). The reduction of the green-blue $ABTS^{\cdot+}$ radical solution yields a decoloration monitored at various wavelengths such as 645 nm, 734 nm, 815 nm, and 415 nm. $ABTS^{\cdot+}$ assay has the potential of being performed either in a lipophilic or hydrophilic solution media (Prior et al., 2005).

2.5.1 Materials

2,2'-azino-bis (3-ethylbenzothiazoline-6-sulphonic acid) diammonium salt (ABTS) and potassium persulfate (potassium peroxodisulfate), were purchased from Sigma-Aldrich (France). Ethanol and distilled water were of analytical grade.

Antioxidants tested: ascorbic acid, gallic Acid, quercetin, rosmarinic acid, and (R)-(+)-6-hydroxy-2,5,7,8-tetramethylchroman-2-carboxylic acid (trolox) were purchased from Sigma-Aldrich (France) and cherries (burlat variety), as a biological source, were supplied from a local market (southeast of France).

2.5.2 Methods

Antioxidant capacity was assessed using a Hewlett Packard 8452A Diode-Array Spectrophotometer and an UV-Vis 2450 Shimadzu for single cuvette analysis (VWR PMMA disposable cuvettes), and a Thermo Scientific Multiskan EX Spectrophotometer adapted for 96-wells microplates.

The antioxidant activity was evaluated following the method developed by Roberta Re with minor modifications. A 7 mM ABTS solution is prepared in phosphate buffer saline solution (PBS) 0.01 M, pH 7.4 and mixed with a 2.45 mM final concentration of potassium persulfate. The solution is vortexed for 2 minutes at room temperature then sonicated for 10 minutes. Stock solution was kept in dark for 12 hours prior to analysis. The $ABTS^{\bullet+}$ or control was diluted until an absorbance of 0.70 +/- 0.03.

2 mM antioxidants stock solution were daily prepared in distilled water. The solutions were vortexed for 2 minutes at room temperature and sonicated for additional 10 minutes. Test solutions were further diluted in distilled water to represent a percentage of $ABTS^{\bullet+}$ scavenged ranging between 20% and 80% approximately. Absorbance was read at an incubation time (endpoint) of 5 minutes and a wavelength of 405 nm.

2.5.3 Results

ABTS$^{\cdot+}$ radical solution was monitored spectrophotometrically in the wavelength range between 250 nm and 800 nm. A representative absorbance of 0.7 +/- 0.03 was fixed at λ= 405 nm for the experimental runs (Figure 2.12).

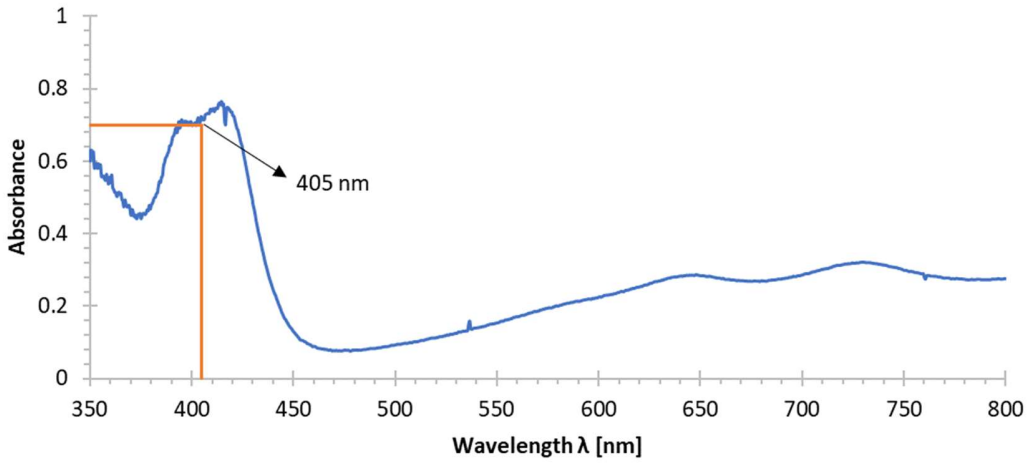

Figure 2.12. UV-VIS Spectrophotometry wavelength scan for an ABTS$^{\cdot+}$ radical solution.

2.5.3.1 Antioxidant capacity determination of natural antioxidants

Figure 2.13 shows the scavenging activity of ascorbic acid, gallic acid, quercetin, rosmarinic acid, α-tocopherol, and trolox toward ABTS$^{\cdot+}$ radical expressed as a molar ratio of antioxidant to ABTS$^{\cdot+}$ radical.

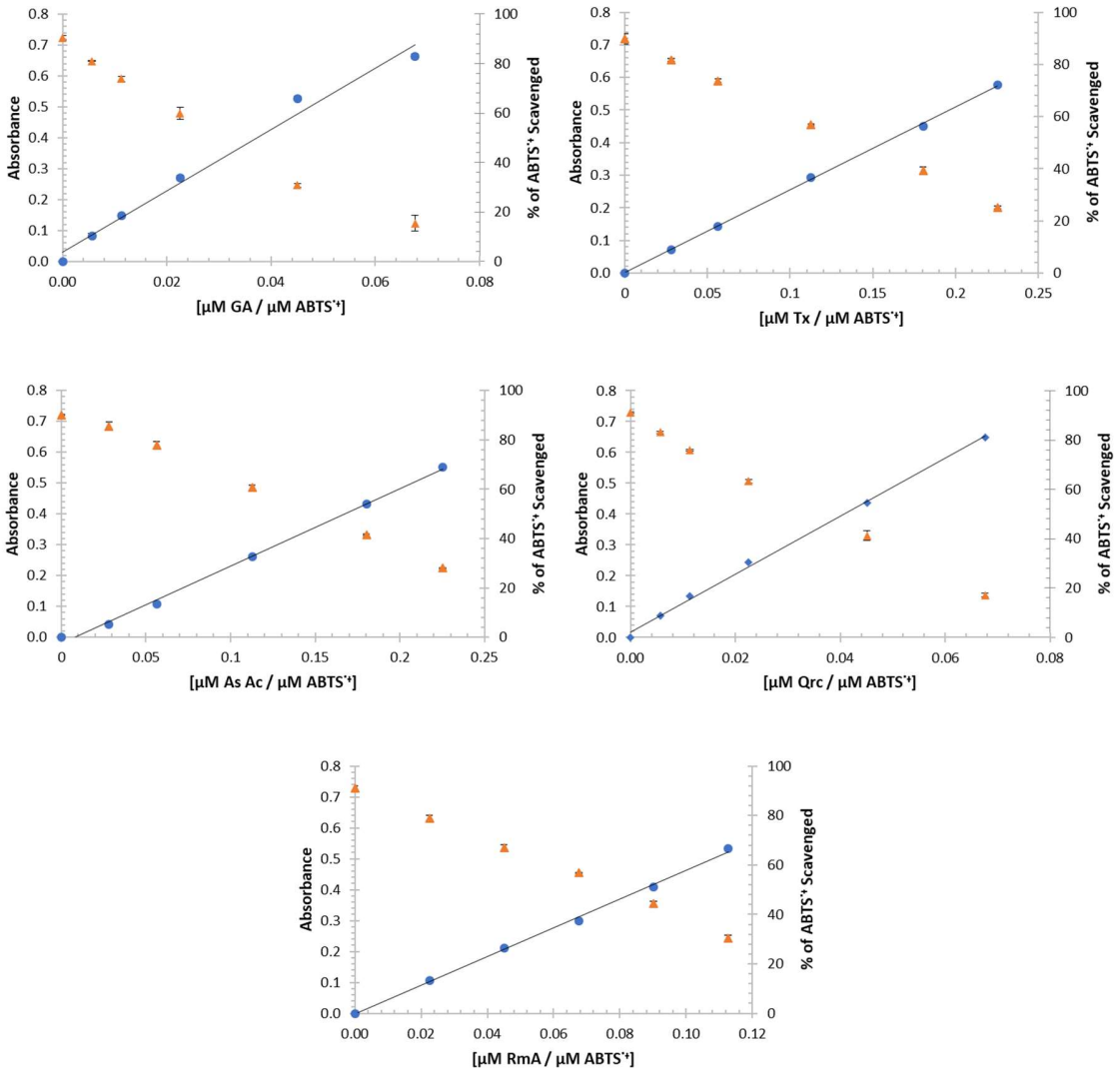

Figure 2.13. $ABTS^{\cdot+}$ antioxidant activity followed spectrophotometrically at a wavelength of 490 nm and 5 minutes (end-point).

All of the antioxidants evaluated experimentally, showed a linear kinetic behavior ($r^2 = 0.99$). The ranked order of $ABTS^{\cdot+}$ scavenging activity is as follows: gallic acid (GA) > quercetin (Qrc) > rosmarinic acid (RmA) > trolox (Tx) > ascorbic acid (As.Ac.).

Gallic acid represented the highest $ABTS^{\cdot+}$ scavenging activity with an EC_{50} value expressed as the molar ratio of antioxidant to $ABTS^{\cdot+}$ radical of 0.037 (the equivalent in GA concentration of ~1.7 μM to scavenged 50% of the $ABTS^{\cdot+}$ radical concentration in solution); followed by Qrc and RmA with calculated EC_{50} values of 0.041 and 0.086 respectively (the equivalent in antioxidant concentration of 1.8 μM and 3.8 μM). Trolox and ascorbic acid showed a similar antioxidant activity toward $ABTS^{\cdot+}$ radical with EC_{50} values of 7 μM and 7.4 μM respectively.

Among the two synthetic radicals evaluated, the $ABTS^{\cdot+}$ method showed a higher sensibility toward the antioxidants assessed. It is observed as an average, a 7.6-fold higher EC_{50} values obtained by $DPPH^{\cdot}$ than those observed in $ABTS^{\cdot+}$ method.

2.6 Super Oxide Anion (SOA) assay

The test-method is founded on the reaction system hypoxanthine (Hx)-xanthine oxidase (XOD), where the XOD enzyme catalyzes the oxidation of hypoxanthine to uric acid. The oxidative hydroxylation generates superoxide radical anions ($O_2^{\cdot-}$) (Kalra, Jena, Tikoo, & Mukhopadhyay, 2007) and hydrogen peroxide (H_2O_2).

This assay involves the presence of nitroblue tetrazolium (NBT) which is reduced in the presence of superoxide radical anions ($O_2^{\cdot-}$) to form formazan blue (F. J. Miller & Griendling, 1994). Antioxidant activity is then measured as a competition between an antioxidant system and NBT to quench superoxide radical anions. The reaction is spectrophotometrically followed at a wavelength of 560 nm (De Gaulejac, Vivas, De Freitas, & Bourgeois, 1999).

2.6.1 General Mechanism

In outline, Hypoxanthine undergoes an enzymatic oxidation in the presence of xanthine oxidase and molecular oxygen. The reaction mechanism involves two steps represented in Figure 2.14 where uric acid is the final product of the degradation pathway (JEŻEWSKA, 1973; P et al., 1998). Additionally, the enzymatic reaction generates superoxide anion radical ($O_2^{\cdot -}$) and hydrogen peroxide (H_2O_2).

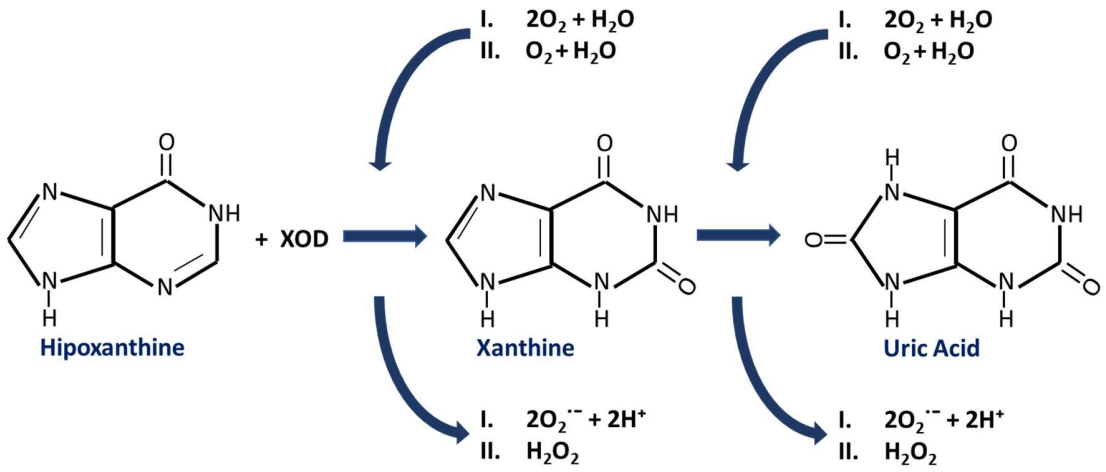

Figure 2.14. Enzymatic oxidation reaction of hypoxanthine.

The presence of a radical scavenger (antioxidant) in the reaction media competes with the NBT reduction reaction by quenching superoxide anion radicals thus, reducing the rate of formazan dye as depicted in Figure 2.15.

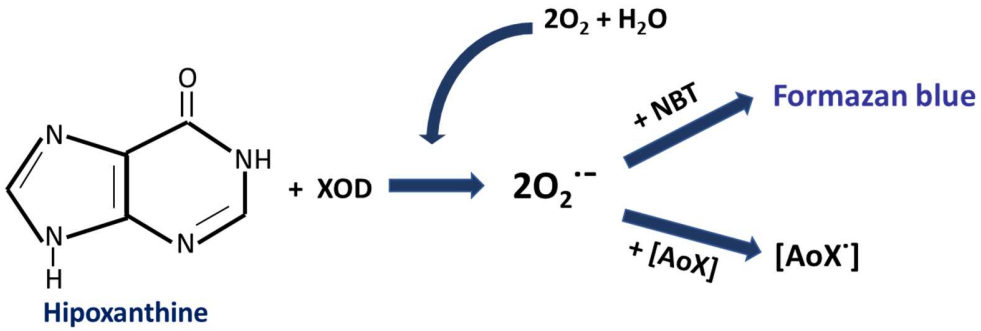

Figure 2.15. Available superoxide radicals. A reduction reaction competition between NBT and an antioxidant system [AoX].

2.6.2 Materials

Xanthine oxidase (XOD), hypoxanthine (Hx), nitroblue tetrazolium (NBT), and hydrogen peroxide solution were purchased from Sigma-Aldrich (France). Antioxidants evaluated: ascorbic acid and ®-(+)-6-hydroxy-2,5,7,8-tetramethylchroman-2-carboxylic acid (trolox) were purchased from Sigma-Aldrich (France).

2.6.3 Methods

The superoxide anion bioassay was produced by a hypoxanthine-xanthine oxidase enzymatic reaction system following the methodology proposed by Saint-Cricq de Gaulejac (De Gaulejac et al., 1999) with modifications. The reaction media consisted of 150 µL of 50 mM potassium phosphate buffer (K-PBS) containing 0.1 mM EDTA (pH 7.5), 25 µL of 50 µM Hx, 25 µL of 75 µM NBT, a 25 µL aliquot for the representative antioxidant sample, and 25 µL of 0.56 U/mL of XOD.

The resulting mixture contained in a final volume assay of 250 µL was followed spectrophotometrically, at room temperature, at λ = 560 nm. Results are expressed as a percentage of inhibition of NBT formazan production. Superoxide radical scavenging was assessed in trolox and ascorbic acid as the standard references.

2.6.4 Antioxidant capacity determination of ascorbic acid and trolox

Figure 2.16 illustrates the percentage of inhibition of NBT Formazan for ascorbic acid and trolox (the water-soluble derivative of vitamin E). The calculated EC_{50} values were 37.42 µM and 177.55 µM respectively. Ascorbic acid showed a higher antioxidant activity against $O_2^{\cdot -}$ radicals than trolox. Furthermore, the antioxidant activity of α-Tocopherol (vitamin E) against $O_2^{\cdot -}$ radicals was lower than trolox (values not shown).

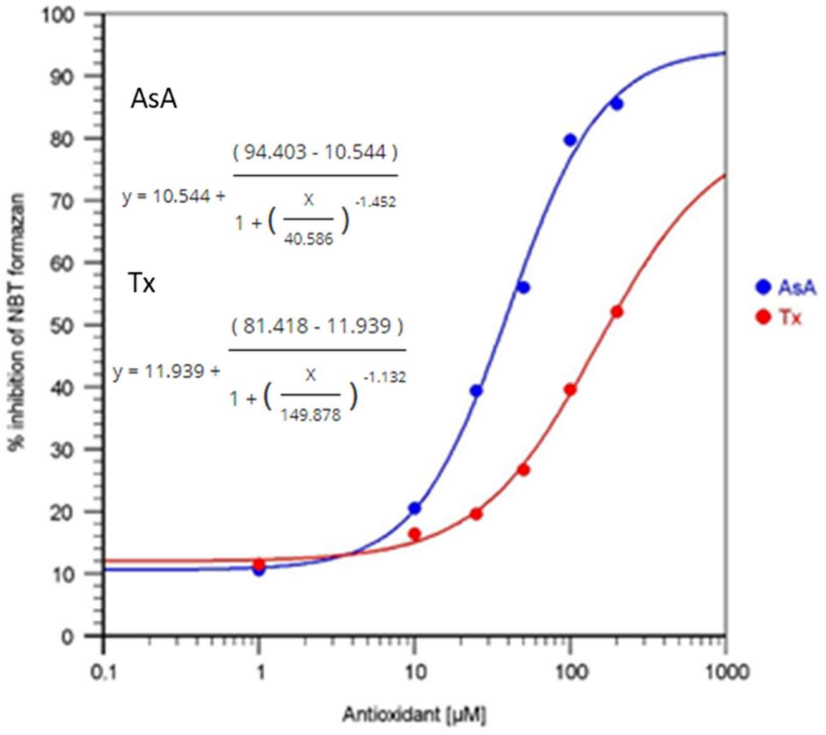

Figure 2.16. Antioxidant activity of ascorbic acid (AsA) and trolox (Tx) against $O_2^{\cdot -}$ radicals (SOA assay).EC_{50} values were calculated using AAT Bioquest, Inc. EC_{50} calculator.

2.6.5 Effect of hydrogen peroxide in the reaction mixture

Hydrogen peroxide is produced during the enzymatic oxidation reaction of hypoxanthine. The radical character of hydrogen peroxides, due to the ability to generate oxygen radical species, was evaluated to determine side reduction reactions on NBT.

The percentage of inhibition of NBT formazan was determined using a 25 μL aliquots of hydrogen peroxide (assessed at two different concentrations in a ten-fold increase) and NBT (under different concentrations) contained in a final volume assay of a 250 μL K-PBS buffer solution.

Reaction mixture was monitored spectrophotometrically at λ = 560 nm and 5 minutes (end-point) with a 24 hours follow-up reading. Table 2.6 illustrates the experimental conditions (individual runs were performed in duplicate).

Experimental run	H_2O_2 [μM]	NBT [μM]
1	5	50
2	5	75
3	5	100
4	50	50
5	50	75
6	50	100

Table 2.6. Experimental conditions of the reaction mixture H_2O_2 and NBT.

2.6.6 Effect of hypoxanthine concentration on the superoxide radical formation

The reaction pathway from hypoxanthine to uric acid yields $O_2^{\cdot -}$. The inhibition of NBT formazan production was followed spectrophotometrically as a function of the concentration of the substrate (Hx).

The reaction media consisted of 175 μL of 50 mM potassium phosphate buffer (K-PBS) containing 25 μL of Hx and 25 μL of NBT. The reaction was initiated with additional 25 μL of 0.56 U/mL of XOD for a total volume assay of 250 μL.

The NBT concentration was kept in excess and in a constant ratio of 2:1 (NBT: Hx). The rate of increase in absorbance followed at λ = 560 nm is representative for the $O_2^{\cdot -}$ formation; individual runs were performed in duplicate. Table 2.7 shows the experimental conditions assessed.

Experimental run	Hx [μM]	NBT [μM]
1	40	80
2	50	100
3	75	150
4	100	200

Table 2.7. Experimental conditions of the reaction mixture Hx and NBT.

2.6.7 Results

Effect of hydrogen peroxide in the reaction mixture

Resulting values of absorbance as shown in table 2.8 indicate no interaction of H_2O_2 with NBT. Hence, only the competition of the reduction reactions from NBT and an antioxidant system on superoxide radicals ($O_2^{\cdot -}$) are assumed. The assay is representative to assess the antioxidant capacity of antioxidant molecules or biological sources.

Experimental run	H_2O_2 [µM]	NBT [µM]	Absorbance	Abs +24 hrs
1	5	50	0.002	-0.001
2	5	75	-0.001	-0.002
3	5	100	-0.002	0.001
4	50	50	0.001	0.001
5	50	75	0.000	0.002
6	50	100	-0.005	0.003

Table 2.8. Effect of hydrogen peroxide (H_2O_2) on NBT followed at λ = 560 nm.

Effect of hypoxanthine concentration on the superoxide radical formation

It is important to validate that the protocol conditions are suitable to assess the effect of an antioxidant system on the inhibition of NBT Formazan. The rapid decoloration from the competitive reduction reaction is followed spectrophotometrically as a decrease in absorbance at λ = 560 nm.

Thus, the delta in absorbance (process window) between the control (NBT Formazan) and the reaction mixture with an antioxidant system must be able to be followed as a function of the reaction time (end-point). Figure 2.17 presents the absorbance values as a function of time at different Hx concentrations.

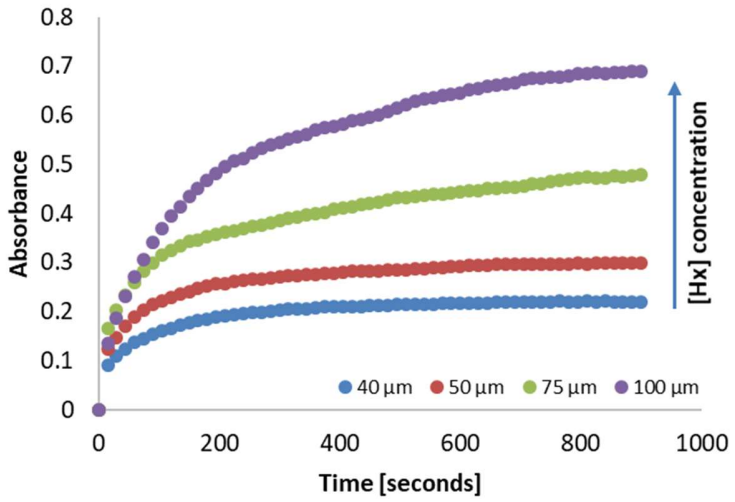

Figure 2.17. Effect of $O_2^{\cdot -}$ radical generation on the reaction mixture Hx and NBT followed at λ= 560 nm.

It was observed within the reaction time t = 1 min that the $O_2^{\cdot -}$ generation is linear (r^2 = 0.99) at the experimental conditions evaluated. A deviation from linearity is observed until a plateau is reached, probably by substrate depletion (Hx at 40 µM and 50 µM).

2.7 Antioxidant capacity determination in foodstuff

Two of the most common synthetic radical antioxidant assays: $DPPH^{\cdot}$ and $ABTS^{\cdot +}$ and superoxide anion assay ($O_2^{\cdot -}$), as a biological radical source, were assessed using UV-VIS spectrophotometry. On the basis of the results presented in this chapter, the standardized antioxidant capacity assays were validated on a biological source.

Fruits and vegetables are rich in natural antioxidant molecules such as phenolic compounds. Fruits such as cherries are rich in bioactive food components such as fiber, polyphenols, carotenoids, vitamin C, and potassium. In addition, anthocyanins are also present (cyanidin-3-glucoside and cyanidine-3-rutinoside) (Kedare & Singh, 2011).

Anthocyanins is a water-soluble antioxidant molecule that forms part of a subgroup of plant constituents known as flavonoids (Bušić, Kovač, Gašo-Sokač, & Lepeduš, 2008) and is of industrial importance not only as an antioxidant source but as a natural pigment (Espín, Soler-Rivas, Wichers, & García-Viguera, 2000).

2.7.1 Extraction Method

The sample preparation during the extraction step was performed following the methodology described by Pérez-Jiménez and Saura Calixto (Pérez & Saura, 2007) with modifications. In outline, the edible part from cherries was grinded and extracted by ultrasound-assisted extraction (UAE) with an aqueous-organic solvent in centrifuge tubes.

Two sequential extraction steps were performed involving solvents with different polarities: first, ethanol/water 50:50 (v/v), pH = 2 (acidified with HCl 2N) and second, acetone/water 70:30 (v/v). Aliquots from the recovered supernatant were directly used in antioxidant capacity assays (Jiménez E., Rincón, Pulido, & Saura C., 2001).

Cacace and Mazza observed that a high solvent to solid ratio leads to lower antioxidant activities (Cacace & Mazza, 2003). Thus, screening solvent to solid ratios were validated to determine the linear domain in terms of the percentage of radical scavenged, within a range between 20% and 80% approximately. It is also important to consider that the foodstuff analyzed has a high water content.

2.7.1.1 Effect of solvents

The proposed methodology considered the effect of solvents in the extraction process. J. E. Cacace and G. Mazza (Cacace & Mazza, 2003) reported that the binary solvent system (aqueous ethanol) used in their research work had a maximum yield of total phenolics extracted at 60% of ethanol. Furthermore, J. Pérez and C. Saura (Perez J. & Saura C.,

2005) reported that, using a two sequential extraction steps enhance the extraction yield of phenolic compounds in cereals.

An important factor to consider in the experimental design is towards a greener extraction condition. Thus, the acidic condition of the binary solvent system (HCl, pH = 2) is considered a variable to validate the effect on the antioxidant capacity determination.

2.7.1.2 Effect of Ultrasound-assisted extraction (UAE)

It is reported that an ultrasound energy higher than 20 kHz may lead to the formation of free radicals from the original active constituents (S. S. Handa, 2008). Hence, the UAE time is also considered a variable to assess in the proposed design of the experiments.

Finally, the last variable involved in the design of experiment is the centrifugation time. Since the antioxidant capacity determination only considered the extractable polyphenols, time is an important variable. Besides maximizing productivity, phase separation (supernatant from the non-extractable polyphenols) (Bravo, Abia, & Saura C., 1994; Bravo, Mañas, & Saura C., 1993) is important in the determination of the antioxidant capacity of the extractable compounds.

2.7.2 Experimental Design

The importance of cherries is twofold: first, the antioxidant activity of the extracted compounds (flavonoids and non-flavonoids compounds) and its potential use in polymer formulation. Second, the potential use of anthocyanins as natural pigment. Hence, the extraction conditions were validated to assess the antioxidant activity considering the following:

- The total antioxidant capacity is also influenced by the presence of phenolic compounds which are best extracted in a hydroalcoholic media (Cuevas V., González R., Wisniak, Apelblat, & Pérez C., 2014),
- Anthocyanins are stable in a pH ranging between 1 and 3, whereas at a pH > 4 the structure is not stable (Bridgers, Chinn, & Truong, 2010).

For the experimental runs, a fractional factorial design was implemented to evaluate the significance of the effects of the variables implied in the extraction process on the antioxidant capacity determination via: $DPPH^{\cdot}$ and $ABTS^{\cdot+}$ assays. Table 2.9 shows the input parameters with two factor levels.

Factor	Notation	Factor Levels	
		low (-)	High (+)
ultrasound (minutes)	U	10	40
Centrifuge (minutes)	C	20	40
Extraction media (pH)	E	7	2

Table 2.9. 2^{k-1} experimental design. Levels were coded as (-1) and (+1) for low and high levels.

2.7.3 $DPPH^{\cdot}$ assay

The methodology followed is based on prior results on the antioxidant capacity determination of single molecules. Briefly, the reaction mixture of a final volume assay of 250 μL containing 25 μL aliquots of extract (supernatant) and $DPPH^{\cdot}$ radical in ethanolic solution (175 μM) is monitored spectrophotometrically at λ = 490 nm and 5 minutes (end-point).

Table 2.10 shows the resulting EC_{50} values of the experimental runs on $DPPH^{\cdot}$ assay. Each corresponding EC_{50} value is calculated from linear regression analysis.

				DPPH·				
Test	U	C	E	EC_{50} mg/mL	r^2	EC_{50} mg/mL	r^2	StdDev
Std Order 1	-1	-1	1	98.8	0.993	99.2	0.995	0.177
Std Order 3	-1	1	-1	87.6	0.990	92.6	0.992	2.543
Std Order 4	1	1	1	90.6	0.989	86.2	0.993	2.192
Std Order 2	1	-1	-1	76.5	0.976	81.5	0.983	2.469

Table 2.10. Effect of factors on EC_{50} determination by DPPH· assay.

Results under the experimental conditions evaluated (at a significance level of 5%) are consistent that there is significant effect from the independent variables on the EC_{50} determination. The coded regression equation of the fitted model is represented by equation 2.6:

$$EC_{50}\ DPPH^{\cdot} = 89.13 - 5.41\ Ultrasound + 0.14\ Centrifuge + 4.58\ pH \quad (2.6)$$

Based on the model, Ultrasound (U) and pH of extraction media (E) are significant terms (ANOVA, $p < 0.05$) influencing on the EC_{50} determination. Figure 2.18 depicts the main effects.

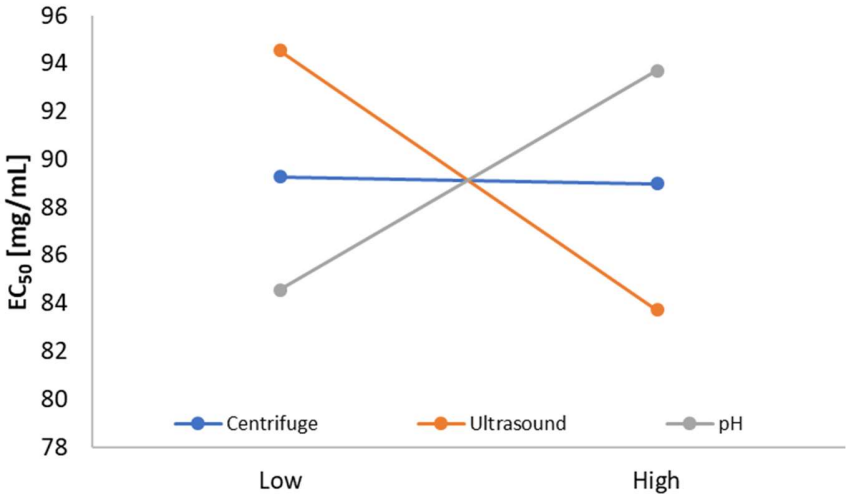

Figure 2.18. Main effects pooled at low (-1) and high (+1) levels for EC_{50} determination on DPPH˙ assay.

The effect of pH on the EC_{50} value determined by DPPH˙ assay shows a reduced antioxidant activity at a pH of 2 (88.4 mg/mL +/- 2.19 compared to 79.0 mg/mL +/- 2.47 at a pH >6). It is reported that acidic conditions inhibit antioxidant activity for phenolic compounds whereas at a pH of 8, the antioxidant activity is higher than the standard reference Trolox (Amorati, Pedullini, Cabrini, Zambonin, & Landi, 2006).

2.7.4 $ABTS^{\cdot+}$ assay

The methodology followed is based on prior results on the antioxidant capacity determination of single molecules. In outline, the reaction mixture of a final volume assay of 250 μL containing 25 μL aliquots of extract (supernatant) and $ABTS^{\cdot+}$ radical in phosphate buffer saline solution (PBS 0.01 M, pH = 7.4) is monitored spectrophotometrically at λ = 405 nm and 5 minutes (end-point).

Table 2.11 illustrates the results from the experimental design on $ABTS^{\cdot+}$ assay. Each corresponding EC_{50} value is calculated from linear regression analysis.

				$ABTS^{\cdot+}$				
Test	U	C	E	EC_{50} mg/mL	r^2	EC_{50} mg/mL	r^2	StdDev
Std Order 1	-1	-1	1	2.33	0.99	2.25	0.99	0.04
Std Order 3	-1	1	-1	2.27	0.99	2.22	0.99	0.02
Std Order 4	1	1	1	2.15	0.99	2.12	0.99	0.01
Std Order 2	1	-1	-1	2.33	1.00	2.26	1.00	0.03

Table 2.11. Effect of factors on EC_{50} determination by $ABTS^{\cdot+}$ assay.

Results under the experimental conditions evaluated (at a significance level of 5%) are consistent that there is significant effect from the independent variables on the EC_{50} determination. The coded regression equation of the fitted model is represented by equation 2.7:

$$EC_{50}\ ABTS^{\cdot+} = 2.2417 - 0.0264\ \text{Ultrasound} - 0.0532\ \text{Centrifuge} - 0.0291\ \text{pH} \quad (2.7)$$

It was observed that the term Centrifuge (C) is significant (ANOVA, $p < 0.05$) on the EC_{50} determination. Figure 2.19 represents the main effects.

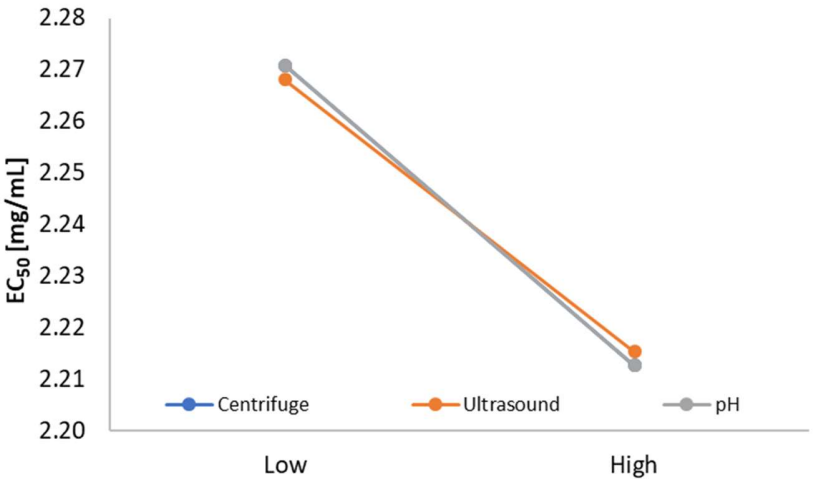

Figure 2.19. Main effects pooled at low (-1) and high (+1) levels for EC_{50} determination on $ABTS^{\bullet+}$ assay.

In general, the extracted compounds presented higher antioxidant activity against $ABTS^{\bullet+}$ radical than $DPPH^{\bullet}$ radical. It was observed for $ABTS^{\bullet+}$ assay a lower coefficient of variation (CV) of 3.21% as compared to $DPPH^{\bullet}$ assay with a CV of 8.29%.

Besides the chemical structure differences between $ABTS^{\bullet+}$ and $DPPH^{\bullet}$ radical, the solvent media is also different: a buffer saline solution (PBS) 0.01 M, pH 7.4 for $ABTS^{\bullet+}$ and an ethanolic solution media for $DPPH^{\bullet}$ (only dissolves in organic media). It is possible that this difference lowers the reaction rate of the antioxidant compounds in $DPPH^{\bullet}$ assay.

Nonetheless, some authors have reported that variations in the extraction conditions evaluated such as solvent to solid ratio, temperature, and ethanol concentration might not be large enough to represent a significant change in the antioxidant capacity determination (Cacace & Mazza, 2003).

2.7.5 Effect of aging on the antioxidant capacity of foodstuff

Lipid oxidation in food induces undesirable changes in organoleptic properties (e.g. aroma, flavor, and color). An antioxidant system inhibits or delays such oxidation process thus, the importance to assess the activity of biological antioxidant sources against radicals as a function of time (aging).

2.7.5.1 DPPH$^{\cdot}$ assay

A fresh stock solution from extracted cherries was stored at 8°C in dark to evaluate the effect of aging on the antioxidant activity against DPPH$^{\cdot}$ radical. Figure 2.20 shows the EC_{50} values.

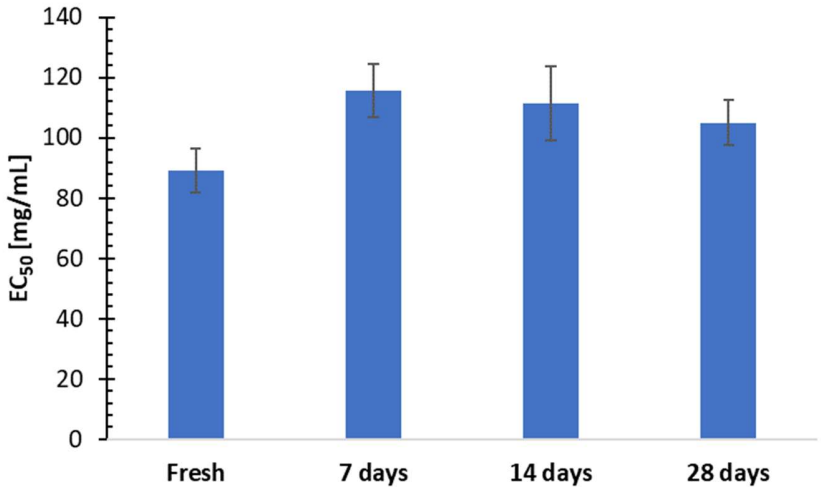

Figure 2.20. EC_{50} determination on DPPH$^{\cdot}$ assay. Each corresponding EC_{50} value is calculated from linear regression analysis (r^2 = 0.99).

During the experimental analysis, particularly for the first DPPH$^{\cdot}$ assay on fresh cherries, it was observed a precipitate in the well (diluted extracted sample + DPPH$^{\cdot}$ radical + ethanol

as solvent media). This precipitate was also observed in the individual blanks (diluted extracted sample + ethanol as solvent media) particularly at higher concentrations of the extracted sample.

It has been reported from authors that polysaccharides and proteins may precipitate from foodstuff in the presence of organic solvents such as methanol. Furthermore, non-extractable polyphenols (high molecular weight) and polyphenols bound to dietary fiber and proteins are found as precipitate in aqueous-organic extracts (Perez J. & Saura C., 2005).

Based on the above, the methodology was changed for the antioxidant determination in day 7, 14, and 28 respectively. A 1.5 mL vials containing the diluted extracted solutions were centrifuge (4000 rpm, 2 minutes). A 25 μL aliquot was utilized for the test-method excluding the precipitate.

These considerations may confirm the lower EC_{50} value obtained from fresh cherries due to the presence of non-diluted compounds with antioxidant activity. Finally, with the new experimental conditions evaluated, there is no significant evidence (ANOVA, $p > 0.05$) to conclude that EC_{50} values are different.

2.7.5.2 $ABTS^{\cdot+}$ assay

A fresh stock solution from extracted cherries was stored at 8°C in dark to assess the effect of aging on the antioxidant activity against $ABTS^{\cdot+}$ radical. Figure 2.21 shows the EC_{50} values.

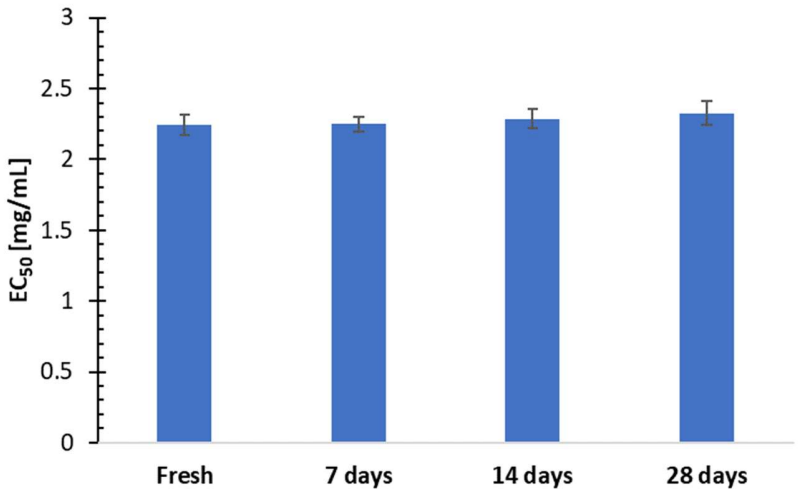

Figure 2.21. EC_{50} determination on $ABTS^{\cdot+}$ assay. Each corresponding EC_{50} value is calculated from linear regression analysis ($r^2 = 0.99$).

There is no significant evidence (ANOVA, $p > 0.05$), within the experimental conditions evaluated, to conclude that EC_{50} values are different. For both assays, the antioxidant activity of the extracted cherries remained constant for a period of 1 month. This finding is similar to the stability analysis reported for black currants, which were stable during 9 months froze at -20°C and evaluated by $DPPH^{\cdot}$ and $ABTS^{\cdot+}$ assays (Bakowska-barczak & Kolodziejczyk, 2011). Srzednicki, et. al., also observed that anthocyanin contents of blueberry froze samples were stable up to three months and no significant difference on the antioxidant activity against $DPPH^{\cdot}$ radical was observed (Lohachoompol, Srzednicki, & Craske, 2004).

2.8 Effect of extraction and aging on the antioxidant capacity of foodstuff

Incorporation of an antioxidant system as a food additive or in polymer formulation provides in some extent stability against reactive oxygen species (ROS). Hence, the importance to determine a priori the antioxidant activity and, in the case of a biological source of

antioxidants, assess the effect of the extraction process and aging on the antioxidant capacity determination.

2.8.1 Super Oxide assay

Test-method was followed based on prior results on single antioxidant molecules. The best fitted model validated for EC_{50} determination was a 4-parameter logistic model (XLfit 5.5.0.5 for MS Excel). Equation 2.8 represents the model equation.

$$y = d + \frac{a-d}{1+\left(\frac{x}{c}\right)^b} \tag{2.8}$$

Where *a* represents the minimum bottom value of the sigmoidal curve, *d* is the maximum value of the sigmoidal curve, *c* represents the inflection point or midway point between the min and max point in the sigmoidal curve, *x* denotes the independent variable (i.e. concentration), and *b* is the slop of the curve at its midpoint. Table 2.12 shows the EC_{50} values and the experimental conditions evaluated.

Cherries			Super Oxide assay $O_2^{\cdot-}$				
Type	Extraction	Condition	EC_{50} mg/mL	r^2	EC_{50} mg/mL	r^2	std dev
Fresh	Yes	fresh extraction	14.0	0.999	18.7	1.000	2.351
Fresh	No		7.9	1.000	11.6	1.000	1.871
Fresh	No	+ 28 days of grinded	11.7	0.997	13.6	1.000	0.927
Aged	Yes	Frozen for 1 year	24.8	1.000	22.4	0.999	1.240
Aged	No	Frozen for 1 year	27.6	0.995	23.6	1.000	1.996

Table 2.12. Effect of extraction and aging from cherries on the scavenging activity of superoxide radicals.

It is observed a slight reduced antioxidant activity between the sample with extraction and without extraction (16.3 mg/mL +/- 2.35 and 9.76 mg/mL +/- 1.87 respectively). This could be explained due to the hydroalcoholic media from the extraction process and their possible interaction in enzyme activity.

Furthermore, Figure 2.22 illustrates the stability of fresh cherries (without extraction). It is observed a decay in approximately 2.5 times to the initial EC_{50} value after 1 year of storage (-20 °C).

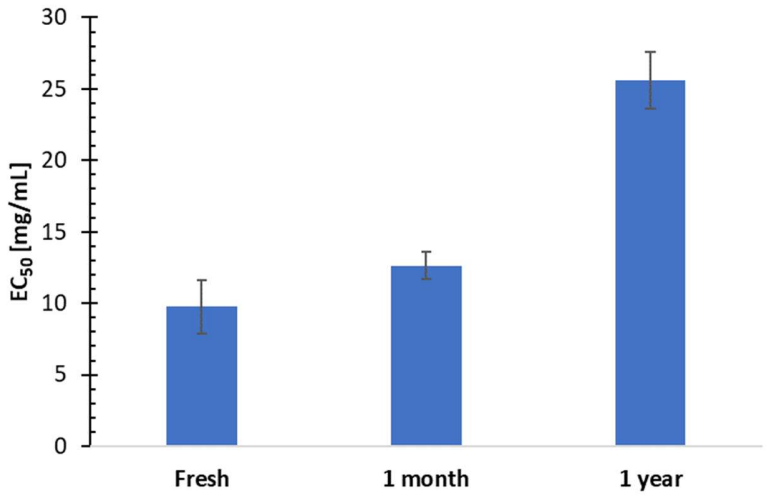

Figure 2.22. Aging effect on EC_{50} determination by $O_2^{\cdot -}$ assay. Fresh cherries without extraction.

2.8.2 DPPH$^{\cdot}$ assay

Test-method was followed based on prior results on single antioxidant molecules. EC_{50} values were calculated from linear regression. Table 2.13 presents the individual EC_{50} values and the experimental conditions evaluated.

Cherries			DPPH$^{\cdot}$ assay				
Type	Extraction	Condition	EC_{50} mg/mL	r^2	EC_{50} mg/mL	r^2	std dev
Fresh	Yes	fresh extraction	90.6	0.989	86.2	0.998	2.192
Fresh	No		81.7	0.971	79.8	0.951	0.963
Fresh	No	+ 28 days of grinded	187.2	0.991	168.0	0.998	9.573
Aged	Yes	Frozen for 1 year	144.7	0.999	143.5	0.998	0.634

Table 2.13. Effect of extraction and aging from cherries on the scavenging activity of DPPH$^{\cdot}$ radical.

It is observed a more rapid decay on the antioxidant activity without an extraction step, an increase of 2.2 times the initial EC_{50} value is observed after 1 month of storage conditions. An extraction step was performed in cherries stored for 1 year (-20 °C) resulting in a lower antioxidant activity (EC_{50} 144.1 mg/mL +/- 0.634) possibly caused by degradation. Finally, there is a slight difference in EC_{50} value between the sample with extraction and without extraction (88.4 mg/mL +/- 2.192 and 80.8 mg/mL +/- 0.963 respectively).

2.8.3 ABTS$^{\cdot+}$ assay

Test-method was followed based on prior results on single antioxidant molecules. EC_{50} values were calculated from linear regression. Table 2.14 presents the EC_{50} values and the experimental conditions evaluated.

Cherries			ABTS$^{\cdot+}$ assay				
Type	Extraction	Condition	EC_{50} mg/mL	r^2	EC_{50} mg/mL	r^2	std dev
Fresh	Yes	fresh extraction	2.15	0.993	2.12	0.991	0.014
Fresh	No		2.06	0.984	1.99	0.981	0.036
Fresh	No	+ 28 days of grinded	2.67	0.747	1.97	0.821	0.352
Aged	Yes	Frozen for 1 year	3.51	0.989	3.08	0.990	0.212

Table 2.14. Effect of extraction and aging from cherries on the scavenging activity of ABTS$^{\cdot+}$ radical.

It is observed a minor difference in the antioxidant activity from an extracted and non-extracted cherry sample (2.13 mg/mL and 2.03 mg/mL respectively). Furthermore, there is no effect of the extraction process on the EC_{50} value after 1 year of storage. A possible sample degradation is represented with a decay in the antioxidant activity of 1.5 times to the initial EC_{50} value (3.30 mg/mL and 2.13 mg/mL respectively).

2.8.4 Effect of lyophilization on the antioxidant capacity

Post-harvest processes such as extraction, freeze drying, fermentation, cooking conditions, storage, and packaging may affect the antioxidant activity of foods (Chang, Lin, Chang, & Liu, 2006; Murcia, López-Ayerra, Martinez-Tomé, Vera, & García-Carmona, 2000; Patthamakanokporn, Puwastien, Nitithamyong, & Sirichakwal, 2008; Pérez-Gregorio, Regueiro, Alonso-González, Pastrana-Castro, & Simal-Gándara, 2011; Robles-Sánchez, Rojas-Graü, Odriozola-Serrano, González-Aguilar, & Martín-Belloso, 2009; Rodrigues, Pérez-Gregorio, García-Falcón, & Simal-Gándara, 2009). Lyophilization is a water removal process commonly used in the pharmaceutical and food industry. The process involves: freezing, primary drying (sublimation), and secondary drying (desorption).

The effect of lyophilization on the antioxidant capacity of foodstuff is addressed to food quality and preservation (shelf-life) performance. Briefly, 50 grams (fresh weight) of cherries contained in centrifuge tubes were froze at -20 °C for 24 hours prior to lyophilization. Lyophilized samples were extracted following the methodology describe above and stored in dark at 8 °C. The effect of lyophilization on the antioxidant capacity of cherries was assessed via: $DPPH^{\cdot}$, $ABTS^{\cdot+}$, and $O_2^{\cdot-}$ assays.

Table 2.15 shows the results as the EC_{50} value in mg/mL for the three radical assays. Results shows that there is a higher antioxidant activity (lower EC_{50} value) for the lyophilized sample under the three different radicals evaluated.

Cherries	DPPH$^{\cdot}$ Assay			$O_2^{\cdot -}$ Assay			$ABTS^{\cdot +}$ Assay		
	EC_{50} mg/mL	r^2	std dev	EC_{50} mg/mL	r^2	std dev	EC_{50} mg/mL	r^2	std dev
fresh extraction	88.4	0.993	2.19	16.3	0.999	2.35	2.13	0.992	0.014
Lyophilized	39.2	0.994	0.06	4.97	0.998	0.20	0.78	0.986	0.012

Table 2.15. Antioxidant capacity determination.

The EC_{50} values assessed by DPPH$^{\cdot}$ for fresh extraction and lyophilized cherries were 5.4-fold and 7.9-fold higher than the corresponding EC_{50} values calculated by SOA ($O_2^{\cdot -}$) assay and 41.5-fold and 50.3-fold higher than the EC_{50} values determine by $ABTS^{\cdot +}$. It may be concluded that the $ABTS^{\cdot +}$ method is more sensitive toward cherries, as a biological source. Figure 2.23 illustrates the sensitivity of the test-methods on the radical scavenging activity expressed as the EC_{50} value.

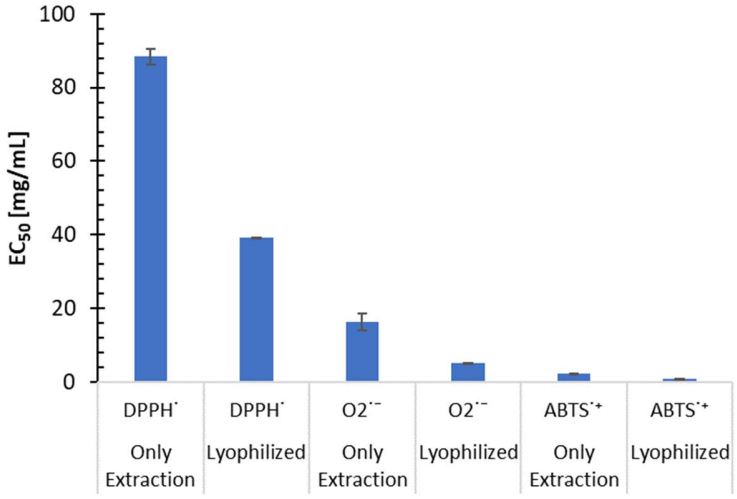

Figure 2.23. Antioxidant capacity determination of cherries against different radical sources.

Figure 2.24 depicts the antioxidant activity of only extracted cherries and lyophilized cherries as the percentage of radical scavenged in the linear domain for DPPH$^{\cdot}$ and $ABTS^{\cdot +}$ assays, and the percentage of NBT formazan inhibition for SOA ($O_2^{\cdot -}$) assay.

a

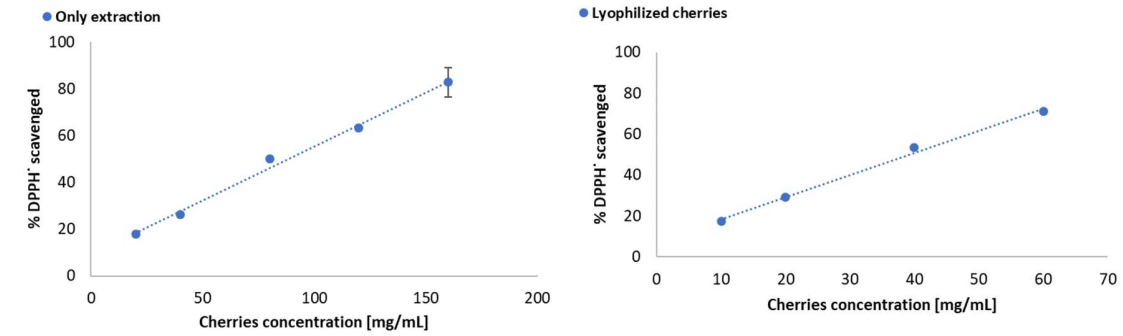

b

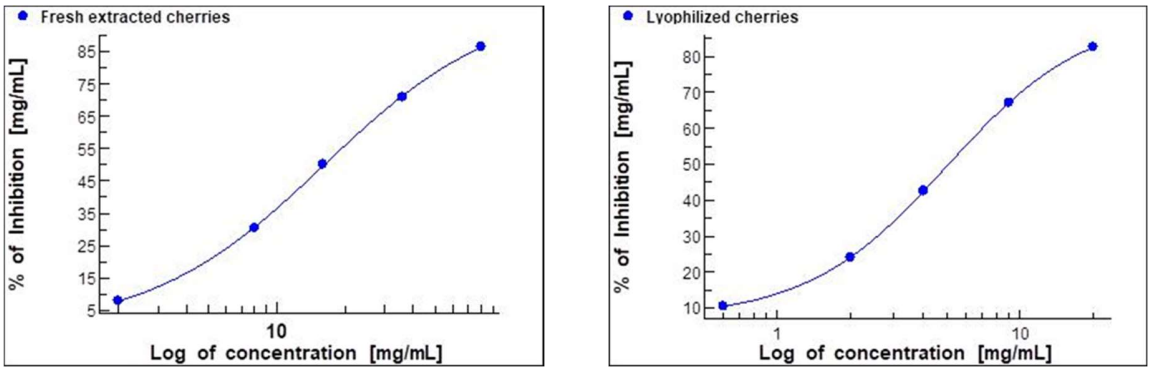

c

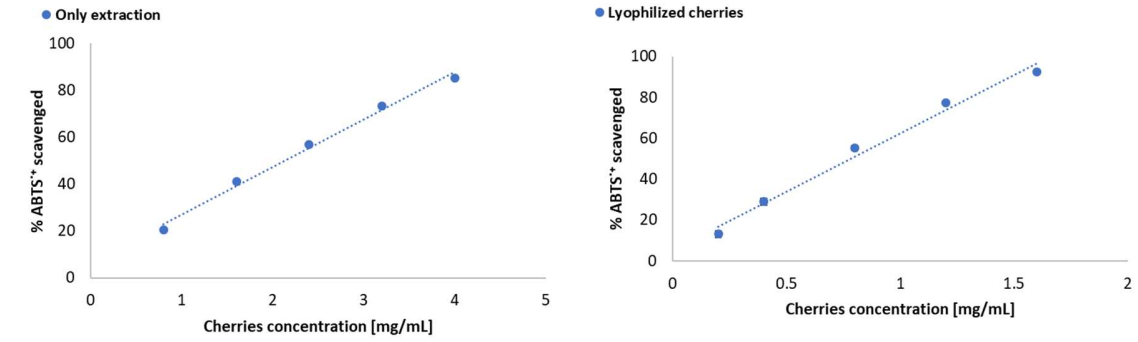

Figure 2.24. Effect of lyophilization on the percentage of radical scavenging. **a** $DPPH^{\cdot}$ radical scavenged curve; **b** $O_2^{\cdot -}$ radical scavenged curve; **c** $ABTS^{\cdot +}$ radical scavenged curve.

It was outlined in chapter I the detrimental effect of reactive oxygen species (ROS) in living systems and also, in polymer degradation during polymer processing. This chapter developed the idea of standardizing an analytical method to screen for the antioxidant capacity of natural molecules and biological samples and their potential incorporation into polymers as thermal stabilizers.

Two synthetic radicals (DPPH$^{\bullet}$ and ABTS$^{\bullet+}$) and one bio-sourced radical (SOA) were proposed to assess the antioxidant activity of natural molecules derived from plants such as gallic acid and rosmarinic acid and from foods such as the case of quercetin. Furthermore, the screening of sweet cherries extracts as a potential antioxidant source were assessed.

The literature review exposed different protocols that assess the antioxidant activity of molecule(s) under the same test-method: DPPH$^{\bullet}$, ABTS$^{\bullet+}$, and SOA. Among them, DPPH$^{\bullet}$ was selected as an indicator for antioxidant capacity studies for further analysis in Chapter III. The sensitivity of the test-method was evaluated within a range in a molar ratio of antioxidant to DPPH$^{\bullet}$ radical of approximately 1 unit of magnitude using trolox as a standard and obeying the beer-lambert law at the experimental conditions utilized, thus concluding its robustness and reproducibility.

Bibliography

Amorati, R., Pedullini, G. F., Cabrini, L., Zambonin, L., & Landi, L. (2006). Solvent and pH Effects on the Antioxidant Activity of Caffeic and Other Phenolic Acids. *Journal of Agricultural and Food Chemistry*, *54*, 2932–2937.

Aruoma, O. I., Ramful, D., Bahorun, T., Tarnus, E., & Bourdon, E. (2011). Polyphenol composition, vitamin C content and antioxidant capacity of Mauritian citrus fruit pulps. *Food Research International*, *44*(7), 2088–2099. https://doi.org/10.1016/j.foodres.2011.03.056

Bakowska-barczak, A. M., & Kolodziejczyk, P. P. (2011). Black currant polyphenols: Their storage stability and microencapsulation. *Industrial Crops & Products*, *34*, 1301–1309. https://doi.org/10.1016/j.indcrop.2010.10.002

Bhagwat, S., & Haytowitz, D. (2015). *USDA Database for the Isoflavone Content of Selected Foods*.

Boly, R., Lamkami, T., Lompo, M., Dubois, J., & Guissou, I. P. (2016). DPPH free radical scavenging activity of two extracts from agelanthus dodoneifolius (Loranthaceae) leaves. *International Journal of Toxicological and Pharmacological Research*, *8*(1), 29–34.

Bozin, B., Mimica-Dukic, N., Simin, N., & Anackov, G. (2004). Antimicrobial and antioxidant activities of Melissa officinalis L. (Lamiaceae) essential oil. *Journal of Agricultural and Food Chemistry*, *52*(5), 2485–2489. https://doi.org/10.1021/jf051922u

Brand-Williams, W., Cuvelier, M. E., & Berset, C. (1995). Use of a Free Radical Method to Evaluate Antioxidant Activity. *LWT - Food Science and Technology*, *28*(1), 25–30.

Bravo, L., Abia, R., & Saura C., F. (1994). Polyphenols as Dietary Fiber Associated Compounds . Comparative Study on in Vivo and in Vitro Properties. *Journal of Agricultural and Food Chemistry*, *42*(7), 1481–1487.

Bravo, L., Mañas, E., & Saura C., F. (1993). Dietary Non-extractable Condensed Tannins as Indigestible Compounds : Effects on Faecal Weight, and Protein and Fat Excretion. *Journal of the Science of Food and Agriculture*, *63*, 63–68.

Bridgers, E. N., Chinn, M. S., & Truong, V.-D. (2010). Extraction of anthocyanins from industrial purple-fleshed sweetpotatoes and enzymatic hydrolysis of residues for fermentable sugars. *Industrial Crops & Products*, *32*(3), 613–620. https://doi.org/10.1016/j.indcrop.2010.07.020

Brody, A. L., Strupinsky, E. P., & Kline, L. R. (2001). Odor Removers. In *Active Packaging for Food Applications* (First, pp. 107–116). CRC Press LLC.

Bušić, V., Kovač, S., Gašo-Sokač, D., & Lepeduš, H. (2008). Antioxidative activity of anthocyanins from sour cherries. *Acta Alimentaria*, *37*(3), 391–397. https://doi.org/10.1556/aalim.2008.0007

Cacace, J. E., & Mazza, G. (2003). Optimization of Extraction of Anthocyanins from Black Currants with Aqueous Ethanol. *JFS: Food Engineering and Physical Properties*, *68*(1), 240–248.

Chang, C., Lin, H.-Y., Chang, C.-Y., & Liu, Y.-C. (2006). Comparisons on the antioxidant properties of fresh, freeze-dried and hot-air-dried tomatoes. *Journal of Food Engineering*, *77*, 478–485. https://doi.org/10.1016/j.jfoodeng.2005.06.061

Chien, P. J., Sheu, F., Huang, W. T., & Su, M. S. (2007). Effect of molecular weight of chitosans on their antioxidative activities in apple juice. *Food Chemistry*, *102*(4), 1192–1198. https://doi.org/10.1016/j.foodchem.2006.07.007

Chun, O. K., Kim, D. O., & Lee, C. Y. (2003). Superoxide Radical Scavenging Activity of the Major Polyphenols in Fresh Plums. *Journal of Agricultural and Food Chemistry*, *51*(27), 8067–8072. https://doi.org/10.1021/jf034740d

Cuevas V., J., González R., Á., Wisniak, J., Apelblat, A., & Pérez C., J. R. (2014). Solubility of (+)-catechin in water and water-ethanol mixtures within the temperature range 277.6–331.2 K: Fundamental data to design polyphenol extraction processes. *Fluid Phase Equilibria*, *382*, 279–285. https://doi.org/10.1016/j.fluid.2014.09.013

De Gaulejac, N. S. C., Vivas, N., De Freitas, V., & Bourgeois, G. (1999). The influence of various phenolic compounds on scavenging activity assessed by an enzymatic method. *Journal of the Science of Food and Agriculture*, *79*(8), 1081–1090. https://doi.org/10.1002/(SICI)1097-0010(199906)79:8<1081::AID-JSFA330>3.0.CO;2-G

de Sousa, P. H. M., Almeida, M. M. B., Maia, G. A., do Prado, G. M., de Lemos, T. L. G., Magalhães, C. E. de C., & Arriaga, Â. M. C. (2011). Bioactive compounds and antioxidant activity of fresh exotic fruits from northeastern Brazil. *Food Research International*, *44*(7), 2155–2159. https://doi.org/10.1016/j.foodres.2011.03.051

Digrak, M., Yildirim, A., Mavi, A., Alma, M. H., & Hirata, T. (2003). Screening Chemical Composition and in Vitro Antioxidant and Antimicrobial Activities of the Essential Oils from Origanum syriacum L. Growing in Turkey. *Biological & Pharmaceutical Bulletin*, *26*(12), 1725–1729. https://doi.org/10.1248/bpb.26.1725

Eklund, P. C., Långvik, O. K., Wärnå, J. P., Salmi, T. O., Willför, S. M., & Sjöholm, R. E. (2005). Chemical studies on antioxidant mechanisms and free radical scavenging properties of lignans. *Organic and Biomolecular Chemistry*, *3*(18), 3336–3347. https://doi.org/10.1039/b506739a

Espín, J. C., Soler-Rivas, C., Wichers, H. J., & García-Viguera, C. (2000). Anthocyanin-based natural colorants: A new source of antiradical activity for foodstuff. *Journal of Agricultural and Food Chemistry*, *48*(5), 1588–1592. https://doi.org/10.1021/jf9911390

Floegel, A., Kim, D. O., Chung, S. J., Koo, S. I., & Chun, O. K. (2011). Comparison of ABTS/DPPH assays to measure antioxidant capacity in popular antioxidant-rich US foods. *Journal of Food Composition and Analysis*, *24*(7), 1043–1048. https://doi.org/10.1016/j.jfca.2011.01.008

Foti, M. C. (2015). The Use and Abuse of the DPPH• Radical. *Journal of Agricultural and Food Chemistry*, *63*(40), 8765–8776.

Gil, M. I., Tomas-Barberan, F. A., Hess-Pierce, B., Holcroft, D. M., & Kader, A. A. (2000). Antioxidant activity of pomegranate juice and its relationship with phenolic composition and processing. *Journal of Agricultural and Food Chemistry*, *48*(10), 4581–4589. https://doi.org/10.1021/jf000404a

Handa, S. S. (2008). An Overview of Extraction Techniques for Medicinal and Aromatic Plants. In Sukhdev Swami Handa, S. P. S. Khanuja, G. Longo, & D. D. Rakesh (Eds.), *Extraction Technologies for Medicinal and Aromatic Plants* (pp. 21–54). ICS UNIDO Iternational Centre for Science and High Technolgy.

Haytowitz, D., Wu, X., & Bhagwat, S. (2018a). *USDA Database for the Flavonoid Content of Selected Foods*.

Haytowitz, D., Wu, X., & Bhagwat, S. (2018b). *USDA Database for the Proanthocyanidin Content of Selected Foods*.

Hicks, R. G. (2010). Verdazyls and Related Radicals Containing the Hydrazyl [R2N−NR] Group. In R. G. Hicks (Ed.), *Stable Radicals: Fundamentals and Applied Aspects of Odd-Electron Compounds* (First, pp. 245–273). WILEY.

Ho, Y. C., Yam, K. L., Young, S. S., & Zambetti, P. F. (1994). Comparison of Vitamin E, Irganox 1010 and BHT as Antioxidants on Release of Off-Flavor from HDPE Bottles. *Journal of Plastic Film and Sheeting*, *10*, 194–212. https://doi.org/10.1177/875608799401000303

JEŻEWSKA, M. M. (1973). Xanthine Accumulation during Hypoxanthine Oxidation by Milk Xanthine Oxidase. *European Journal of Biochemistry*, *36*(2), 385–390. https://doi.org/10.1111/j.1432-1033.1973.tb02923.x

Jiménez E., A., Rincón, M., Pulido, R., & Saura C., F. (2001). Guava Fruit (Psidium guajava L .) as a New Source of Antioxidant Dietary Fiber. *Journal of Agricultural and Food Chemistry*, *49*, 5489–5493. https://doi.org/10.1021/jf010147p

Kalra, S., Jena, G., Tikoo, K., & Mukhopadhyay, A. K. (2007). Preferential inhibition of xanthine oxidase by 2-amino-6-hydroxy-8- mercaptopurine and 2-amino-6-purine thiol. *BMC Biochemistry*, *8*, 1–11. https://doi.org/10.1186/1471-2091-8-8

Kedare, S. B., & Singh, R. P. (2011). Genesis and development of DPPH method of antioxidant assay. *Journal of Food Science and Technology*, *48*(4), 412–422. https://doi.org/10.1007/s13197-011-0251-1

Kim, H. J., Chen, F., Wu, C., Wang, X., Chung, H. Y., & Jin, Z. (2004). Evaluation of Antioxidant Activity of Australian Tea Tree (Melaleuca alternifolia) Oil and Its Components. *Journal of Agricultural and Food Chemistry*, *52*(10), 2849–2854. https://doi.org/10.1021/jf035377d

Lohachoompol, V., Srzednicki, G., & Craske, J. (2004). The Change of Total Anthocyanins in Blueberries and Their Antioxidant Effect After Drying and Freezing. *Journal of Biomedicine and Biotechnology*, *5*, 248–252.

López-Rubio, A., Almenar, E., Hernandez-Muñoz, P., Lagarón, J. M., Catalá, R., & Gavara, R. (2004). Overview of Active Polymer-Based Packaging Technologies for Food

Applications. *Food Reviews International*, *20*(4), 357–387. https://doi.org/10.1081/FRI-200033462

Lu, Y., & Foo, L. Y. (2001). Antioxidant activities of polyphenols from sage (Salvia officinalis). *Food Chemistry*, *75*, 197–202.

Lu, Y., & Yeap Foo, L. (2000). Antioxidant and radical scavenging activities of polyphenols from apple pomace, *68*, 81–85. https://doi.org/10.1016/S0308-8146(99)00167-3

Miller, F. J., & Griendling, K. K. (1994). *Functional evaluation of nonphagocytic NAD(P)H oxidases*. *Methods in Enzymology* (Vol. 353). Elsevier Masson SAS. https://doi.org/10.1016/S0076-6879(02)53050-0

Miller, N. J., & Rice-Evans, C. A. (1997). Factors Influencing the Antioxidant Activity Determined by the ABTS•+ Radical Cation Assay. *Free Radical Research*, *26*, 195–199.

Miller, N. J., Rice-Evans, C., Davies, M. J., Gopinathan, V., & Milner, A. (1993). A novel method for measuring antioxidant capacity and its application to monitoring the antioxidant status in premature neonates. *Clinical Science*, *84*, 407–412.

Mishra, K., Ojha, H., & Chaudhury, N. K. (2012). Estimation of antiradical properties of antioxidants using DPPH- assay: A critical review and results. *Food Chemistry*, *130*(4), 1036–1043. https://doi.org/10.1016/j.foodchem.2011.07.127

Montoro, P., Braca, A., Pizza, C., & De Tommasi, N. (2005). Structure-antioxidant activity relationships of flavonoids isolated from different plant species. *Food Chemistry*, *92*(2), 349–355. https://doi.org/10.1016/j.foodchem.2004.07.028

Murcia, M., López-Ayerra, B., Martinez-Tomé, M., Vera, A., & García-Carmona, F. (2000). Evolution of ascorbic acid and peroxidase during industrial processing of broccoli. *Journal of the Science of Food and Agriculture*, *80*, 1882–1886.

Nenadis, N., & Tsimidou, M. Z. (2018). DPPH (2,2-di(4-tert-octylphenyl)-1- picrylhydrazyl) radical scavenging mixed-mode colorimetric assay(s). In Reşat Apak, E. Capanoglu, & F. Shahidi (Eds.), *Measurement of Antioxidant Activity & Capacity Recent Trends and Applications* (First, pp. 141–164). WILEY.

Olszowy, M., & Dawidowicz, A. L. (2018). Is it possible to use the DPPH and ABTS methods for reliable estimation of antioxidant power of colored compounds? *Chemical Papers*,

72(2), 393–400. https://doi.org/10.1007/s11696-017-0288-3

P, C., L, Y., M, C., JP, H., K, C., B, V. P., … D, V. B. (1998). Structure-activity relationship and classification of flavonoids as inhibitors of xanthine oxidase and superoxide scavengers. *Journal of Natural Products*, *61*(1), 71–76.

Patthamakanokporn, O., Puwastien, P., Nitithamyong, A., & Sirichakwal, P. P. (2008). Changes of antioxidant activity and total phenolic compounds during storage of selected fruits. *Journal of Food Composition and Analysis*, *21*, 241–248. https://doi.org/10.1016/j.jfca.2007.10.002

Pérez-Gregorio, M. R., Regueiro, J., Alonso-González, E., Pastrana-Castro, L. M., & Simal-Gándara, J. (2011). Influence of alcoholic fermentation process on antioxidant activity and phenolic levels from mulberries (Morus nigra L .). *LWT - Food Science and Technology*, *44*(8), 1793–1801. https://doi.org/10.1016/j.lwt.2011.03.007

Perez J., J., & Saura C., F. (2005). Literature Data May Underestimate the Actual Antioxidant Capacity of Cereals. *Journal of Agricultural and Food Chemistry*, *53*, 5036–5040.

Pérez, J., & Saura, F. (2007). Metodología para la evaluación de capacidad antioxidante en frutas y hortalizas. In *V Congreso iberoamericano de tecnologia postcosecha y agroexportaciones* (Vol. 2007, p. 11). Retrieved from http://www.horticom.com/pd/imagenes/71/429/71429.pdf

Prior, R. L., Wu, X., & Schaich, K. (2005). Standardized methods for the determination of antioxidant capacity and phenolics in foods and dietary supplements. *Journal of Agricultural and Food Chemistry*, *53*(10), 4290–4302. https://doi.org/10.1021/jf0502698

Proteggente, A. R., Pannala, A. S., Paganga, G., Van Buren, L., Wagner, E., Wiseman, S., … Rice-Evans, C. A. (2002). The antioxidant activity of regularly consumed fruit and vegetables reflects their phenolic and vitamin C composition. *Free Radical Research*, *36*(2), 217–233. https://doi.org/10.1080/10715760290006484

Re, R., Pellegrini, N., Proteggente, A., Pannala, A., Yang, M., & Rice-Evans, C. (1999). ANTIOXIDANT ACTIVITY APPLYING AN IMPROVED ABTS RADICAL CATION DECOLORIZATION ASSAY. *Free Radical Biology and Medicine*, *26*(98), 1231–1237.

Robak, J., & Gryglewski, R. J. (1988). FLAVONOIDS ARE SCAVENGERS OF

SUPEROXIDE ANIONS. *Biochemical Pharmacology*, *37*(5), 837–841.

Robles-Sánchez, R. M., Rojas-Graü, M. A., Odriozola-Serrano, I., González-Aguilar, G. A., & Martín-Belloso, O. (2009). Effect of minimal processing on bioactive compounds and antioxidant activity of fresh-cut 'Kent ' mango (Mangifera indica L.). *Postharvest Biology and Technology*, *51*, 384–390. https://doi.org/10.1016/j.postharvbio.2008.09.003

Rodrigues, A. S., Pérez-Gregorio, M. R., García-Falcón, M. S., & Simal-Gándara, J. (2009). Effect of curing and cooking on flavonols and anthocyanins in traditional varieties of onion bulbs. *Food Research International*, *42*(9), 1331–1336. https://doi.org/10.1016/j.foodres.2009.04.005

Russo, A., Longo, R., & Vanella, A. (2002). Antioxidant activity of propolis: role of caffeic acid phenethyl ester and galangin. *Fitoterapia*, *73 Suppl 1*, S21–S29. Retrieved from http://www.ncbi.nlm.nih.gov/pubmed/12495706

Skaltsa, H., Hadjipavlou-Litina, D., Fleischer, T. C., Karioti, A., & Mensah, M. L. K. (2004). Composition and Antioxidant Activity of the Essential Oils of Xylopia aethiopica (Dun) A. Rich. (Annonaceae) Leaves, Stem Bark, Root Bark, and Fresh and Dried Fruits, Growing in Ghana. *Journal of Agricultural and Food Chemistry*, *52*(26), 8094–8098. https://doi.org/10.1021/jf040150j

Strljbe, M., Haenen, G. R. M. M., Van Den Berg, H., & Bast, A. (1997). Pitfalls in a Method for Assessment of Total Antioxidant Capacity. *Free Radical Research*, *26*(6), 515–521. https://doi.org/10.3109/10715769709097822

Sun, Y., Yang, C., & Tsao, R. (2018). Nomenclature and general classification of antioxidant activity/capacity assays. In Resat Apak, E. Capanoglu, & F. Shahidi (Eds.), *Measurement of Antioxidant Activity & Capacity Recent Trends and Applications* (First). John Wiley & Sons Ltd.

TAKAYANAGI, T., KANO, M., HARADA, K., ISHIKAWA, F., & MAKINO, K. (2005). Antioxidative Activity of Anthocyanins from Purple Sweet Potato, Ipomoera batatas Cultivar Ayamurasaki . *Bioscience, Biotechnology, and Biochemistry*, *69*(5), 979–988. https://doi.org/10.1271/bbb.69.979

Van Den Berg, R., Haenen, G. R. M. M., Van Den Berg, H., & Bast, A. (1999). Applicability of an improved Trolox equivalent antioxidant capacity (TEAC) assay for evaluation of antioxidant capacity measurements of mixtures. *Food Chemistry*, *66*(4), 511–517.

https://doi.org/10.1016/S0308-8146(99)00089-8

Xie, J., & Schaich, K. M. (2014). Re-evaluation of the 2,2-Diphenyl-1-picrylhydrazyl Free Radical (DPPH) Assay for Antioxidant Activity. *Journal of Agricultural and Food Chemistry*, *62*(19), 4251–4260.

Yordanov, N. D. (1996). Is our knowledge about the chemical and physical properties of DPPH enough to consider it as a primary standard for quantitative EPR spectrometry. *Applied Magnetic Resonance*, *10*(1–3), 339–350. https://doi.org/10.1007/BF03163117

CHAPTER III

POLYMERS

3.1 Introduction

As described in chapter I, polymer processing involves different operations: starting with the polymerization reactor where the resin is fabricated, then processed in post-reactor operations where the first thermo-mechanical event is present (extrusion) to produce virgin plastic pellets and finally, the plastics product fabricating operations where the finished plastic part, for the end-user, is manufactured.

It is required to ensure the stability of the physical properties of the polymer resin along the value chain of the individual unit operations. In the case of polyolefins, the incorporation of thermal stabilizers (antioxidants) is important. Hence, the need to assess the effect of thermal and mechanical events.

The industrial polymer processing temperature conditions for most of the thermoplastic resins relies in a range between 400 K and 650 K. Although higher processing temperatures (resulting in a lower melt viscosity) may lead to cost savings by using less mechanical energy, the processing conditions utilized are constrained to polymer thermal stability (Colin & Verdu, 2006).

Thus, the optimal process window involves a compromise between the integrity of the polymer end use properties and the processing temperature: at low processing temperatures thermal degradation is neglected but poor product quality is presented due to high melt viscosity, whereas at high processing temperatures thermal degradation occurs and product quality is affected mainly by molecular weight variations.

This chapter deals with the state of the art of the selected resins characterized by classical thermal analysis and by polymer melt rheology. It addresses the effect of processing conditions on the polymer thermal stability and proposes two thermal test-methods that best describes the degradation effect caused by the extrusion process.

3.2 Specific Objectives

- To assess the thermal stability of un-stabilized isotactic polypropylene (i-PP) and un-stabilized low-density polyethylene (LDPE) during polymer processing by thermal analysis and polymer melt rheology analysis,

- To assess the effect of extrusion process on i-PP and LDPE at different processing conditions.

3.3 Thermal Analysis

According to The International Union of Pure and Applied Chemistry (IUPAC) and the International Confederation of Thermal Analysis and Calorimetry (ICTAC), thermal analysis (TA) is defined as the study of the relationship between a sample property and its temperature as the sample is heated or cooled in a controlled manner.

Thermal transport and conductivity are the driving processes during a thermal analysis. Hence, sample mass, ramp rate, and purge gas are the most important variables (Menczel, Prime, & Gallagher, 2009).

Thermal analysis is widely used by the plastic industry as a tool to determine thermal and mechanical histories, in the design of manufacturing processes commonly used for plastic converters, and to estimate the lifetime of a polymer material under different environments.

The main analytical techniques are: differential scanning calorimetry (DSC), thermogravimetric analysis (TGA), thermomechanical analysis (TMA), dynamic mechanical analysis (DMA), dielectric analysis (DEA), and micro/nano-thermal analysis (μ/n-TA) (Menczel, Prime, et al., 2009).

3.3.1 DSC

A widely used technique for materials characterization in food (Larrea-Wachtendorff, Tabilo-Munizaga, Moreno-Osorio, Villalobos-Carvajal, & Pérez-Won, 2015), pharmaceutical (Klímová & Leitner, 2012), ceramics (Herek et al., 2012), and polymer applications (Majewsky, Bitter, Eiche, & Horn, 2016) among others. Briefly, a sample and a reference material are heated under a specific controlled temperature program. The heat flow rate difference is measured as a function of temperature thus, determining the thermal properties of the sample such as glass transition temperature (Tg), melt temperature (Tm), crystallization, cure reactions, oxidation, and decomposition (Menczel, Judovits, et al., 2009).

3.3.2 TGA

Thermogravimetric analysis is an analytical technique where the mass of a substance is measured as a function of temperature or time under a controlled temperature program and a controlled atmosphere. A thermobalance monitors the sample mass variation (loss or gain) upon heating within a specific temperature rage (Prime, Bair, Vyazovkin, Gallagher, & Riga, 2009).

Thermal analysis of polymers generally exhibits mass loss involving volatile components such as water content, residual solvents, monomers, oligomers, or low molar mass additives. Furthermore, the generation of volatile degradation products derived from chain scission may be characterized by TGA analysis resulting in thermal, thermo-oxidative stability, and kinetic analyses (Prime et al., 2009).

3.4 isotactic Polypropylene (i-PP)

A semi-crystalline olefin resin derived from the polymerization of propylene with a melting temperature (Tm) of approximately 165 °C and a glass transition temperature (Tg) of

approximately -15 °C. Polypropylene is divided into isotactic, syndiotactic, and atactic polypropylene. Among these three categories, Isotactic PP is the most relevant in the industry, its end-use applications are: film for packaging, fibres, crates, pipes, and automotive parts (usually modified PP with reinforcing fillers) (Becker, Burton, & Amos, 1996)(Van der Vegt, 2002). Figure 3.1 shows the chemical structure.

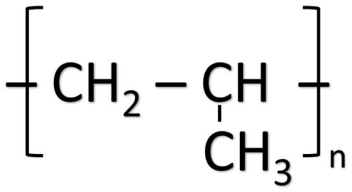

Figure 3.1. Polypropylene chemical structure.

3.4.1 DSC Thermal analysis

Bare un-stabilized isotactic polypropylene (i-PP, MFI= 40 g/10 min) was supplied from REPSOL Spain. Thermal analysis was performed with a TA instrument DSC Q100. A representative sample contained in a closed aluminum pan was evaluated under inert conditions (nitrogen, 50 mL/min) and according to the following summarized methodology: ramp 20.00°C/min to 190.00°C / Isothermal for 1 min / Ramp 10 °C/min to -10 °C / Isothermal for 1.0 min / Ramp 10 °C/min to 190 °C. The representative sample mass was kept similar (7.4 mg +/- 0.1).

3.4.1.1 Results

Endothermic events

Figure 3.2 presents the corresponding endothermic events from the DSC thermograms. The averaged melting point of the crystallites (Tm), the extrapolated onset melting point (Tm_{onset}), and the heat of fusion (Hm) values are presented in Table 3.1.

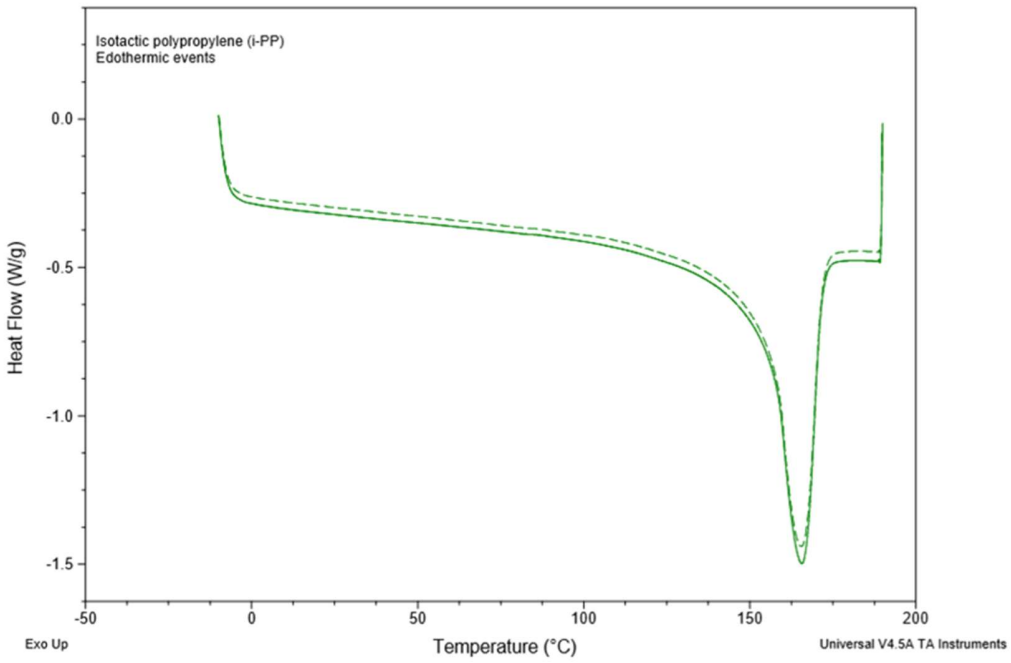

Figure 3.2. DSC thermal runs (endothermic events) for bare i-PP.

Material	Tm [°C]	+/-	Tm_{onset} [°C]	+/-	Hm [J/g]	+/-
i-PP	165.6	0.05	154.9	0.07	101.7	1.79

Table 3.1. Endothermic events values for bare isotactic polypropylene (i-PP). Results are expressed as the average of two replicates.

Exothermic events

Figure 3.3 shows the corresponding exothermic events from the DSC thermogram. The crystallization temperature (Tc), the extrapolated onset crystallization point (Tc_{onset}), and the heat of crystallization (Hc) values are presented in Table 3.2.

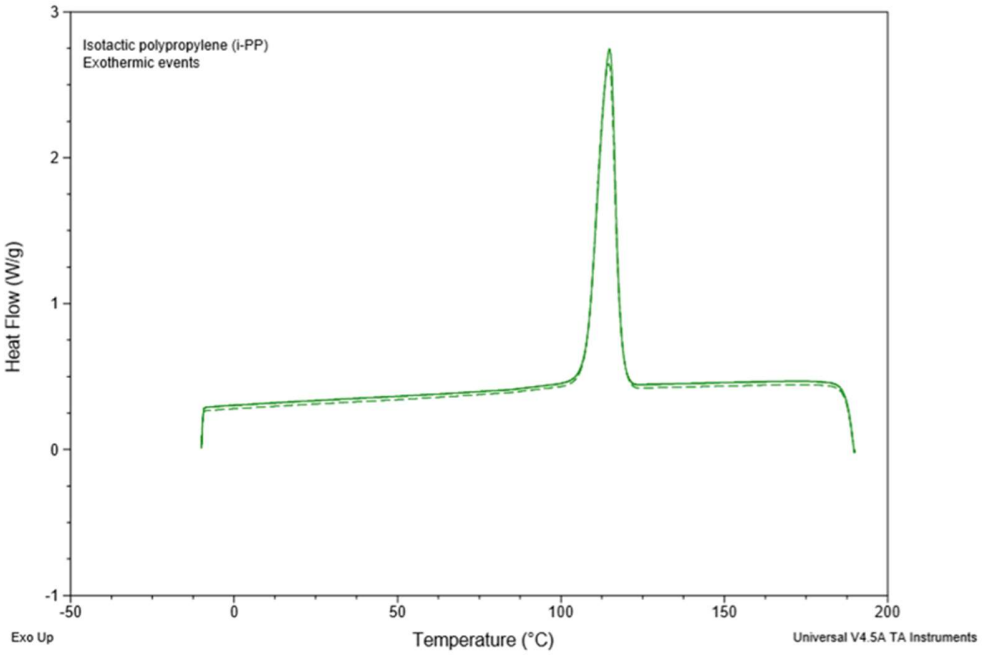

Figure 3.3. DSC thermal runs (exothermic events) for bare i-PP.

Material	Tc [°C]	+/-	Tc_{onset} [°C]	+/-	Hc [J/g]	+/-
i-PP	114.7	0.14	118.3	0.05	99.2	0.30

Table 3.2. Exothermic events values for bare isotactic polypropylene (i-PP). Results are expressed as the average of two replicates.

The endothermic peak observed for bare isotactic polypropylene (i-PP) from the DSC curve, corresponding to the averaged melting point of the crystallites (Tm), was at 166 °C with an extrapolated onset melting point at 155 °C. The crystallization process for i-PP followed by the DSC curve showed an exotherm peak (Tc) at 115 °C with an extrapolated initial crystallization temperature (TC_{onset}) at 118 °C.

Also, the degree of crystallinity (%c) was calculated according to the following equation:

$$\%c = \frac{Hm}{Hm_0} \quad (3.1)$$

Where Hm is the observed i-PP heat of fusion and Hm_0 is the heat of fusion of a 100% crystalline material, in the case of polypropylene Hm_0 is 207 J/g (Ehrenstein, Riedel, & Trawiel, 2004). Thus, the calculated percentage of crystallinity for bare i-PP is 49.1%.

3.4.2 TGA Thermal analysis

Bare un-stabilized isotactic polypropylene (i-PP, MFI= 40 g/10 min) was supplied from REPSOL Spain. Thermal analysis was performed with a TA instrument TGA Q50 in a dynamic mode from room temperature to 600°C at a heating rate of 10 °C/min under an inert atmosphere of nitrogen (60 mL/min).

3.4.2.1 Results

Figure 3.4 shows the TGA thermogram and the corresponding derivative curve (dTGA). Thermal degradation was assessed as the onset temperature (Tonset), maximum temperature (Tmax), the extrapolated end-set temperature (Tendset), and the temperature profile at 1% and 5% of mass loss ($T_{1\%}$, $T_{5\%}$). Table 3.3 presents the thermal events.

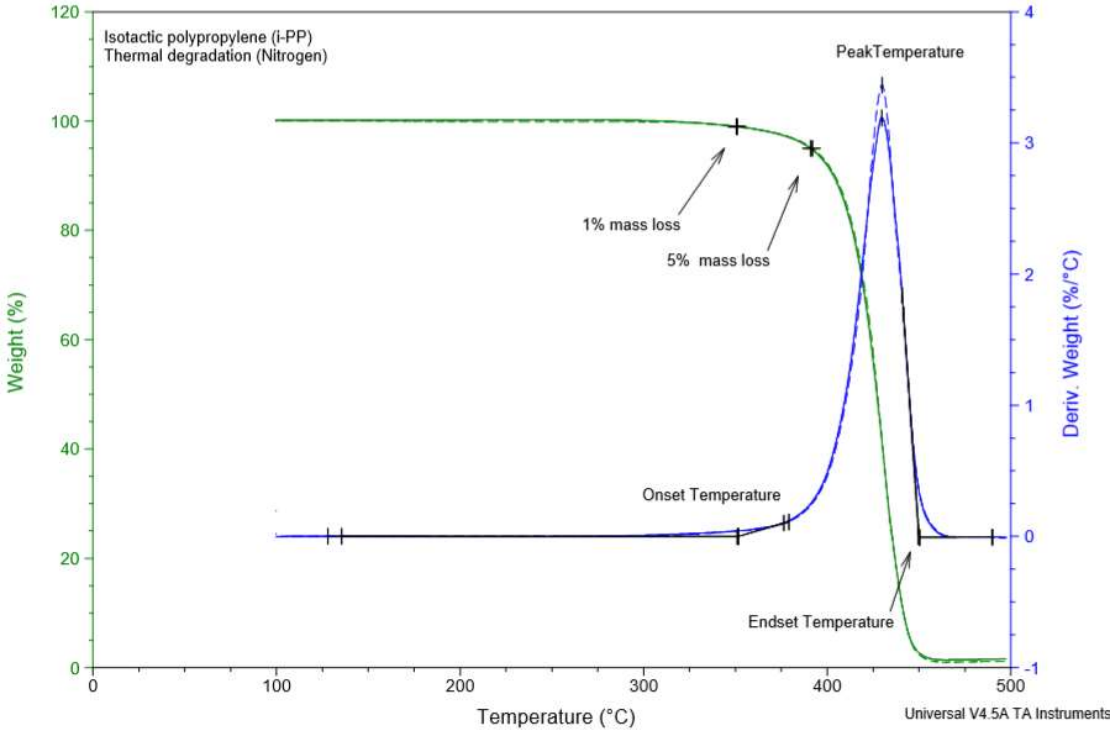

Figure 3.4. TGA and dTGA thermograms for bare isotactic polypropylene (i-PP).

Material	Tonset [°C]	+/-	Tmax [°C]	+/-	Tendset [°C]	+/-	$T_{1\% loss}$ [°C]	+/-	$T_{5\% loss}$ [°C]	+/-
i-PP	353.0	0.68	429.8	0.09	450.0	0.24	350.8	0.32	391.4	0.43

Table 3.3. TGA thermal degradation events for bare isotactic polypropylene (i-PP). Results are expressed as the average of two replicates.

The TGA thermogram for i-PP showed a single step thermal decomposition with an onset temperature (Tonset) of 353 °C, an observed peak temperature (Tmax) corresponding to the maximum rate of mass change, at 430 °C, and an extrapolated endset temperature (Tendset) of 450 °C. The thermal decomposition profile for i-PP assessed at 1 and 5% of mass showed temperatures of 351 and 391 °C respectively.

3.5 Low-density polyethylene (LDPE)

Polyethylene is a semi-crystalline olefin resin derived from the polymer synthesis of ethylene. It is produced mainly on three types: low-density polyethylene (LDPE) with a significant concentration of ethyl and butyl groups as branches resulting in a relative low density value in the range between 0.90 and 0.94 g/cm^3, high-density polyethylene (HDPE) with a high degree of crystallinity resulting in a higher density in the range between 0.94 and 0.97 g/cm^3, and linear-low-density polyethylene (LLDPE), a linear polyethylene backbone with random alkyl groups attached. LLDPE presents a density value between 0.90 and 0.94 g/cm^3.

The stiffness of polyethylene highly increases with density and presents melting points varying between 105 to 130 °C. The principal end-use applications are: packaging film, bags, pipes, crates, pails, bottles among others. Figure 3.5 shows the chemical structure (Peacock, 2000; Van der Vegt, 2002).

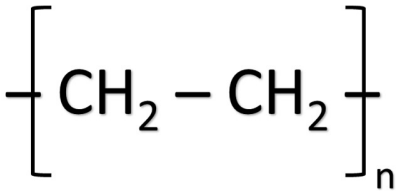

Figure 3.5. Low-density polyethylene chemical structure.

3.5.1 DSC Thermal analysis

Un-stabilized low-density polyethylene ($LDPE_{15}$, MFI= 1 g/10 min) was supplied from REPSOL Spain. Thermal analysis was performed with a TA instrument DSC Q100. A representative sample contained in a closed aluminum pan was evaluated under inert conditions (nitrogen, 50 mL/min) and according to the following summarized methodology: ramp 20.00°C/min to 190.00°C / Isothermal for 1 min / Ramp 10 °C/min to -10 °C / Isothermal

for 1.0 min / Ramp 10 °C/min to 190 °C. The averaged weigh of the samples was 6.9 mg +/- 0.2.

3.5.1.1 Results

Endothermic events

Figure 3.6 presents the corresponding DSC thermograms. The averaged melting point of the crystallites (Tm), the extrapolated onset melting point (Tm_{onset}), and the heat of fusion (Hm) values are presented in Table 3.4.

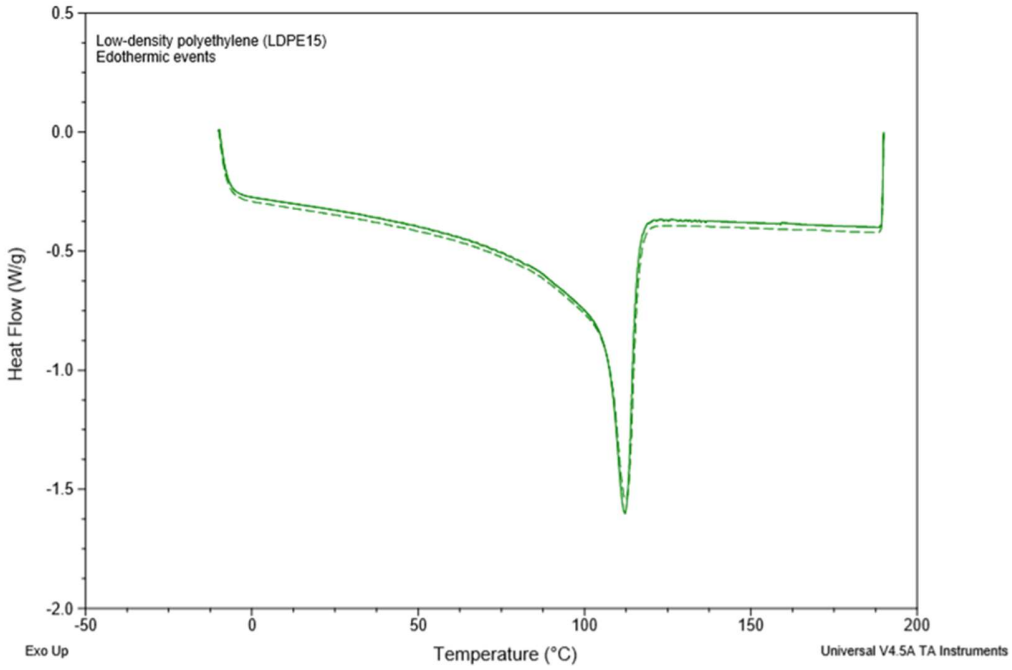

Figure 3.6. DSC thermal runs (endothermic events) for bare $LDPE_{15}$.

Material	Tm [°C]	+/-	Tm_{onset} [°C]	+/-	Hm [J/g]	+/-
$LDPE_{15}$	112.3	0.10	104.6	0.11	126.4	5.85

Table 3.4. Endothermic events values for bare low-density polyethylene ($LDPE_{15}$). Results are expressed as the average of two replicates.

Exothermic events

Figure 3.7 presents the corresponding DSC thermograms. The crystallization temperature (Tc), the extrapolated onset crystallization point (Tc_{onset}), and the heat of crystallization (Hc) values are presented in Table 3.5.

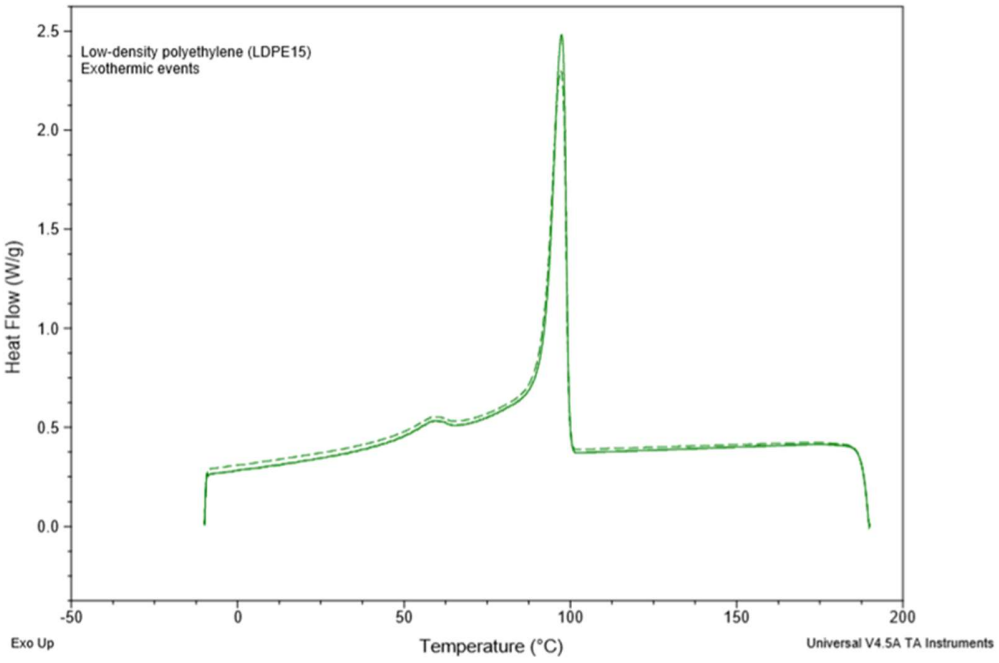

Figure 3.7. DSC thermal runs (exothermic events) for bare $LDPE_{15}$.

Material	Tc [°C]	+/-	Tc_{onset} [°C]	+/-	Hc [J/g]	+/-
$LDPE_{15}$	97.2	0.13	99.6	0.01	118.7	1.25

Table 3.5. Exothermic events values for bare low-density polyethylene ($LDPE_{15}$). Results are expressed as the average of two replicates.

Low-density polyethylene ($LDPE_{15}$) presented a melting point of approximately 112 °C and an extrapolated onset temperature (Tm_{onset}) of 105 °C. The crystallization process for $LDPE_{15}$ followed by the DSC curve showed an exotherm peak (Tc) at 97 °C with an extrapolated initial crystallization temperature (TC_{onset}) at 100 °C. Apparently, it is observed a second crystallization event at lower temperatures (~ 58 °C) nonetheless, there was not observed any melting peak in the same region possibly, due to the small crystallization peak area and a broad melting peak. The calculated percentage of crystallinity (%Xc) for $LDPE_{15}$ was 43.1% based on a Hm_0 of 293 J/g (Ehrenstein et al., 2004).

3.5.2 TGA Thermal analysis

Bare un-stabilized low-density polyethylene ($LDPE_{15}$, MFI= 1 g/10 min) was supplied from REPSOL Spain. Thermal analysis was performed with a TA instrument TGA Q50 in a dynamic mode from room temperature to 600°C at a heating rate of 10 °C/min under an inert atmosphere of nitrogen (60 mL/min).

3.5.2.1 Results

Figure 3.8 shows the TGA thermogram and the corresponding derivative curve (dTGA). Thermal degradation was assessed as the onset temperature (Tonset), maximum temperature (Tmax), the extrapolated end-set temperature (Tendset), and the temperature profile at 1% and 5% of mass loss ($T_{1\%}$, $T_{5\%}$). Table 3.6 presents the thermal events.

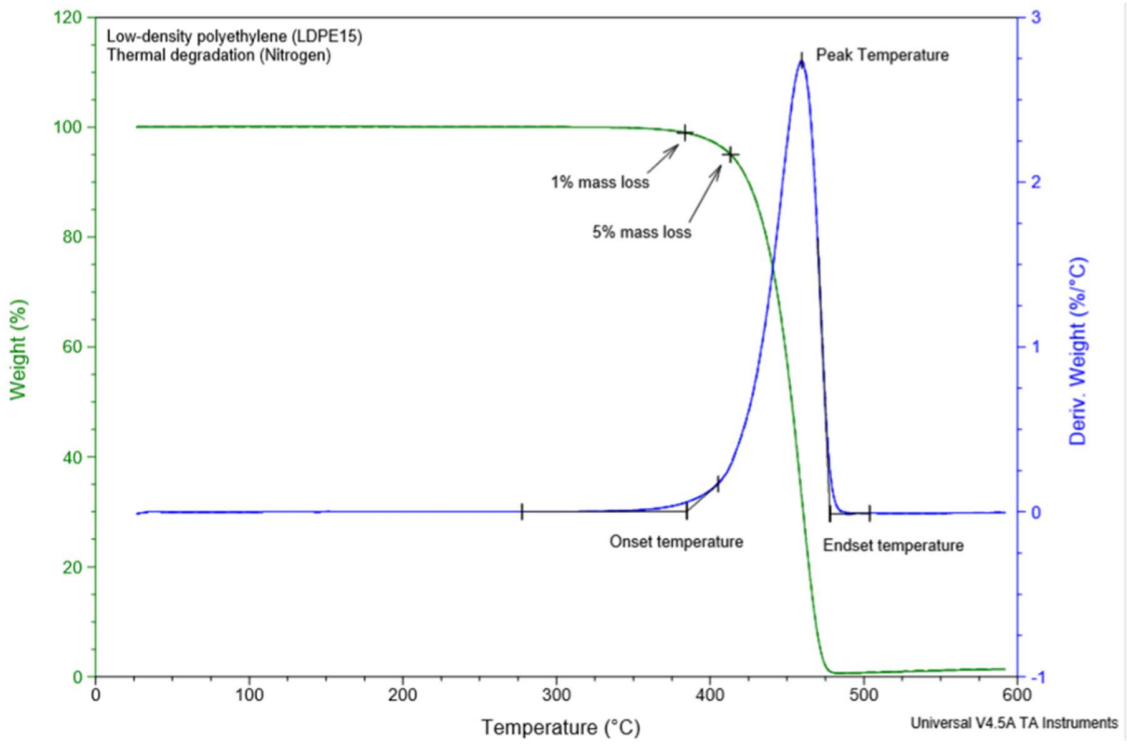

Figure 3.8. TGA and dTGA thermograms for bare low-density polyethylene ($LDPE_{15}$).

Material	Tonset [°C]	+/-	Tmax [°C]	+/-	Tendset [°C]	+/-	$T_{1\%\,loss}$ [°C]	+/-	$T_{5\%\,loss}$ [°C]	+/-
$LDPE_{15}$	373.3	0.54	459.4	0.19	478.0	0.13	384.2	0.52	413.6	0.25

Table 3.6. TGA thermal degradation events for bare low-density polyethylene ($LDPE_{15}$). Results are expressed as the average of two replicates.

The TGA thermogram for $LDPE_{15}$ showed a single step thermal decomposition with an extrapolated onset temperature (Tonset) of 373 °C, an observed peak temperature (Tmax) corresponding to the maximum rate of mass change at 459 °C, and an extrapolated endset temperature (Tendset) of 478 °C. The thermal decomposition profile for $LDPE_{15}$ assessed at 1 and 5% of mass showed temperatures of 384 and 414 °C respectively.

Both un-stabilized resins were evaluated by DSC and TGA. From DSC curves it is important to consider the melting point (Tm) as the temperature where the averaged crystals melt thus, providing an estimation of the processing conditions in terms of temperature during extrusion. In the case of the TGA analysis, both resins presented a single step thermal decomposition profile where $LDPE_{15}$ showed a higher thermal stability compared to i-PP with observed initial thermal degradation temperatures (Tonset) of 373 °C and 353 °C respectively.

3.6 Extrusion

The extrusion process of polyolefins is a sequential process where the extrusion step comprises: the feeding of a polymer in the form of powders, beads, flakes, pellets, and/or their combination, the heating and transport of the molten polymer through a heated barrel (screw) forcing the melted polymer to exit through a dye to shape the final plastic product (Rosato, Rosato, & Rosato, 2004). The following scheme presented in Figure 3.9 illustrates the overall sequential steps to produce the finished product.

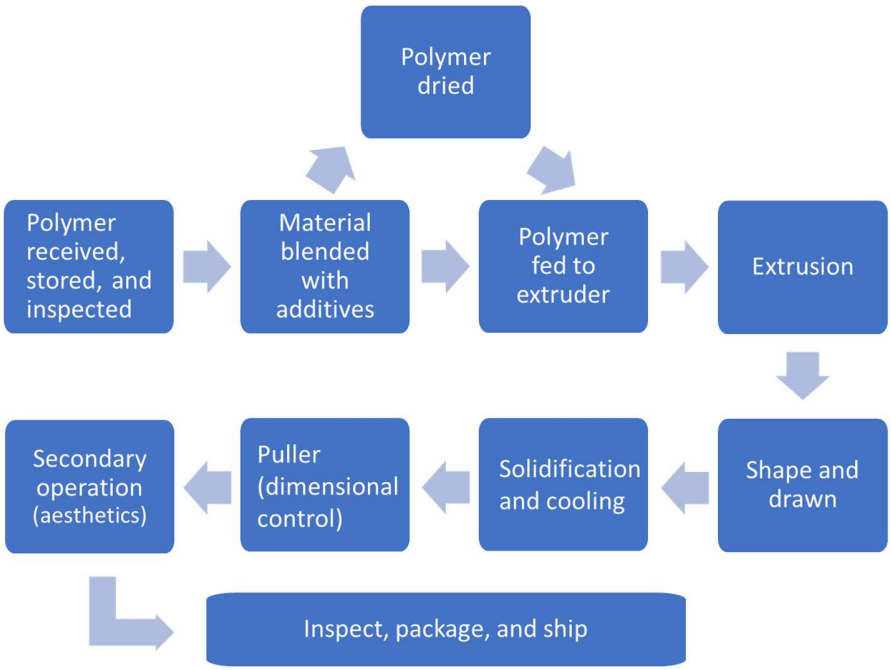

Figure 3.9. Representation of a basic extrusion process (Wagner Jr, Mount III, & Giles Jr, 2014a).

Prior to polymer formulation, bare un-stabilized low-density polyethylene ($LDPE_{15}$) and bare un-stabilized isotactic polypropylene (i-PP) were processed as received by extrusion process at different temperatures and a constant rate. The effect of temperature and mechanical stresses were assessed by thermal analysis evidencing possibly, any molecular weight variations by means of thermal stability.

3.6.1 Materials and Methods

Bare un-stabilized isotactic polypropylene (i-PP, MFI= 40 g/10 min) and bare un-stabilized low-density polyethylene ($LDPE_{15}$, MFI= 1 g/10 min) were supplied from REPSOL Spain (Technical data sheet in Annex A).

3.6.1.1 Thermal Analysis

The thermal stability of the extrudate $LDPE_{15}$ and i-PP was characterized by DSC and TGA on a TA instrument DSC Q100 and a TA instrument TGA Q50 respectively.

DSC analysis

A representative sample contained in a closed aluminum pan was evaluated under inert conditions (nitrogen) and according to the following summarized methodology: ramp 20.00°C/min to 190.00°C / Isothermal for 1 min / Ramp 10 °C/min to -10 °C / Isothermal for 1.0 min / Ramp 10 °C/min to 190 °C.

TGA analysis

TG analysis was performed in a dynamic mode from room temperature to 600°C at a heating rate of 10 °C/min under an inert atmosphere of nitrogen (60 mL/min).

3.6.1.2 Experimental

Extrusion was performed on a LabTech twin co-rotating extruder with 16 mm diameter screw and length to diameter (L/D) ratio of 40. The extrusion system is provided with a water bath, a puller band system, and a pelletizer. Table 3.7 presents the extrusion temperature profiles for i-PP and $LDPE_{15}$.

Extrusion temperatures profile [°C]										
DIE	**Z9**	**Z8**	**Z7**	**Z6**	**Z5**	**Z4**	**Z3**	**Z2**	**Z1**	**Input Material**
230	230	230	230	230	230	160	150	120	80	i-PP
220	220	220	220	220	220	160	150	120	80	
210	210	210	210	210	210	160	150	120	80	
200	200	200	200	200	200	160	150	120	80	
190	190	190	190	190	190	160	150	120	80	
180	180	180	180	180	180	160	150	120	80	
190	190	190	190	190	180	150	140	120	80	$LDPE_{15}$
180	180	180	180	180	170	150	140	120	80	
170	170	170	170	170	170	150	140	120	80	
160	150	150	150	150	150	150	140	120	80	

Table 3.7. Extrusion temperatures profiles for un-stabilized isotactic polypropylene (i-PP) and low-density polyethylene ($LDPE_{15}$).

Extrusion experimental runs

Calibration curves for the dosing feeder system on i-PP and $LDPE_{15}$ were performed prior to extrusion to fix constant the output rate. The screw speed was set at 300 rpm and the individual extrusion temperatures profiles according to Table 3.7. The puller speed was kept constant and the strand (extrudate) grinded into a 1 mm pellet size.

3.6.1.3 Results

The effect of extrusion temperature on i-PP and $LDPE_{15}$ was evaluated by DSC. In the case of i-PP (Table 3.8), it is observed no significant difference between the means of melting temperature (Tm) and crystallization temperature (Tc) under the experimental conditions evaluated (ANOVA analysis, α= 0.05).

Material	Extrusion [°C]	Tm [°C]	Hm [J/g]	Tc [°C]	Hc [J/g]	Crystallinity [%c]
i-PP	190	165.5	102.2	114.7	93.4	49.4
	210	166.0	110.5	115.5	100.6	53.4
	220	165.6	103.2	117.0	95.1	49.9
	230	165.5	118.6	116.2	107.4	57.3

Table 3.8. Summarized DSC results for isotactic polypropylene (results are expressed as the average of two replicates): melting Temperature (Tm), heat of fusion (Hm), crystallization temperature (Tc), heat of crystallization (Hc), and percentage of crystallinity (%c).

Also, DSC thermal results on $LDPE_{15}$ (Table 3.9) showed no significant difference between the means of melting temperature (Tm) and crystallization temperature (Tc) under the experimental conditions evaluated (ANOVA analysis, α= 0.05).

Material	Extrusion [°C]	Tm [°C]	Hm [J/g]	Tc [°C]	Hc [J/g]	Crystallinity [%c]
$LDPE_{15}$	150	112.3	101.0	97.3	85.2	34.5
	170	112.0	95.7	97.0	76.9	32.7
	180	112.3	102.9	96.8	79.3	35.1
	190	112.4	102.3	96.8	79.5	34.9

Table 3.9. Summarized DSC results for low-density polyethylene (results are expressed as the average of two replicates): melting Temperature (Tm), heat of fusion (Hm), crystallization temperature (Tc), heat of crystallization (Hc), and percentage of crystallinity (%c).

Polypropylene and polyethylene undergo different degradation paths. It is observed a higher percentage of crystallinity in i-PP extruded at 230 °C (%c 57%) as compared to the rest of the extrusion temperatures evaluated. This result may be possibly attributed to the thermo-oxidative degradation mechanism of polypropylene which involves predominantly β-scission reactions, where the shorter length of the resulting n^{th} degraded molecules enhances the mobility of polymer chains (lower viscosity) thus, the ease of further crystal growth represented as an increment in the percentage of crystallinity.

Furthermore, this increment in crystallinity is also represented by an increment in the heat of fusion (Hm). It is also reported that, at various injection molding cycles no changes in the melting temperature was observed thus, confirming that the crystal conformation remained constant (da Costa, Ramos, & de Oliveira, 2007; Guerrica-Echevarría, Eguiazábal, & Nazábal, 1996).

In the case of polyethylene, the thermo-oxidative degradation mechanism involves competition reactions between chain-scission and crosslinking reactions. It is reported from literature that the crosslinking reactions are dominant at lower temperatures whereas chain scission reactions dominate at higher temperatures (thermal scission) (Hoàng, Allen, Liauw, Fontán, & Lafuente, 2006; Johnston & Morrison, 1996; Ono & Yamaguchi, 2009). Probably, a higher stability during processing may be observed.

All these observations have been corroborated in literature when either the polymer is exposed under an oxidative source for prolonged times such as photo-oxidation (Rabello & White, 1997) and extended processing times such as multi-extrusion cycles analysis (Guerrica-Echevarría et al., 1996).

The residence time for a single extrusion is in the order of minutes. For example, in a co-rotating twin-screw extruder system (40 mm diameter) at different screw speeds, ranging between 75 rpm and 225 rpm, it is reported a residence time between 70 and 105 seconds (Wagner Jr, Mount III, & Giles Jr, 2014b).

Hence, the experimental results show that, under the experimental conditions evaluated, there are no changes in the melting temperature and crystallization temperature for i-PP and $LDPE_{15}$ possibly due to a very short residence time. Figure 3.10 and Figure 3.11 show the plotted results of the experimental runs for i-PP and $LDPE_{15}$ respectively.

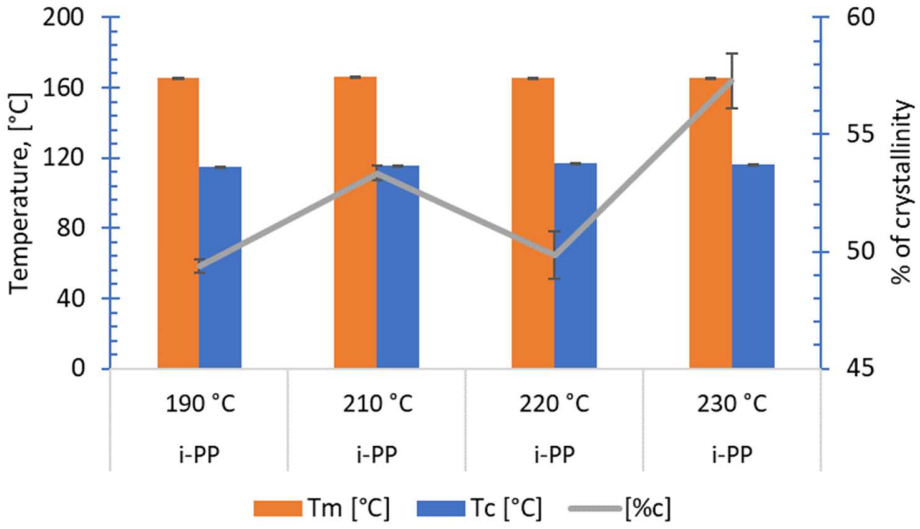

Figure 3.10. Polypropylene melting temperature (Tm), crystallization temperature (Tc), and percentage of crystallization (%c) results.

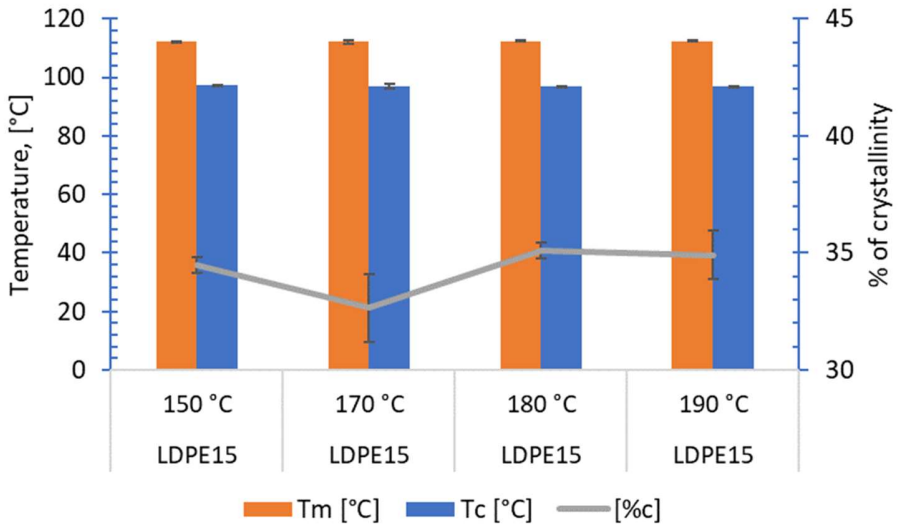

Figure 3.11. Low-density polyethylene melting temperature (Tm), crystallization temperature (Tc), and percentage of crystallinity (%c) results.

Samples were analyzed by TGA to assess the degradation profile on i-PP and $LDPE_{15}$ after extrusion trials. Two representative extrusion temperatures were evaluated: 220 °C and 190 °C for i-PP and 190 °C and 150 °C for $LDPE_{15}$ respectively. Figure 3.12 and 3.13 show the corresponding percentages of residual mass as a function of temperature.

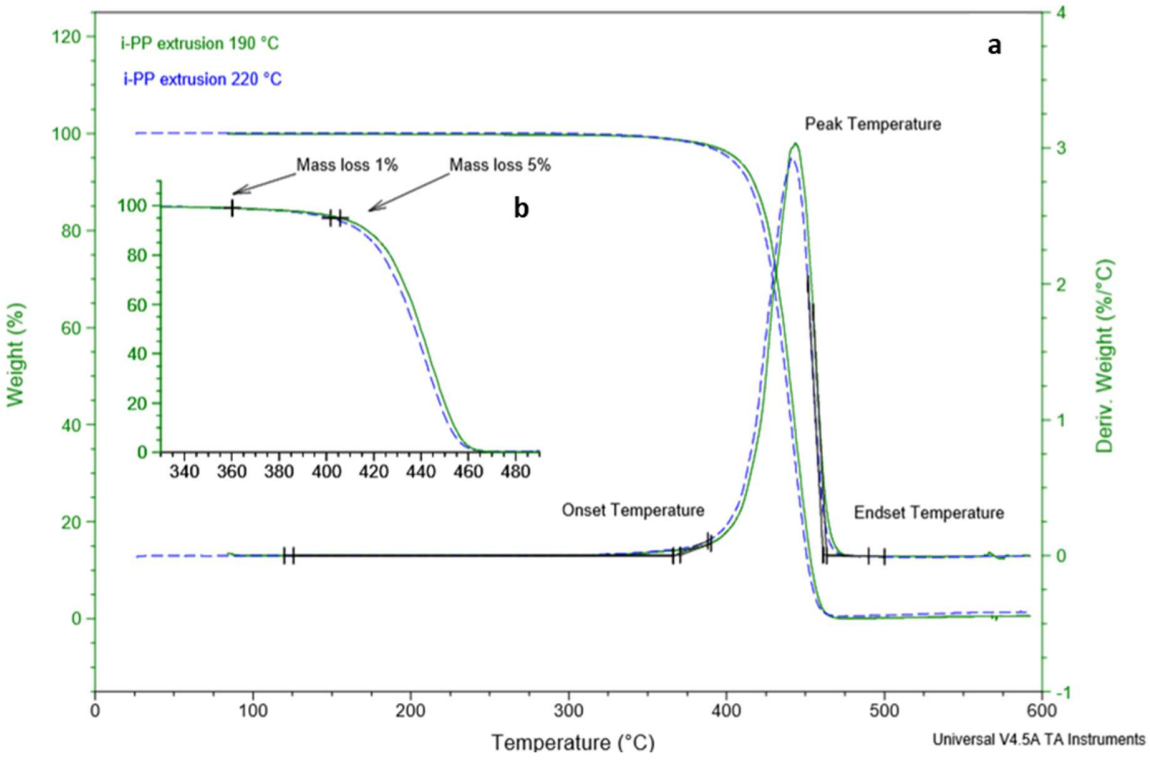

Figure 3.12. **a** TGA and dTGA thermograms for polypropylene. **b** Insert of TGA curve of mass loss.

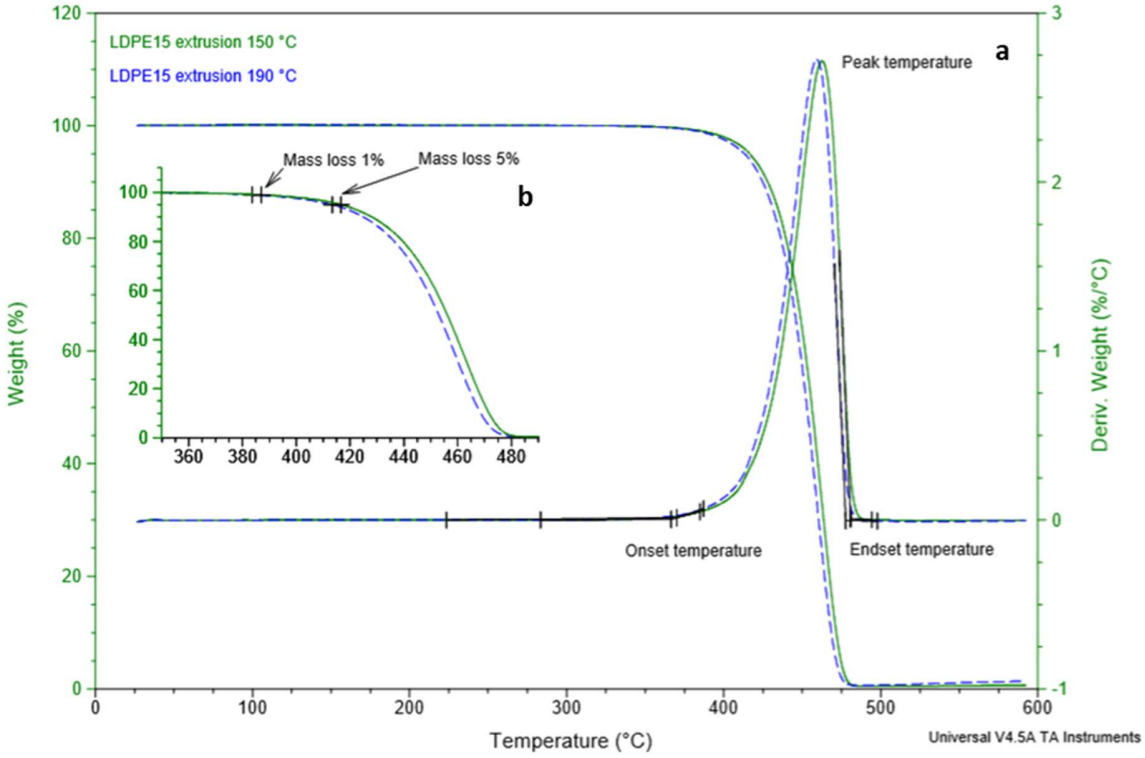

Figure 3.13. **a** TGA thermograms for low-density polyethylene. **b** Insert of TGA curve of mass loss.

Material	Extrusion [°C]	Tonset [°C]	Tmax [°C]	Tendset [°C]	$T_{1\% loss}$ [°C]	$T_{5\% loss}$ [°C]
i-PP	190	358.1	443.6	463.5	360.1	405.8
i-PP	220	352.3	441.5	461.1	360.5	401.7

Table 3.10. TGA thermal degradation events for bare isotactic polypropylene (i-PP).

Material	Extrusion [°C]	Tonset [°C]	Tmax [°C]	Tendset [°C]	$T_{1\% loss}$ [°C]	$T_{5\% loss}$ [°C]
$LDPE_{15}$	150	370.3	462.6	480.6	387.0	416.6
$LDPE_{15}$	190	361.5	459.3	477.7	383.7	413.3

Table 3.11. TGA thermal degradation events for bare low-density polyethylene ($LDPE_{15}$).

TGA results confirmed the effect of extrusion temperatures on i-PP and $LDPE_{15}$ as it is observed that, higher processing extrusion temperatures lower the initial decomposition temperature as shown in Table 3.10 and Table 3.11. Thus, indicating an extent of polymer degradation.

Align to the scope of this chapter, it is proposed and standardized two test-methods followed by thermal analysis to best assessed the thermal stability of i-PP and $LDPE_{15}$: the oxidation onset temperature (OOT) and thermal decomposition kinetics.

3.7 Onset Induction Time (OIT) and Oxidation Onset Temperature (OOT)

Previously discussed in chapter I, polyolefins induced by an energy source (heat and light) produce alkyl radicals and, in the presence of oxygen yield peroxy radicals which further abstracts a hydrogen from a contiguous polyolefin molecule thus, propagating in a chain reaction (degrading the polyolefin).

The presence of an antioxidant system delays polymer degradation and this may be followed by DSC as the oxidation induction time (OIT) and oxidation onset temperature (OOT) test methods. The analytical methods are well established and simple to perform.

According to the ASTM D3895 standard, the OIT test method consists of heating a sample at 200°C at a constant rate (dynamic mode) under an inert atmosphere (Nitrogen). When the fixed temperature is reached, the atmosphere is changed to oxygen (or air) and the sample is held at a constant temperature (isothermal). The oxidation reaction process is represented as an exothermic event thus, the time from the initial oxygen flow exposure to the time of the inflection point of oxidation is considered as the OIT value. The higher the OIT value the higher the thermo-oxidative stability. Figure 3.14 illustrates the schematic representation of the OIT procedure.

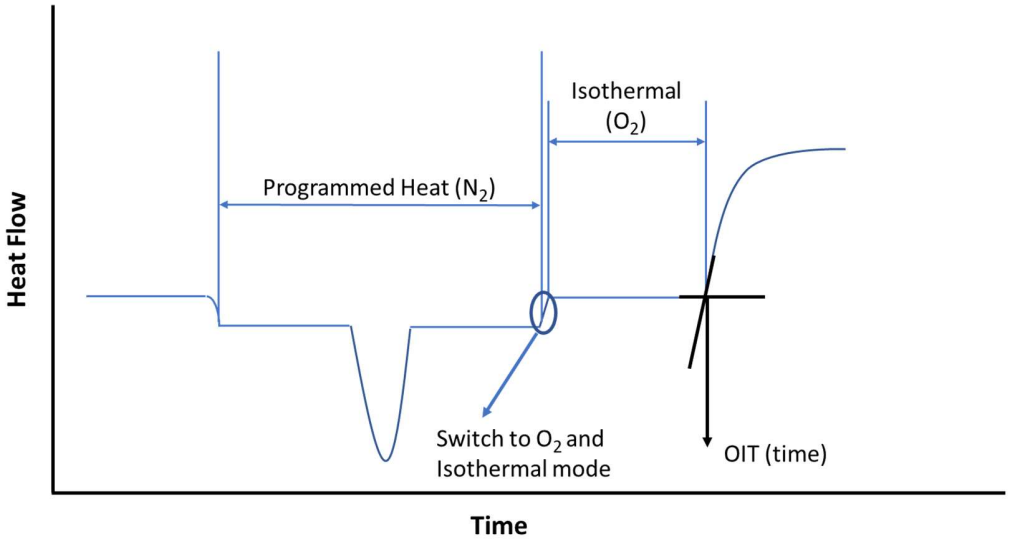

Figure 3.14. Schematic diagram for the OIT procedure (adapted from ASTM D3895).

The standardize method (ASTM D3895) recommends a temperature range between 180 °C and 200 °C depending on the stabilization (known antioxidant concentration). Isothermal heating conditions ranging between 190 °C and 220 °C (Fearon, Bigger, & Billingham, 2004) have been also reported for different polymers. Table 3.12 illustrate the test method conditions.

Onset Induction Time (OIT)						
Sample mass [mg]	Gas flow [mL/min]	Inert atmosphere	Oxidative atmosphere	heating rate [°C/min]	Isothermal [°C]	Reference
5 - 10	50	N_2	O_2	20	200	a
2 & 8	20 & 60	N_2	O_2	10 & fast*	210	b
5 - 15	50	N_2	O_2	20	210	c
15	20 under N_2 150 under Air	N_2	O_2	2, 10, 40	120 - 250	d
~71.5	50	N_2	O_2	20	180	e
5 - 10	50	Ar	O_2	20	200	f
94.6	50	N_2	O_2	20	200	g

Table 3.12. Summary of test method (OIT). *heating rate not reported. a. (*ASTM D3895-14, Standard Test Method for Oxidative-Induction Time of Polyolefins by Differential Scanning Calorimetry*, 2014) b. (Rosa, Sarti, Mei, Filho, & Silveira, 2000) c. (M Schmid, Ritter, & Affolter, 2006) d. (Wallius, 1993) e. (Volponi, Innocentini Mei, & dos Santos Rosa, 2004) f. (Araújo, Waldman, & De Paoli, 2008) g. (Gao et al., 2007).

The isothermal conditions depend on the polymer resin evaluated but also, it may be considered the total running test time to optimize the test-method. Sample mass reported in literature varied between 2 mg and 94.6 mg, the recommendation is to keep less mass variation between measurements for comparison purpose. The inert atmosphere mostly used is nitrogen, whereas the oxidative atmosphere is oxygen, though air may be also utilized.

The oxidation onset temperature (OOT) test method determines the stability of a polymer-based material when is exposed into an oxidative atmosphere (O_2 or air) and temperature. Figure 3.15 shows a schematic layout representing the OOT test method.

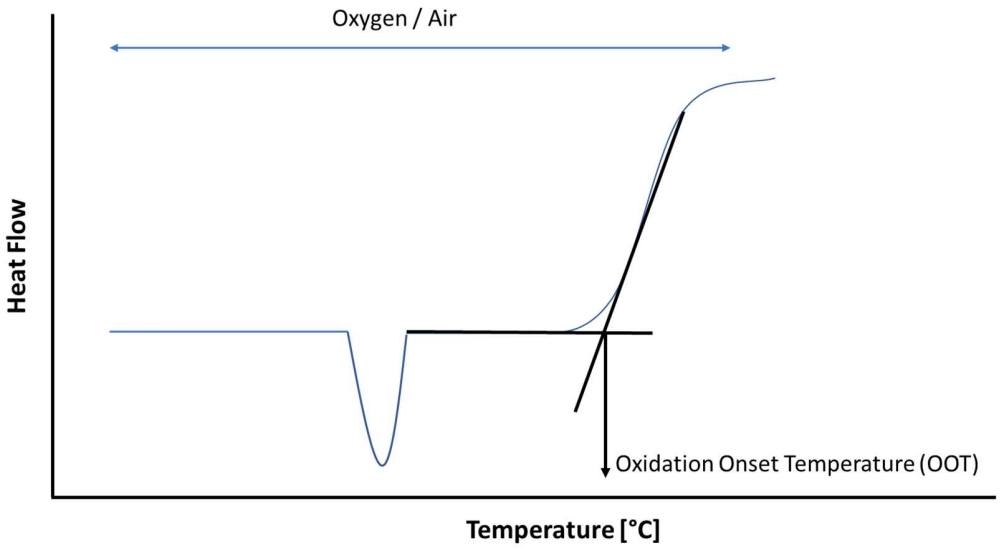

Figure 3.15. Schematic representation for the determination of OOT by DSC (Manfred Schmid & Affolter, 2003).

A sample is heated in dynamic conditions (constant rate in °C/min) and the onset point (inflection point) in temperature, represented as an exothermic peak resulting from the oxidation reaction, represents the oxidation onset temperature. The higher the OOT value the more stable the material (higher thermo-oxidative stability). Table 3.13 depicts the main variables involved in the test method.

Oxidation Onset Temperature (OOT)					
Sample mass [mg]	Gas flow [mL/min]	Oxidative atmosphere	heating rate [°C/min]	Range of temperature [°C]	Reference
5	50	O_2	10	50 - 250	h
3	50	O_2	10	250	i
4	50	O_2	10	50 - 500	j
5	100	Air	20	280	k
5	*	Air	3	130 - 300	l
*	20	Air	10	30-300	m

Table 3.13. Summary of test method (OOT). * Data not reported. h. (Okamba-Diogo et al., 2016) i. (Astruc, Bartolomeo, Fayolle, Audouin, & Verdu, 2004) j. (Fiorio, D'hooge, Ragaert, & Cardon, 2018) k. (Blom, Yeh, Wojnarowski, & Ling, 2006) l. (Gregorová, Cibulková, Košíková, & Šimon, 2005) m. (Grabmayer et al., 2014).

The dynamic heating conditions reported in literature varied from 3 °C/min to 20 °C/min, being more common the range between 10 °C and 20 °C. Same consideration for sample mass, a reduced mass variation between measurements ensures reproducibility. The sample working gas reported is air and oxygen and the range of temperature for the test is dependent on the polymer sample evaluated.

3.7.1 Assumptions

Oxidation induction time (OIT) test method is used to assess the stability of polymers in the solid state (Mason & Reynolds, 1997) to predict the polymer lifetime based mainly, on their working conditions (temperature and environment) (Pospíšil et al., 2003; Woo, Khare, Sandford, Ling, & Ding, 2001) or as a complement to evaluate polymer stability in accelerated testing methods such as accelerated weathering test (exposure to carbon and xenon arc lamps and to fluorescent UV lamps), outdoor weathering of plastics (ASTM D 1435, ISO-877), and long-term heat resistance test (ASTM D794) (Vishu, 2006).

Oxidation induction time is a reproducible and standardize method to assess polymer stability under thermo-oxidative conditions however, there are some disadvantages:

- The uncertainty of the method when analyzing non-stabilized polymers is high due to a rapid oxidation after oxygen flow is fed during the analysis (Manfred Schmid & Affolter, 2003),

- OIT is time consuming, depending on the experimental temperature, test method may take up to hours with an additional time to determine the best isothermal test temperature (Ilie & Senetscu, 2009),

- Inter-laboratory studies confirmed a higher variation (standard deviation) for OIT measurements particularly, when lower OIT times are present (10 – 20 minutes) a high variation is observed (up to a 60% of variation) (Manfred Schmid & Affolter, 2003).

Based on the above, the oxidation onset temperature (OOT) test method is proposed considering the following assumption:

- To assess the thermo-oxidative stability of the polymer during polymer processing: a solid sample is fed, heated, melted, and forced to exit through a die. Followed by DSC analysis in a dynamic mode: from room temperature (solid state) up to the inflection point in temperature that corresponds to the oxidation onset temperature (generally above polymer melting temperature).

3.7.2 Effect of extrusion process on polymer degradation

Olefin resins are prone to degradation during extrusion process derived from thermal and mechanical stresses. Thus, it is of importance to assess the effect of polymer processing conditions such as extrusion temperature, screw speed (shear), and output on the degradation process to design a formulation with thermal stabilizers.

3.7.2.1 Materials and Methods

Bare un-stabilized isotactic polypropylene (i-PP), MFI= 40 g/10 min; bare un-stabilized low-density polyethylene ($LDPE_{15}$), MFI= 1 g/10 min and commercial low-density polyethylene ($LDPE_{33}$) with an antioxidant package formulation and MFI= 0.3 g/10 min, were supplied from REPSOL Spain.

Oxidation onset temperature (OOT) for bare i-PP and $LDPE_{15,33}$

Thermo-oxidative stability of bare un-stabilized i-PP, bare un-stabilized $LDPE_{15}$, and commercial $LDPE_{33}$ was assessed by DSC analysis following the methodology for OOT determination. Briefly, a representative sample is heated in an open aluminum pan under air (60 mL/min), as the oxidative atmosphere, in a dynamic heating mode: 10°C/min.

Extrusion processing

Extrusion was performed on a LabTech twin co-rotating extruder with 16 mm diameter screw and length to diameter (L/D) ratio of 40. The extrusion system is provided with a water bath, a puller band system, and a pelletizer.

3.7.2.2 Experimental

A fractional factorial design of experiments was implemented to evaluate the significance of the effects of the variables implied in the extrusion process on OOT determination. For this, i-PP was selected for experimentation based on their degradation mechanism and its susceptibility to degrade. Table 3.14 shows the input parameters with two factors.

Factor	Notation	Factor Levels	
		Low (-)	High (+)
Extrusion Temperature (°C)	ET	170	220
Dosing Feeder (rpm)	FR	10	30
Screw Speed (rpm)	SS	425	150

Table 3.14. 2^{k-1} experimental design. Levels were coded as (-1) and (+1) for low and high levels.

3.7.2.3 Results

Oxidation onset temperature determination on bare materials

Oxidation onset temperature (OOT) measurements were performed by DSC (Table 3.15). Results are expressed as the average of two replicates.

Material	Formulation	OOT [°C]	StdDev
$LDPE_{33}$	Bare	225.1	1.40
$LDPE_{15}$	Bare	215.8	0.68
i-PP	Bare	206.9	0.29

Table 3.15. DSC results on OOT for un-stabilized bare polypropylene (i-PP), un-stabilized bare low-density polyethylene ($LDPE_{15}$), and commercial bare low-density polyethylene ($LDPE_{33}$).

It is important to determine the thermo-oxidative stability of the bare resins before experimental manipulation. From Table 3.15 it is observed a higher OOT value for the commercial $LDPE_{33}$ as compared to $LDPE_{15}$ this, is probably derived from the antioxidant system present in the commercial resin. In addition, there is a difference of approximately 9 °C between LDPE samples whereas the standard deviation represented less than 1% of the averaged OOT values. Thus, the OOT results differentiated the thermo-oxidative stability for LDPE samples. The lower OOT value observed is for i-PP, approximately 18 °C lower than the commercial $LDPE_{33}$.

3.7.2.3.1 Effect of extrusion parameters on i-PP stability

Prior to extrusion trials, a calibration curve was performed in triplicate for the dosing feeder (Figure 3.16) to corroborate the output in grams per minute.

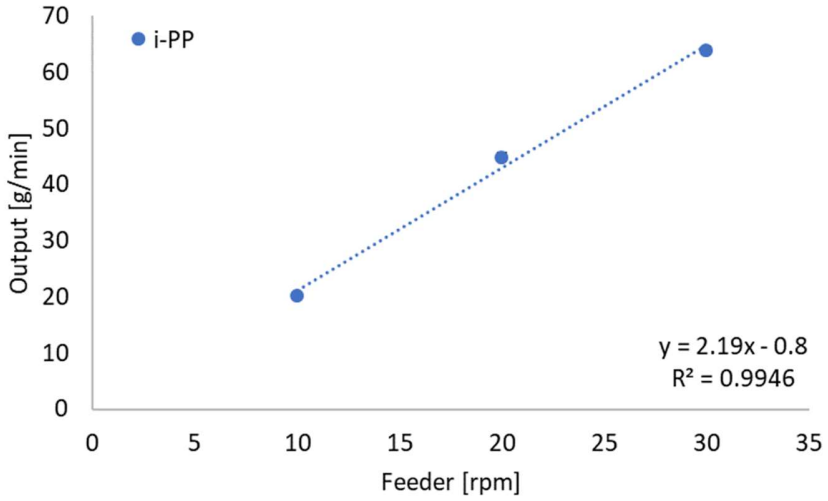

Figure 3.16. Isotactic polypropylene (i-PP) calibration curve for the dosing feeder.

Extrudate was analyze by DSC under the methodology above described. Table 3.16 shows the results in OOT for the experimental runs (results are expressed as the average of three replicates).

				OOT	
Test	ET	FR	SS	°C	StdDev
Std Order 3	-1	1	-1	206.7	2.04
Std Order 5	-1	-1	1	207.9	1.00
Std Order 2	1	-1	-1	212.7	1.88
Std Order 8	1	1	1	203.5	3.08

Table 3.16. Effect of factors on i-PP thermal stability by OOT test method.

Results from the fractional factorial design, show that, under the experimental conditions evaluated, there is a significant effect (ANOVA, $p < 0.05$, $r^2 = 0.75$) from the dosing feeder (FR) and screw speed (SS) terms on the i-PP thermo-oxidative stability by means of OOT. The coded regression equation of the fitted model is represented by equation 3.2:

$$OOT = 207.970 + 0.100\ ET - 2.320\ FR - 2.290\ SS \quad (3.2)$$

Were both, FR and SS terms, influence negatively on the OOT value. In other words, the higher the screw speed and output, the lower the OOT value indicating lesser thermo-oxidative stability. Figure 3.17 shows the Pareto of the standardized effects.

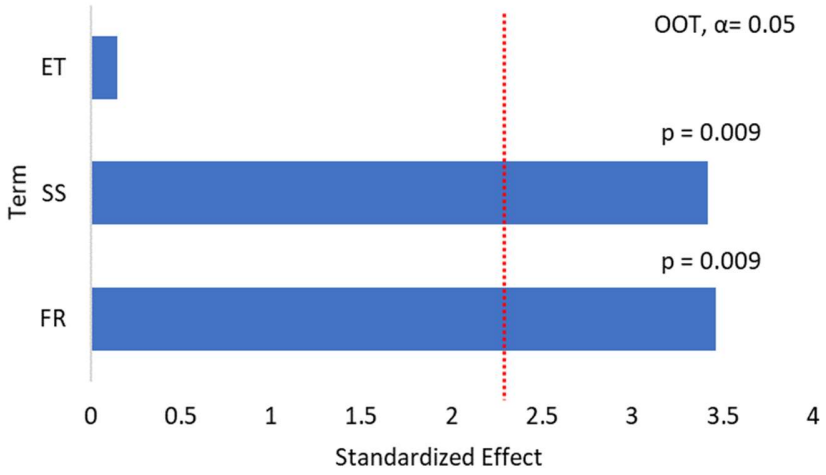

Figure 3.17. Pareto of standardized effects on i-PP thermo-oxidative stability analysis.

Figure 3.17 illustrates the significance of the standardized effects of the independent variables ($p < 0.05$). Results are in line with those observed in (da Costa et al., 2007). Authors concluded that degradation is more important at high shear levels than at high extrusion temperatures.

3.7.4 Effect of heating rate on OOT determination (Test-method optimization)

As mentioned before, two of the most important parameters in thermal analysis are sample mass and heating rate. In light of this information, it was evaluated the effect of different heating rates (°C/min) on the OOT value determined by DSC analysis (sample mass pooled standard deviation of +/- 0.49 mg).

Polypropylene formulated with Vitamin E (i-PP/Vit. E) was selected as the control sample to assess the experimental runs. Table 3.17 shows the DSC results of OOT determination at different heating rates.

Material	Formula	Heating Rate [°/min]	Sample Mass [mg]	StdDev +/-	OOT [°C]	StdDev
i-PP	i-PP/Vit. E	5	8.6	0.1	246.8	0.04
		10	9.9	0.25	259.8	0.24
		15	9.0	0.15	266.4	0.13
		20	8.6	0.2	272.2	0.43
		30	9.1	0.15	280.4	0.43

Table 3.17. OOT results. Results are expressed as the mean of two replicates.

Results were plotted in a semi-log plot to validate linearity as shown in Figure 3.18. It is observed that, at a heating rate of 5 ºC and 30 ºC the OOT value is out of the linear domain. Linearity is observed within a heating range between 10 ºC and 20 ºC (shadowed region).

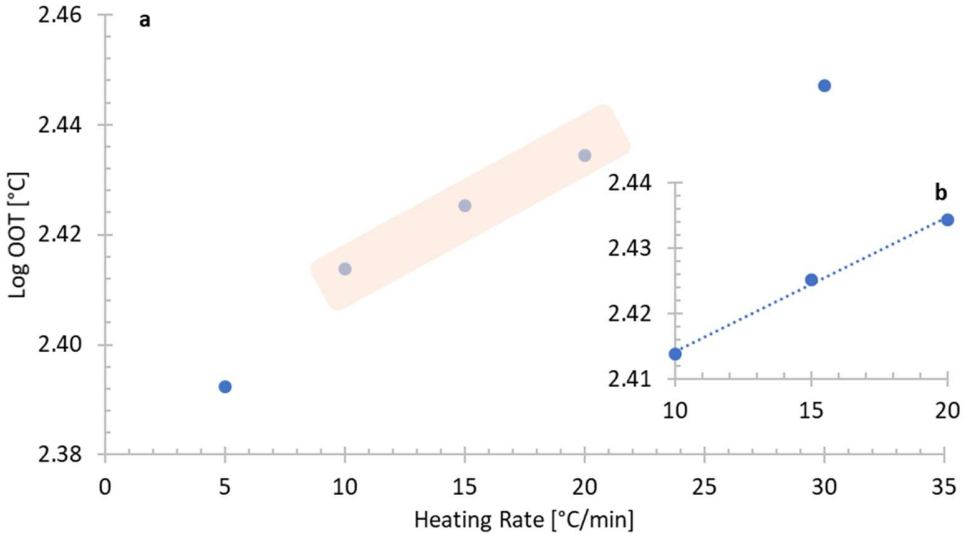

Figure 3.18. OOT values at different heating rates. **a**. Log of OOT vs heating rate **b**. Linear domain.

It was shown in Table 3.17, the different heating rate conditions used in the OOT determination reported from bibliography. Different authors have performed the test method within a heating range between 10 ºC and 20 ºC, this is also recommended in the standard

BS EN ISO 11357-6:2018. Within the linear domain observed in Figure 3.18 results are reproducible (r^2 = 0.998).

3.8 Decomposition Kinetics

Kinetic analysis in TGA correlates the time (t), temperature (T), and conversion (α) to estimate or predict the processing conditions, service lifetimes, and storage of materials. In thermal analysis, the rate of change in thermally stimulated processes, at a constant (ambient) pressure, can be expressed in terms of two mayor variables: temperature and conversion. Where temperature is controlled by the instrument (programmed) and the extent of conversion at a determined temperature is calculated from mass loss measurements (Equation 3.3).

$$\alpha = \left(\frac{m_i - m_t}{m_i - m_f}\right) \tag{3.3}$$

Where m_i, m_t, and m_f are the initial mass of the sample, the actual mass at a specific point in the curve, and the final mass for a given step of mass change respectively. Equation 3.4 represents the extent of conversion for a single step process (Prime et al., 2009; Vyazovkin et al., 2011).

$$\frac{d\alpha}{dt} = k(T)f(\alpha) \tag{3.4}$$

The dependence of the process rate on temperature is represented by the rate constant, k(T), and the dependence on the extent of conversion by the reaction model, f(α). The temperature dependence is generally defined through the Arrhenius equation (Equation 3.5) (Prime et al., 2009; Vyazovkin et al., 2011).

$$k(T) = Aexp\left(\frac{-E}{RT}\right) \quad (3.5)$$

A (min^{-1}) and E (kJ/mol) are kinetic parameters, preexponential factor and the activation energy respectively, R is the universal gas constant and T (K) is temperature. Substituting equation 3.5 in equation 3.4 (Prime et al., 2009; Vyazovkin et al., 2011):

$$\frac{d\alpha}{dt} = Aexp\left(\frac{-E}{RT}\right) f(\alpha) \quad (3.6)$$

From equation 3.5, the reaction rate depends on the conversion, represented by a reaction model [f(α)] which is based on physical mechanisms assumed as a mathematical derivation. In polymer degradation, the rate of conversion is proportional to the concentration of the unreacted material (Equation 3.7).

$$f(\alpha) = (1-\alpha)^n \quad (3.7)$$

Finally, combining equation 3.6 and 3.7 gives the differential equation from which kinetic parameters are estimated (equation 3.8) (Prime et al., 2009; Vyazovkin et al., 2011).

$$\frac{d\alpha}{dt} = Aexp\left(\frac{-E}{RT}\right) f(1-\alpha)^n \quad (3.8)$$

3.8.1 Material and Methods

Bare un-stabilized isotactic polypropylene (i-PP), MFI= 40 g/10 min; bare un-stabilized low-density polyethylene ($LDPE_{15}$), MFI= 1 g/10 min and commercial low-density polyethylene ($LDPE_{33}$) with an antioxidant package formulation and MFI= 0.3 g/10 min, were supplied

from REPSOL Spain. Ascorbic Acid (As. Ac.), α-tocopherol (α-toc), and linseed oil (LSO) were supplied from Sigma, France; flaxseed oil (FSO) was provided by Terpenic Labs, Spain.

3.8.2 Experimental

For i-PP, $LDPE_{15}$ and $LDPE_{33}$, TGA degradation analysis were performed in dynamic mode at three different heating rates: 10 °C/min, 20 °C/min, and 30 °C/min, in open aluminum pans under inert atmosphere (nitrogen) and a gas flow of 60 mL/min. In the case of antioxidants, thermal and thermo-oxidative degradation analyses were carried out in nitrogen and air respectively and under the same dynamic conditions.

Premises and assumptions

- Friedman and Kissinger isoconversional methods assessed. The reaction rate at a constant degree of conversion is only a function of temperature (model-free methods) (Vyazovkin et al., 2011),

- ASTM E 1641 method for decomposition kinetics by thermogravimetry. The apparent activation energy is independent of reaction order at earlier decomposition stages (10% of decomposition or in some instances up to 20 %) (*ASTM E1641-99, Standard Test Method for Decomposition Kinetics by Thermogravimetry*, 1999).

Friedman isoconversional method

The general equation illustrated in equation (3.9) represents the method.

$$\ln\left(\frac{d\alpha}{dt}\right)_{\alpha,i} = \ln[f(\alpha)A_{\alpha}] - \frac{E_{\alpha}}{RT_{\alpha,i}} \quad (3.9)$$

Where, at a fixed degree of conversion (α) for non-isothermal analysis, the value of the apparent energy of activation (Ea_{deg}) can be estimated by plotting the left side of the equation against the reciprocal of the absolute temperature (Friedman, 1964; Vyazovkin et al., 2011).

Kissinger isoconversional method

The Kissinger equation under non-isothermal conditions is shown in equation (3.10).

$$\ln\left(\frac{\beta}{T^2 m,i}\right) = \ln\left(-\frac{AR}{E}\, f'(\alpha_m)\right) - \frac{E}{RT_{m,i}} \quad (3.10)$$

Where the plot of the left side of the equation against the reciprocal of the absolute temperature (T_m) at the maximum rate, yields the apparent activation energy (Kissinger, 1957; Vyazovkin et al., 2011).

ASTM E 1641

The methodology involves non-isothermal conditions under a series of different heating rates. The main assumption defines that, the apparent energy of activation (Ea_{deg}) is independent of the reaction order at early decomposition stages (maximum 20% of decomposition).

The plot of the logarithm of the heating rate, at a specific extent of conversion (α), against the reciprocal of the absolute temperature yields a straight line whose slope is ran in an iterative process with numerical integration constants to calculate the apparent energy of activation (Ea_{deg}) within 1% of variation (*ASTM E1641-99, Standard Test Method for Decomposition Kinetics by Thermogravimetry*, 1999).

3.8.3 Results

Figure 3.19, 3.20, and 3.21 represent the TGA thermograms for i-PP, $LDPE_{15}$, and $LDPE_{33}$ respectively for non-isothermal conditions.

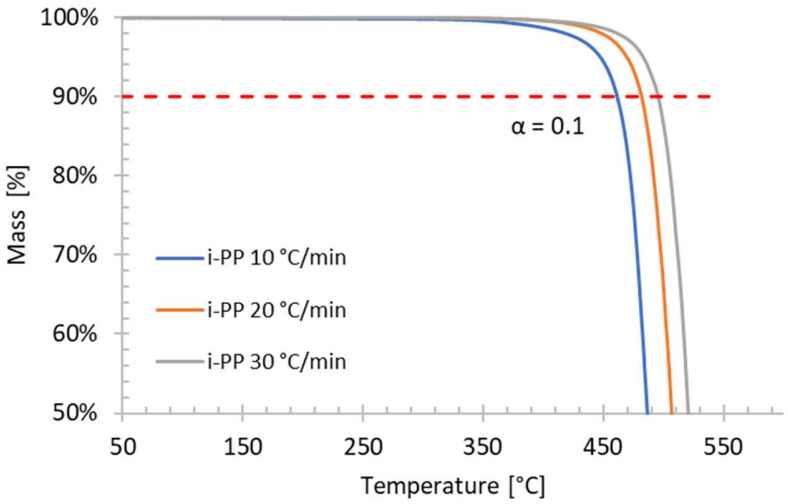

Figure 3.19. TGA thermograms for i-PP at different heating rates.

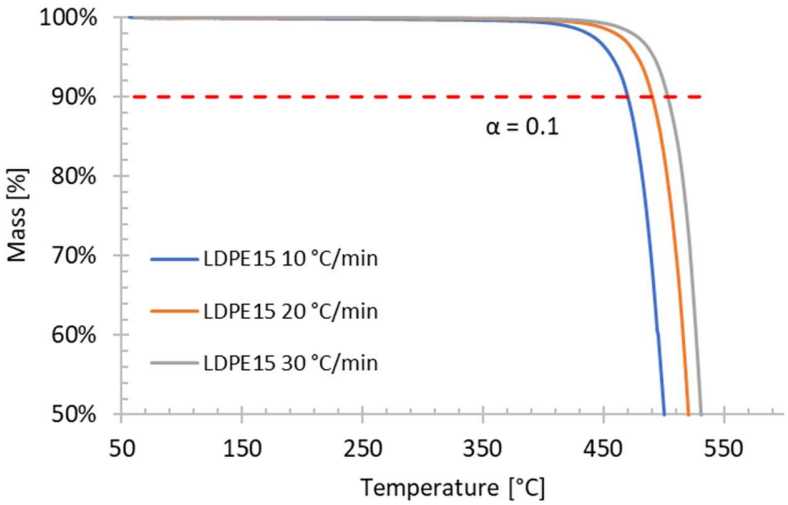

Figure 3.20. TGA thermograms for $LDPE_{15}$ at different heating rates.

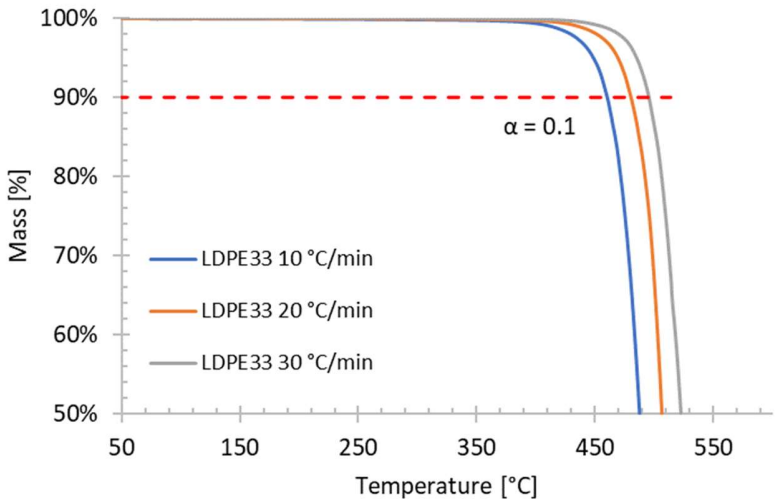

Figure 3.21. TGA thermograms for $LDPE_{33}$ at different heating rates.

Resulting treatment data from above thermograms, yield a straight line at a corresponding degree of conversion (α) from where the apparent energy of activation is calculated.

Polypropylene (i-PP)

Figure 3.22 shows the plots based on the ASTM E1641, Kissinger, and Friedman Decomposition Kinetics methods.

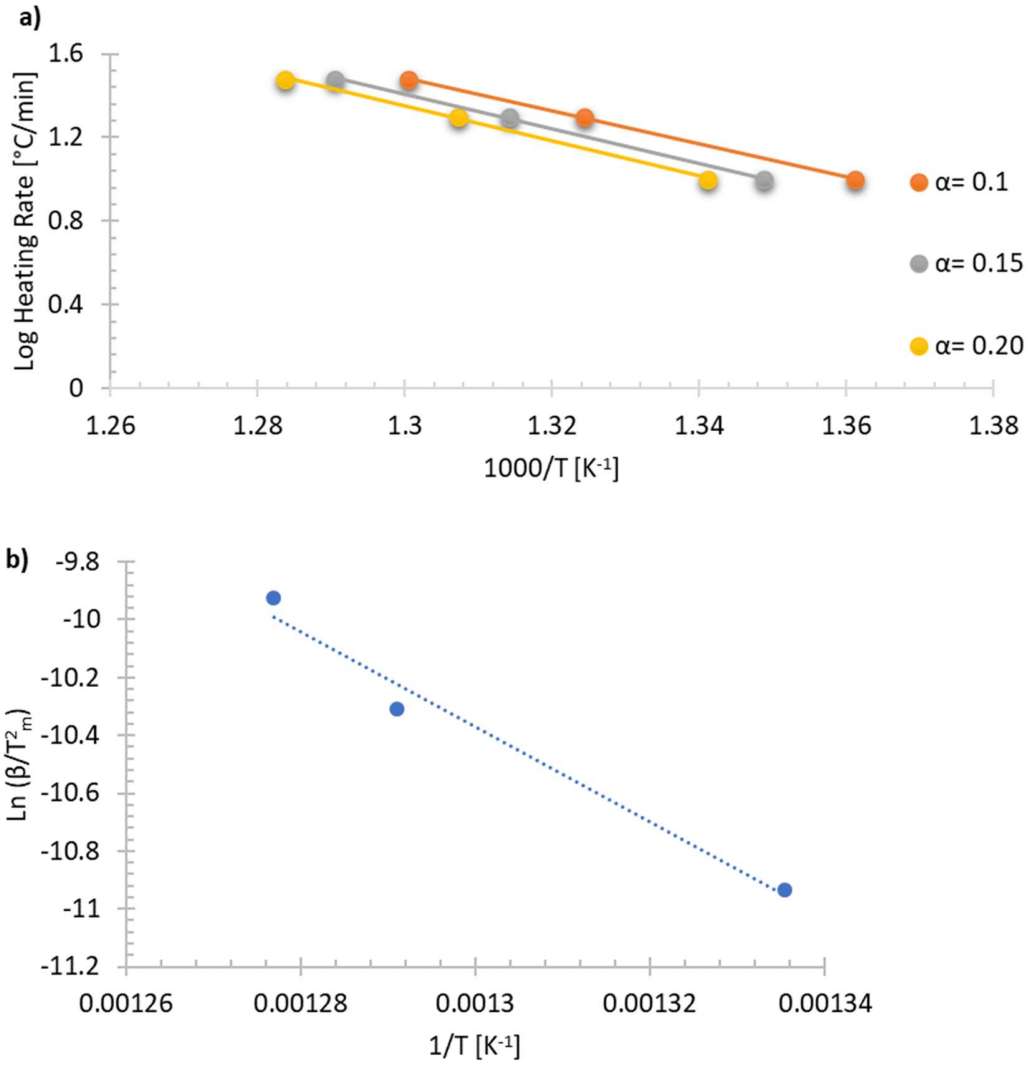

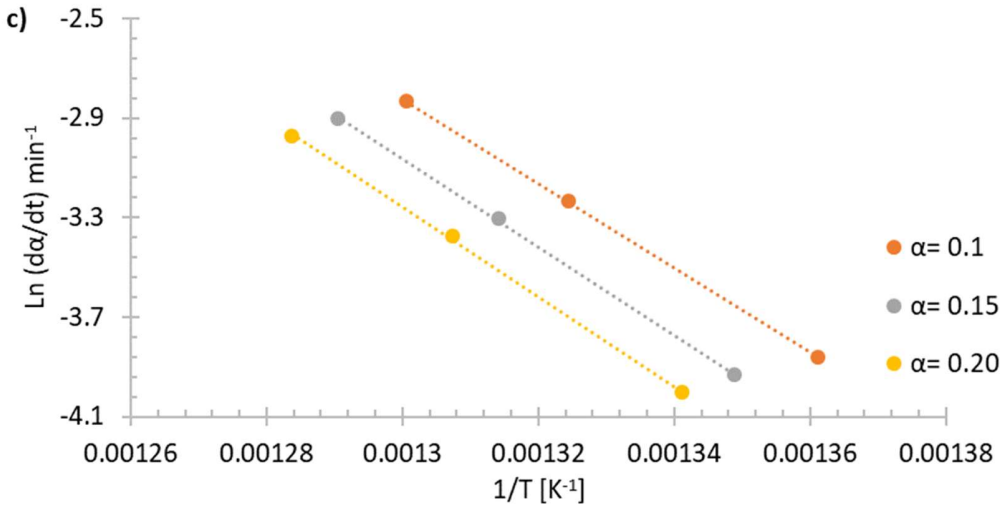

Figure 3.22. Arrhenius plot of isoconversional methods. a) ASTM E1641, b) Kissinger, c) Friedman.

Low-Density Polyethylene (LDPE$_{15}$)

Figure 3.23 shows the plots based on the ASTM E1641, Kissinger, and Friedman Decomposition Kinetics methods.

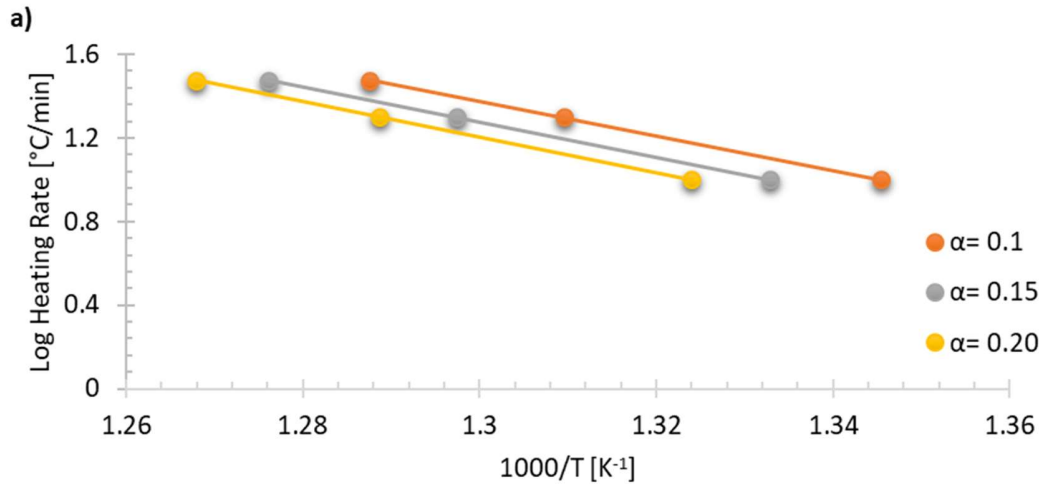

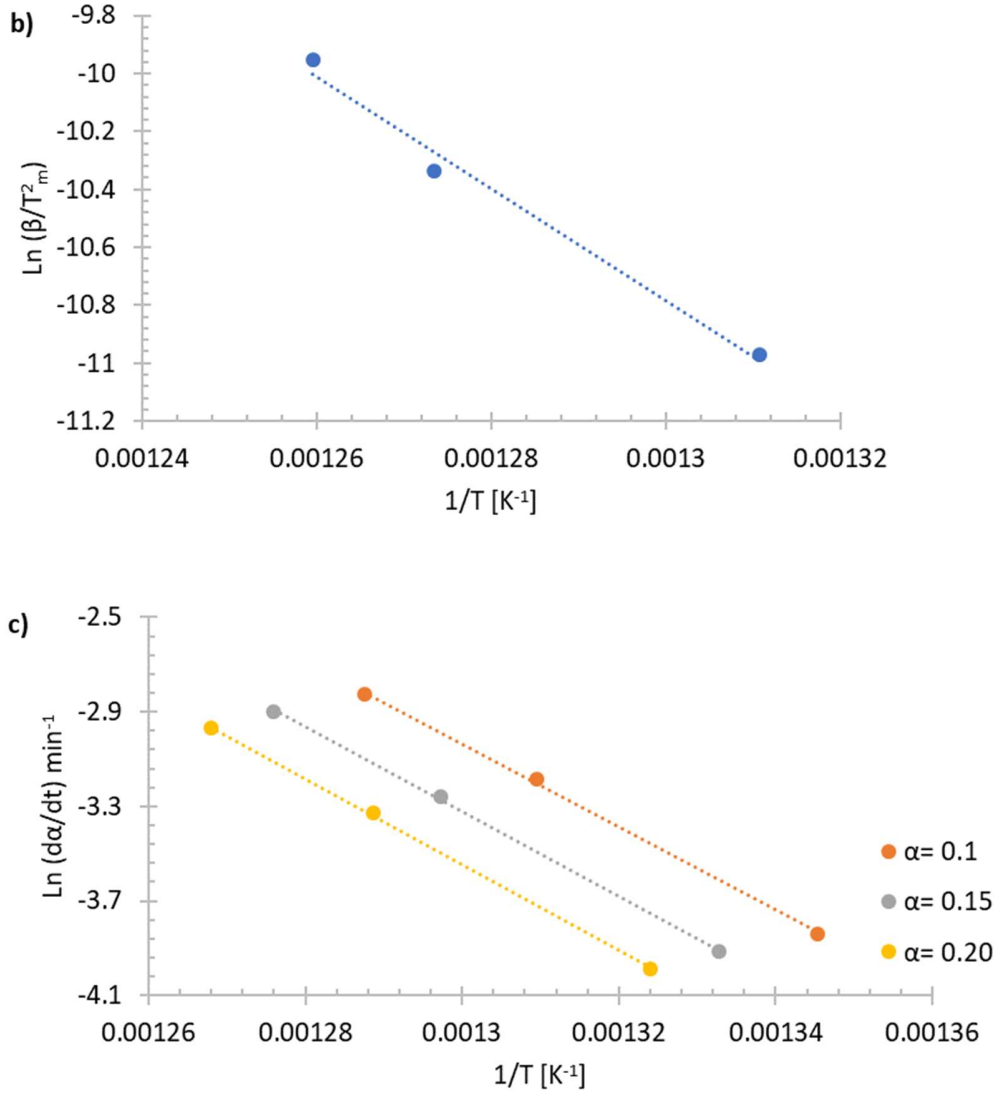

Figure 3.23. Arrhenius plot of isoconversional methods. a) ASTM E1641, b) Kissinger, c) Friedman.

Low-Density Polyethylene (LDPE$_{33}$)

Figure 3.24 shows the plots based on the ASTM E1641, Kissinger, and Friedman Decomposition Kinetics methods.

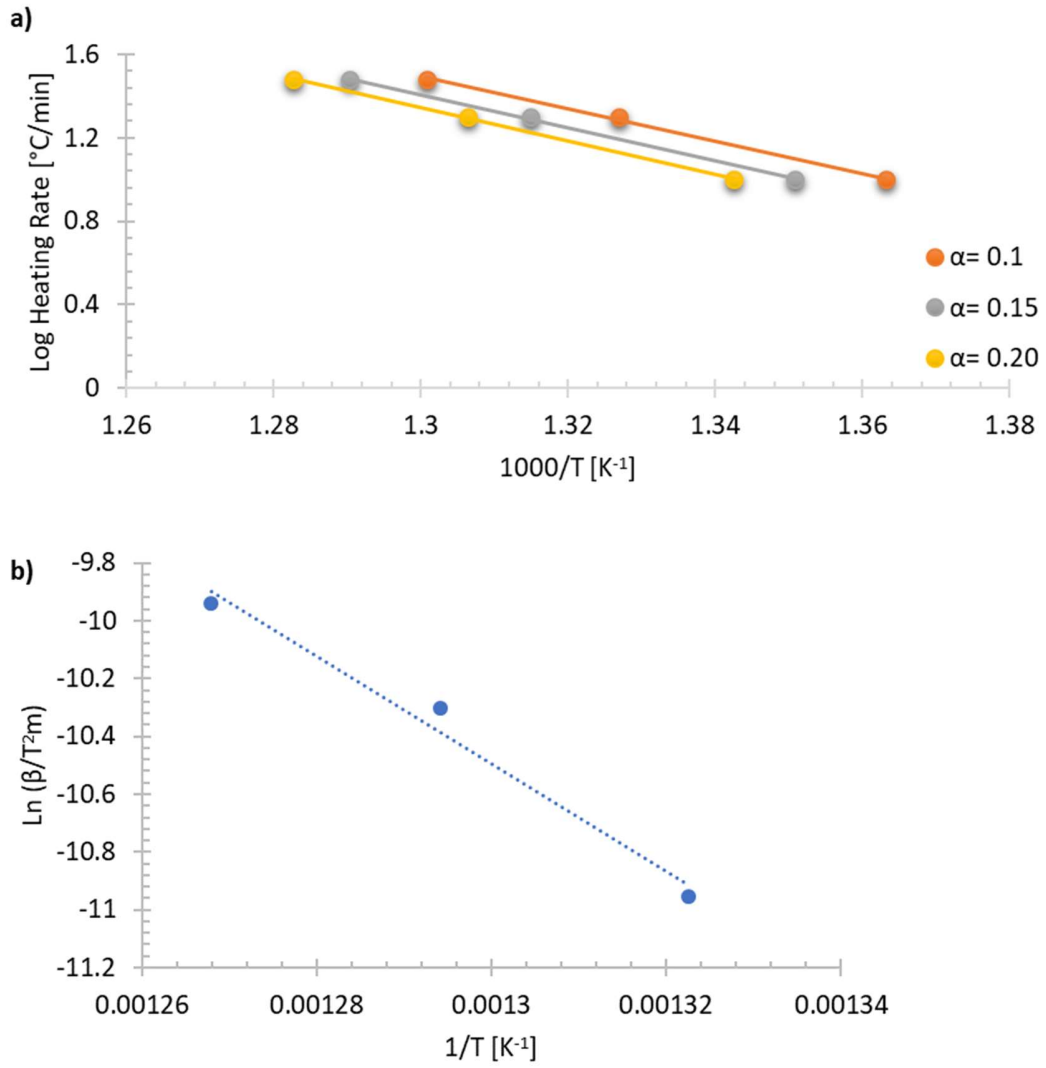

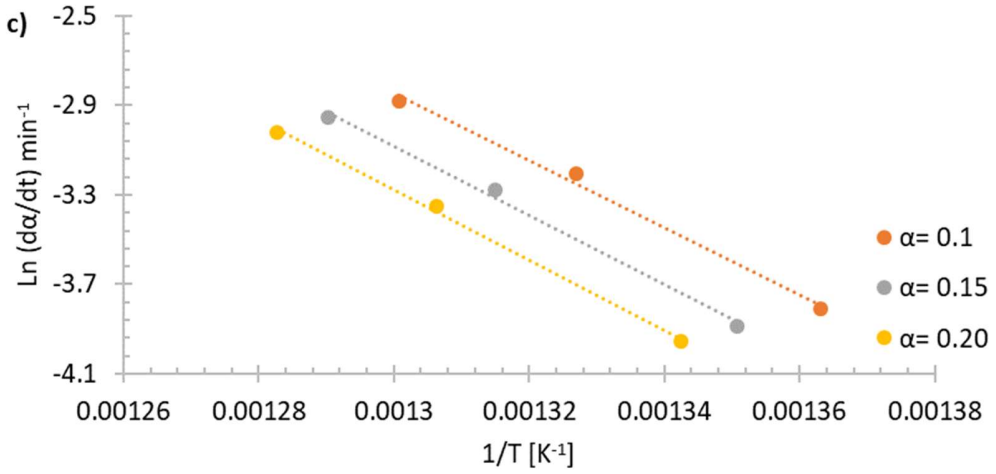

Figure 3.24. Arrhenius plot of isoconversional methods. a) ASTM E1641, b) Kissinger, c) Friedman.

Table 3.18 represents the resultant apparent energy of activation (Ea_{deg}) by the isoconversional methods approach. Following the assumption of the ASTM E1641 test method, the averaged Ea_{deg} calculated from the Friedman method, represents a decomposition (% of mass loss) between 90% and 80% for comparison analysis.

Material	Method	Ea [Kj/mol]	Std Dev. +/-
i-PP	ASTM E1641	143.7	3.7
	Kissinger	136.9	*
	Friedman	145.9	3.6
$LDPE_{15}$	ASTM E1641	148.2	4.1
	Kissinger	160.6	*
	Friedman	148.9	1.9
$LDPE_{33}$	ASTM E1641	138.4	2.35
	Kissinger	154.7	*
	Friedman	128.0	2.49

Table 3.18. Apparent energy of activation for bare polypropylene (i-PP) and bare low-density polyethylene (LDPE). * Kissinger approach considers the temperature at the maximum rate of decomposition ($d^2\alpha/d^2t$).

Antioxidants

Apparent energy of activation was evaluated, under the same methods, for Ascorbic Acid (As. Ac.), α-tocopherol (α-toc), linseed oil (LSO), and flaxseed oil (FSO). Antioxidants were evaluated under inert (nitrogen) and oxidative (air) atmospheres to assess the effect of oxygen in the degradation analysis of the antioxidant molecule. Figure 3.25 illustrates the degradation analysis by the ASTM E1641 method.

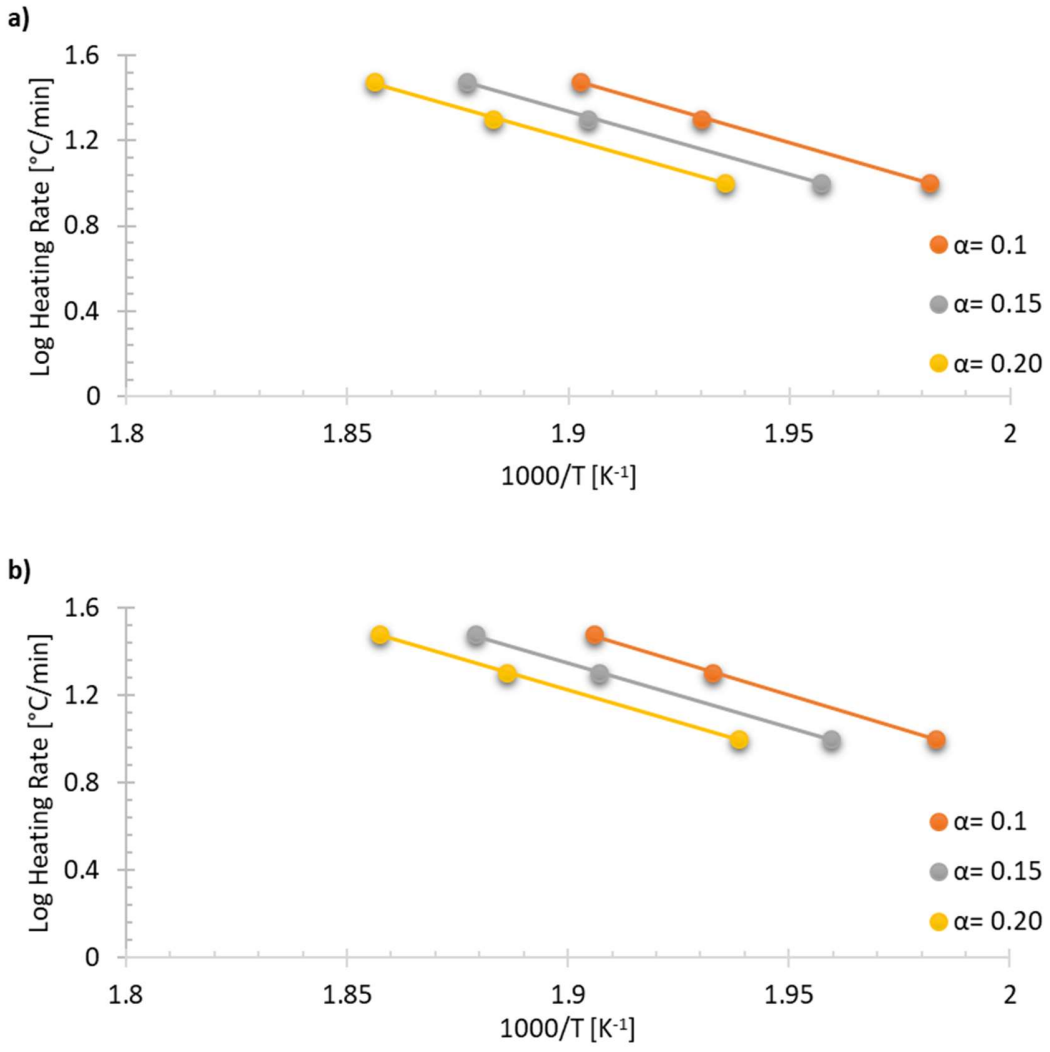

Figure 3.25. Calculated apparent energy of activation (Ea_{deg}) for ascorbic acid by ASTM E1641 method. a) nitrogen and b) air.

Figure 3.26 represents the degradation analysis by Kissinger method.

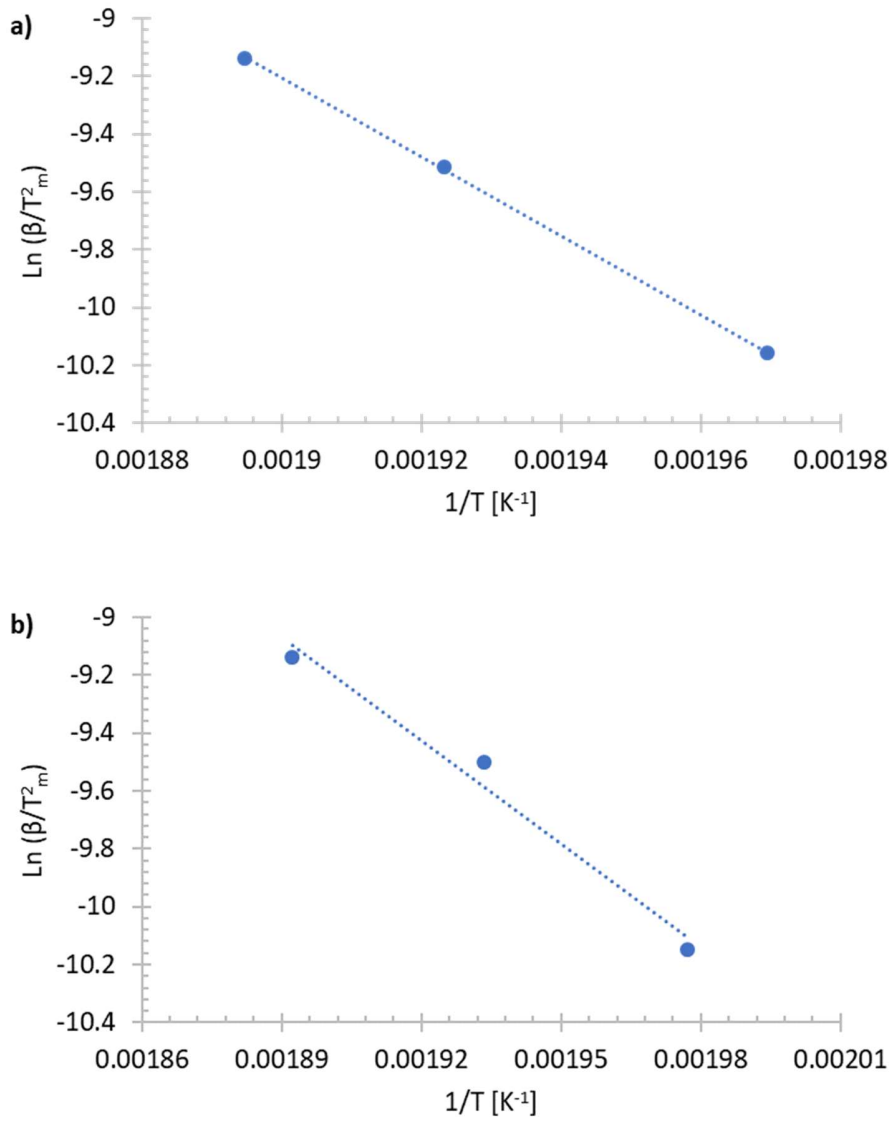

Figure 3.26. Calculated apparent energy of activation (Ea_{deg}) for ascorbic acid by Kissinger method. a) nitrogen and b) air.

Figure 3.27 represents the degradation analysis by Friedman method.

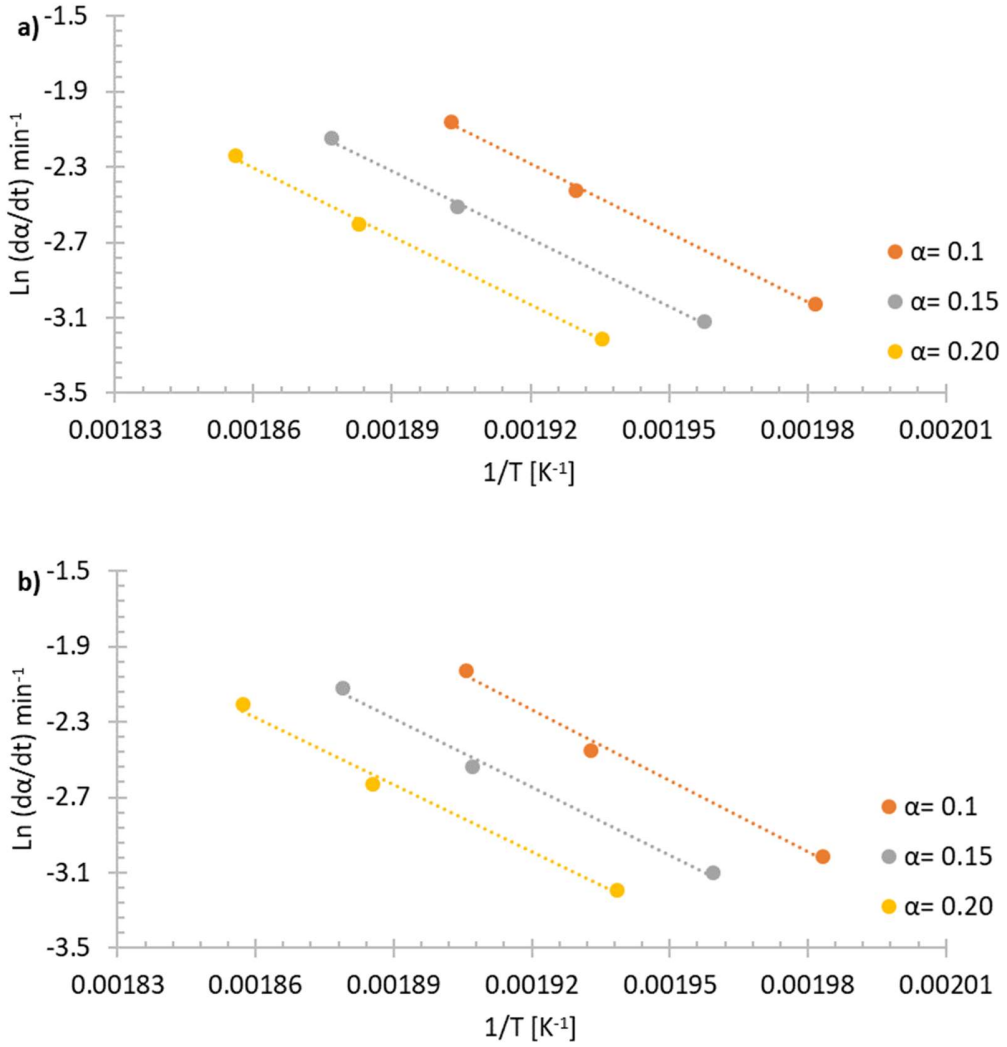

Figure 3.27. Calculated apparent energy of activation (Ea_{deg}) for ascorbic acid by Friedman method. a) nitrogen and b) air.

The degradation analysis plots for α-tocopherol (α-toc), linseed oil (LSO), and flaxseed oil (FSO) are presented in Annex A. Resulting apparent activation energies are described in Table 3.19.

		Nitrogen		Air	
Material	Method	Ea [Kj/mol]	Std Dev. +/-	Ea [Kj/mol]	Std Dev. +/-
As. Ac.	ASTM E1641	105.4	0.84	105.4	2.3
	Kissinger	113.7	*	99.3	*
	Friedman	100.6	0.97	101.1	2.2
α-Toc	ASTM E1641	84.8	1.50	80.5	0.6
	Kissinger	86.2	*	69.8	*
	Friedman	100.6	0.97	69.3	0.4
LSO	ASTM E1641	103.3	2.76	67.0	7.4
	Kissinger	132.5	*	59.3	*
	Friedman	104.1	3.03	64.1	7.3
FSO	ASTM E1641	111.9	2.72	60.7	7.2
	Kissinger	116.2	*	55.0	*
	Friedman	113.7	2.62	61.1	6.6

Table 3.19. Apparent energy of activation for Ascorbic Acid (As. Ac.), α-tocopherol (α-toc), linseed oil (LSO), and flaxseed oil (FSO). * Kissinger approach considers the temperature at the maximum rate of decomposition ($d^2\alpha/d^2t$).

The apparent activation energy reported in literature for ascorbic acid under isothermal conditions and different relative humidities (less than 70%, 97%, 93%, and 79.5%) are 104.33, 86.87, 88.22, and 202 kJ/mol respectively. Whereas the observed averaged Ea_{deg} values from the experimental runs were 106.6 +/- 0.91 and 101.9 +/- 2.2 for nitrogen atmosphere and air atmosphere respectively (He, Yin, & Ma, 1990).

Furthermore, the potential antioxidant effect of antioxidants such as alpha-tocopherol has been validated when incorporated into edible oils and assessed by the activation energies of the decomposition process under oxidative conditions. The incorporation of 0.04 g/L in soybean oil, sunflower oil, and their blends resulted in higher Ea_{deg} values (Arora, Bagoria, & Kumar, 2010).

In the case of linseed oil, it is reported activation energy values, determined by pressure differential scanning calorimetry (PDSC) and Rancimat, in the range of 93.14 to 94.53 kJ/mol and 74.03 to 77.76 kJ/mol respectively (Symoniuk, Ratusz, & Krygier, 2016). Whereas the observed averaged Ea_{deg} values from the experimental runs were 113.3 +/- 2.90 and 63.5 +/- 7.4 for nitrogen atmosphere and air atmosphere respectively. In the case of linseed oil and flaxseed oil, it was more evident the effect of air (oxidative atmosphere) on the Ea_{deg} value. Lower Ea_{deg} values observed are possibly due to the presence of polyunsaturated fatty acids, which are highly oxidable compounds present in edible oils.

3.9 Melt Flow Index

Melt Flow index (MFI) is a quality control test on thermoplastics, the method involves the flow per unit of time of a molten polymer material through a die of specific length and diameter under standardized parameters such as temperature, load, and piston position in the barrel (*ASTM D1238-04 Standard Test Method for Melt Flow Rates of Thermoplastics by Extrusion Plastomers*, 2004). MFI provides an estimation of the viscosity of the material and is inversely correlated: the higher the melt flow rate, the lower the viscosity of the material. An indirect method to estimate the molecular weight of the polymer.

It is reported in literature MFI analysis on polyethylene and polypropylene in multiple extrusions in which MFI results are correlated with polymer degradation mechanisms. A resulting higher MFI on polypropylene through multiple extrusion cycles indicates a predominant chain scission mechanism occurring during reprocessing. On the other hand, the presence of additives, such as compatibilizers for polymer blends, increased the MFI value under the same experimental conditions (Delva, Ragaert, Degrieck, & Cardon, 2016).

On the contrary, the melt stability of un-stabilized low-density polyethylene during multiple extrusion cycles was assessed by MFI, authors observed a decrease in the MFI value after multiple extrusion cycles. Furthermore, the incorporation of antioxidants such as irganox 1010, irganox 1076, and alpha-tocopherol in LDPE showed lesser changes in the MFI

values under the same experimental conditions (multi-extrusion); being alpha-tocopherol the antioxidant that exhibited the higher melt stability in terms of MFI value (Al-Malaika, Ashley, & Issenhuth, 1994).

3.9.1 Materials and Methods

Bare un-stabilized isotactic polypropylene (i-PP), MFI= 40 g/10 min; bare un-stabilized low-density polyethylene ($LDPE_{15}$), MFI= 1 g/10 min and commercial low-density polyethylene ($LDPE_{33}$) with an antioxidant package formulation and MFI= 0.3 g/10 min, were supplied from REPSOL Spain.

Premises and assumptions

Melt flow index rely on the average molecular weight and molecular weight distribution (Abbas-Abadi, Haghighi, & Yeganeh, 2012), but the effect of additives such as compatibilizers and processing aids alter in some extent the MFI without modification of the average molecular weight.

The lipophilic character of alpha-tocopherol may act as a processing aid in polymer formulation and, possibly, the same behavior would be expected for oil-based antioxidant sources. Thus, effect of degradation (thermal, thermo-oxidative, and thermo-mechanical) on multiple extrusion cycles is assessed by MFI for pure i-PP and LDPE resins.

Average molecular weight for polypropylene was calculated considering the Bremner approximation (Bremner, Rudin, & Cook, 1990) (equation 3.11).

$$Mw^{3.7} = \frac{1.675}{MFI\ x\ 10^{-21}} \qquad (3.11)$$

3.9.2 Experimental

Extrusion

Polymer resins were processed during 9 extrusion cycles on a LabTech twin co-rotating extruder; screw speed of 300 RPM and a temperature profile of 190°C for i-PP and $LDPE_{15,33}$ were utilized.

MFI

Melt flow index (MFI) measurements were performed according to ASTM D1238. The reported MFI values represents the average of 4 independent measurements. Briefly, the following methodology was considered:

- Set temperature and heating time 15 min (LDPE 190 °C /2.16 Kg and PP 230 °C /2.16 Kg),
- Pack time (sample mass added) 1 minute,
- Hold time with piston inserted 4 minutes,
- Dead load added,
- 1st cutoff discarded,
- Take cutoffs as per Standard.

3.9.3 Results

i-PP

Figure 3.28 illustrates the effect of sequential extrusion cycles on MFI. It is observed that, for the first extrusion cycle there is no change in MFI (variation is within the standard deviation) comparing with the MFI value for bare i-PP (control). Higher MFI values were observed from extrusion cycle 2 to extrusion cycle 9.

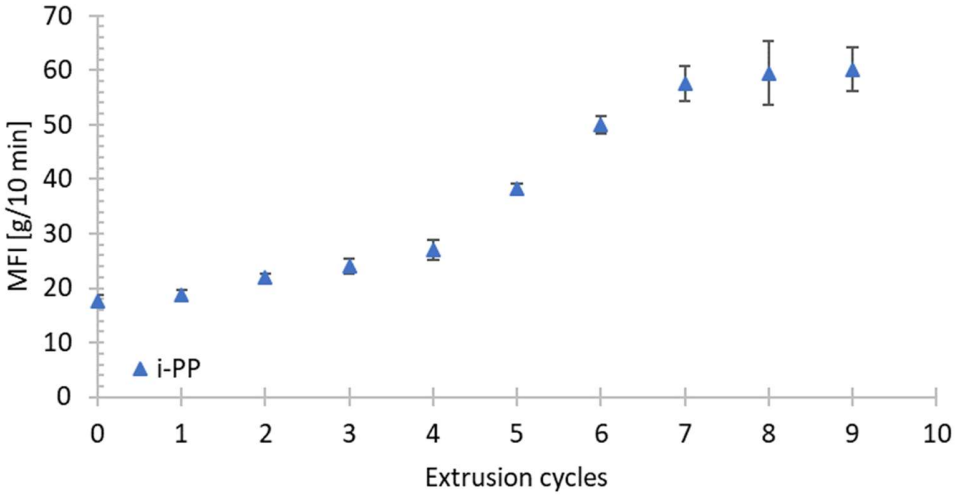

Figure 3.28. Melt Flow Index for i-PP as function of number of extrusion cycles.

Figure 3.29 illustrates the percentage of variation of MFI as function of extrusion cycles. The representation of the variation of MFI showed a maximum or plateau at extrusion cycle 7, with a total variation of 28% under the experimental conditions evaluated.

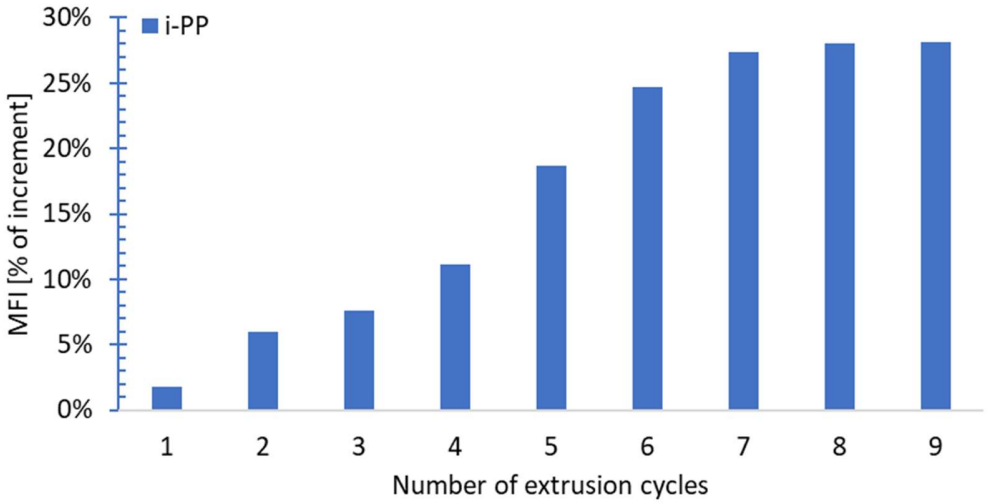

Figure 3.29. Percentage of variation on MFI for i-PP as function of number of extrusion cycles.

The degradation mechanism represented by an increment in the MFI or a loss in the averaged molecular way is by chain-scission. Figure 3.30 shows a correlation between the calculated averaged molecular weight (Mw) and the number of extrusion cycles. Results showed a thermo-oxidative degradation on i-PP during processing, mainly dominated by chain-scission reactions.

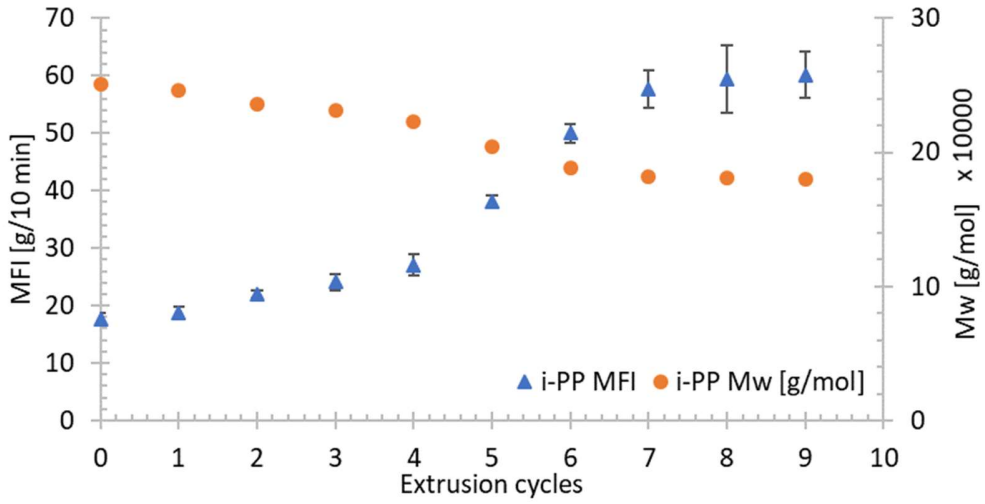

Figure 3.30. Correlation of the calculated averaged molecular weight (Mw) and the number of extrusion cycles for un-stabilized isotactic polypropylene (ii-PP).

$LDPE_{15,33}$

Figure 3.31 shows the effect of sequential extrusion cycles on MFI. It is observed that, $LDPE_{15}$ presented the steepest slope thus, a more rapid degradation effect as a function of number of extrusion cycles. Being in agreement with the technical data sheet for the resins (see Annex A), where $LDPE_{33}$ is formulated with an antioxidant system thus, delaying in some extent the thermo-oxidative degradation during processing.

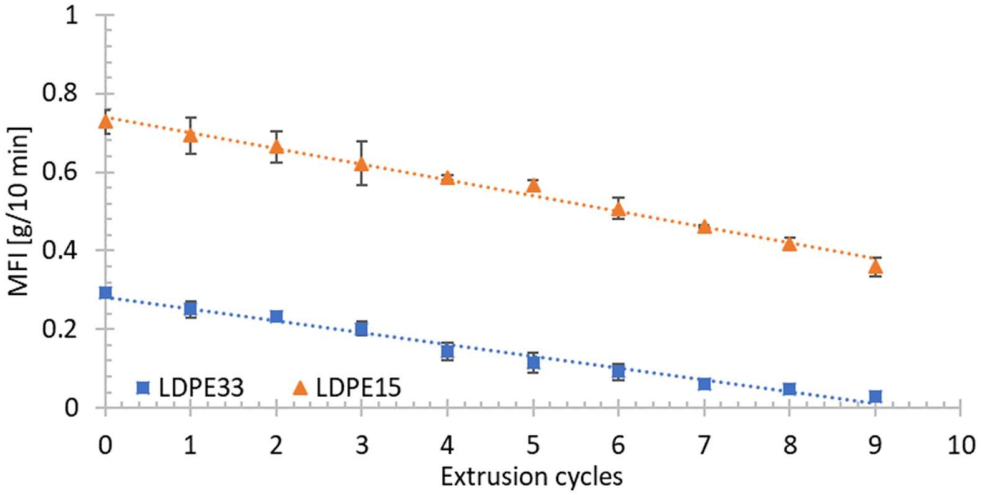

Figure 3.31. Melt Flow Index for $LDPE_{15}$ and $LDPE_{33}$ as function of number of extrusion cycles.

It is up to the best knowledge of author from literature research that, there is not an accurate relationship between MFI and averaged molecular weight for low density polyethylene. Hence, data is only represented as the averaged MFI values.

3.10 Rheological analysis

Sample preparation

25 mm diameter disk samples were compressed molded at a temperature of 150 °C for $LDPE_{15,33}$ and 180 °C for i-PP during 7 minutes and a mold pressure of 78.4 bar. Polymer melt rheology analysis were performed in an Ares rotational rheometer with a parallel plate geometry (25 mm diameter). The gap distance was fixed approximately to 1.8 mm and the percentage of strain utilized under the linear viscoelasticity region. Strain sweep analysis and frequency sweep analysis were performed in nitrogen atmosphere to avoid degradation. The test temperatures were selected considering the melting temperature of the polymer resins.

3.10.1 Methodology

Dynamic oscillatory test

Strain sweep analysis were performed to assess the linear viscoelastic region for all the test-temperatures evaluated. Test conditions were fixed at a frequency of 1 rad/s and between an initial strain of 0.1% and a final strain of 10%. Frequency sweep test were performed at a fixed percentage of strain (2.5%) in the frequency range between 0.1 and 100 rad/s. Master curves were generated using the TA Orchestrator software at a reference temperature of 160°C for bare un-stabilized resins (i-PP, $LDPE_{15}$) and bare commercial $LDPE_{33}$. In the case of multi-extrusion cycle analysis, a broader temperature range was covered: 140 °C to 180 °C for low-density polyethylene ($LDPE_{15,33}$) and 150 °C to 230 °C for isotactic polypropylene (i-PP).

Samples were characterized as a function of complex viscosity (η^*), the calculated energy of activation (Ea), and the zero-shear viscosity (η_0) calculated from the complex viscosity (η^*) data using the cross model fitting and the TA Orchestrator software.

3.10.2 Results

A preliminary time sweep analysis (test temperature 200 °C, N_2 as inert atmosphere, 2.5% of strain, frequency of 10 rad/s for 1 hour) was performed to ensure no polymer degradation represented as a deviation in Tan δ. Figure 3.32 shows the relationship between complex viscosity (η^*) and frequency (ω) for bare un-stabilized i-PP, bare un-stabilized $LDPE_{15}$ and bare commercial $LDPE_{33}$.

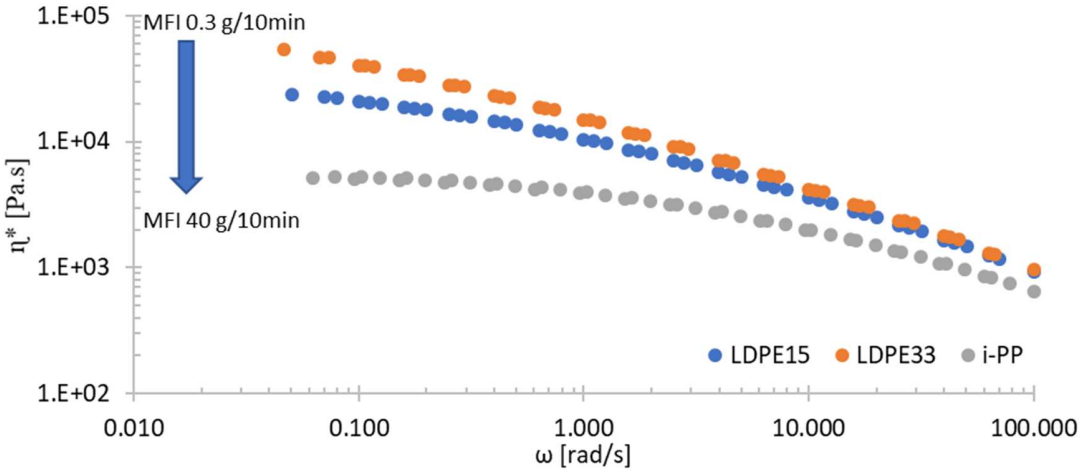

Figure 3.32. Complex viscosity (η*) versus frequency (ω) for bare un-stabilized isotactic polypropylene (i-PP), bare un-stabilized low-density polyethylene ($LDPE_{15}$), and commercial low-density polyethylene ($LDPE_{33}$).

Isotactic polypropylene and low-density polyethylene present different molecular structures with different physical properties such as the reported melt flow index (MFI). The calculated zero-shear viscosity (η_0) and the energy of activation will be a reference point to evaluate the effect of thermo-mechanical events by extrusion process and further antioxidant formulation (chapter IV). Table 3.20 presents the rheological data.

Polymer sample	η0 [Pa.s]	+/-	r^2	Ea [kJ/mol]	+/-	r^2	Gc [Pa]	ωc [Rad/s]	1/ωc [s]
$LDPE_{15}$ bare	2.33E+04	2.0	1.00	61.2	2.5	1.00	20175	6.3	0.16
$LDPE_{33}$ bare	5.10E+04	1711	1.00	68.2	1.2	1.00	11900	1.2	0.85
i-PP bare	5.31E+03	867	1.00	42.5	7.5	1.00	32107	40.4	0.02

Table 3.20. Summary of rheological properties for bare un-stabilized $LDPE_{15}$, bare commercial $LDPE_{33}$, and bare un-stabilized i-PP: zero-shear viscosity (η_0), energy of activation (Ea), crossover modulus (ωc) and crossover frequency (ωc).

All samples were characterized as received. In general, it is observed higher Ea values for bare $LDPE_{15}$ and bare $LDPE_{33}$ (61.2 and 68.2 kJ/mol respectively) than bare i-PP with a resulting Ea value of 42.5 kJ/mol. The inherent zero-shear viscosity (η_0) for $LDPE_{15}$ and $LDPE_{33}$ was $2.33x10^4$ Pa.s and $5.10x10^4$ Pa.s respectively. Whereas i-PP reported a lower zero-shear value (η_0) of $5.31x10^3$.

The crossover point (G'/G'') for $LDPE_{33}$ is shifted toward lower frequencies (ωc) as compared to $LDPE_{15}$. This may be attributed to either a longer or more branched molecules resulting in a higher average molecular weight, this is also represented with a lower MFI value (0.3 g/10 min) for $LDPE_{33}$. Isotactic polypropylene (i-PP) presented the lowest relaxation time ($1/\omega c$) of 0.02 s.

Effect of multi-extrusion cycles on rheological properties

Polymer resins were exposed to 9 sequential extrusion cycles to assess the thermo-mechanical effect on the rheological properties. Extrusion was performed on a LabTech twin co-rotating extruder with 16 mm diameter screw and length to diameter (L/D) ratio of 40. Averaged extrusion temperatures profile for i-PP and LDPE were 180 °C and 150 °C respectively.

The effect of extrusion cycles on zero-shear viscosity (η_0) and energy of activation (Ea) were evaluated for $LDPE_{15,33}$ and i-PP. Figures 3.33, 3.35, and 3.37 present the relationship between complex viscosity (η^*) and frequency (ω).

LDPE$_{15}$

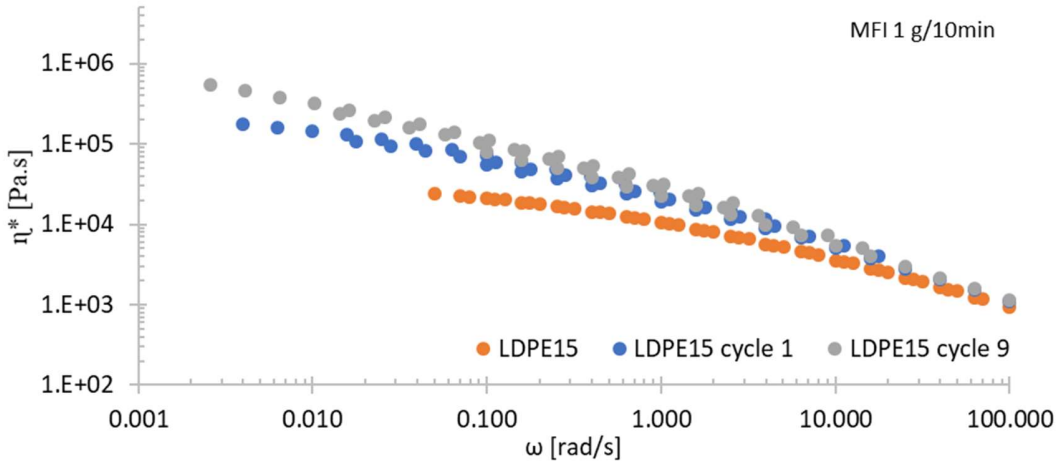

Figure 3.33. Complex viscosity (η*) versus frequency (ω) for bare un-stabilized low-density polyethylene (LDPE$_{15}$).

Resulting data from master curves showed a higher complex viscosity (η*) value after extrusion process. It is observed, at a fixed frequency of ~0.05 rad/s, a difference in the complex viscosity (η*) from the extruded samples cycle 1 and cycle 9 in the order of 3.5-fold and 7.3-fold higher than the complex viscosity (η*) value of the bare un-processed LDPE$_{15}$ sample. Table 3.21 presents the rheological data.

Polymer sample	η_0 [Pa.s]	+/-	r^2	Ea [kJ/mol]	+/-	r^2	Gc [Pa]	ωc [Rad/s]	1/ωc [s]
LDPE$_{15}$ bare	2.33E+04	2.0	1.00	61.248	2.5	1.00	20175	6.257	0.16
LDPE$_{15}$ cycle 1	1.56E+05	---	0.98	68.326	---	1.00	28420	0.738	1.35
LDPE$_{15}$ cycle 9	4.87E+05	---	0.99	77.317	---	1.00	7023	0.148	6.75

Table 3.21. Summary of rheological properties for bare un-stabilized LDPE$_{15}$ and bare un-stabilized LDPE$_{15}$ extrusion cycle 1 and extrusion cycle 9: zero-shear viscosity (η_0), energy of activation (Ea), crossover modulus (ωc) and crossover frequency (ωc).

The zero-shear viscosity values (η_0) from the extruded samples where higher than the corresponding zero-shear viscosity value (η_0) from the un-processed $LDPE_{15}$ sample. Thus, it may be concluding that the continuous thermo-mechanical degradation on $LDPE_{15}$ is mainly dominated by cross-linking reactions. Furthermore, the more the extrusion cycles the higher the energy of activation (Ea) value thus, corroborating the degradation mechanism path as shown in Figure 3.34.

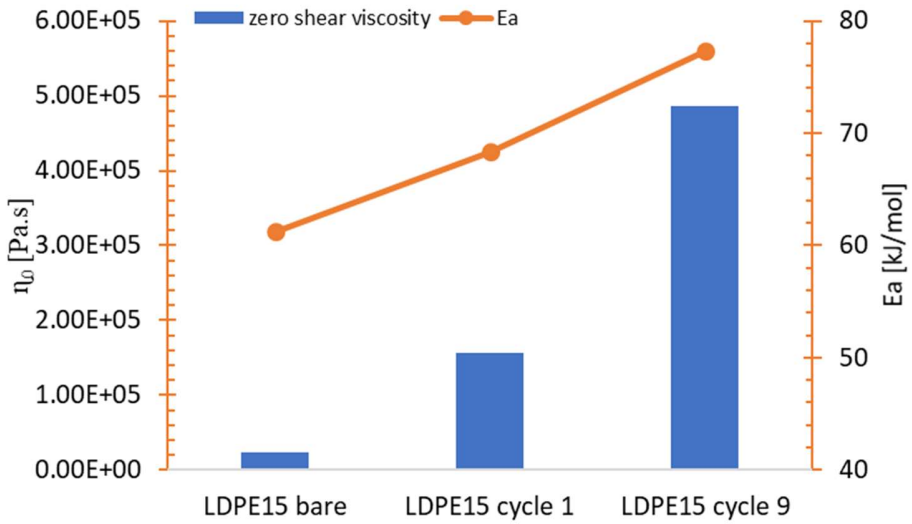

Figure 3.34. Zero-shear viscosity (η_0) and energy of activation (Ea) for bare un-processed $LDPE_{15}$ and extruded $LDPE_{15}$.

LDPE$_{33}$

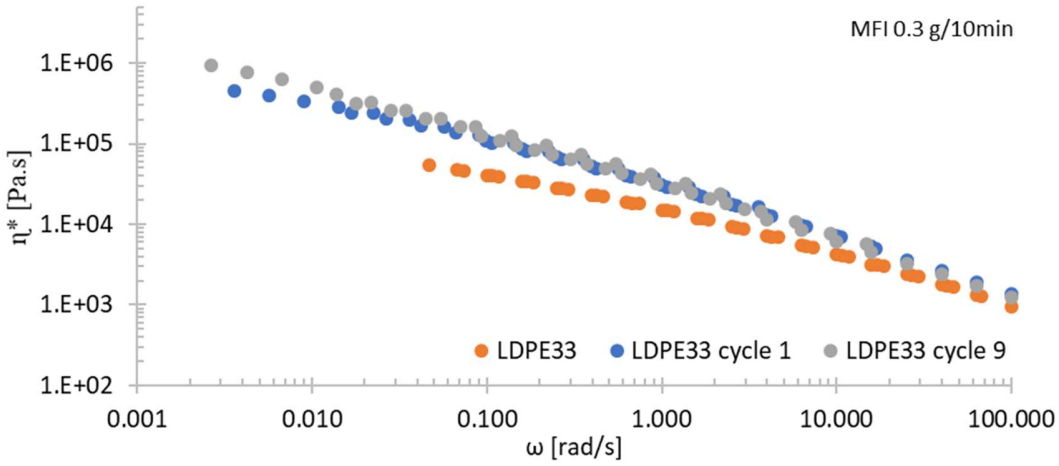

Figure 3.35. Complex viscosity (η*) versus frequency (ω) for commercial low-density polyethylene (LDPE$_{33}$).

A higher complex viscosity (η*) value after extrusion process is observed from retrieved master curves data. It is also observed, at a fixed frequency of ~0.05 rad/s, a difference in the complex viscosity (η*) from the extruded samples cycle 1 and cycle 9 in the order of 3.1-fold and 3.8-fold higher than the complex viscosity (η*) value of the bare un-processed LDPE$_{33}$ sample. Table 3.22 presents the rheological data.

Polymer sample	η_0 [Pa.s]	+/-	r^2	Ea [kJ/mol]	+/-	r^2	Gc [Pa]	ωc [Rad/s]	1/ωc [s]
LDPE$_{33}$ bare	5.10E+04	1711	1.00	68.2	1.2	1.00	11900	1.182	0.85
LDPE$_{33}$ cycle 1	4.05E+05	31046	0.99	70.4	0.75	1.00	10105	0.137	7.32
LDPE$_{33}$ cycle 9	1.25E+06	81615	0.99	83.5	5.1	1.00	2782	0.004	245.9

Table 3.22. Summary of rheological properties for bare commercial LDPE$_{33}$ and bare commercial LDPE$_{33}$ extrusion cycle 1 and extrusion cycle 9: zero-shear viscosity (η_0), energy of activation (Ea), crossover modulus (ωc) and crossover frequency (ωc).

The zero-shear viscosity values (η_0) from the extruded samples where higher than the corresponding zero-shear viscosity value (η_0) from the un-processed $LDPE_{33}$ sample. It also may be concluded that the degradation path is mainly by cross-linking reactions. Figure 3.36 shows the relationship between extrusion cycles and rheological properties. Also, it is observed that, the more the extrusion cycles the higher the energy of activation (Ea) value. Thus, corroborating the same degradation mechanism path as observed in $LDPE_{15}$ and presented in Figure 3.34.

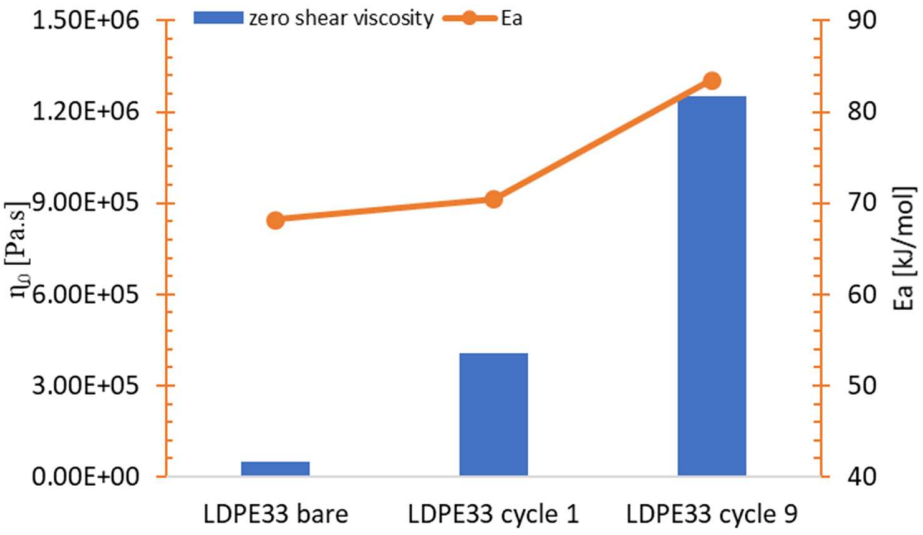

Figure 3.36. Zero-shear viscosity (η_0) and energy of activation (Ea) for bare un-processed $LDPE_{33}$ and extruded $LDPE_{33}$.

i-PP

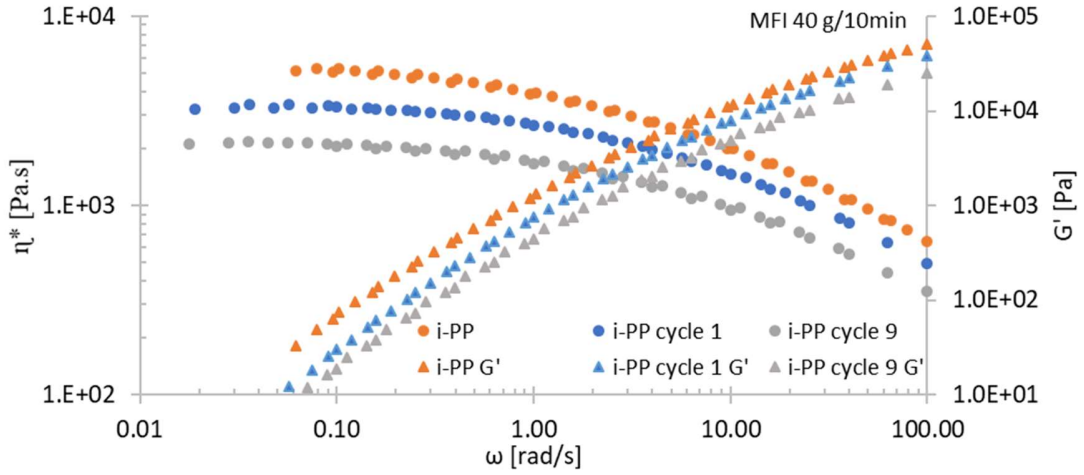

Figure 3.37. Complex viscosity (η*) versus frequency (ω) for bare un-stabilized isotactic polypropylene (i-PP).

The resulting MFI values for i-PP on multi-extrusion cycle analysis (Figure 3.30) showed a degradation dominated by chain scissions of the i-PP macromolecule and correlated with a reduction on the average molecular weight determined by theoretical calculations. The rheological properties are in agreement with the MFI values for i-PP, the complex viscosity (n*) and the dynamic storage modulus (G') are reduced as a function of the extrusion cycle. It may be concluded that continuous thermo-mechanical degradation on i-PP is possibly derived mainly by chain scissions.

A different degradation path was observed for i-PP, lower complex viscosity (η*) values after extrusion process were obtained. At a fixed frequency of ~0.05 rad/s, a difference in the complex viscosity (η*) values from the extruded samples cycle 1 and cycle 9 were 66% and 42% lower than the complex viscosity (η*) value of the bare un-processed i-PP sample. Table 3.23 presents the rheological data.

Polymer sample	η_0 [Pa.s]	+/-	r^2	Ea [kJ/mol]	+/-	r^2	Gc [Pa]	ωc [Rad/s]	1/ωc [s]
i-PP bare	5.31E+03	867	1.00	42.5	7.5	1.00	32107	40.406	0.025
i-PP cycle 1	3.41E+03	484.8	0.99	37.0	0.04	0.99	25265	49.705	0.020
i-PP cycle 9	5.33E+02	65.68	0.97	39.1	0.5	0.99	n.a.	n.a.	n.a.

Table 3.23. Summary of rheological properties for bare un-stabilized i-PP and bare un-stabilized i-PP extrusion cycle 1 and extrusion cycle 9: zero-shear viscosity (η0), energy of activation (Ea), crossover modulus (ωc) and crossover frequency (ωc).

The resulting zero-shear viscosity values (η_0) from the extruded samples were lower than the corresponding zero-shear viscosity value (η_0) from the un-processed i-PP sample. Thus, it may be concluding that the continuous thermo-mechanical degradation on i-PP is mainly dominated by chain scission reactions. Furthermore, it is observed a slight difference in the energy of activation (Ea) values across the extrusion cycles, possibly a plateau is reached in terms of the sufficient energy to produce movement in the polymer chains due to polymer degradation. Results are present in Figure 3.34.

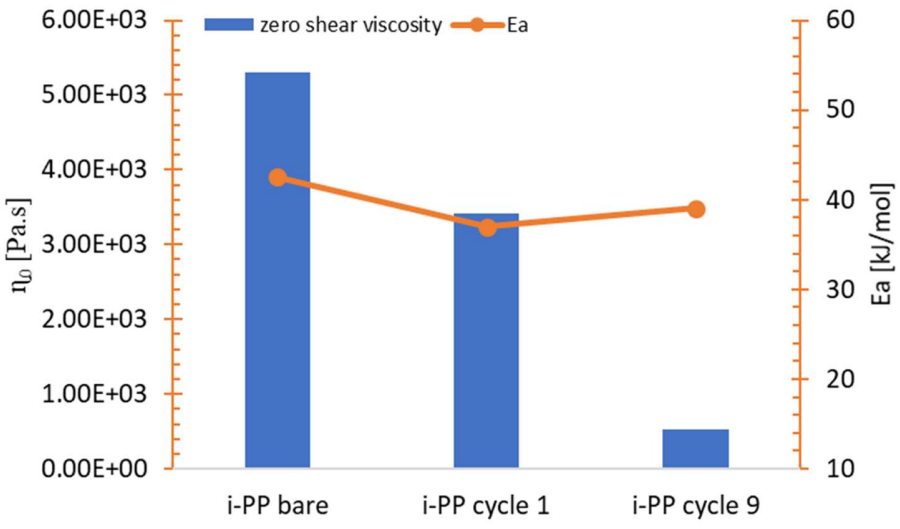

Figure 3.38. Zero-shear viscosity (η_0) and energy of activation (Ea) for bare un-processed i-PP and extruded i-PP.

It is important to define the optimum processing conditions for the selected resins. This chapter presented the thermal and rheological properties of bare i-PP and bare $LDPE_{15,33}$. The importance of analysis and characterization was twofold: first, it was aimed to propose the degradation mechanisms involved in polymer degradation during extrusion process, and on the other hand, to define and optimize a test-method that, with reproducibility, characterize the potential formulated resins within a processability window. Finally, chapter IV presents the potential formulas incorporated into un-stabilized low-density polyethylene ($LDPE_{15}$) and un-stabilized isotactic polypropylene (i-PP).

Bibliography

Abbas-Abadi, M. S., Haghighi, N. M., & Yeganeh, H. (2012). Effect of the Melt Flow Index and Melt Flow Rate on the Thermal Degradation Kinetics of Commercial Polyolefins. *Journal of Applied Polymer Science*, *126*(5), 1739–1745.

Al-Malaika, S., Ashley, H., & Issenhuth, S. (1994). The Antioxidant Role of a-Tocopherol in Polymers . I . The Nature of Transformation Products of a-tocopherol Formed during Melt Processing of LDPE *. *Journal of Polymer Science Part A: Polymer Chemistry*, *32*, 3099–3113.

Araújo, J. R., Waldman, W. R., & De Paoli, M. A. (2008). Thermal properties of high density polyethylene composites with natural fibres: Coupling agent effect. *Polymer Degradation and Stability*, *93*(10), 1770–1775. https://doi.org/10.1016/j.polymdegradstab.2008.07.021

Arora, S., Bagoria, R., & Kumar, M. (2010). Effect of alpha-tocopherol (vitamin E) on the thermal degradation behavior of edible oils Multiple-heating rate kinetics. *Journal of Thermal Analysis and Calorimetry*, *102*(1), 375–381. https://doi.org/10.1007/s10973-009-0460-2

ASTM D1238-04 Standard Test Method for Melt Flow Rates of Thermoplastics by Extrusion Plastomers. (2004). West Conshohocken, PA.

ASTM D3895-14, Standard Test Method for Oxidative-Induction Time of Polyolefins by Differential Scanning Calorimetry. (2014). West Conshohocken, PA.

ASTM E1641-99, Standard Test Method for Decomposition Kinetics by Thermogravimetry. (1999). West Conshohocken, PA.

Astruc, A., Bartolomeo, P., Fayolle, B., Audouin, L., & Verdu, J. (2004). Accelerated oxidative ageing of polypropylene fibers in aqueous medium under high oxygen pressure as studied by thermal analysis. *Polymer Testing*, *23*(8), 919–923. https://doi.org/10.1016/j.polymertesting.2004.05.002

Becker, R. F., Burton, L. P. J., & Amos, S. E. (1996). Additives. In E. P. Moore (Ed.), *Polypropylene Handbook: Polymerization, Characterization, Properties, Processing, Applications* (pp. 177–210). Hanser Publishers.

Blom, H., Yeh, R., Wojnarowski, R., & Ling, M. (2006). Detection of degradation of ABS materials via DSC. *Journal of Thermal Analysis and Calorimetry*, *83*(1–2), 113–115. https://doi.org/10.1016/j.tca.2006.01.015

Bremner, T., Rudin, A., & Cook, D. G. (1990). Melt flow index values and molecular weight distributions of commercial thermoplastics. *Journal of Applied Polymer Science*, *41*(7–8), 1617–1627. https://doi.org/10.1002/app.1990.070410721

Colin, X., & Verdu, J. (2006). Polymer degradation during processing. *Comptes Rendus Chimie*, *9*(11–12), 1380–1395. https://doi.org/10.1016/j.crci.2006.06.004

da Costa, H. M., Ramos, V. D., & de Oliveira, M. G. (2007). Degradation of polypropylene (PP) during multiple extrusions: Thermal analysis, mechanical properties and analysis of variance. *Polymer Testing*, *26*(5), 676–684. https://doi.org/10.1016/j.polymertesting.2007.04.003

Delva, L., Ragaert, K., Degrieck, J., & Cardon, L. (2016). The effect of extrusion reprocessing on the properties of montmorillonite filled polypropylene. In *AIP Conference Proceedings* (Vol. 1779). https://doi.org/10.1063/1.4965584

Ehrenstein, G. W., Riedel, G., & Trawiel, P. (2004). *Thermal Properties of Plastics. Theory and Practice*. Carl Hanser Verlag GmbH & Co.

Fearon, P. K., Bigger, S. W., & Billingham, N. C. (2004). DSC combined with chemiluminescence for studying polymer oxidation. *Journal of Thermal Analysis and Calorimetry*, *76*(1), 75–83. https://doi.org/10.1023/B:JTAN.0000027805.48648.c2

Fiorio, R., D'hooge, D. R., Ragaert, K., & Cardon, L. (2018). A statistical analysis on the effect of antioxidants on the thermal-oxidative stability of commercial massand emulsion-polymerized ABS. *Polymers*, *11*(1). https://doi.org/10.3390/polym11010025

Friedman, H. L. (1964). Kinetics of thermal degradation of char-forming plastics from thermogravimetry. Application to a phenolic plastic. *Journal of Polymer Science Part C: Polymer Symposia*, *6*(1), 183–195. https://doi.org/10.1002/polc.5070060121

Gao, X., Hu, G., Qian, Z., Ding, Y., Zhang, S., Wang, D., & Yang, M. (2007). Immobilization of antioxidant on nanosilica and the antioxidative behavior in low density polyethylene. *Polymer*, *48*(25), 7309–7315. https://doi.org/10.1016/j.polymer.2007.10.015

Grabmayer, K., Wallner, G. M., Beißmann, S., Schlothauer, J., Steffen, R., Nitsche, D., …

Lang, R. W. (2014). Characterization of the aging behavior of polyethylene by photoluminescence spectroscopy. *Polymer Degradation and Stability*, *107*, 28–36. https://doi.org/10.1016/j.polymdegradstab.2014.04.030

Gregorová, A., Cibulková, Z., Košíková, B., & Šimon, P. (2005). Stabilization effect of lignin in polypropylene and recycled polypropylene. *Polymer Degradation and Stability*, *89*(3), 553–558. https://doi.org/10.1016/j.polymdegradstab.2005.02.007

Guerrica-Echevarría, G., Eguiazábal, J. I., & Nazábal, J. (1996). Effects of reprocessing conditions on the properties of unfilled and talc-filled polypropylene. *Polymer Degradation and Stability*, *53*(1), 1–8. https://doi.org/10.1016/0141-3910(96)00018-3

He, X., Yin, G., & Ma, B. (1990). A study on the decomposition kinetics of vitamin C powder. *Acta Pharmaceutica Sinica*, *25*(7), 543–550.

Herek, L. C. S., Hori Eponina, C., Miranda Reis, M. H., Mora Diaz, N., Granhem Tavares, C. R., & Bergamasco, R. (2012). Characterization of ceramic bricks incorporated with textile laundry sludge. *Ceramics International*, *38*(2), 951–959. https://doi.org/10.1016/j.ceramint.2011.08.015

Hoàng, E. M., Allen, N. S., Liauw, C. M., Fontán, E., & Lafuente, P. (2006). The thermo-oxidative degradation of metallocene polyethylenes: Part 2: Thermal oxidation in the melt state. *Polymer Degradation and Stability*, *91*(6), 1363–1372. https://doi.org/10.1016/j.polymdegradstab.2005.07.018

Ilie, S., & Senetscu, R. (2009). *Polymeric Materials Review on Oxidation, Stabilization and Evaluation using CL and DSC Methods*. Retrieved from https://cds.cern.ch/record/1201650

Johnston, R. T., & Morrison, E. J. (1996). Thermal Scission and Cross-Linking during Polyethylene Melt Processing. In R. L. Clough, N. C. Billingham, & K. T. Gillen (Eds.), *Polymer Durability: Degradation, Stabilization, and Lifetime Prediction* (Vol. 249, pp. 651–682). American Chemical Society. https://doi.org/10.1021/ba-1996-0249.ch039

Kissinger, H. E. (1957). Reaction Kinetics in Differential Thermal Analysis. *Analytical Chemistry*, *29*(11), 1702–1706. https://doi.org/10.1021/ac60131a045

Klímová, K., & Leitner, J. (2012). DSC study and phase diagrams calculation of binary systems of paracetamol. *Thermochimica Acta*, *550*(2), 59–64.

https://doi.org/10.1016/j.tca.2012.09.024

Larrea-Wachtendorff, D., Tabilo-Munizaga, G., Moreno-Osorio, L., Villalobos-Carvajal, R., & Pérez-Won, M. (2015). Protein Changes Caused by High Hydrostatic Pressure (HHP): A Study Using Differential Scanning Calorimetry (DSC) and Fourier Transform Infrared (FTIR) Spectroscopy. *Food Engineering Reviews*, *7*(2), 222–230. https://doi.org/10.1007/s12393-015-9107-1

Majewsky, M., Bitter, H., Eiche, E., & Horn, H. (2016). Determination of microplastic polyethylene (PE) and polypropylene (PP) in environmental samples using thermal analysis (TGA-DSC). *Science of the Total Environment*, *568*, 507–511. https://doi.org/10.1016/j.scitotenv.2016.06.017

Mason, L. R., & Reynolds, A. B. (1997). Standardization of oxidation induction time testing used in life assessment of polymeric electric cables. *Journal of Applied Polymer Science*, *66*(9), 1691–1702. https://doi.org/10.1002/(sici)1097-4628(19971128)66:9<1691::aid-app7>3.3.co;2-5

Menczel, J. D., Judovits, L., Prime, B. R., Bair, H. E., Reading, M., & Swier, S. (2009). Differential Scanning Calorimetry (DSC). In J. D. Menczel & B. R. Prime (Eds.), *Thermal Analysis of Polymers: Fundamentals and Applications* (pp. 7–239). WILEY.

Menczel, J. D., Prime, B. R., & Gallagher, P. K. (2009). Introduction. In J. D. Menczel & B. R. Prime (Eds.), *Thermal Analysis of Polymers: Fundamentals and Applications* (pp. 1–7). WILEY.

Okamba-Diogo, O., Richaud, E., Verdu, J., Fernagut, F., Guilment, J., Pery, F., & Fayolle, B. (2016). Quantification of hindered phenols in polyamide 11 during thermal aging. *Polymer Testing*, *52*, 63–70. https://doi.org/10.1016/j.polymertesting.2016.03.023

Ono, K., & Yamaguchi, M. (2009). Thermal and Mechanical Modification of LDPE in Single-Screw Extruder. *Journal of Applied Polymer Science*, *113*, 1462–1470. https://doi.org/10.1002/app

Peacock, A. J. (2000). *Handbook of Polyethylene: Structures, Properties, and Applications*. New York: Marcel Dekker.

Pospíšil, J., Horák, Z., Pilař, J., Billingham, N. C., Zweifel, H., & Nešpůrek, S. (2003). Influence of testing conditions on the performance and durability of polymer stabilisers

in thermal oxidation. *Polymer Degradation and Stability*, *82*(2), 145–162. https://doi.org/10.1016/S0141-3910(03)00210-6

Prime, B. R., Bair, H. E., Vyazovkin, S., Gallagher, P. K., & Riga, A. (2009). Thermogravimetric Analysis (TGA). In J. D. Menczel & B. R. Prime (Eds.), *Thermal Analysis of Polymers: Fundamentals and Applications* (pp. 241–318). WILEY.

Rabello, M. S., & White, J. R. (1997). Crystallization and melting behaviour of photodegraded polypropylene — I. Chemi-crystallization. *Polymer*, *38*(26), 6379–6387.

Rosa, D. S., Sarti, J., Mei, L. H. I., Filho, M. M., & Silveira, S. (2000). A study of parameters interfering in oxidative induction time (OIT) results obtained by differential scanning calorimetry in polyolefin. *Polymer Testing*, *19*(5), 523–531. https://doi.org/10.1016/S0142-9418(99)00022-7

Rosato, D. V., Rosato, D. V., & Rosato, M. V. (2004). Extrusion. In D. V. Rosato, D. V. Rosato, & M. V. Rosato (Eds.), *Plastic Product Material and Process Selection Handbook* (pp. 227–281). Elsevier Science.

Schmid, M, Ritter, A., & Affolter, S. (2006). Determination of oxidation induction time and temperature by DSC. *Journal of Thermal Analysis and Calorimetry*, *83*(2), 367–371. https://doi.org/10.1007/s10973-005-7142-5

Schmid, Manfred, & Affolter, S. (2003). Interlaboratory tests on polymers by differential scanning calorimetry (DSC): determination and comparison of oxidation induction time (OIT) and oxidation induction temperature (OIT*). *Polymer Testing*, *22*(4), 419–428. https://doi.org/10.1016/S0142-9418(02)00122-8

Symoniuk, E., Ratusz, K., & Krygier, K. (2016). Comparison of the oxidative stability of linseed (Linum usitatissimum L.) oil by pressure differential scanning calorimetry and Rancimat measurements. *Journal of Food Science and Technology*, *53*(11), 3986–3995. https://doi.org/10.1007/s13197-016-2398-2

Van der Vegt, A. K. (2002). *From Polymers to Plastics*. Delft: Delft University Press.

Vishu, S. (2006). Weathering Properties. In S. Vishu (Ed.), *Handbook of Plastics Testing and Failure Analysis* (3rd ed., pp. 139–156). John Wiley & Sons, Inc.

Volponi, J. E., Innocentini Mei, L. H., & dos Santos Rosa, D. (2004). Use of oxidation onset temperature measurements for evaluating the oxidative degradation of isotatic

polypropylene. *Journal of Polymers and the Environment*, *12*(1), 11–16. https://doi.org/10.1023/B:JOOE.0000003123.68569.0e

Vyazovkin, S., Burnham, A. K., Criado, J. M., Pérez-Maqueda, L. A., Popescu, C., & Sbirrazzuoli, N. (2011). ICTAC Kinetics Committee recommendations for performing kinetic computations on thermal analysis data. *Thermochimica Acta*, *520*(1–2), 1–19. https://doi.org/10.1016/j.tca.2011.03.034

Wagner Jr, J. R., Mount III, E. M., & Giles Jr, H. F. (2014a). Extrusion Process. In J. R. Wagner Jr, E. M. Mount III, & H. F. Giles Jr (Eds.), *Extrusion: The Definitive Processing Guide and Handbook* (2nd ed., pp. 3–11). Elsevier.

Wagner Jr, J. R., Mount III, E. M., & Giles Jr, H. F. (2014b). Plastic Behavior in Twin Screw Extruders. In J. R. Wagner Jr, E. M. Mount III, & H. F. Giles Jr (Eds.), *Extrusion: The Definitive Processing Guide and Handbook* (2nd ed., pp. 149–169). Elsevier.

Wallius, S. (1993). Methodological investigations on the thermal stability of polypropylene. *Die Angewandte Makromolekulare Chemie*, *212*(1), 103–119. https://doi.org/10.1002/apmc.1993.052120110

Woo, L., Khare, A. R., Sandford, C. L., Ling, M. T. K., & Ding, S. Y. (2001). Relevance of high temperature oxidative stability testing to long term polymer durability. *Journal of Thermal Analysis and Calorimetry*, *64*(2), 539–548. https://doi.org/10.1023/A:1011594901752

CHAPTER IV

POLYMER FORMULATION: Incorporation of natural antioxidant molecules

Polyolefins, as carbon-based materials, are prone to degradation and two different degradation mechanisms were observed for bare un-stabilized isotactic polypropylene (i-PP) and bare un-stabilized low-density polyethylene ($LDPE_{15}$). Also, two test-methods followed by DSC and TGA were proposed and standardized to assess the effect of thermo-mechanical events present during extrusion process.

This chapter embodies the characterization and analysis of selected natural antioxidants and their incorporation into i-PP and $LDPE_{15}$ and sustains the hypothesis of this thesis dissertation: natural antioxidants do provide thermal stability during industrial transformation. The oxidation onset temperature (OOT) and the energy of activation at degradation (E_{adeg}) were evaluated for different polymer formulations. Furthermore, rheological analysis was carried out to study the effect of antioxidant(s) incorporation into i-PP and $LDPE_{15}$ by extrusion process.

4.1 Antioxidants

Olefin resins are prone to deterioration induced by the oxidative atmospheric attack during its processing but also, handling and storage conditions are important factors to consider in the development of detrimental properties such as optical and mechanical properties. The incorporation of additives to stabilize polymer resins are thus of importance.

Antioxidants are molecules that retard the effect of degradation in the polymer backbone induced by the presence of radical species acting as polymer thermal stabilizers. The involved mechanism is by the inactivation of free radical species and the resulting oxidized antioxidants react with another radical form yielding a nonradical specie in a termination step.

4.2 Flaxseed oil

A polyunsaturated oil derived from the seed of the flax plant. It is one of the most unsaturated common oils. Among the total fatty acids content, around 50% corresponds to alpha-linoleic acid (ALA), 18% to Oleic acid, and 14% to linoleic acid (LA) (Daun, Barthet, Chornick, & Duguid, 2003) (figure 4.1 represents the chemical structures).

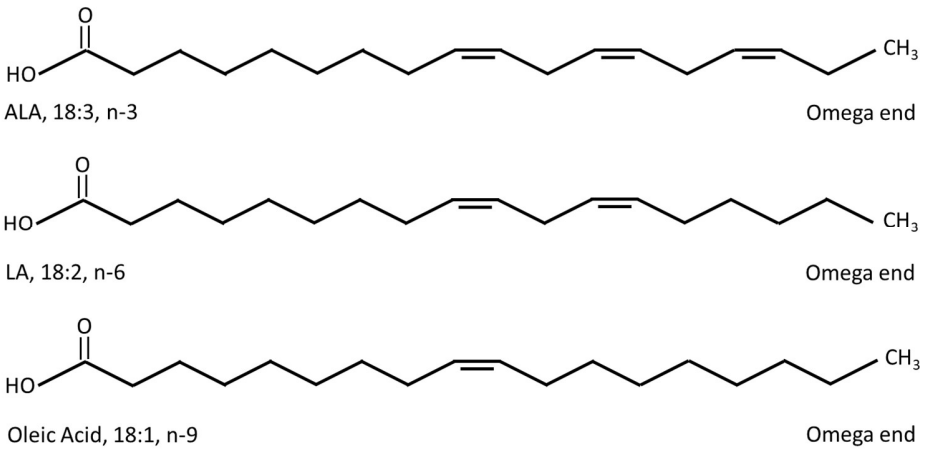

Figure 4.1. Fatty acid structures.

4.2.1 Thermal Analysis

The thermal degradation of flaxseed oil was performed by thermogravimetric analysis (TGA). The onset temperature (Tonset), maximum temperature (Tmax), end-set temperature (Tendset), and the temperature profile at 1% and 5% of mass loss ($T_{1\%}$, $T_{5\%}$) were assessed.

4.2.1.1 Methodology

Linseed oil (LSO) and Flaxseed oil (FSO) were supplied by Sigma, France and Terpenic Labs, Spain respectively. Thermal analysis was performed with a TA instrument TGA Q50; the carrier gas used was nitrogen (inert atmosphere) and air (oxidative atmosphere) at a flow rate of 60 mL/min and a heating rate of 10 °C/min.

4.2.2.1 Results

Figure 4.2 and Figure 4.3 represent the differential thermogravimetry (dTGA) and the thermogravimetry (TGA) curves of the thermal degradation of FSO in nitrogen and air respectively.

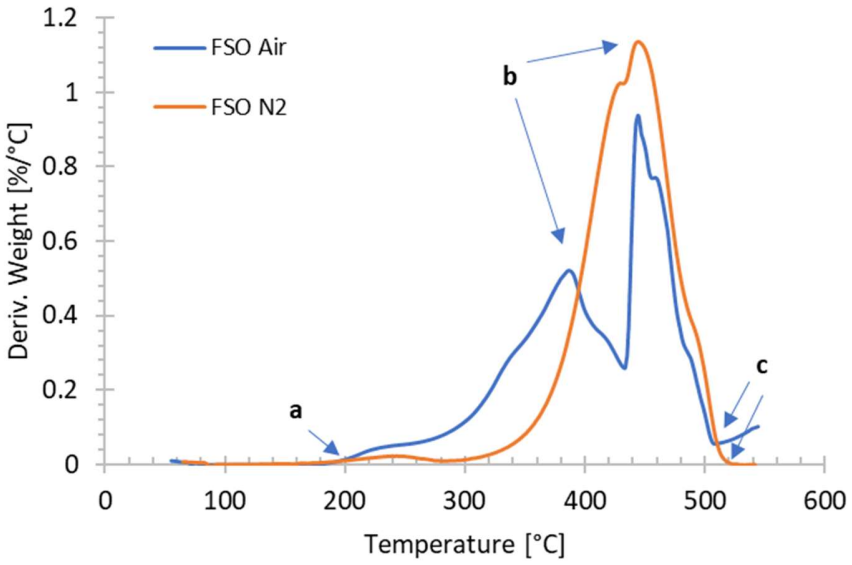

Figure 4.2. dTGA thermograms of the thermal degradation of FSO in nitrogen (N_2) and air (Air). **a**. Tonset, **b**. Tmax, **c**. Tendset.

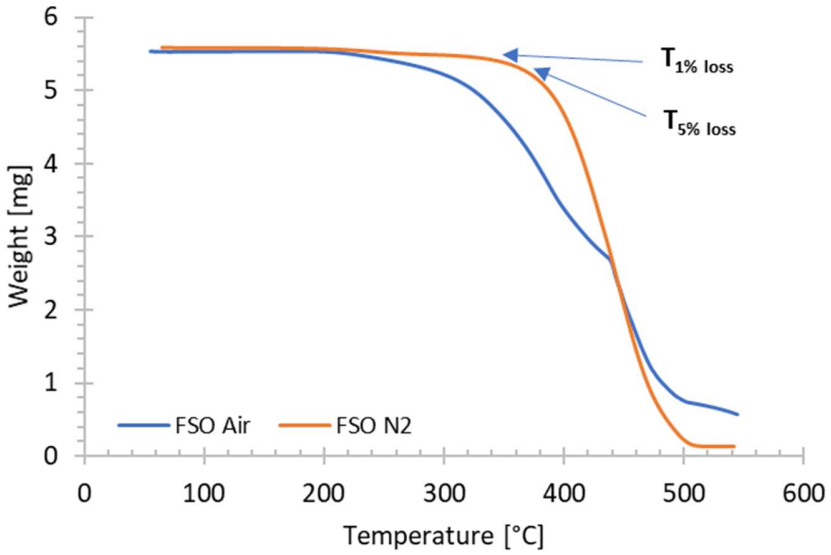

Figure 4.3. TGA thermograms of the thermal degradation of FSO in nitrogen (N_2) and air (Air).

Table 4.1 shows the corresponding dTGA and TGA calculated values.

Antioxidant	Atmosphere	Tonset [°C]	Tmax [°C]	Tendset [°C]	$T_{1\% loss}$ [°C]	$T_{5\% loss}$ [°C]
FSO	Air	198.4	386.4	391.2	230.5	293.2
FSO	Nitrogen	196.7	444.8	455.6	240.0	361.6

Table 4.1 Thermal degradation temperatures for FSO.

The peak temperature observed from the dTGA curves indicates the maximum rate of mass change. From Table 4.1, it is observed the effect of an oxidative atmosphere on the thermal degradation of FSO with an observed reduction in the peak temperature (Tmax) of approximately 58 °C as compared to the FSO degradation profile in nitrogen (inert atmosphere). This reduction is also observed from the TGA curves at 1% and 5% of mass loss being approximately 10 °C and 68°C of difference respectively.

Figure 4.4 and Figure 4.5 represent the differential thermogravimetry (dTGA) and the thermogravimetry (TGA) curves of the thermal degradation of LSO in nitrogen and air respectively.

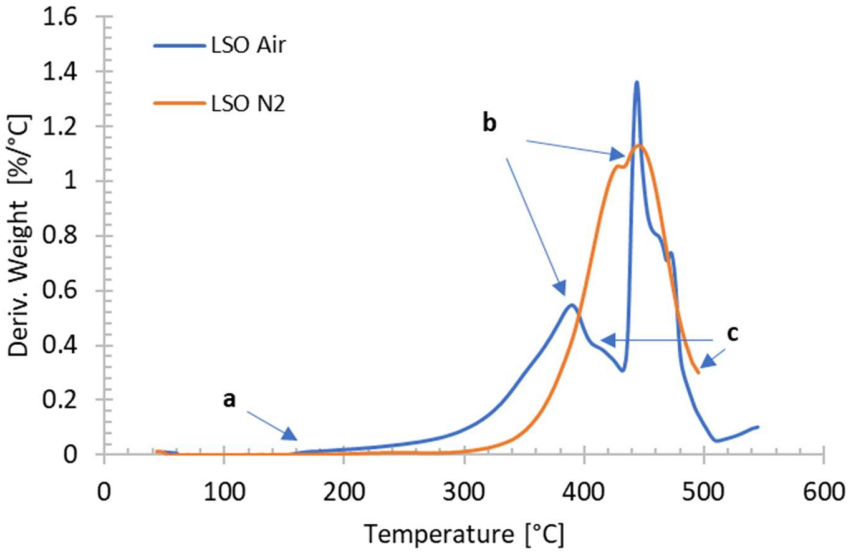

Figure 4.4. dTGA thermograms of the thermal degradation of LSO in nitrogen (N_2) and air (Air). **a**. Tonset, **b**. Tmax, **c**. Tendset.

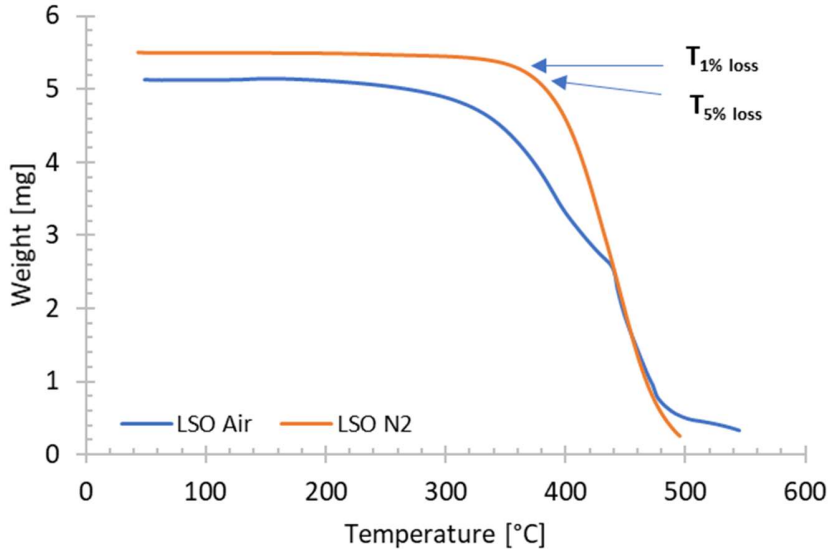

Figure 4.5. TGA thermograms of the thermal degradation of LSO in nitrogen (N_2) and air (Air).

Table 4.2 shows the corresponding dTGA and TGA results.

Antioxidant	Atmosphere	Tonset [°C]	Tmax [°C]	Tendset [°C]	$T_{1\% loss}$ [°C]	$T_{5\% loss}$ [°C]
LSO	Air	186.0	389.2	394.1	229.3	302.7
LSO	Nitrogen	204.4	444.7	455.4	300.7	367.1

Table 4.2 Thermal degradation temperatures for LSO.

From Table 4.2, it is observed the oxidative effect of air on the thermal degradation of LSO with an observed reduction in the peak temperature (Tmax) of approximately 55 °C as compared to the FSO degradation profile in nitrogen (inert atmosphere). This reduction is also observed from the TGA curves at 1% and 5% of mass loss being approximately 71 °C and 74°C of difference respectively. Table 4.3 and Table 4.4 presents the thermal degradation temperatures for FSO and LSO.

Antioxidant	Atmosphere	Tonset [°C]	Tmax [°C]	Tendset [°C]
FSO	Air	198.4	386.4	391.2
LSO	Air	186.0	389.2	394.1
FSO	Nitrogen	196.7	444.8	455.6
LSO	Nitrogen	204.4	444.7	455.4

Table 4.3 Thermal degradation temperatures for FSO and LSO in nitrogen and air.

		Percentage of mass loss [°C]						
Antioxidant	Atmosphere	$T_{1\% loss}$	$T_{5\% loss}$	$T_{10\% loss}$	$T_{15\% loss}$	$T_{20\% loss}$	$T_{25\% loss}$	$T30_{\% loss}$
FSO	Air	230.5	293.2	326.3	344.5	359.1	371.3	381.7
LSO	Air	229.3	302.7	336.5	355.0	368.7	379.9	389.4
FSO	Nitrogen	240.0	361.6	385.0	397.1	405.5	412.2	417.9
LSO	Nitrogen	300.7	367.1	385.9	397.2	405.3	411.8	417.4

Table 4.4 Degradation temperature profiles at specific percentage of mass loss for FSO and LSO.

From Table 4.3 it is observed the effect of an oxidative atmosphere on the thermal degradation of FSO and LSO. This is possibly attributed to the rapid oxidation of polyunsaturated fatty acids present in flaxseed oil. It is also observed a lower onset degradation temperature for LSO (186 °C) as compared to FSO (198.4 °C). Nonetheless, the peak temperature and the endset temperature in both, air and nitrogen atmospheres, are similar.

Furthermore, Table 4.4 presents the degradation temperature profiles for FSO and LSO. In the case of FSO, results show that, within the mass loss range from 5% to 30%, there is an averaged difference in temperature of 9.3 °C lower than the mass loss profile for LSO, both evaluated in air. In the case of thermal degradation of FSO and LSO carried out in nitrogen and within the same mass loss range, there is no significant difference (0.9 °C) between the mass loss profiles of FSO and LSO. The TGA thermograms are shown in Figure 4.6.

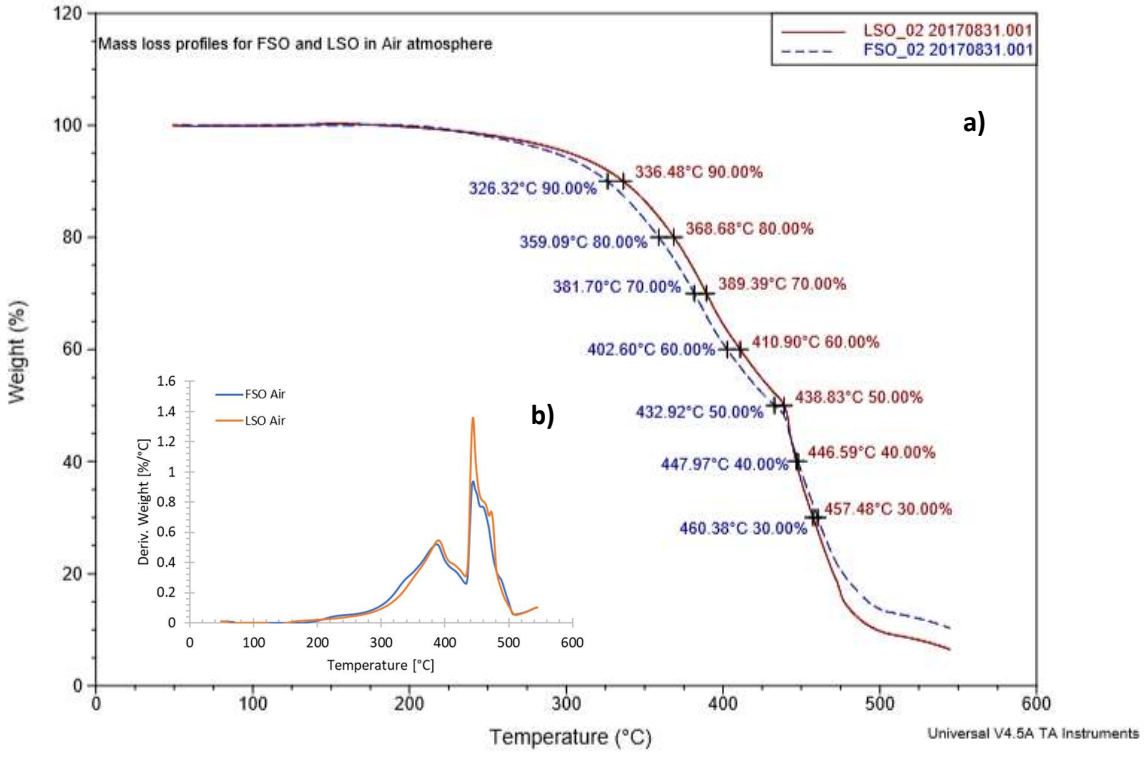

Figure 4.6. **a**. TGA mass loss temperature profiles and **b**. dTGA curves for FSO and LSO in air atmosphere.

The degradation profile under an oxidative atmosphere for flaxseed oil is represented by an exothermic process caused by the oxidation of unsaturated fatty acids in the range of 150 to 250 °C. A second decomposition step is observed between 250 and 400 °C and finally, above 400 °C the main processes of decomposition (combustion) are present. Figure 4.7 represents the TGA and dTGA thermograms for FSO where it is observed the same degradation profile as reported in literature (Lazzari & Chiantore, 1999).

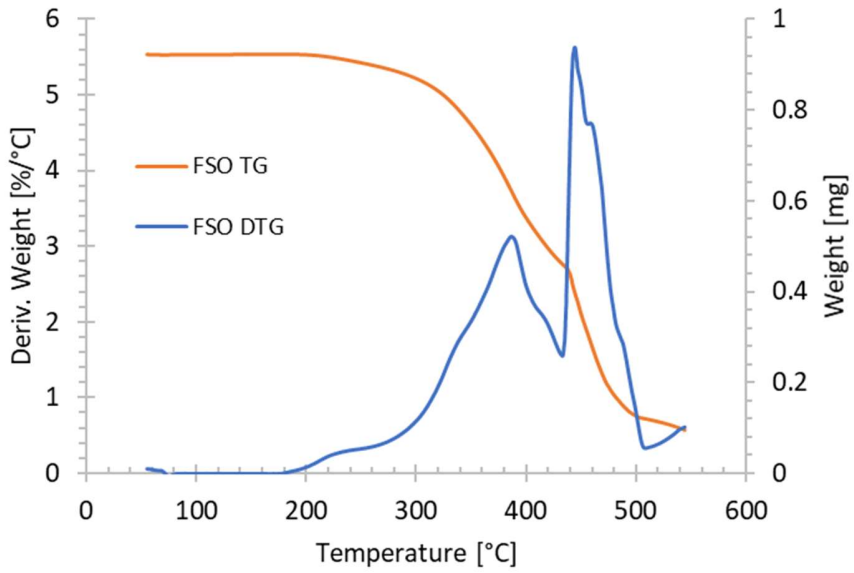

Figure 4.7. TGA and dTGA thermograms of the thermal degradation of FSO in air.

A step-wise isothermal analysis was performed in LSO and FSO to assess the degradation profile to best validate quantitatively the weight loss events. Figure 4.8 represents the TGA thermograms for both, LSO and FSO. It is osberved that, compounds present in both oils degrade at approximately the same temperature within three main weight loss events as reported in literature.

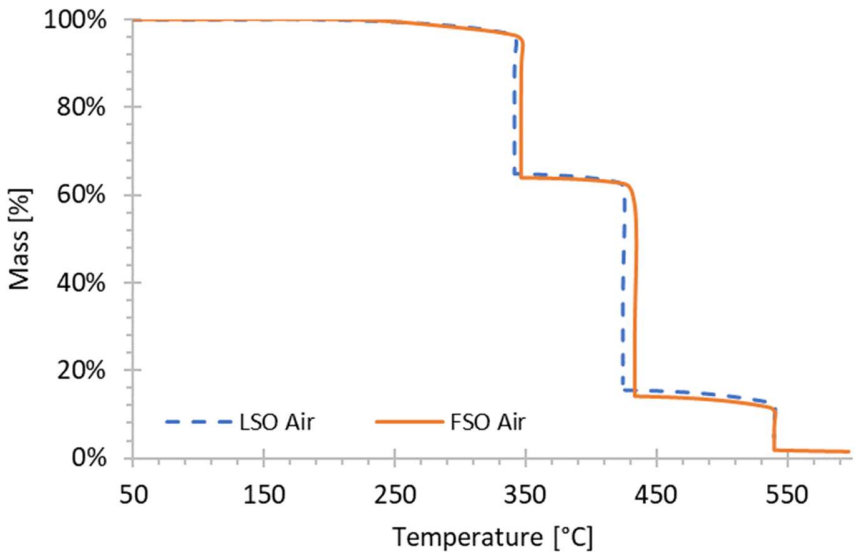

Figure 4.8. TGA thermograms for LSO (dashed line) and FSO (solid line).

4.2.1.3 Conclusions

Resulting thermograms shown in Figure 4.6a showed a slight lower degradation temperature profile for FSO than LSO. Although, the maximum rate of change of mass loss represented by the peak maxima in temperature (Figure 4.6b) showed an observed value of 386.4 °C and 389.2 °C for FSO and LSO respectively. Thus, there is not a significant difference in the thermal-degradation and thermo-oxidative degradation of FSO and LSO.

It is important to mentioned that FSO from Terpenic Labs specifies the extraction method (cold-pressed extraction), whereas LSO from Sigma, France does not provide information. This is of importance in order to estimate the thermal stability for both oils under oxidative conditions. It is reported in literature that oxidation in oils are dependent on the extraction process but also, among other factors such as storage conditions, temperature, light, and oxygen availability.

4.2.2 Oxidative degradation analysis

It is known the susceptibility of oils with high content of polyunsaturated fatty acids to deteriorate (oxidation) partially induced by heat and storage conditions. Furthermore, oxidation in oils lead to undesirable products that affects sensorial properties such as flavors. The thermo-oxidative stability of flaxseed oils must be evaluated in order to determine its viability as a potential source of natural antioxidants for polymer stabilization during processing.

Oxidative degradation of oils can be assessed by UV-Vis spectrophotometry following the specific extinction coefficient value. The degree of oxidation can be assessed in a wavelength range between 232 nm and 274 nm. At 232 nm, primary oxidation products are absorbed (peroxydes and hydroperoxydes) whereas secondary oxidation products such as aldehydes, ketones, and acids are absorbed at higher wavelengths: 262, 268, 270, and 274 nm (Antolín & Meneses, 2000).

Thermal stability of FSO and LSO under oxidative conditions is assessed experimentally to validate the combined effect of temperature and incubation time when oil is exposed to a continuous air flux. The specific extinction coefficient value (K_{270}) was calculated according to equation 4.1.

$$K_\lambda = \frac{D_\lambda}{C\ x\ L} \tag{4.1}$$

Where K_λ is the specific extinction coefficient for a fixed wavelength, D_λ is the absorbance reading, C is the sample concentration (in g/100 mL), and L is the path length of light (Antolín & Meneses, 2000).

4.2.2.1 Methodology

The effect of thermal stability of FSO and LSO was evaluated on temperature, air atmosphere, and exposure time. Approximately 25 mL of either FSO and LSO were exposed to a continuous air-flux. Table 4.5 shows schematically the experimental runs. For UV-Vis spectrophotometry analysis, a fixed oil concentration of 2.5 g/100 mL was utilized.

Sample	Heating conditions [°C]	Incubation time [hr]
FSO	w/o heating	w/o incubation
FSO	120	3
LSO	w/o heating	w/o incubation
LSO	120	3

Table 4.5. Experimental conditions to assess thermal stability in flaxseed oil (FSO) and (LSO).

Two representative samples for both, FSO and LSO, were used as control (without treatment).

4.2.2.2 Results

Figure 4.9 and Figure 4.10 show the full spectrum wavelength analysis. Within the analysis range corresponding to oxidation products absorbed during oxidation (232 nm to 274 nm) It is observed, in the case of FSO, an increment in absorbance. Whereas LSO showed a higher absorbance increment in the wavelength range of 250 nm to 274 nm.

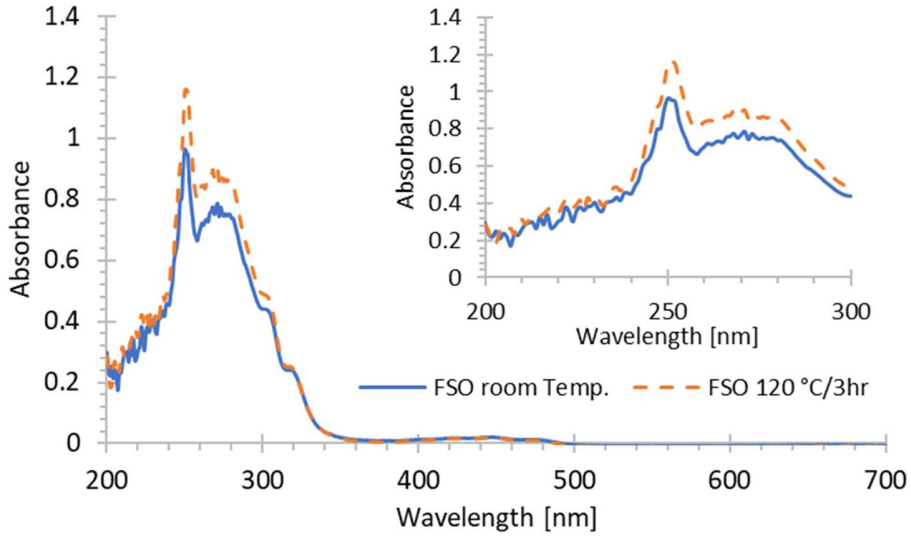

Figure 4.9. UV-VIS Spectrophotometry wavelength scan for FSO solution.

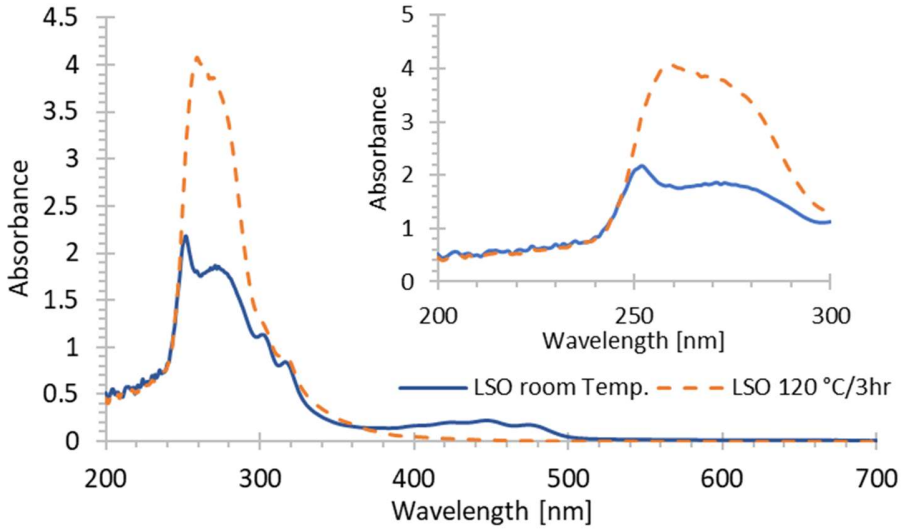

Figure 4.10. UV-VIS Spectrophotometry wavelength scan for LSO solution.

Determination of the specific extinction coefficient, K_{270}.

Individual absorbance reading corresponding to each experimental run was utilized to calculate the specific extinction coefficient (K_{270}). Figure 4.11 illustrates the resulting values. Furthermore, the wavelength range in the region of 234 nm to 274 nm, that corresponds to the absorption of oxidation products, were evaluated by calculating the area under the curve (Figure 4.12) and correlated to the specific extinction coefficient for the experimental runs.

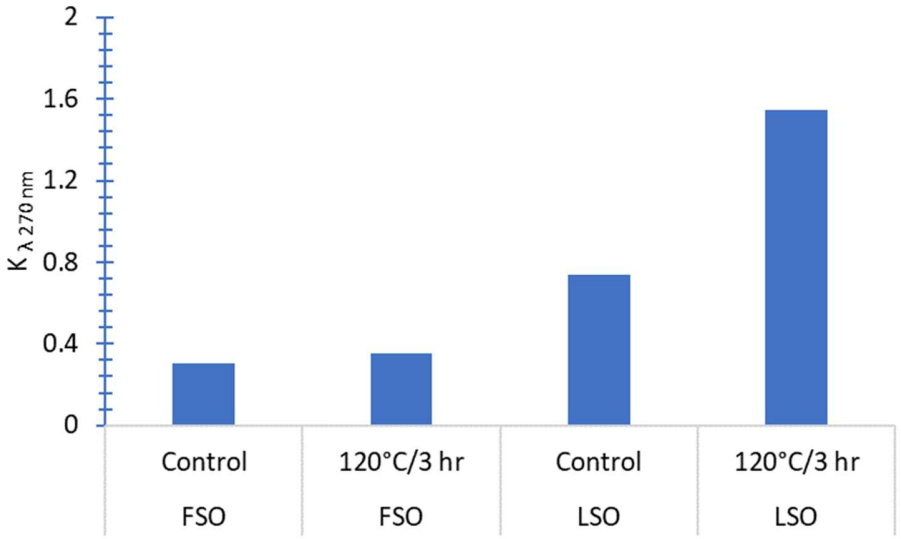

Figure 4.11. Specific coefficient of extinction, K_{270}.

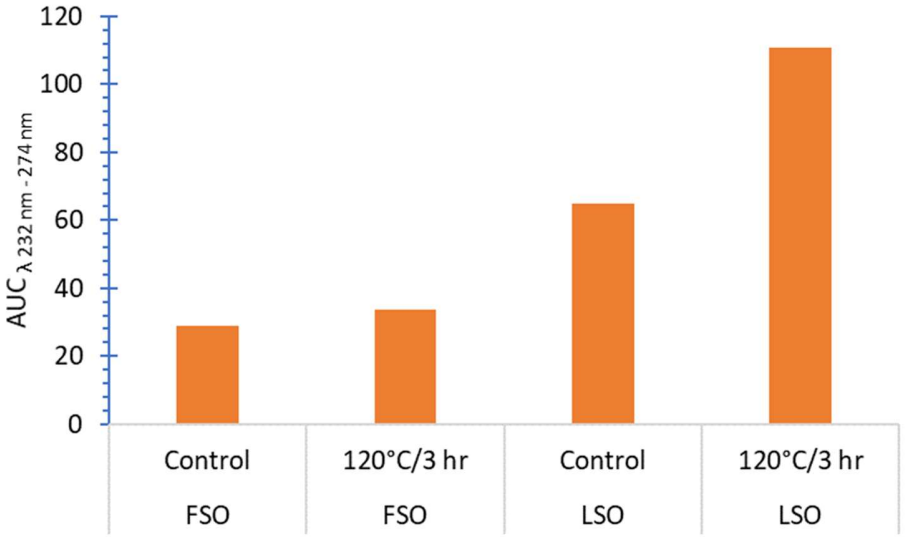

Figure 4.12. Area under the curve in the region of the spectrum 234 nm to 274 nm.

4.2.2.3 Conclusions

Both methods determined the thermo-oxidative stability of FSO and LSO. It is observed that FSO presented a higher thermo-oxidative stability, under the experimental conditions evaluated, than LSO. This is represented by either a lower K_{270} value or a lower area under the curve (AUC) within the wavelength region analyzed.

Furthermore, the effect of temperature, exposure time, and air atmosphere on LSO, followed by the K_{270} value, is almost two times higher as compared to the control LSO sample. On the other hand, FSO only presented an increment of approximately 16% as compared with its control sample counterpart. Figure 4.13 presents the correlation fit between the two UV-VIS Spectrophotometry test-methods.

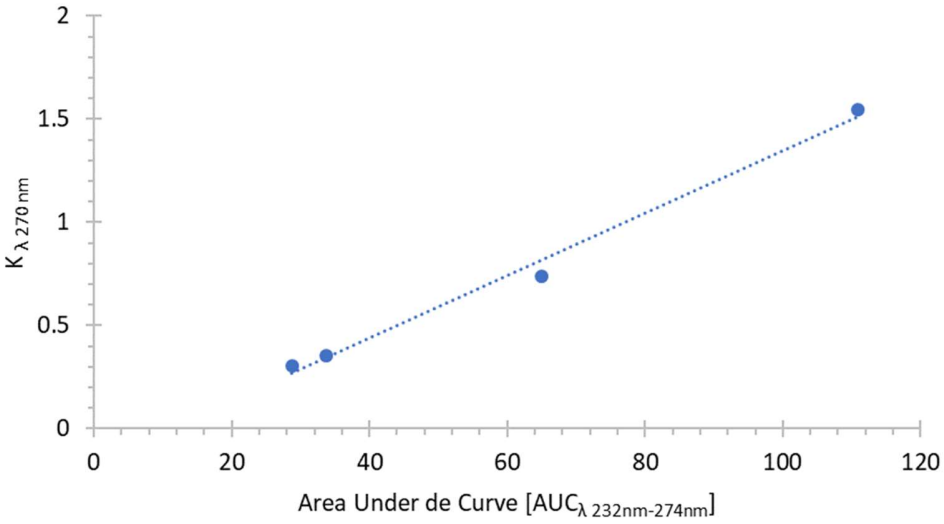

Figure 4.13. Correlation between the specific coefficient of extinction, K_{270} and the area under the curve in the region of the spectrum 234 nm to 274 nm.

The calculated Pearson correlation coefficient from figure 4.13 is r = 0.995 resulting in a positive and robust correlation between the two test-methods.

4.2.3 Antioxidant Capacity determination of FSO

It is confirmed, under the experimental conditions evaluated, a higher thermo-oxidative stability of FSO. One step further and prior to incorporation into a polymer matrix, is to determine the antioxidant activity. The DPPH$^{\cdot}$ method was selected to assess the antioxidant capacity of FSO.

4.2.3.1 Methodology

Briefly, the reaction mixture of a final volume assay of 1000 µL containing a 100 µL aliquot of extracted edible oil (in ethanol and ethyl acetate) and a 100 µL aliquot of DPPH$^{\cdot}$ radical

solution (175 μM) was monitored spectrophotometrically at λ = 520 nm and at two kinetic end-points: 5 minutes and 1 hour.

Sample preparation

Flaxseed oil was diluted with ethanol, stirred for 5 minutes, and centrifuge for additional 5 minutes at 5000 rpm and room temperature. The ethanolic fraction was separated from the lipidic phase for antioxidant capacity determination. Same procedure was followed for flaxseed oil dissolved in ethyl acetate. Figure 4.14 and Figure 4.15 illustrate the maxima wavelength selected and the respective diluted oil samples in presence of DPPH$^{\cdot}$ radical.

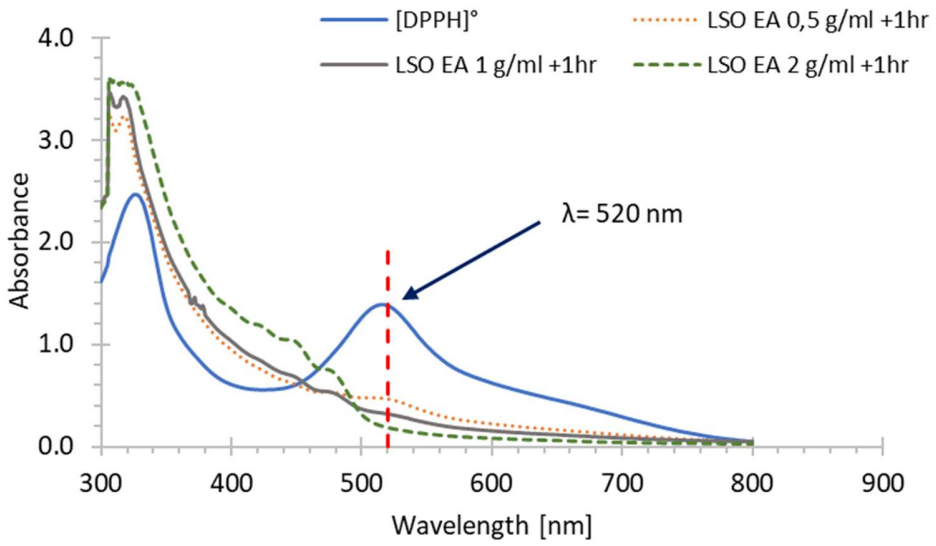

Figure 4.14. UV-VIS Spectrophotometry wavelength scan for FSO antioxidant determination by DPPH$^{\cdot}$ method (ethyl acetate as solvent).

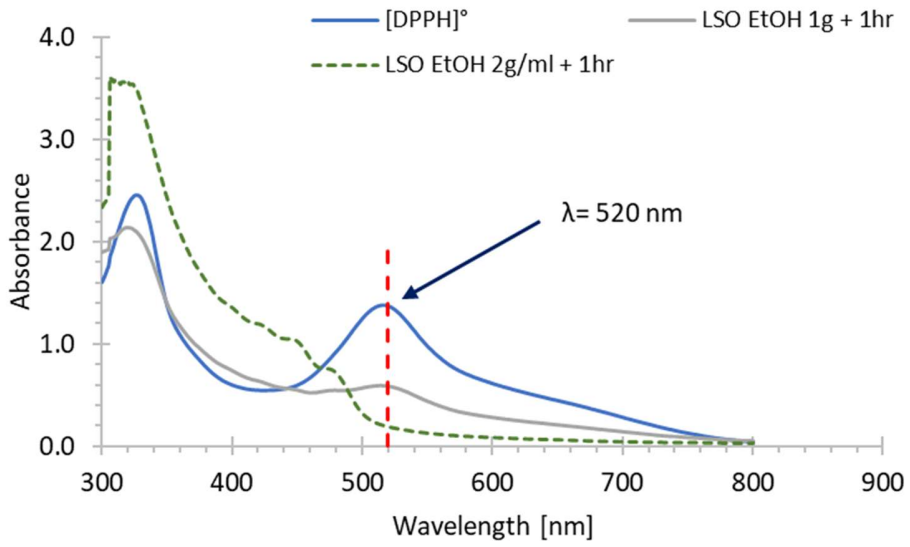

Figure 4.15. UV-VIS Spectrophotometry wavelength scan for FSO antioxidant determination by DPPH· method (ethanolic extraction).

At λ = 520 nm, the delta in absorbance between the control (DPPH· radical) and the diluted samples allowed to follow the radical scavenging activity against DPPH· radical. Figure 4.16 and Figure 4.17 illustrate the antioxidant activity of flaxseed oil (FSO).

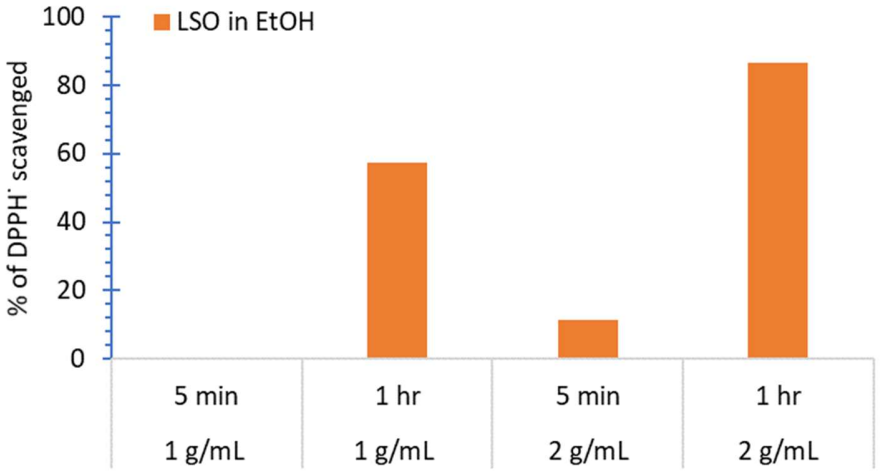

Figure 4.16. Antioxidant capacity determination of FSO in ethanol (EtOH) solution.

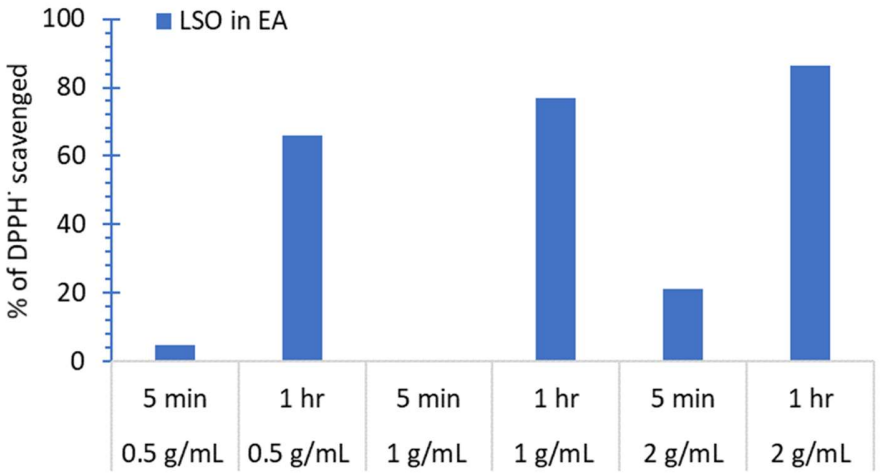

Figure 4.17. Antioxidant capacity determination of FSO in ethyl acetate (EA) solution.

4.2.3.2 Results

Results showed antioxidant activity of FSO toward DPPH· radical. There is a solvent interaction on the percentage of DPPH· radical scavenged, being ethyl acetate (EA) the solvent system that presented the higher antioxidant activity (34% higher) at a concentration of 1 g/mL and an end-point reading of 1 hour. Additionally, the antioxidant activity of flaxseed oil dissolved in ethyl acetate includes hydrophobic compounds which are non-soluble in ethanol hence, a higher antioxidant activity may be expected (Espín, Soler-Rivas, & Wichers, 2000).

4.2.3.3 Conclusions

Thus far, it has been assessed the thermal-oxidation stability of FSO and LSO and corroborated experimentally the potential antioxidant activity of FSO. The incorporation of natural antioxidants such as ascorbic acid and α-tocopherol, with an observed fast reaction

rate on scavenging $DPPH^{\cdot}$ and $ABTS^{\cdot+}$ radicals, may provide protection to FSO and a synergistic effect for thermal stability in polymers.

4.3 Ascorbic acid

Ascorbic acid (AsA) is a low molar mass antioxidant molecule (176.12 g/mol g) with potential antioxidant activity. The molecular structure presents two hydroxyl groups with a high reductive potential able to scavenge superoxide anion radicals, singlet oxygen, hydrogen peroxide, and hydroxyl radicals (Bennette, Logan, Shiferaw-Terefe, Singh, & Robin, 2014; Jomova, Lawson, & Valko, 2014). The hydroxyl groups on adjacent carbon atoms can chelate metal ions and quench singlet oxygen (Brewer, 2011). Figure 4.18 represents the chemical structure.

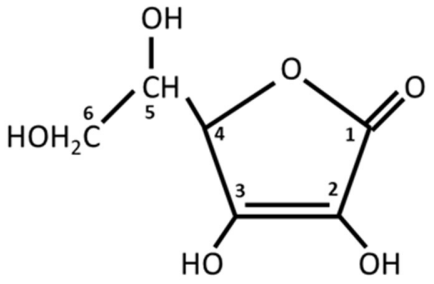

Figure 4.18. Ascorbic acid (AsA) chemical structure.

4.3.1 Thermal analysis

The thermal degradation of AsA was performed by thermogravimetric analysis (TGA). The onset temperature (Tonset), maximum temperature (Tmax), end-set temperature (Tendset), and the temperature profile at 1% and 5% of mass loss ($T_{1\%}$, $T_{5\%}$) were assessed.

4.3.1.1 Methodology

Ascorbic acid (AsA) was supplied by Sigma, France. Thermal analysis was performed with a TA instrument TGA Q50; the carrier gas used was nitrogen (inert atmosphere) and air (oxidative atmosphere) at a flow rate of 60 mL/min and a heating rate of 10 °C/min.

4.3.1.2 Results

Figure 4.19 and Figure 4.20 represent the differential thermogravimetry (dTGA) and the thermogravimetry (TGA) curves of the thermal degradation of AsA in nitrogen and air respectively.

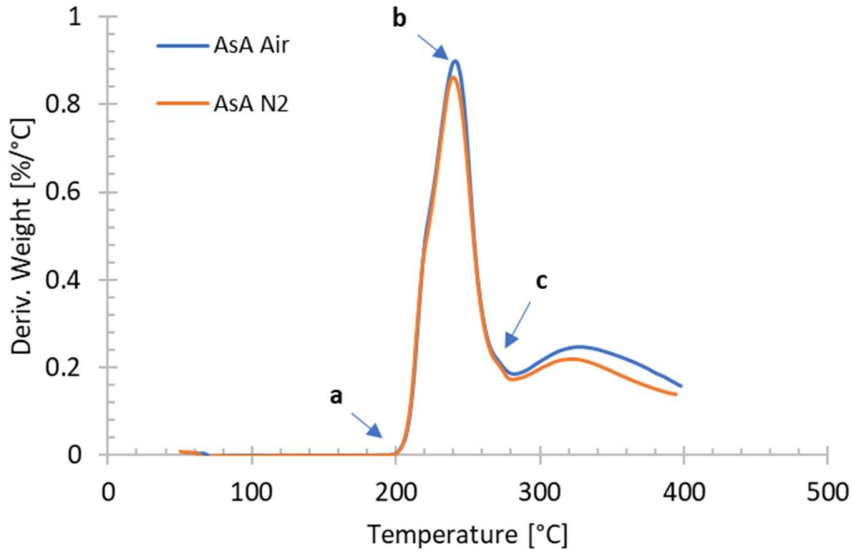

Figure 4.19. dTGA thermograms of the thermal degradation of AsA in nitrogen (N_2) and air (Air). **a**. Tonset, **b**. Tmax, **c**. Tendset.

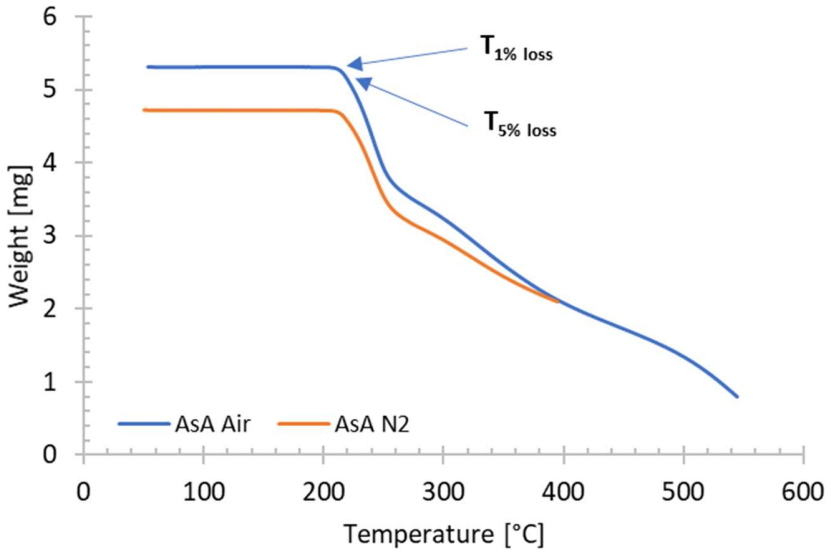

Figure 4.20. TGA thermograms of the thermal degradation of AsA in nitrogen (N_2) and air (Air).

The analysis of an oxidative atmosphere (Figure 4.19 and Figure 4.20) showed that AsA started to decompose at approximately 180 °C with the maximum rate of decomposition (Tmax) at 220 °C.

In a nitrogen atmosphere a similar degradation behavior at the onset degradation temperature and at the temperature of the maximum rate of decomposition is observed. For the two dTGA curves (air and nitrogen atmospheres) and within an interval temperature of analysis between room temperature and 500 °C it is observed two decomposition steps. The first one between the range of 180 °C and 240 °C approximately with a peak temperature at 220 °C. The second decomposition step observed is in the range of temperature between 260 °C and 430 °C approximately with a peak temperature at 310 °C approximately.

It is important to mention that the TA instrument TGA Q50 has passed through several calibrations within 2017. It has been evaluated the bias with a former TGA run on ascorbic acid and found a positive deviation of approximately +20 °C with the actual conditions. Thus, results expressed by the thermograms presented needs to be adjusted to – 20 °C, that

corresponds to the original profile of ascorbic acid. Table 4.6 and Table 4.7 show the corresponding dTGA and TGA results.

Antioxidant	Atmosphere	Tonset [°C]	Tmax [°C]	Tendset [°C]
AsA	Oxygen	202.0	240.5	259.6
AsA	Nitrogen	204.6	239.7	259.6

Table 4.6. Thermal degradation temperatures for AsA.

		Percentage of mass loss [°C]						
Antioxidant	Atmosphere	$T_{1\%\,loss}$	$T_{5\%\,loss}$	$T_{10\%\,loss}$	$T_{20\%\,loss}$	$T_{30\%\,loss}$	$T_{40\%\,loss}$	$T_{50\%\,loss}$
AsA	Air	214.0	223.1	231.0	242.7	258.0	304.1	345.6
AsA	Nitrogen	213.6	223.3	231.4	243.5	261.1	311.1	359.4

Table 4.7. Degradation temperature profiles at specific percentage of mass loss for AsA.

From Table 4.6 it is observed no significant effect of the atmosphere (nitrogen or oxygen) on the thermal degradation of ascorbic acid. This is further detailed in Table 4.7 where it is presented the degradation temperature profiles of AsA. It is observed, in the range of mass loss between 1% and 30% no significant effect on the degradation temperature profiles for both, air and nitrogen atmospheres with an averaged difference of 0.8 °C. A higher thermal degradation on AsA is observed on air atmosphere at a mass loss percentage range between 40% and 50% with an averaged difference of 8°C as compared to the same mass loss range performed in an inert atmosphere (nitrogen). Results are in agreement with those observed by (Nieva-Echevarría, Manzanos, Goicoechea, & Guillén, 2015). The TGA thermograms are shown in Figure 4.21.

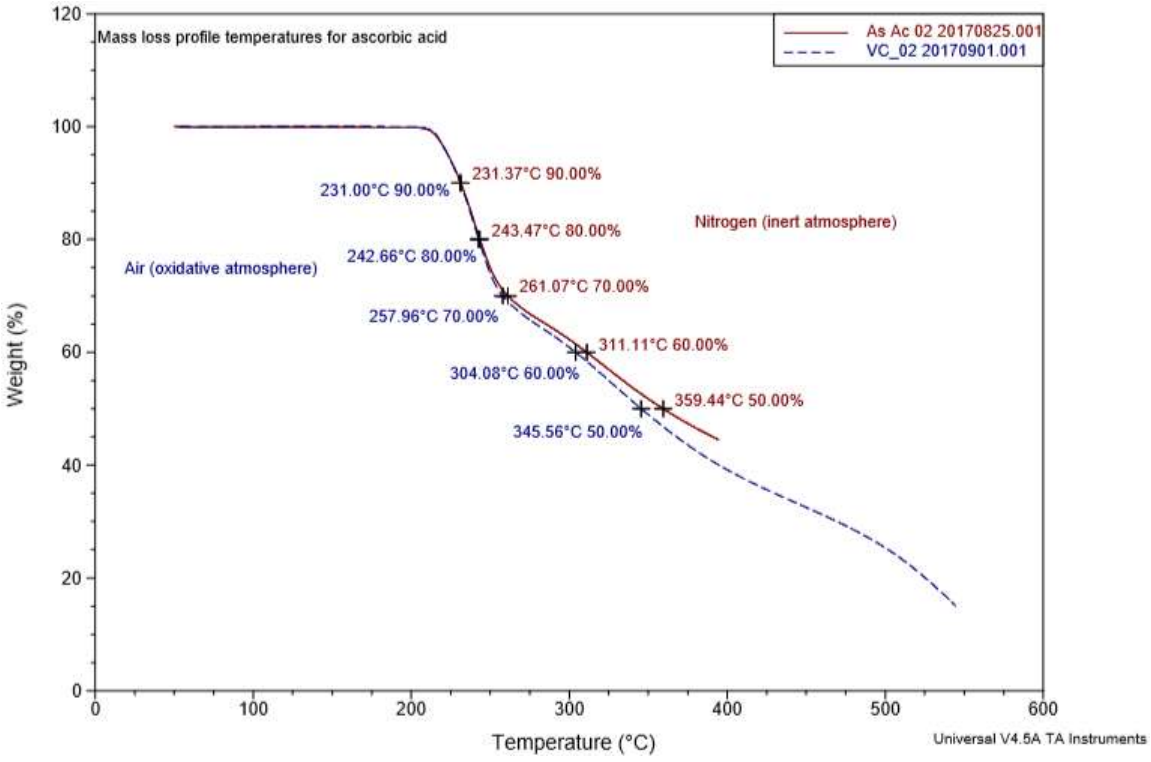

Figure 4.21. TGA mass loss profiles for AsA in air and nitrogen atmosphere.

4.3.1.3 Conclusions

It is observed a slightly higher degradation temperature profile for AsA in air atmosphere than in nitrogen atmosphere. Although, the maximum rate of change of mass loss, represented by the peak maxima in temperature, observed for AsA in air is 240.5 °C and 239.7 °C for AsA in nitrogen. The main observation is the initial degradation temperature of AsA which is in the order of 180°C and the effect of initial AsA degradation on its antioxidant activity and the potential use as thermal stabilizer during polymer processing with temperatures normally higher than 180°C.

4.3.2 Antioxidant capacity determination of AsA

Align to the objective of incorporation of a natural source of antioxidants as thermal stabilizers for polymers, the antioxidant activity of AsA is assessed. The effect of different incubation temperatures and incubations times on the antioxidant capacity of AsA are evaluated by the $DPPH^{\cdot}$ method.

4.3.2.1 Methodology

Briefly, the reaction mixture of a final volume assay of 1000 µL containing a 100 µL aliquot of AsA diluted in ethanol and a 100 µL aliquot of $DPPH^{\cdot}$ radical solution (175 µM) was monitored spectrophotometrically at λ = 490 nm and at two kinetic end-points: 5 minutes and 30 minutes.

Thermal runs on ascorbic acid

Samples of approximately 20 mg of AsA were placed in an open aluminum pan in a TA instrument TGA Q50. Tests were conducted in isothermal mode at different temperatures and incubation times under nitrogen atmosphere. Table 4.8 shows the experimental runs evaluated.

Test run	Temp. [°C]	Incubation time [min]
1	70	5
2	140	30
3	70	5
4	140	30
5	180	5

Table 4.8. Experimental conditions on thermal stability analysis of AsA under nitrogen atmosphere.

4.3.2.2 Results

Figure 4.22 illustrates the percentage of DPPH· radical scavenged by AsA at three different incubation temperatures and two different kinetic end-points.

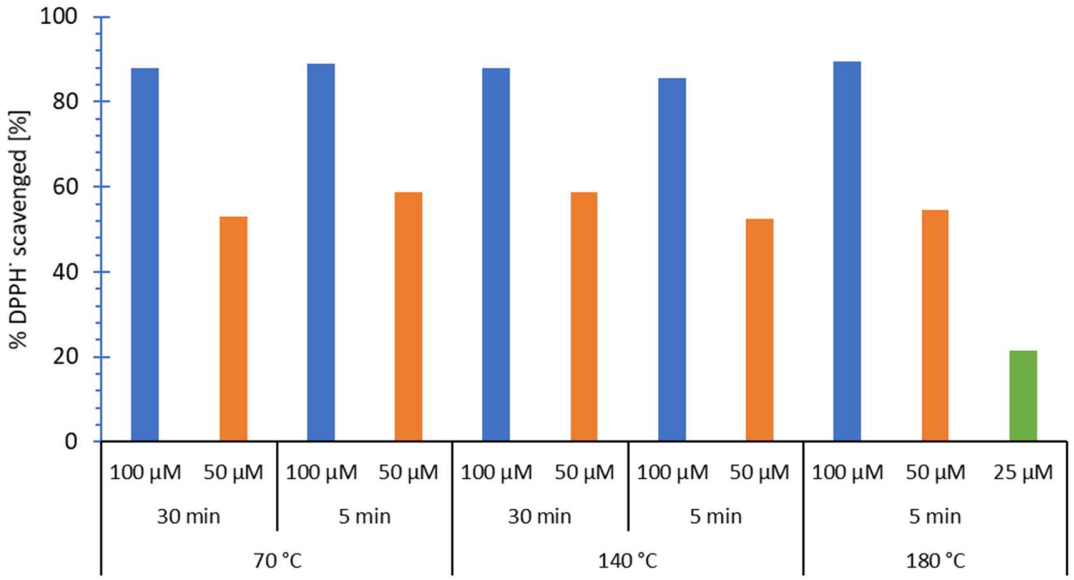

Figure 4.22. Percentage of DPPH· radical scavenged by AsA.

It can be inferred that there is no significant change in the resulting percentages of DPPH· radical scavenged under the experimental conditions assessed. Furthermore, for a fixed AsA concentration of 100 µM, the observed percentage of DPPH· radical scavenged at the extreme experimental condition in terms of incubation temperature (70°C and 180 °C) were 89.0 % and 89.4% respectively.

On the other hand, evaluating the extreme experimental condition in terms of incubation time (5 minutes and 30 minutes) for a fixed temperature (140°C), the resulting percentage of DPPH· radical scavenged were 85.6% and 88.0% respectively.

4.3.2.3 Conclusions

The effect of heating time and temperature on the antioxidant activity of AsA is not significant under the experimental conditions evaluated. Furthermore, the results obtained in terms of percentage of $DPPH^{\cdot}$ radical scavenged are close to the values obtained at ambient temperature.

It is also observed a physical discoloration (brownish) for the sample evaluated at 180°C for 5 minutes, this possibly could induce coloration in the polymer during industrial transformation.

4.4 α-tocopherol

The family of tocopherols comprise 4 structure-related phenolic compounds, varying only in the position and number of the methyl group on the aromatic ring. Being α-tocopherol (α-Toc-OH) fully methylated and the most biologically active compound among tocopherols (Burton & Ingold, 1986; Kiokias, Varzakas, & Oreopoulou, 2008).

α-tocopherol is considered the most effective lipid-soluble chain-breaking antioxidant in biological activities. It is known in metabolism that α-tocopherol inhibits lipid autoxidation via hydrogen transfer to lipid peroxy radicals. The radical scavenge activity leads the formation of a stable tocopheroxyl radical which further undergo termination reactions to yield nonradical products (Al-Malaika, Ashley, & Issenhuth, 1994). Figure 4.23 depicts the chemical structures.

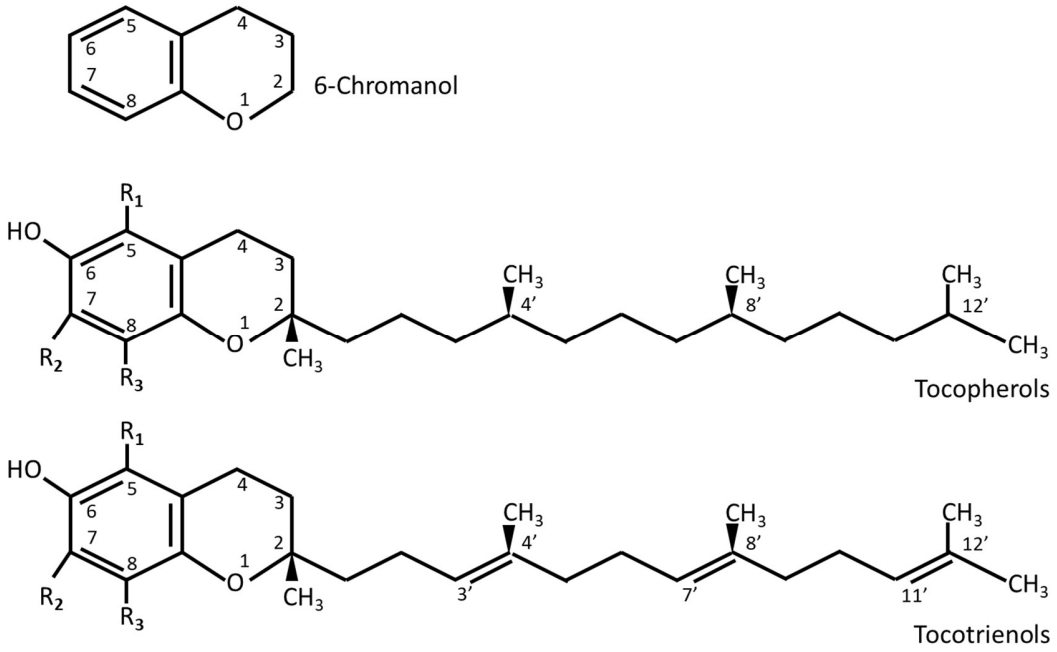

Vitamin E compounds	R_1	R_2	R_3
5,7,8-Trimethyl Tocopherol (α-tocopherol) 5,7,8-Trimethyl Tocotrienol (α-tocotrienol)	CH_3	CH_3	CH_3
7,8-Dimethyl Tocopherol (β-tocopherol) 7,8-Dimethyl Tocotrienol (β-tocotrienol)	H	CH_3	CH_3
5,8-Dimethyl Tocopherol (ϒ-tocopherol) 5,8-Dimethyl Tocotrierol (ϒ-tocotrienol)	CH_3	H	CH_3
8-Methyl Tocopherol (δ-tocopherol) 8-Methyl Tocotrienol (δ-tocotrienol)	H	H	CH_3

Figure 4.23. chemical structures (Gliszczynska-Swigło & Oszmianski, 2014; Shahidi & Ambigaipalan, 2015).

4.4.1 Thermal analysis

The thermal degradation of α-tocopherol (α-Toco) was performed by thermogravimetric analysis (TGA). The onset temperature (Tonset), maximum temperature (Tmax), end-set temperature (Tendset), and the temperature profile at 1% and 5% of mass loss ($T_{1\%}$, $T_{5\%}$) were assessed.

4.4.1.1 Methodology

α-tocopherol was supplied by Sigma, France. Thermal analysis was performed with a TA instrument TGA Q50; the carrier gas used was nitrogen (inert atmosphere) and air (oxidative atmosphere) at a flow rate of 60 mL/min and a heating rate of 10 °C/min.

4.4.1.2 Results

Figure 4.24 and Figure 4.25 represent the differential thermogravimetry (dTGA) and the thermogravimetry (TGA) curves of the thermal degradation of α-Toco in nitrogen and air respectively.

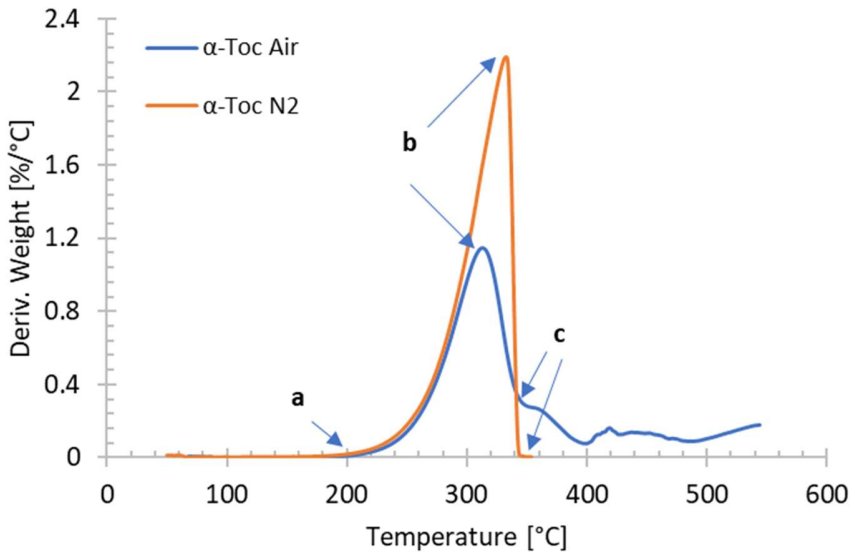

Figure 4.24. dTGA thermograms of the thermal degradation of α-tocopherol in nitrogen (N_2) and air (Air). **a**. Tonset, **b**. Tmax, **c**. Tendset.

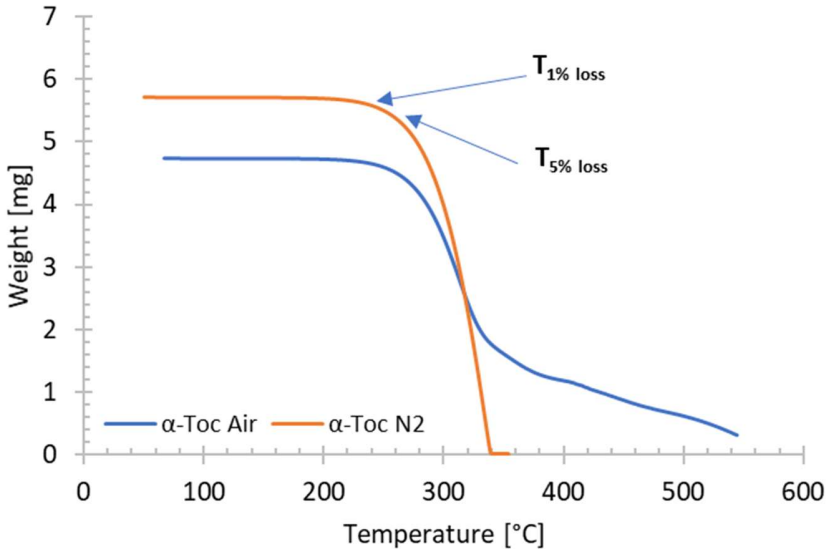

Figure 4.25. TGA thermograms of the thermal degradation of α-tocopherol in nitrogen (N_2) and air (Air).

Table 4.9 and Table 4.10 show the corresponding dTGA and TGA results.

Antioxidant	Atmosphere	Tonset [°C]	Tmax [°C]	Tendset [°C]
α-Toco	Air	210.0	312.6	338.4
α-Toco	Nitrogen	219.0	332.7	342.1

Table 4.9. Thermal degradation temperatures for α-tocopherol (α-Toco).

		Percentage of mass loss [°C]						
Antioxidant	Atmosphere	$T_{1\%\,loss}$	$T_{5\%\,loss}$	$T_{10\%\,loss}$	$T_{20\%\,loss}$	$T_{30\%\,loss}$	$T_{40\%\,loss}$	$T_{50\%\,loss}$
α-Toco	Air	226.3	260.6	275.7	292.3	303.2	312.2	321.2
α-Toco	Nitrogen	221.1	256.2	272.1	289.0	299.7	307.7	314.3

Table 4.10. Degradation temperature profiles at specific percentage of mass loss for α-Toco.

The analysis of Figure 4.24 and Figure 4.25 in an oxidative atmosphere showed that α-Toco started to decompose at approximately 210 °C with the maximum rate of decomposition (Tmax) at 312.6°C.

In a nitrogen atmosphere the initial degradation and the maximum rate of decomposition took place at higher temperatures (312.6 °C and 332.7 °C respectively). Table 4.9 and Table 4.10 show the TGA and dTGA results and Figure 4.26 presents the corresponding thermograms for α-Toco.

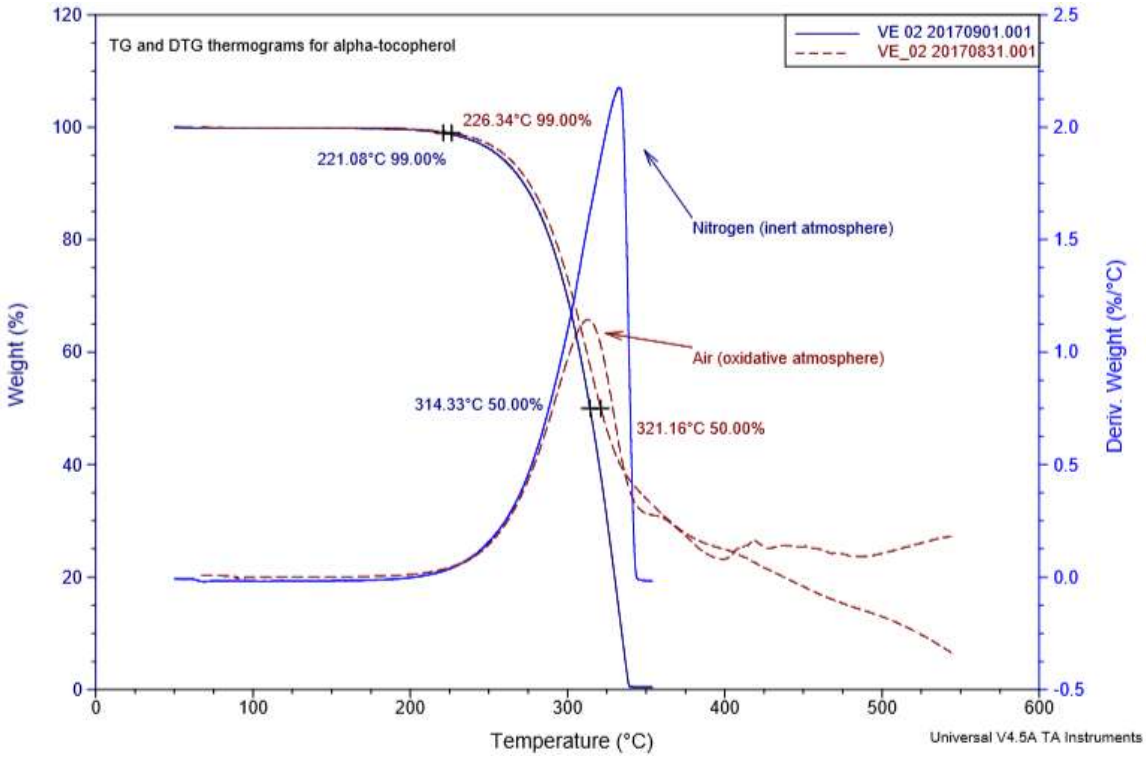

Figure 4.26. TGA and dTGA thermograms for α-tocopherol in air and nitrogen atmosphere.

At earlier degradation stages such as 1% of mass loss, α-tocopherol showed similar degradation profiles in air and nitrogen atmospheres (226.3°C and 221.1 °C respectively). As the temperature rises, the degradation paths for α-tocopherol deviates. At a 50% of mass

loss, the degradation temperature of α-tocopherol under nitrogen was 314.3°C whereas in air atmosphere the observed temperature was 321.2 °C.

Under inert atmosphere (nitrogen) it is observed a single and sharp degradation step for α-tocopherol. On the other hand, in air atmosphere, the first degradation step is broader with an apparent second degradation step in the range between 400 °C and 480°C. Figure 4.27 shows the dTGA of α-tocopherol in air at different heating rates showing the same second degradation step shifted towards higher temperature as the heating rate increased.

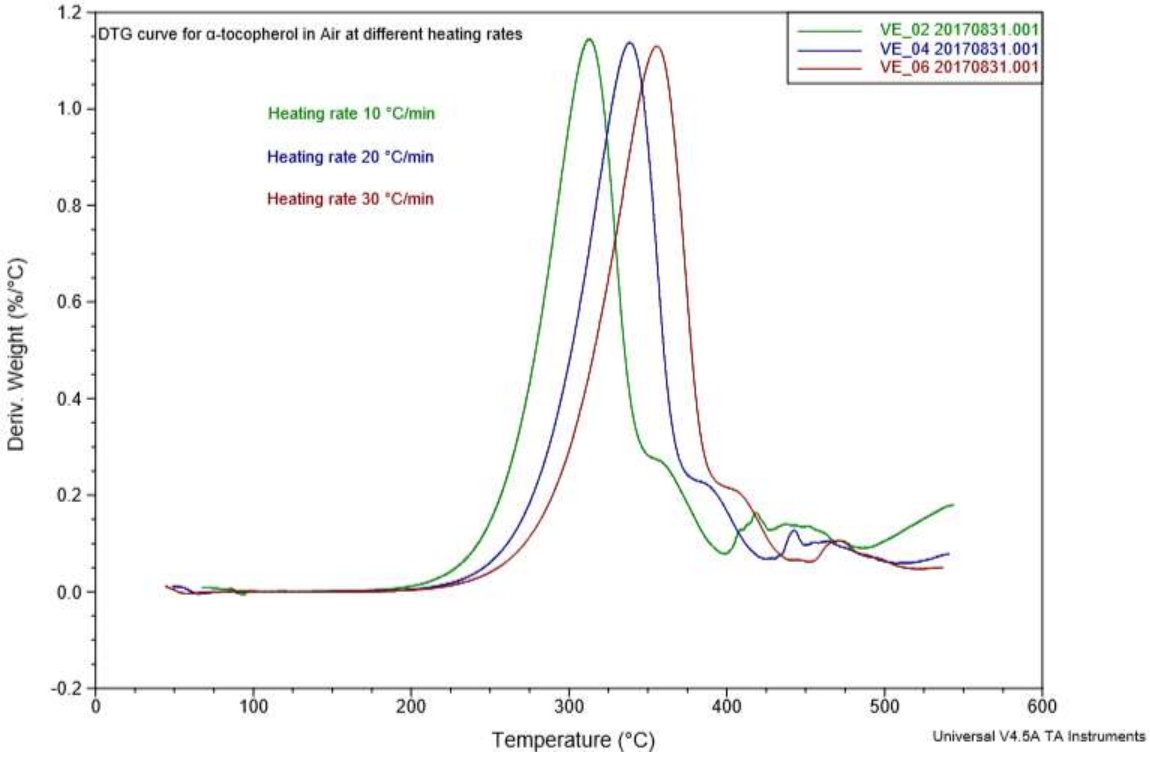

Figure 4.27. dTGA thermogram for α-tocopherol in air atmosphere at different heating rates.

4.4.1.3 Conclusions

The presence of a second degradation step in an oxidative atmosphere such as air may be attributed to the oxidation reaction mechanism of α-tocopherol. One of the reaction pathways

from the general reaction mechanism of an antioxidant towards a free radical is the possible dimerization of two tocopherol radicals. Thus, induced by oxidative conditions and temperature, may formed higher molar mass sub-products that decompose at higher temperatures. These results must be compared with the antioxidant activity of α-tocopherol and the effect of temperature and the surrounding atmosphere.

4.4.2 Antioxidant capacity determination of α-tocopherol

α-tocopherol is a well-known and effective chain-breaking antioxidant. To validate the potential incorporation into polymers as thermal stabilizer it is needed to assess the effect of temperature and different atmosphere conditions on the radical scavenging activity. To address this objective, it is proposed to evaluate the antioxidant activity of α-tocopherol by the $DPPH^{\cdot}$ method.

4.4.2.1 Methodology

Briefly, the reaction mixture of a final volume assay of 1000 μL containing a 100 μL aliquot of α-Toco diluted in ethanol and a 100 μL aliquot of $DPPH^{\cdot}$ radical solution (175 μM) was monitored spectrophotometrically at λ = 490 nm and at a kinetic end-point of 5 minutes.

Thermal runs on α-tocopherol

Samples of approximately 20 mg of α-Toco were placed in an open aluminum pan in a TA instrument TGA Q50. Tests were conducted in isothermal mode under air and nitrogen atmospheres. Table 4.11 shows the experimental runs evaluated.

Test run	Atmosphere	Temperature [°C]	Incubation Time [min]
1	Air	180	5
2	Nitrogen	180	5

Table 4.11. Experimental conditions on α-tocopherol.

4.4.2.2 Results

Figure 4.28 shows the percentage of DPPH· radical scavenged by α-tocopherol.

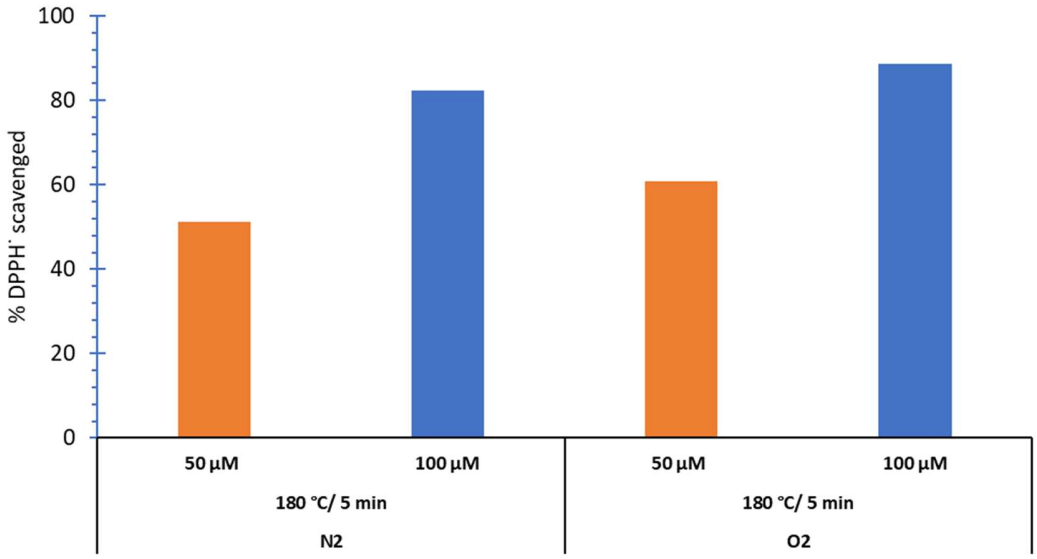

Figure 4.28. Percentage of DPPH· radical scavenged by α-Toco.

It is observed no significant change in the DPPH· radical scavenging activity under the experimental conditions assessed. At the highest α-Toco concentration (100 µM) the resulting percentage of radical scavenged were in the same order of magnitude: 82.2% in nitrogen atmosphere and 88.6% in air atmosphere.

4.4.2.3 Conclusions

The effect of temperature and atmosphere (nitrogen/air) on the antioxidant activity of α-tocopherol is not significant under the experimental conditions evaluated. Furthermore, the results obtained in terms of percentage of $DPPH^{\cdot}$ radical scavenged are close to the values obtained at ambient temperature (Table 2.4).

4.5 BHT

2,6-di-tert-butyl-4-methylphenol or Butylated hydroxytoluene (BHT) is a conventional synthetic phenolic antioxidant used as a radical quencher in the food, cosmetic, and plastic industries. At authorized levels it is considered safe for human health but with an increasing customer awareness on health risks associated with synthetic materials in contact with food (Berdhal, Nahas, & Barren, 2010; Nieva-Echevarría et al., 2015). Figure 4.29 illustrates the chemical structure.

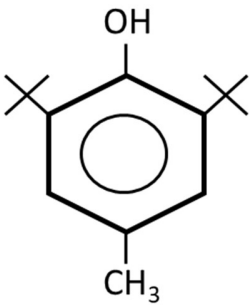

Figure 4.29. 2,6-di-tert-butyl-4-methylphenol (BHT) chemical structure.

In light of this information, a thermal degradation analysis is performed on BHT to have a comparison reference to natural antioxidant sources.

4.5.1 Thermal analysis

The thermal degradation of BHT was performed by thermogravimetric analysis (TGA). The onset temperature (Tonset), maximum temperature (Tmax), end-set temperature (Tendset), and the temperature profile at 1% and 5% of mass loss ($T_{1\%}$, $T_{5\%}$) were assessed.

4.5.1.1 Methodology

BHT was supplied by Sigma, France. Thermal analysis was performed with a TA instrument TGA Q50; the carrier gas used was nitrogen (inert atmosphere) at a flow rate of 60 mL/min and a heating rate of 10 °C/min, 20°C/min, 30°C/min.

4.5.1.2 Results

Figure 4.30 and Figure 4.31 represent the differential thermogravimetry (dTGA) and the thermogravimetry (TGA) curves of the thermal degradation of BHT.

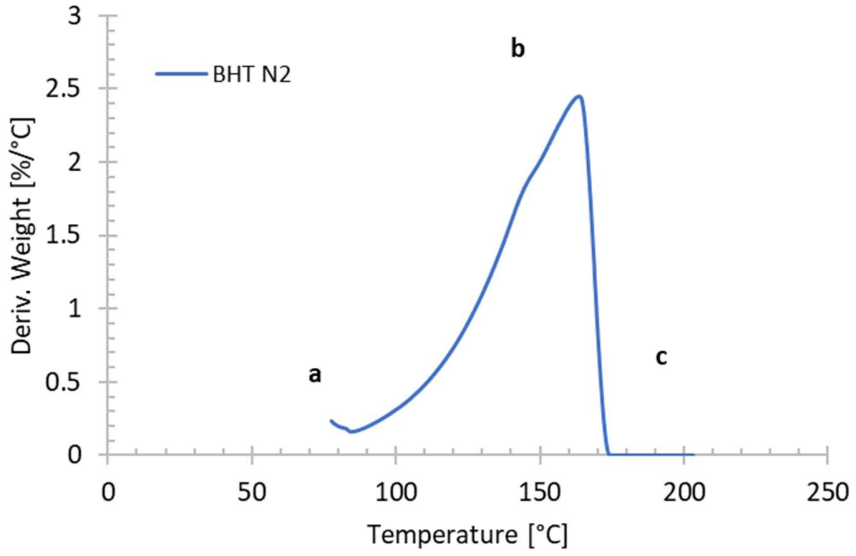

Figure 4.30. dTGA thermograms of the thermal degradation of BHT in nitrogen (N_2). **a**. Tonset, **b**. Tmax, **c**. Tendset.

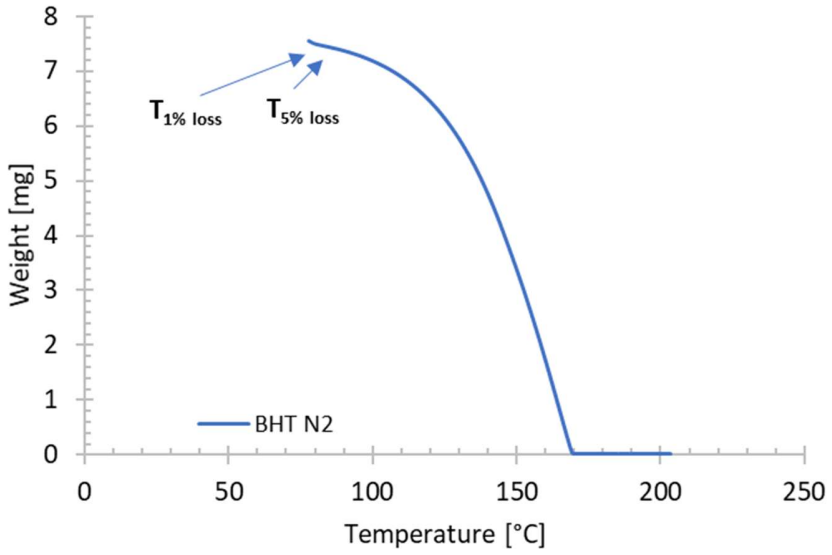

Figure 4.31. TGA thermograms of the thermal degradation of BHT nitrogen (N_2).

The analysis of the curves shows that BHT decomposes in a single step and at temperatures below 100 °C. It is observed an initial degradation temperature of approximately 78.5 °C with a peak maximum at 163.9 °C. Table 4.12 and Table 4.13 show the corresponding dTGA and TGA results.

Antioxidant	Atmosphere	Tonset [°C]	Tmax [°C]	Tendset [°C]
BHT	Nitrogen	78.5	163.9	172.5

Table 4.12. Thermal degradation temperatures for BHT.

		Percentage of mass loss [°C]						
Antioxidant	Atmosphere	$T_{1\%\ loss}$	$T_{5\%\ loss}$	$T_{10\%\ loss}$	$T_{20\%\ loss}$	$T_{30\%\ loss}$	$T_{40\%\ loss}$	$T_{50\%\ loss}$
BHT	Nitrogen	81.6	100.5	112.6	126.5	135.3	14.9	147.4

Table 4.13. Degradation temperature profiles at specific percentage of mass loss for BHT.

Thermal degradation of BHT was assessed under dynamic conditions at 10 °C/min, 20 °C/min, and 30 °C/min and nitrogen atmosphere to address the effect of heating rate on the degradation temperature profiles. Particularly, the onset degradation temperature (Tonset), the maximum rate of decomposition (Tmax), and the end-set temperature of mass loss from the corresponding degradation step. Figure 4.32 shows the TGA curve and the insert of dTGA curve for BHT.

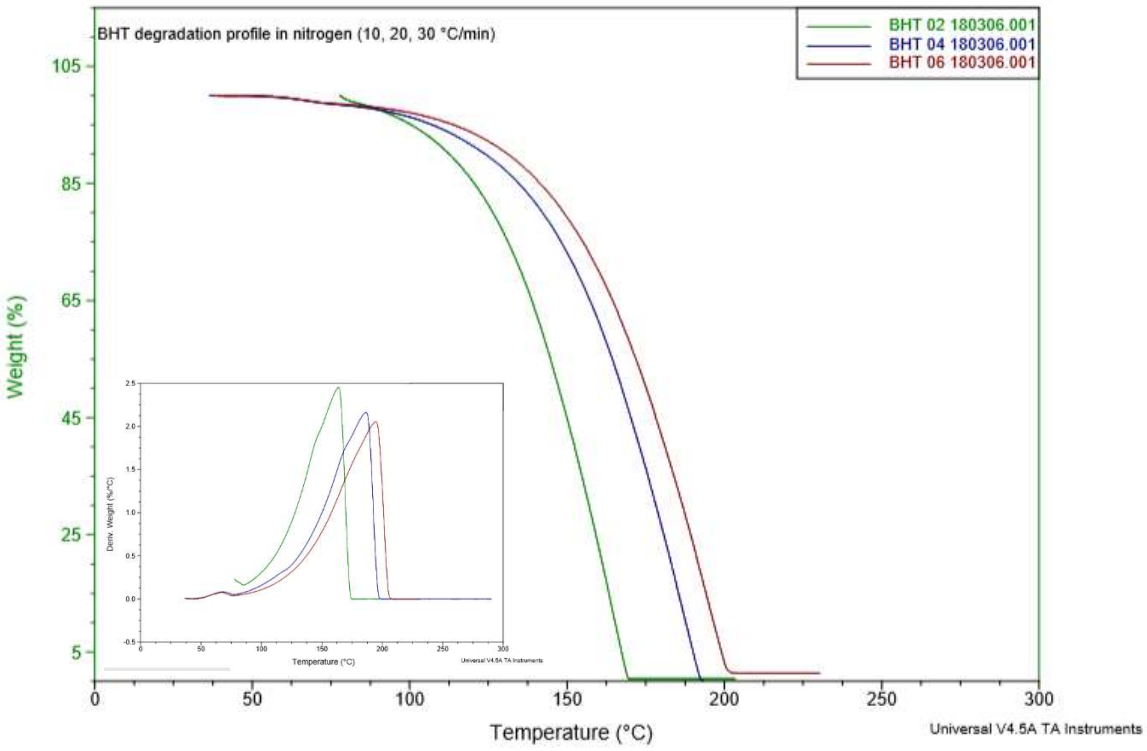

Figure 4.32. BHT degradation profile in nitrogen. TGA curves and corresponding dTGA curves at different heating rates.

As mentioned before, BHT degrades in a single step. In Figure 4.32 it is observed that BHT degraded almost completely (approximately 1.4 % residue) at a maximum temperature of approximately 206 °C. Furthermore, it was evaluated the effect of heating conditions on the specific degradation temperature assessed (Tonset, Tmax, Tendset).

Equation 4.2, 4.3, and 4.4 represent the calculated linear equations for the thermal degradation temperatures obtained from the experimental runs at different heating rates. It is also reported the coefficient of correlation (r) indicating a linear response and good fit between the heating rate and the specific degradation temperature.

$$T_{onset} = (1.0095\ (\text{heating rate}) + 70.983),\ r = 0.92 \quad (4.2)$$

$$T_{max} = (1.5395\ (\text{heating rate}) + 150.97),\ r = 0.97 \quad (4.3)$$

$$T_{endset} = (1.5855\ (\text{heating rate}) + 159.08),\ r = 0.96 \quad (4.4)$$

4.5.1.3 Conclusions

BHT was used as the commercial antioxidant counterpart; it is a synthetic antioxidant widely used in industry. BHT presented a poor thermal stability under nitrogen atmosphere with initial degradation temperatures lower than 100 °C.

In the case of low-density polyethylene (LDPE) and isotactic polypropylene (i-PP), it is observed a melting point (Tm) of approximately 113 °C and 166 °C respectively, at least extrusion temperatures must be above the corresponding melting temperature, thus possibly compromising the stability and performance of BHT.

4.6 General overview

Natural antioxidants have been characterized prior to incorporation into a polymer matrix. Thermal analysis has been carried out by TGA to assess thermal degradation and the effect of air and nitrogen atmospheres. Figure 4.33 and Figure 4.34 present the TGA curves of thermal degradation for all the antioxidants tested.

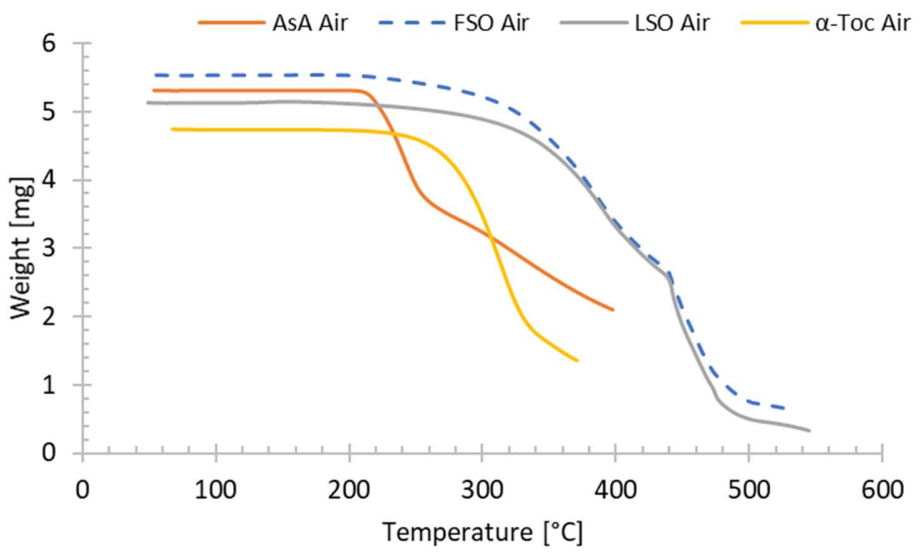

Figure 4.33. TGA curves of the thermal degradation of ascorbic acid (AsA), flaxseed oil (FSO), linseed oil (LSO), and α-tocopherol in air.

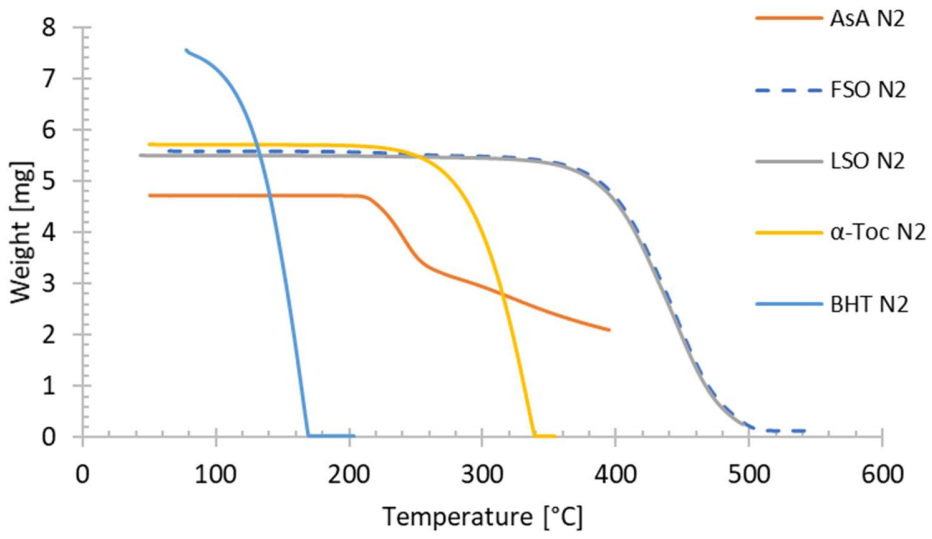

Figure 4.34. TGA curves of the thermal degradation of ascorbic acid (AsA), flaxseed oil (FSO), linseed oil (LSO), α-tocopherol, and butylated hydroxytoluene (BHT) in nitrogen (N_2).

Two specific degradation temperatures may provide sufficient information for antioxidant screening. The onset temperature (Tonset) which is the initial temperature at which degradation starts and the temperature at the maximum rate of mass loss (Tmax).

Thermal degradation under nitrogen presented a single degradation profile for all the antioxidants evaluated. In the case of oxidative conditions such as air, antioxidants presented two or more degradation steps. The first decomposition step is considered for antioxidant screening which is observed, in all the cases, in the range of temperature between 100 °C and 400 °C approximately.

It is important to remark that despite the low onset temperatures observed in flax oils (166 °C and 178 °C in air atmosphere for LSO and FSO respectively), the representative total mass loss within a range between 150 °C and 250 °C was only 1.916% whereas ascorbic acid reported a mass loss of 26% under the same temperature interval.

The above temperature range evaluated corresponds to the first degradation step in flax oil and is related to the oxidation of unsaturated fatty acids. It may be possible to incorporate additional antioxidants to suppress oxidation and exploit the potential use as thermal stabilizer in polymers since it is observed that the temperature at the highest rate of mass loss (Tmax) in air atmosphere were 369 °C and 366 °C for LSO and FSO respectively. In this scenario, the decreasing order in terms of thermal stability and thermo-oxidative stability for the antioxidants evaluated were: α-toco > Flax oils > AsA > BHT.

The potential antioxidant activity of natural molecules may provide thermal stability in polymers during processing by free radical scavenging. The effect of temperature, carrier gas (air or nitrogen), and incubation time on the antioxidant capacity were studied and followed by UV-Vis spectrophotometry and the $DPPH^{\cdot}$ method. Incubation temperatures up to 180°C were evaluated in ascorbic acid and α-tocopherol and it was observed no significant difference on the antioxidant activity.

In the case of ascorbic acid with an initial degradation temperature in the range of 180 °C, the combined effect of incubation time (30 minutes) and incubation temperature (180 °C) on the antioxidant capacity was assessed. From results shown, it may be concluded that the antioxidant capacity of ascorbic acid remained in the same order of magnitude compared to the antioxidant capacity of ascorbic acid at standard ambient temperature. It is important to conclude that the effect of the test temperature lead to coloration, a brownish effect on ascorbic acid that may restrict the processing temperatures if used in polymer formulation.

Two different flax oils were thermally characterized by UV-Vis spectrophotometry. The specific extinction coefficient K_{270} and the area under the curve in the region between 234 nm and 274 nm confirmed the extent of oxidation in both flax oils. It may be concluded that flaxseed oil (Terpenic Labs) presented the highest thermo-oxidative stability under the experimental conditions evaluated. Also, it may be concluded that there is no significant difference on the antioxidant activity against $DPPH^{\cdot}$ radical from both flax oils.

4.7 Encapsulation of ascorbic acid

Ascorbic acid (AsA) possesses antioxidant activity against free radicals. The antioxidant capacity of AsA was followed spectrophotometrically by the $DPPH^{\cdot}$, $ABTS^{\cdot+}$, and SOA methods. Furthermore, the effect of exposure time and a temperature close to the initial degradation temperature of AsA on the antioxidant activity were assessed by the $DPPH^{\cdot}$ method.

The potential use of AsA as a radical scavenger providing thermal resistance to polymers at temperatures in the order of 180 °C was confirmed by its antioxidant activity. It was observed no significant difference in the percentage of $DPPH^{\cdot}$ radical scavenged comparing with the results obtained at standard ambient temperature. The major constrain is the observed initial degradation temperature of AsA and the processing conditions in terms of temperature to incorporate in isotactic polypropylene (i-PP).

One possibility to explore is the encapsulation of AsA using a food grade carrier. The aim is to protect AsA (core material) by casing in a sealed microcapsule. The capsule has the advantage to preserve the core material and provide protection against degradation such as UV light, heat, moisture, air oxidation and chemical attack. An additional feature is that the capsule masks taste or odors from the active compounds present in the core material. Furthermore, it may provide a controlled release of the active compound (Mishra, 2016).

The spray-drying encapsulation process is a feasible and economical operation unit commonly used in the food industry. The process entails the mixture and homogenization of the core material and the carrier. The resulting mixture is fed into a spray dryer and atomized with a nozzle or spinning wheel. Water is evaporated by hot air and the carrier solidifies onto the core material as solvent evaporates yielding dried spherical capsules. The averaged particle size is in the range between 10 and 100 μm (Fang & Bhandari, 2010; Mishra, 2016; Nedovic, Kalusevic, Manojlovic, Levic, & Bugarski, 2011).

4.7.1 Methodology

Ascorbic acid (AsA), chitosan (CHT), and maltodextrin (MDX) were purchased from Sigma, France. Ascorbic acid was encapsulated by the spray-drying process and supplied by the UPVD in collaboration with an external laboratory. Table 4.14 shows the final composition of the core material in the carrier matrix.

Core Material	% in weight of AsA incorporated	Carrier
AsA	6	Chitosan (CHT)
AsA	6	Maltodextrin (MDX)

Table 4.14. Core material composition (as a percentage in weight of AsA incorporated) and carrier agent.

4.7.2 Thermal analysis

Thermal analysis was performed with a TA instrument TGA Q50; the carrier gas used was nitrogen (inert atmosphere) and air (oxidative atmosphere) at a flow rate of 60 mL/min and a heating rate of 20 °C/min. The thermal degradation was assessed at the onset temperature (Tonset), maximum temperature (Tmax), and end-set temperature (Tendset).

4.7.3 Results

Fresh AsA samples were characterized by TGA to set a control reference for further analysis on the encapsulation process. Figure 4.35 shows the differential thermogravimetry (dTGA) and the thermogravimetry (TGA) curves of the thermal degradation of AsA in air and nitrogen atmospheres at the first degradation step.

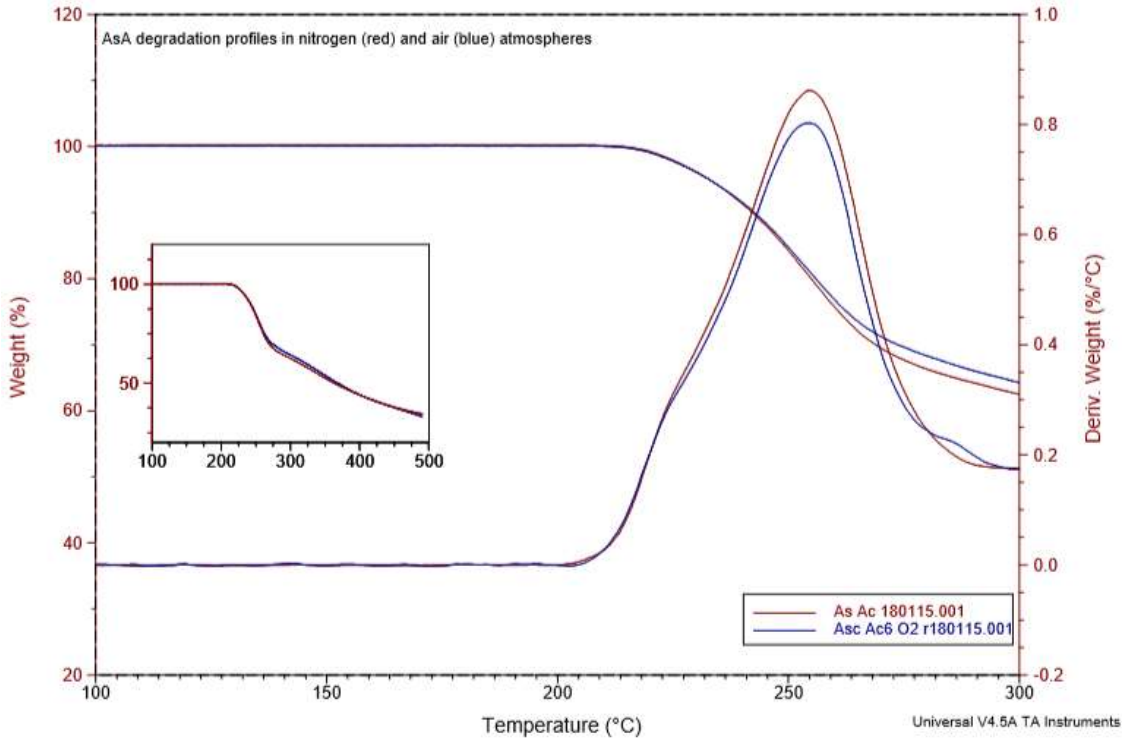

Figure 4.35. First thermal degradation step for AsA in nitrogen and air atmospheres. **b**. Complete TGA curves of the thermal degradation of AsA.

The first corresponding degradation step of AsA occurred in the range between 200°C and 300 °C (similar results were previously observed). From the insert plot, it is shown the complete thermal degradation of AsA under nitrogen and air atmospheres showing similar degradation paths. Figure 4.36 and Figure 4.37 present the individual analysis for each atmosphere condition.

Thermal degradation of AsA was first assessed in two regions. The first range of temperature evaluated was between 100 °C and 200 °C which includes the initial decomposition temperature of AsA. The second region of temperatures comprised the range between 100 °C up to the peak temperature (Tmax) which is the maximum rate of mass loss. The covered range is within the processing temperatures utilized in polymer processing particularly for low-density polyethylene (LDPE) and isotactic polypropylene (i-PP). The initial degradation temperature (Tonset), maximum temperature (Tmax), and the end-set temperature (Tendset) were also determined for comparison analysis.

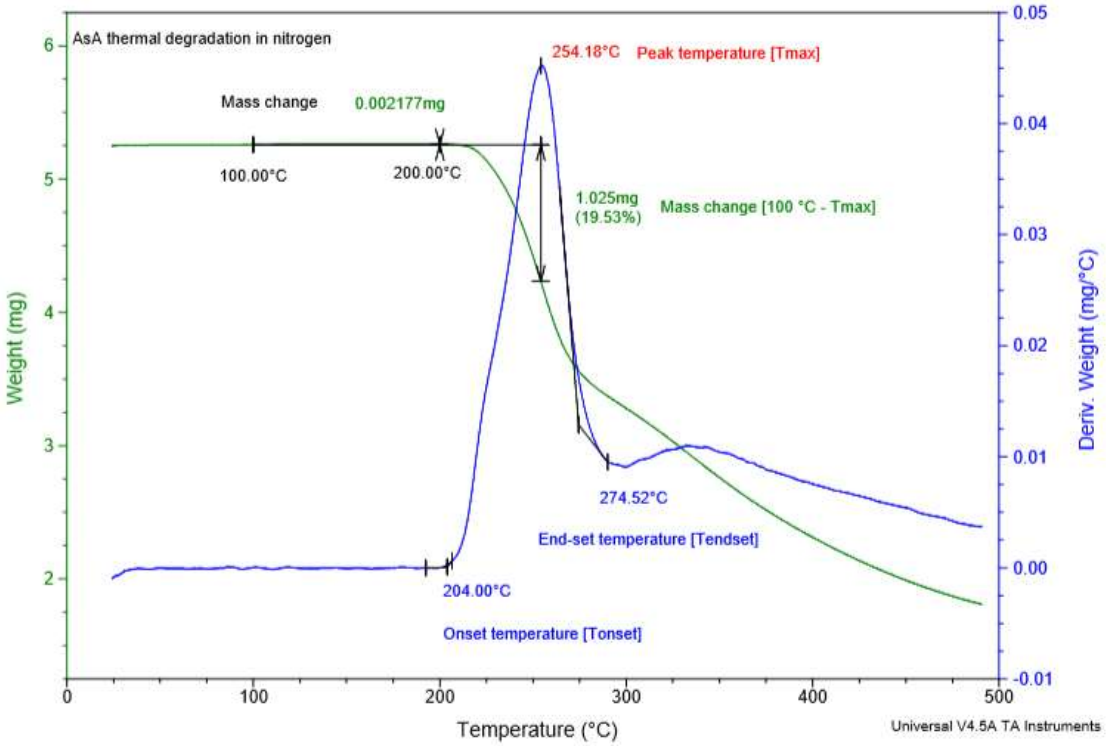

Figure 4.36. TGA and dTGA curves for AsA in nitrogen atmosphere.

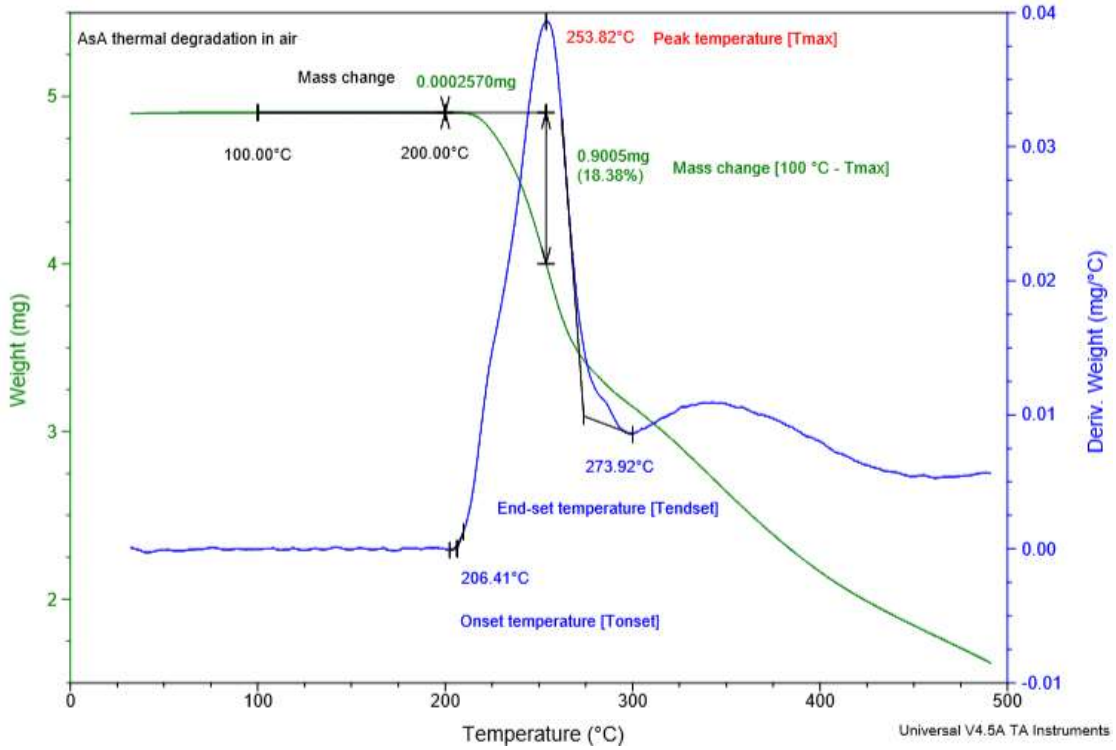

Figure 4.37. TGA and dTGA curves for AsA in air atmosphere.

The analysis of AsA under nitrogen and air showed that, within the first temperature range evaluated (from 100 °C to 200 °C) there is no significant change of mass loss (< 1%). A mass loss of 19.53% and 18.38% is observed within the range of temperature between 100 °C and the corresponding point in temperature of the maximum rate of mass loss under nitrogen and air atmosphere respectively. Table 4.15 shows the specific degradation temperatures.

Antioxidant	Atmosphere	Tonset [°C]	Tmax [°C]	Tendset [°C]
AsA	Nitrogen	204.0	254.2	274.5
AsA	Air	206.4	253.8	273.9

Table 4.15. Thermal degradation temperatures of AsA.

4.7.4 Chitosan as encapsulate agent

Chitosan (CHT) is a natural biodegradable polymer, a linear polysaccharide composed of β-(1-4)-linked N-acetyl-D-glucosamine (acetylated unit) and D-glucosamine (deacetylated unit) sourced from shells of shrimps, crabs, and sea crustaceans. It is a polymer widely used in the pharmaceutical industry to encapsulate drugs (Hussain, Abdelkader, Abdullah, & Kmaruddin, 2018).

(Hong et al., 2007) performed a thermogravimetric analysis of chitosan in nitrogen atmosphere. Authors observed a single degradation step and evaluated the relationship between different heating rates and degradation temperatures such as onset temperature, peak temperature, and end-set temperature. Also, the equilibrium thermal degradation temperature (T^0) was calculated as the intersect of the linear fit equation when X or the heating rate equals to 0. Resulting equilibrium temperatures reported were 326.8 °C, 355.2 °C, 369.7 °C for onset temperature, peak temperature, and end-set temperature respectively.

D. de Brito and S. P. Campana-Filho assessed the thermal degradation of chitosan under nitrogen atmosphere and several heating rates. Authors reported a first thermal degradation step (6% of weight loss) in the range between 25 °C and 140 °C associated to water evaporation. The second thermal degradation step is reported in the range between 200 °C and 400 °C attributed to continuing dehydration, deacetylation and depolymerization of chitosan, and a third event at temperatures higher than 400 °C associated to residual decomposition reactions. Authors reported for the second degradation step peak temperatures ranging between 294.3 °C and 328.6 °C corresponding to a heating rate of 2.5 °C/min and 15 °C/min respectively (de Britto & Campana-Filho, 2007).

(Peniche-Covas, Argüelles-Monal, & San Román, 1993) studied the thermal degradation behavior of chitosan under nitrogen and air atmospheres in dynamic conditions at a heating rate of 10 °C/min. Authors observed a first thermal degradation step occurring in the range between 35 °C and 192 °C derived from water loss. A second degradation step was observed associated with polymer dehydration, depolymerization, and decomposition of

acetylated and deacetylated units with a peak temperature of 311 °C and an end-set temperature observed at 360 °C.

4.7.4.1 Thermal analysis

Thermal analysis was performed with a TA instrument TGA Q50; the carrier gas used was nitrogen (inert atmosphere) and air (oxidative atmosphere) at a flow rate of 60 mL/min and a heating rate of 20 °C/min. The thermal degradation was assessed at the onset temperature (Tonset), maximum temperature (Tmax), and end-set temperature (Tendset).

4.7.4.2 Results

Figure 4.38 and Figure 4.39 show the differential thermogravimetry (dTGA) and the thermogravimetry (TGA) curves of the thermal degradation of ascorbic acid encapsulated in chitosan (CHT-AsA) in nitrogen and air atmospheres respectively.

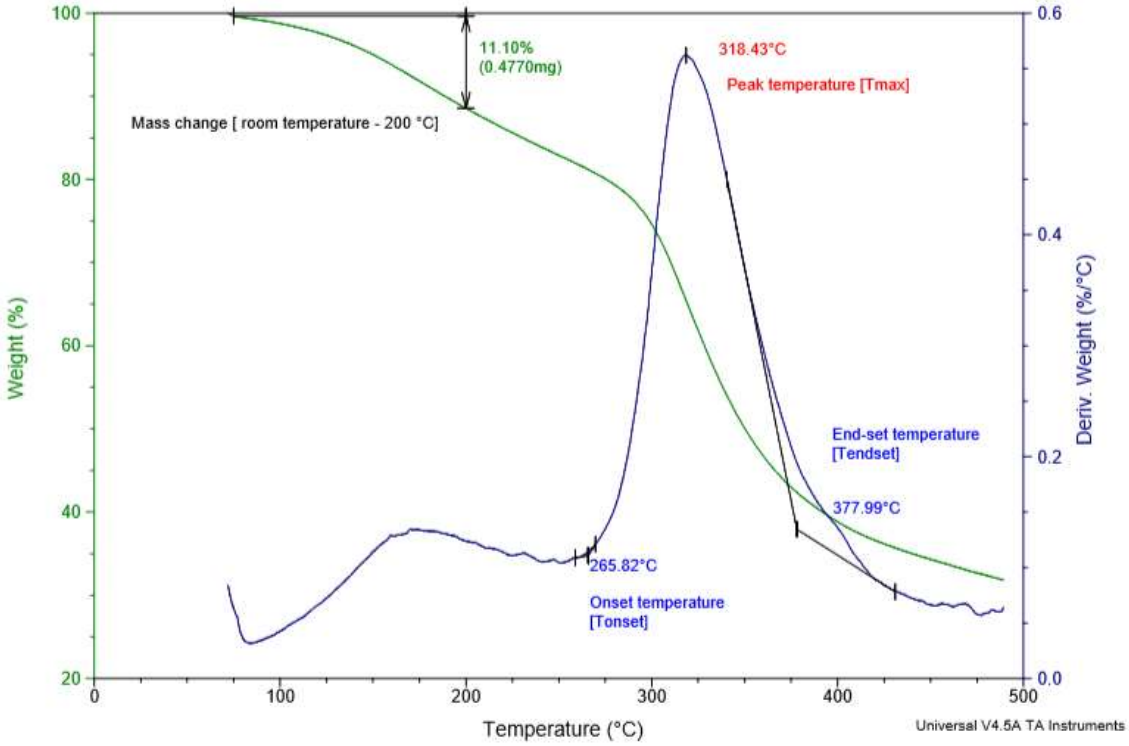

Figure 4.38. TGA and dTGA curves for CHT – AsA (6% w/w) in nitrogen atmosphere.

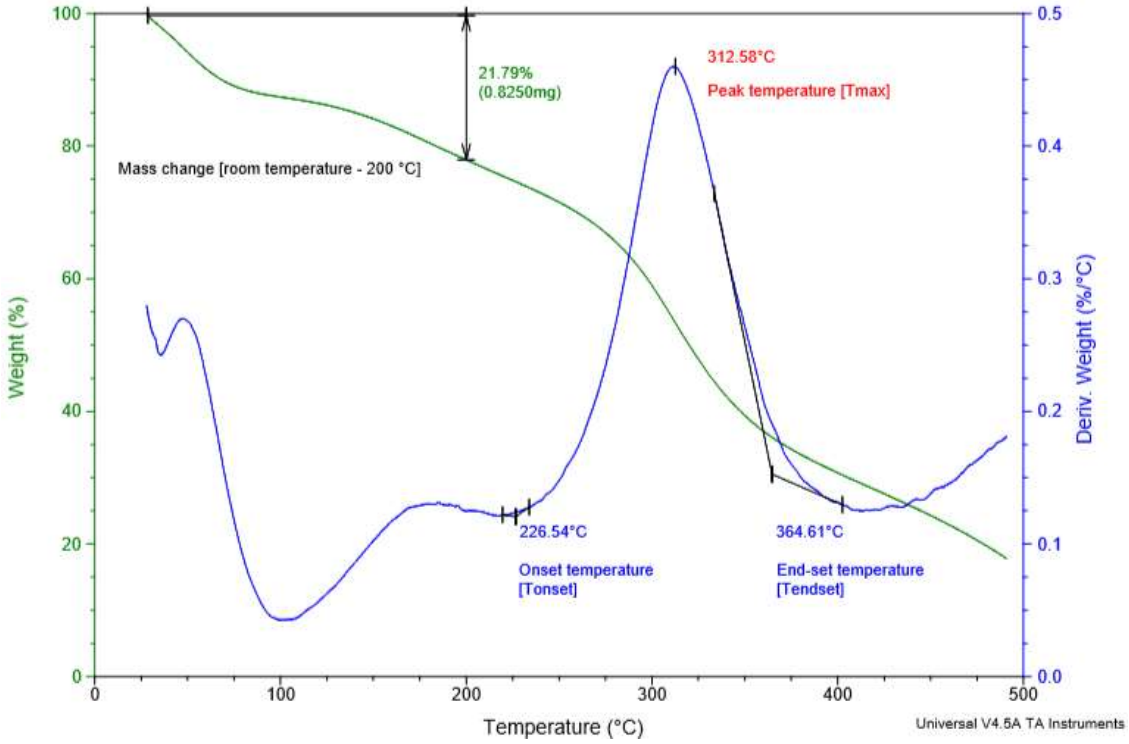

Figure 4.39. TGA and dTGA curves for CHT – AsA (6% w/w) in air atmosphere.

The first degradation step of CHT-AsA associated to water evaporation occurred within a range in temperature between room temperature and 200 °C in both, nitrogen and air atmospheres, with an observed weight loss of 11.1% and 21.8% respectively. The observed temperature corresponding to the maximum rate of mass loss was at 318.4 °C and 312.6 °C respectively. Table 4.16 shows the specific degradation temperatures.

Antioxidant	Atmosphere	Tonset [°C]	Tmax [°C]	Tendset [°C]
CHT-AsA	Nitrogen	265.8	318.4	378.0
CHT-AsA	Air	226.5	312.6	364.6

Table 4.16. Thermal degradation temperatures of CHT-AsA.

Thermal results are in line with those reported in literature, the total percentage of mass loss observed at 200 °C for CHT-AsA is one order of magnitude higher than the percentage of mass loss at the same temperature for AsA.

4.7.5 Maltodextrin as encapsulating agent

Maltodextrin (CAS# 9050-36-6) is a polysaccharide derived from acid or enzymatic hydrolysis of starch. It is considered a polymer of D-glucose chains with dextrose equivalent in the range between 3 and 20 with a molecular weight (Mw < 4000 Da). Maltodextrin (MDX) is widely used in the food industry as an encapsulating agent, the encapsulation technologies usually used are: spray-drying, fluidized bed coating and extrusion (Saavedra-Leos, Leyva-Porras, Araujo-Díaz, Toxqui-Terán, & Borrás-Enríquez, 2015; Wandrey, Bartkowiak, & Harding, 2010).

(Saavedra-Leos et al., 2015) assessed the thermal degradation of maltodextrins at different dextrose equivalents (DE). Authors observed a first thermal degradation step in the range of temperature between 70 °C and 110 °C associated to evaporation (3.5% to 7% of water

loss) and a second thermal degradation step reported in the range of temperature between 200 °C and 350 °C corresponding to long molecular chains decomposition. At lower water content, the reported peak temperature was in the range of 300 °C.

4.7.5.1 Thermal analysis

Thermal analysis was performed with a TA instrument TGA Q50; the carrier gas used was nitrogen (inert atmosphere) and air (oxidative atmosphere) at a flow rate of 60 mL/min and a heating rate of 20 °C/min. The thermal degradation was assessed at the onset temperature (Tonset), maximum temperature (Tmax), and end-set temperature (Tendset).

4.7.5.2 Results

Figure 4.40 and Figure 4.41 present the differential thermogravimetry (dTGA) and the thermogravimetry (TGA) curves of the thermal degradation of ascorbic acid encapsulated in maltodextrin (MDX-AsA) in nitrogen and air atmospheres respectively.

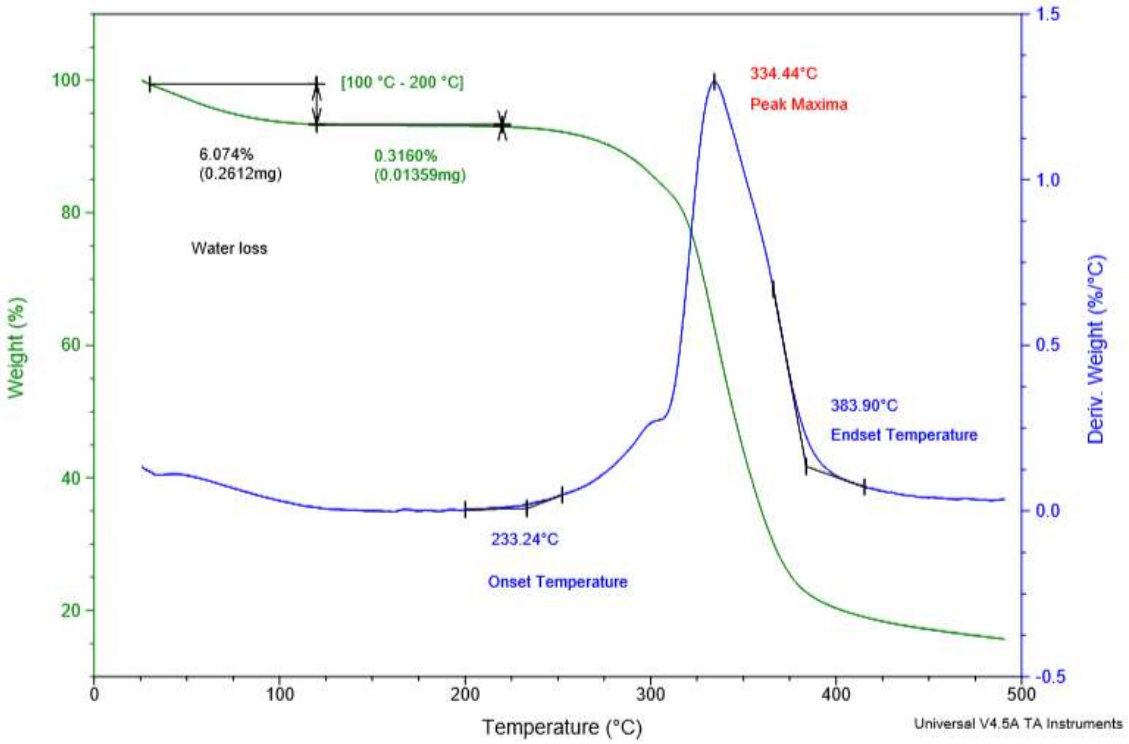

Figure 4.40. TGA and dTGA curves for MDX – AsA (6% w/w) in nitrogen atmosphere.

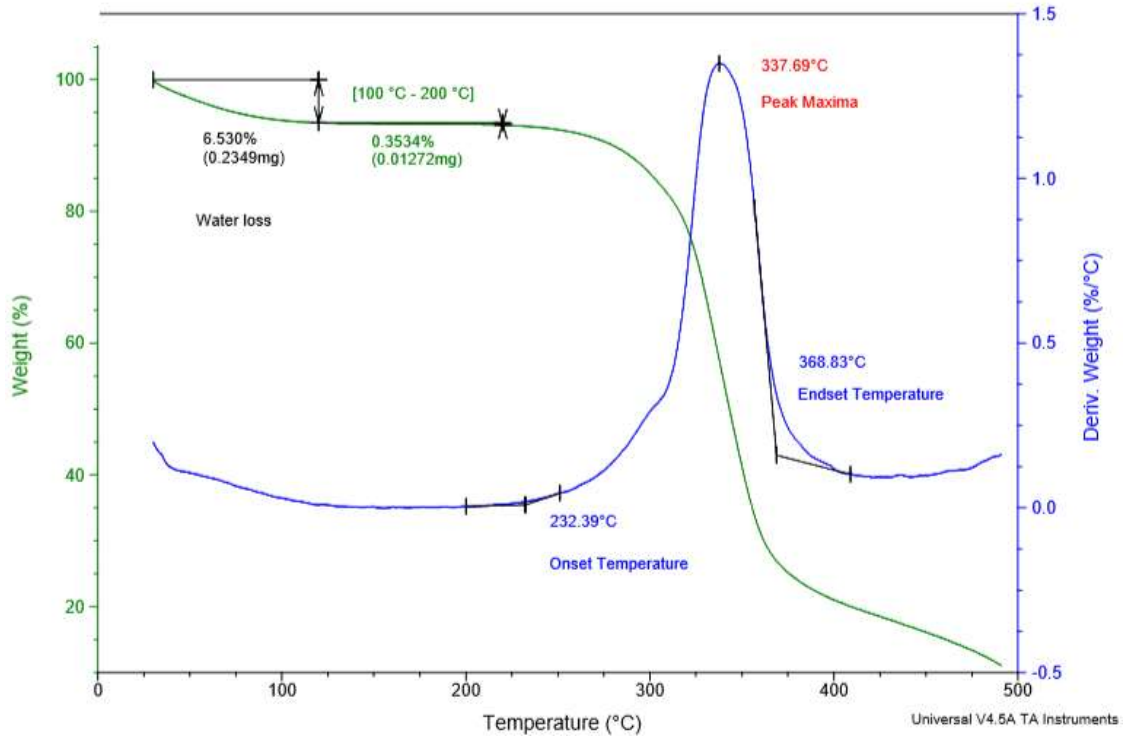

Figure 4.41. TGA and dTGA curves for MDX – AsA (6% w/w) in air atmosphere.

The first thermal degradation event associated to water evaporation for the system MDX-AsA reported a mass loss percentage of 6.1% and 6.5% in nitrogen and air atmosphere respectively. The observed weight change was followed in the temperature region between ambient temperature and 100 °C.

A second region of temperature in the range of 100 °C to 200 °C was evaluated to assess the initial degradation temperature (Tonset) observed for ascorbic acid alone. Corresponding results showed a mass loss percentage less than 0.4% in both, nitrogen and air atmosphere. The main degradation event corresponding to molecular chains decomposition is observed at a second thermal degradation event. The observed temperature at the maximum rate of mass loss for MDX-AsA in nitrogen and air atmosphere was 334.4 °C and 337.7 °C respectively. Table 4.17 presents the specific degradation temperatures.

Antioxidant	Atmosphere	Tonset [°C]	Tmax [°C]	Tendset [°C]
MDX-AsA	Nitrogen	233.2	334.4	383.9
MDX-AsA	Air	232.4	337.7	368.8

Table 4.17. Thermal degradation temperatures of MDX-AsA.

Figure 4.42 presents a TGA step-wise analysis on the thermal degradation of MDX-AsA and a comparison to the thermal degradation of AsA, both in air atmosphere. Resulting TGA curves provide a clearer degradation components separation. Basically, the TGA instrument heat the sample under a constant rate (dynamic mode) until a significant weight loss is detected. Then, the TGA instrument keeps constant the temperature (isothermal mode) until the rate of the sample mass loss becomes negligible. The TGA instrument works in loop until a fixed end test-temperature. Furthermore, Figure 4.44 shows the corresponding dTGA curves where it is clearly observed the peak maxima for both systems.

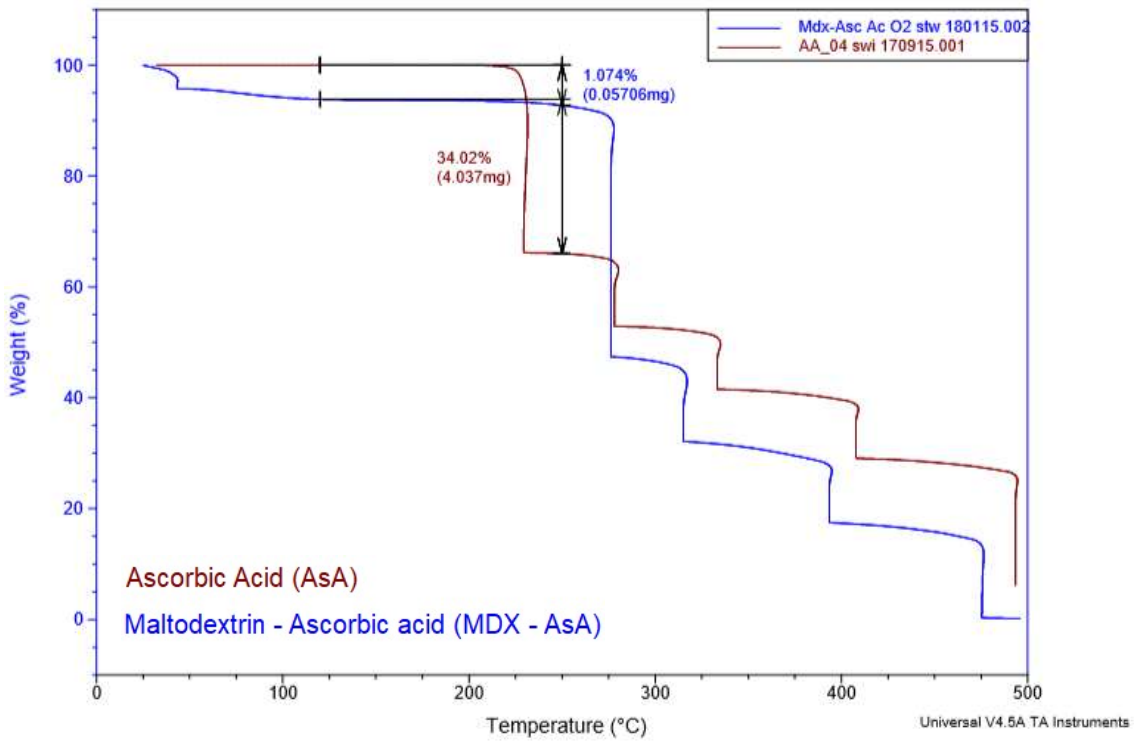

Figure 4.42. Stepwise isothermal thermogram of AsA and MDX-AsA in air atmosphere.

Figure 4.42 shows the components separation steps for MDX-AsA and AsA in air atmosphere. The temperature region for analysis was in the range between 120 °C and 250 °C for both systems. It was not considered the mass loss associated to water evaporation observed in MDX-AsA at temperatures below 100 °C.

The first weight loss change for AsA represented 34% of mass loss compared to 1.1 % of mass loss for MDX-AsA. Furthermore, the initial thermal degradation temperature of MDX-AsA is shifted towards higher temperatures.

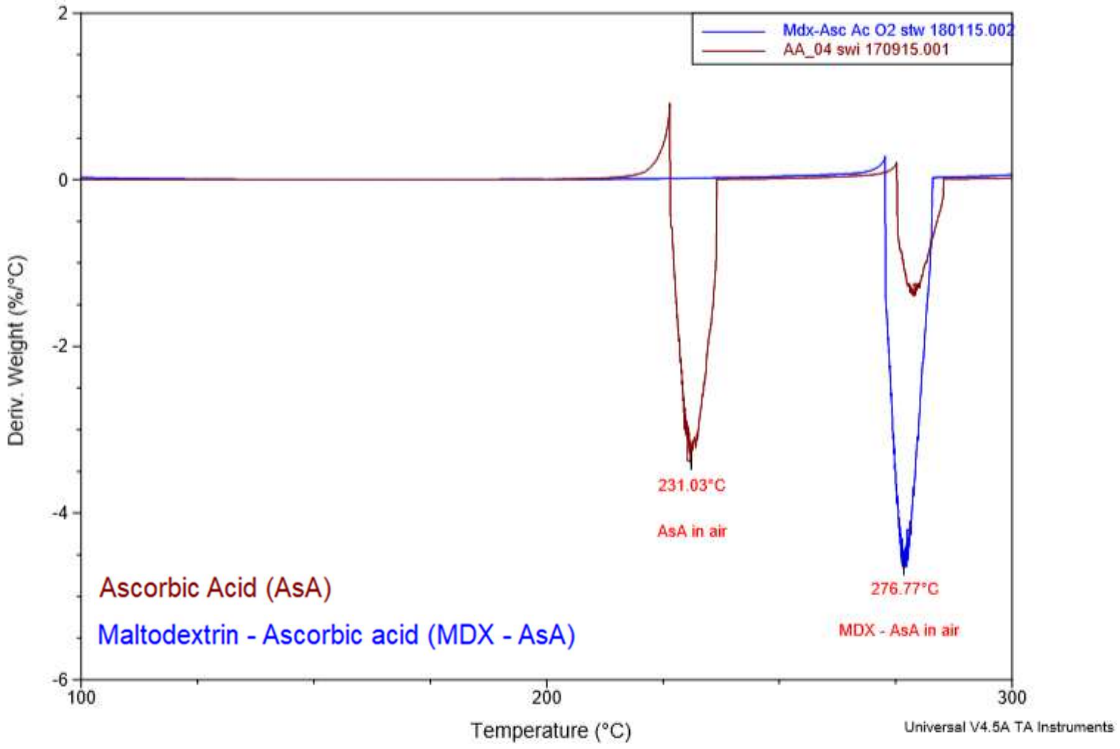

Figure 4.43. Stepwise isothermal dTGA curves of AsA and MDX-AsA in air atmosphere.

Figure 4.43 presents the derivative TGA curves for AsA and MDX-AsA. The maximum rate of mass loss occurred at different temperatures for both systems. In the case of ascorbic acid, it is observed a peak temperature of 231 °C whereas the system MDX-AsA reported a peak temperature of 276.8 °C. A positive difference of approximately 46 °C is observed, hence a possible thermal protection of the encapsulated agent on AsA is achieved.

4.7.6 Conclusions

The effect of encapsulation on ascorbic acid to provide thermal protection was evaluated using chitosan and maltodextrin. Results shown that both encapsulated products presented higher peak temperatures compared to single ascorbic acid. Prior to analysis, samples were kept at the same storage conditions: ambient temperature and in a dark place.

Chitosan – Ascorbic acid system

Thermal degradation of CHT-AsA system in nitrogen and air atmosphere presented a first thermal event associated with water loss. The region of temperature assess was between ambient temperature and 200 °C with an observed mass loss percentage of 11.1% and 21.8% respectively. It was observed degradation above 100 °C which may be attributed to low-molecular weight compounds. Observed peak temperatures were 318.4 °C and 312.6 °C in nitrogen and air atmosphere respectively.

Maltodextrin – Ascorbic acid system

The thermal degradation of MDX-AsA system in nitrogen and air atmosphere presented a first thermal event associated with water loss. The region of temperature analysis was kept the same as CHT-AsA system. The observed mass loss percentages were 6.4% and 6.9% in nitrogen and air atmosphere respectively. Within the range in temperature between 100 °C and 200 °C the mass loss associated to low-molecular weight compounds volatilization is negligible: in both atmospheres, a total mass loss percentage lower than 0.4% was observed.

General overview

It may be concluded that the combined effect of water content and oxidative conditions such as air atmosphere presented a higher mass loss percentage for the system CHT-AsA. Possibly derived from oxidation degradation reactions and hydrolysis reactions as reported by (Saavedra-Leos et al., 2015). Also, a broad molecular weight distribution could increase the region of thermal degradation temperatures.

The system MDX-AsA presented a lesser mass loss percentage associated to water evaporation (below 100°C). One important point to remark is the thermal degradation analysis in the range between 100 °C and 200 °C with an observed mass loss percentage

lower than 0.4%. Hence, it may represent that there is no significant volatilization of low-molecular weight compounds and also, the onset degradation temperature observed in ascorbic acid is not present. The onset degradation temperatures reported in nitrogen and air atmosphere is shifted towards higher temperatures: 233.2 °C and 232.4 °C respectively. It may be concluded that maltodextrin is more thermally stable and protected the thermal degradation of the core material ascorbic acid.

4.7.7 Antioxidant capacity determination of encapsulated ascorbic acid

The encapsulation of ascorbic acid in maltodextrin provided a higher thermal stability as compared to the single ascorbic acid molecule. The antioxidant capacity of AsA at standard conditions proved its antioxidant activity against free radicals such as $DPPH^{\cdot}$, $ABTS^{\cdot+}$ and SOA.

Prior to incorporation of MDX-AsA in polymer formulation as thermal stabilizer, it is important to evaluate the effect of the encapsulation process on the antioxidant activity of AsA. In light of this information, the antioxidant capacity of AsA (control reference) and MDX-AsA were assessed by the $DPPH^{\cdot}$ method.

4.7.7.1 Methodology

Antioxidant capacity was assessed using a Thermo Scientific Multiskan EX Spectrophotometer adapted for 96-wells microplates. The reaction mixture of a final volume assay of 250 µL containing a 25 µL aliquot of either AsA or MDX-AsA diluted in ethanol and a 25 µL aliquot of $DPPH^{\cdot}$ radical solution (175 µM) was monitored spectrophotometrically at λ = 490 nm and at a kinetic end-points of 5 and 10 minutes. Results are expressed as the percentage of $DPPH^{\cdot}$ scavenged and the EC_{50} value, which corresponds to the antioxidant concentration that causes a reduction of 50% from the initial concentration of $DPPH^{\cdot}$ radical.

4.7.7.2 Results

Figure 4.44 and Figure 4.45 present the antioxidant activity of ascorbic acid (AsA) and encapsulated ascorbic acid in maltodextrin (MDX-AsA) by the DPPH$^{\cdot}$ method followed as the percentage of DPPH$^{\cdot}$ radical scavenged.

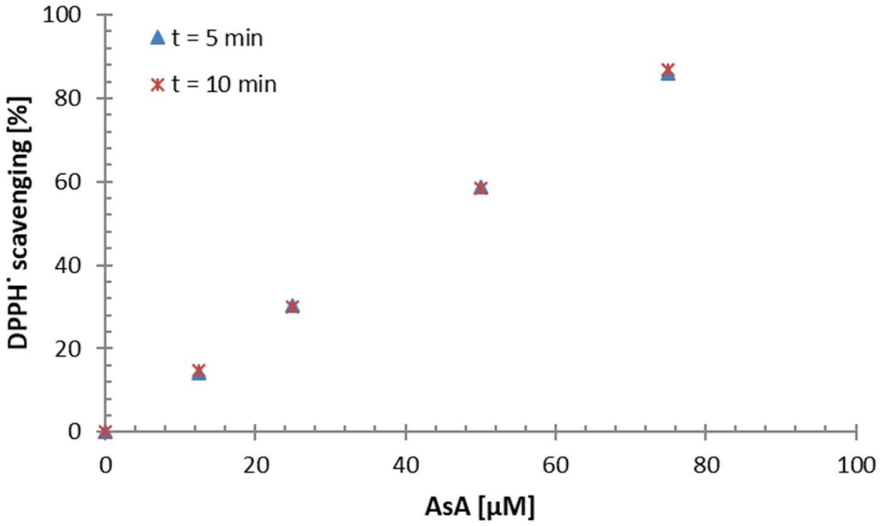

Figure 4.44. Percentage of DPPH$^{\cdot}$ radical scavenged by ascorbic acid (AsA).

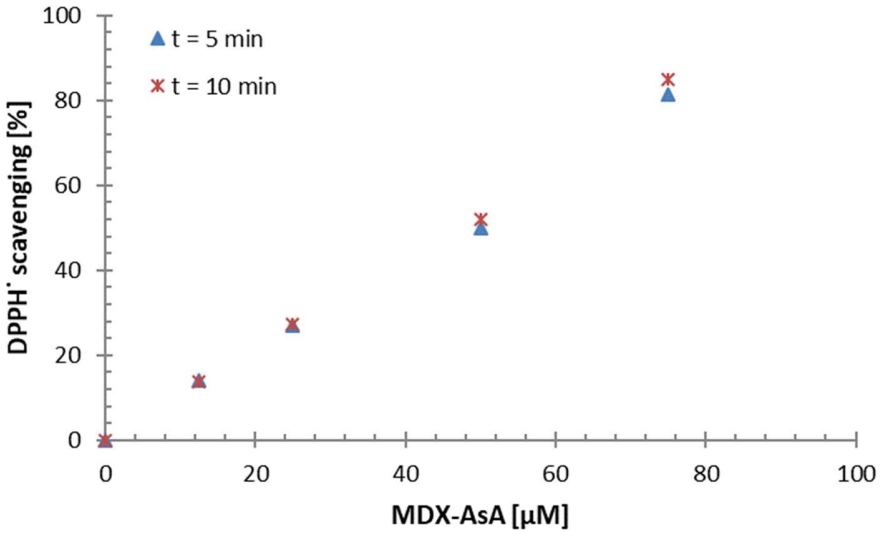

Figure 4.45. Percentage of DPPH$^{\cdot}$ radical scavenged by encapsulated ascorbic acid (MDX-AsA).

From Figure 4.44 it is observed, as shown in chapter 2, that ascorbic acid followed a fast reaction rate against DPPH$^{\cdot}$ radical. Within the percentage of DPPH$^{\cdot}$ radical scavenged, under the experimental conditions assessed, there were no significant difference between an end-point of 5 and 10 minutes. The system MDX-AsA shown in Figure 4.45 presented also a fast reaction rate against DPPH$^{\cdot}$ radical and no significant difference in the percentage of DPPH$^{\cdot}$ radical scavenged at the kinetic end-points of 5 and 10 minutes. Table 4.18 presents the corresponding DPPH$^{\cdot}$ radical scavenged at different antioxidant (AoX) concentrations.

	AsA		**MDX - AsA**	
AoX [μM]	t = 5 min [%]	t= 10 min [%]	t = 5 min [%]	t= 10 min [%]
75	86.0	86.8	81.3	85.0
50	58.8	58.4	49.9	52.1
25	30.3	30.0	27.0	27.3
12.5	14.2	14.7	14.1	13.9
0	0	0	0	0

Table 4.18. DPPH$^{\cdot}$ radical scavenged at different antioxidant concentrations for ascorbic acid (AsA) and encapsulated ascorbic acid in maltodextrin (MDX-AsA).

Table 4.19 shows the calculated EC_{50} values for AsA and MDX-AsA.

Material	Kinetic [min]	Linear fit	r^2	EC_{50} [μM]
AsA	5	[DPPH scvg] = 1.1518 [AsA] + 0.4311	0.999	43.0
AsA	10	[DPPH scvg] = 1.1571 [AsA] + 0.3805	0.999	42.9
MDX-AsA	5	[DPPH scvg] = 1.0604 [MDX-AsA] - 0.0045	0.996	47.2
MDX-AsA	10	[DPPH scvg] = 1.1146 [MDX-AsA] - 0.5781	0.997	45.4

Table 4.19. EC_{50} values for AsA and MDX-AsA at a kinetic end point of 5 and 10 minutes.

It is observed from Table 4.19 that ascorbic acid and the antioxidant system MDX-AsA presented a good linear fit with similar values of EC_{50}. Furthermore, Figure 4.46 presents a

correlation between AsA and MDX-AsA as a function of the percentage of DPPH$^{\cdot}$ radical scavenged.

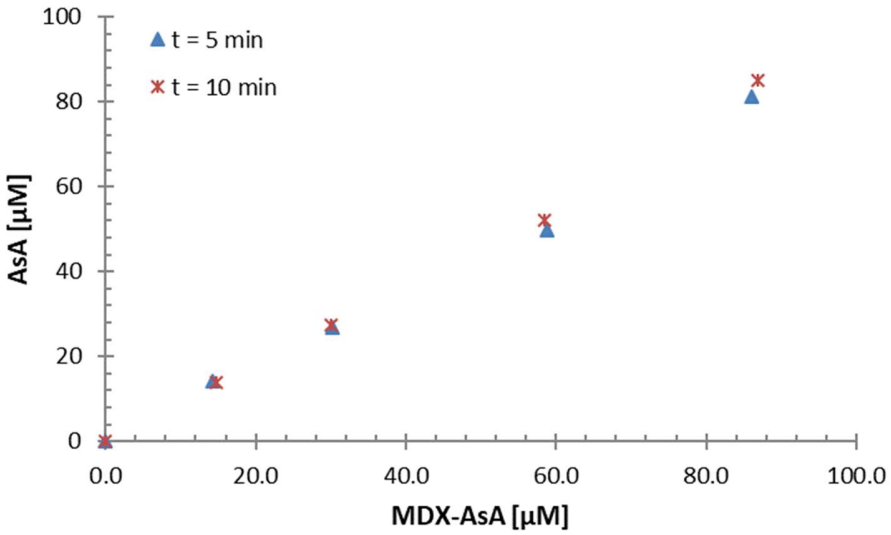

Figure 4.46. Correlation plot between ascorbic acid (AsA) and encapsulated ascorbic acid (MDX-AsA) on the percentage of DPPH$^{\cdot}$ radical scavenging.

The calculated Pearson correlation coefficient from figure 4.46 at the kinetic points t= 5 minutes and t= 10 minutes were r= 0.997 and r= 0.998 respectively. Resulting in a positive and robust correlation between ascorbic acid and encapsulated ascorbic acid. Thus, it may be concluded that the effect of the encapsulation process on the antioxidant activity of ascorbic acid against DPPH$^{\cdot}$ radical is not significant.

4.8 Antioxidant capacity of binary antioxidant blends

The incorporation of exogenous antioxidants in food and polymer resins is of importance to either prolonged the shelf-life of food products such as edible oils or to provide thermal resistance against oxidation caused by free radicals to polymer resins during its processing.

According to literature, α-tocopherol radical can be reduced to its original form by ascorbic acid, this positive effect may open the possibility to incorporate antioxidant blends in polymer formulation.

Ascorbic acid and α-tocopherol were previously assessed as a function of its antioxidant activity and thermal stability. The effect of a binary antioxidant blend on the antioxidant activity has been reported in literature to determine a synergistic, antagonistic, or additive effect on the antioxidant capacity determination (Colon & Nerín, 2016). The proposed methodology is to evaluate the interaction of the binary antioxidant system of ascorbic acid (AsA) and trolox (Tx), the α-tocopherol analogous, by the $DPPH^{\cdot}$ method.

Statistical Analysis

A simplex lattice mixture design was assessed in Minitab 18 and evaluated using ANOVA. Model terms are significant for a p value < 0.05.

Simplex Lattice Design

A mixture design was utilized to assess the antioxidant activity of a binary antioxidant formulation. Two components were evaluated: ascorbic acid (AsA) and trolox (Tx) within a range in concentration between 0 and 60 μM each and a total maximum binary antioxidant concentration of 60 μM. The general equations to predict the response for two components are the following:

$$\hat{Y} = \beta_1 X_1 + \beta_2 X_2 \quad (4.5)$$

$$\hat{Y} = \beta_1 X_1 + \beta_2 X_2 + \beta_{12} X_1 X_2 \quad (4.6)$$

Where $\hat{Y}$ is the response or dependent variable represented as the percentage of $DPPH^{\cdot}$ radical scavenged and β_1 and β_2 are the fitted coefficients for component X_1 and X_2 respectively. Equation 1 represents a first order (linear) model fit whereas equation 2 stands for a second order (quadratic) model fit.

4.8.1 Methodology

Antioxidant capacity was assessed using a Thermo Scientific Multiskan EX Spectrophotometer adapted for 96-wells microplates. 2 mM ethanolic stock solutions for $DPPH^{\cdot}$, ascorbic acid (AsA), and trolox (Tx) were prepared. Further dilutions were performed in ethanol according to the experimental runs shown in Table 4.20.

Briefly, the reaction mixture of a final volume assay of 250 µL containing a 25 µL aliquot from the dilutions presented in Table 4.20 and a 25 µL aliquot of $DPPH^{\cdot}$ radical solution (200 µM) was monitored spectrophotometrically at λ = 490 nm and at a kinetic end-point of 5 minutes. Results are expressed as the percentage of $DPPH^{\cdot}$ radical scavenged.

StdOrder	RunOrder	AsA [µM]	Tx [µM]
1	1	60	0
5	2	30	30
4	3	0	60
7	4	15	45
6	5	45	15
2	6	40	20
3	7	20	40

Table 4.20. Design table for experimental runs on the antioxidant capacity of ascorbic acid (AsA) and trolox (Tx) as a binary antioxidant system.

4.8.2 Results

The 7 experimental runs were randomized and assessed by DPPH$^{\cdot}$ method. Figure 4.47 shows the experimental results in terms of percentage of DPPH$^{\cdot}$ radical scavenged.

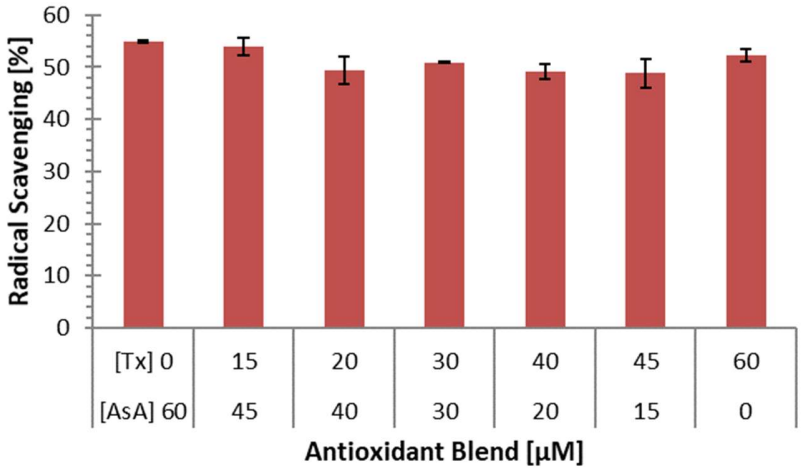

Figure 4.47. DPPH$^{\cdot}$ radical scavenging results for ascorbic acid (AsA) and trolox (Tx) as a binary antioxidant system.

The resulting fitted mixture model (r^2 = 0.71) is represented in equation 4.7:

$$\%\ DPPH^{\cdot}\ scvg = 0.924104\ [AsA] + 0861048\ [Tx] - 000409842\ [AsA]\ [Tx] \quad (4.7)$$

ANOVA results ($p > 0.05$) infers that there is no significant statistical evidence of association between the dependent variable with the individual components and their interaction.

4.8.3 Conclusions

The use of a simplex lattice mixture design provided a systematic approach on a binary antioxidant formulation in terms of antioxidant capacity. The use of ascorbic acid and trolox as a binary antioxidant blend did not affect the performance (antagonism effect) on the antioxidant capacity against $DPPH^{\cdot}$ free radical.

Perhaps it is reasonable to assess antioxidants with different reaction rates against free radicals. In the case of ascorbic acid and trolox, both present similar bond dissociation energies (69 – 83 Kcal/mol and 77.1 – 79.3 Kcal/mol respectively) (Decker, Chen, Panya, & Elias, 2010). Thus, may confirm the observed results with similar antioxidant activities against $DPPH^{\cdot}$ radical.

4.9 Polymer Formulation

The industrial transformation of polymers involves thermo-mechanical events such as the case in post-reactor operations, where the resulting polymer resin is dried and formulated with stabilizers and processing aids prior to extrusion to produce resin pellets. Other post-processing operations such as compounding and plastics product operations include additional thermo-mechanical events.

Olefin resins in particular, low-density polyethylene (LDPE) and isotactic polypropylene (i-PP) are susceptible to degradation during polymer processing. Chapter III dealt with the state of the art of LDPE and i-PP, it addressed the effect of thermo-mechanical events on the thermal stability of these polymer resins followed by thermal analysis (oxidation onset temperature and degradation kinetic analysis), polymer melt rheology, and melt flow index to evidence the corresponding degradation mechanism.

Align to the scope of this thesis dissertation, natural sources of antioxidants were assessed in terms of antioxidant activity and thermal stability prior to incorporation into LDPE and i-PP by extrusion process.

4.9.1 Materials

Un-stabilized low-density polyethylene ($LDPE_{15}$) and un-stabilized isotactic polypropylene (i-PP) were provided by Repsol, Spain; ascorbic acid, α-tocopherol, and linseed oil were supplied by Sigma, France, and flaxseed oil was obtained from Terpenic Labs, Spain.

4.9.2 Methodology

Antioxidant(s) incorporation into $LDPE_{15}$ and i-PP were carried out by extrusion process using a LabTECH co-rotating twin extruder with 16 mm diameter screw and length to diameter (L/D) ratio of 40; extruder is provided with 10 temperature-controlled heating zones (from zone 1 to die). Screw speed was fixed constant at 300 RPM and the extrusion temperatures profiles as shown in Table 4.21.

Extrusion temperatures profile [°C]										
DIE	**Z9**	**Z8**	**Z7**	**Z6**	**Z5**	**Z4**	**Z3**	**Z2**	**Z1**	**Input Material**
190	190	190	190	190	190	160	150	120	80	i-PP
160	150	150	150	150	150	150	140	120	80	$LDPE_{15}$

Table 4.21. Extrusion temperatures profiles for i-PP and $LDPE_{15}$.

4.9.2.1 Thermal analysis

The thermal stability of the extrudate $LDPE_{15}$ and i-PP, under the experimental conditions evaluated, were characterized by DSC and TGA on a TA instrument DSC Q100 and a TA instrument TGA Q50 respectively. Two test methods were studied:

Oxidation onset temperature (OOT)

Thermo-oxidative degradation can be assessed at the onset of oxidation induced by the effect of temperature and oxidative conditions such as air or oxygen. The oxidation onset temperature (OOT) is determined as the intersection of the baseline with the slope at the inflection point of the oxidation exotherm peak, the resulting temperature represents the OOT value. The higher the OOT value, the higher the thermal resistance of the sample.

Briefly, a representative sample is placed in an open aluminum pan and heated, in dynamic conditions, at a rate of 10 °C/min under a flux of air atmosphere (60 mL/min).

Thermal degradation kinetic analysis

Kinetics of thermal degradation were performed by TGA in dynamic mode at three different heating rates: 10 °C/min, 20 °C/min, and 30 °C/min, in open aluminum pans under inert atmosphere (nitrogen) and a gas flow of 60 mL/min. Two iso-conversional methods were assessed: Friedman and Kissinger and the ASTM E 1641 method for decomposition kinetics by thermogravimetry.

4.9.2.2 Rheological analysis

Sample preparation

25 mm diameter disk samples were compressed molded at a temperature of 150 °C for $LDPE_{15,33}$ and 180 °C for i-PP during 7 minutes and a mold pressure of 78.4 bar.

Dynamic tests

Polymer melt rheology analysis was performed in an Ares rotational rheometer with a parallel plate geometry (25 mm diameter). The gap distance was fixed approximately between 1.8 mm and 1.9 mm and the percentage of strain utilized under the linear viscoelasticity region. Strain sweep analysis and frequency sweep analysis were performed in nitrogen atmosphere to avoid degradation.

Strain sweep analysis

The linear viscoelastic region was assessed between an initial strain of 0.1% and a final strain of 10%, with a frequency of 1 rad/s.

Frequency sweep analysis

The frequency range evaluated was 0.1 – 100 rad/s and a 2.5% of strain used to ensure linear viscoelasticity.

Complex viscosity (η*), storage modulus (G'), and loss modulus (G'') were assessed as a function of frequency (ω) and analyzed by the TA orchestrator software. Equation 4.8 represents de relationship.

$$\eta* = (G' + G'')^{\frac{1}{2}}/\omega \quad (4.8)$$

4.9.3 Extrusion and formulation of low-density polyethylene ($LDPE_{15}$)

Individual antioxidants at a constant concentration (% w/w) were incorporated into $LDPE_{15}$ in order to assess the effect of antioxidant type on the thermal stability of $LDPE_{15}$ followed by thermal and rheological analyses. Also, the thermal degradation of bare $LDPE_{15}$ was studied as a control reference. Table 4.22 shows the experimental conditions assessed.

Polymer	Extrusion temperature [°C]	Antioxidant	% in formula
$LDPE_{15}$[a]	150	--	--
$LDPE_{15}$[b]	150	--	--
$LDPE_{15}$	150	LSO	2.5%
$LDPE_{15}$	150	FSO	2.5%
$LDPE_{15}$	150	α-toco	2.5%

Table 4.22. Extrusion process conditions and formulation for $LDPE_{15}$. **a**. unprocessed $LDPE_{15}$ **b**. extruded $LDPE_{15}$ w/o antioxidants.

Furthermore, Table 4.23 depicts the formulation by extrusion process of $LDPE_{15}$ under the same processing temperatures to assess the individual performance of antioxidants on the thermal stability of $LDPE_{15}$.

Polymer	Extrusion temperature [°C]	Antioxidant	% in formula
$LDPE_{15}$[a]	150	--	--
$LDPE_{15}$[b]	150	--	--
$LDPE_{15}$	150	FSO	1.5%
$LDPE_{15}$	150	FSO	2%
$LDPE_{15}$	150	FSO	3%
$LDPE_{15}$	150	α-toco	1.5%
$LDPE_{15}$	150	α-toco	2%
$LDPE_{15}$	150	α-toco	3%
$LDPE_{15}$	150	α-toco	6%

Table 4.23. Test conditions and formulation of $LDPE_{15}$. **a**. unprocessed $LDPE_{15}$ **b**. extruded $LDPE_{15}$ w/o antioxidants.

4.9.3.1 Thermal analysis

Oxidation onset temperature (OOT)

The incorporation of individual antioxidants by extrusion process into $LDPE_{15}$ were assessed by OOT. Figure 4.48 shows the DSC curves.

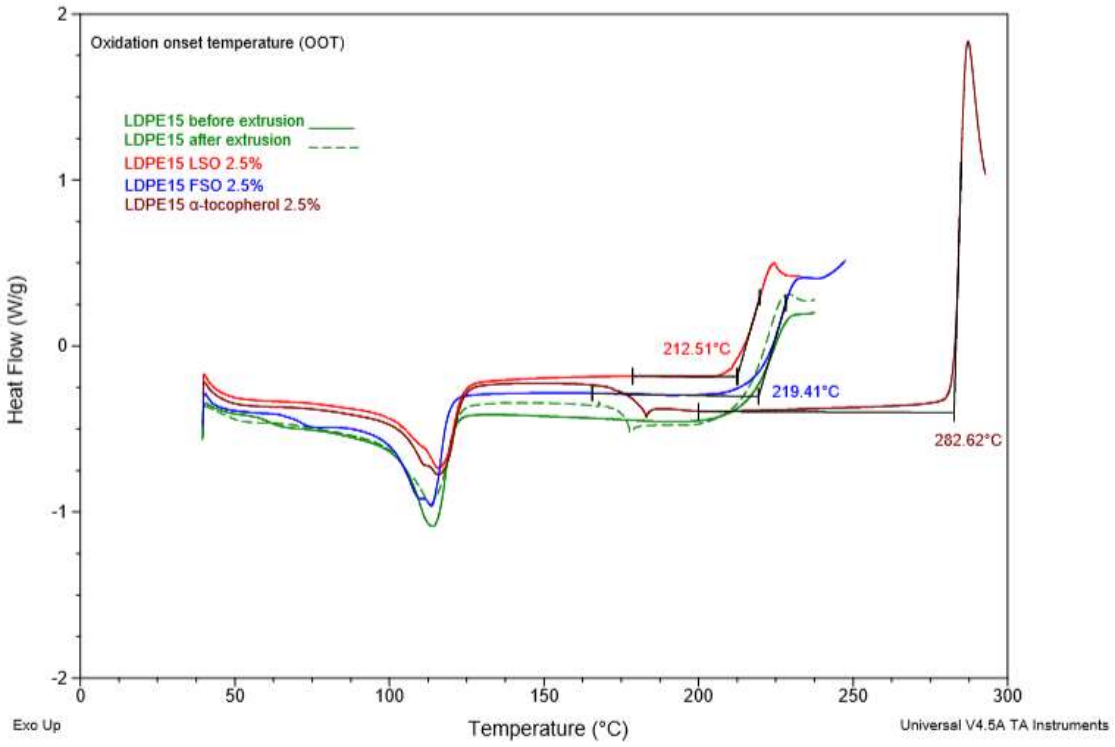

Figure 4.48. DSC curves on $LDPE_{15}$ formulated with individual antioxidants at a fixed concentration (%w/w).

It is observed from Figure 4.48 that α-tocopherol presented the highest thermo-oxidative stability as compared to flaxseed and linseed oil respectively, and with a difference of approximately + 66°C comparing to the OOT value of the control reference ($LDPE_{15}$ un-stabilized after extrusion).

In the case of flax oils, within the experimental conditions assessed, there is a slight difference observed between flaxseed oil (FSO) and linseed oil (LSO), 219.2 °C +/- 0.25 and 212.8 °C +/- 0.31 respectively. Table 4.24 shows the resulting OOT values.

Polymer	Antioxidant	% in formula	OOT [°C]	+/-
$LDPE_{15}^{a}$	--	--	215.6	0.53
$LDPE_{15}^{b}$	--	--	214.2	0.23
$LDPE_{15}$	LSO	2.5%	212.8	0.31
$LDPE_{15}$	FSO	2.5%	219.2	0.25
$LDPE_{15}$	α-toco	2.5%	280.7	1.88

Table 4.24. OOT results for $LDPE_{15}$ after extrusion process.

It is observed a lower thermo-oxidative stability of LSO than the unprocessed material and the control reference ($LDPE_{15}^{a, b}$) in terms of OOT. This may corroborate prior results observed on the effect of oxidation stability on flax oils, where it was observed a higher oxidation on LSO.

Antioxidants were incorporated as a percentage in weight (% w/w) into $LDPE_{15}$, the effect of the final percentage of antioxidant on the oxidation onset temperature is shown in Figures 4.49 and 4.50 for flaxseed oil (FSO) and α-tocopherol respectively.

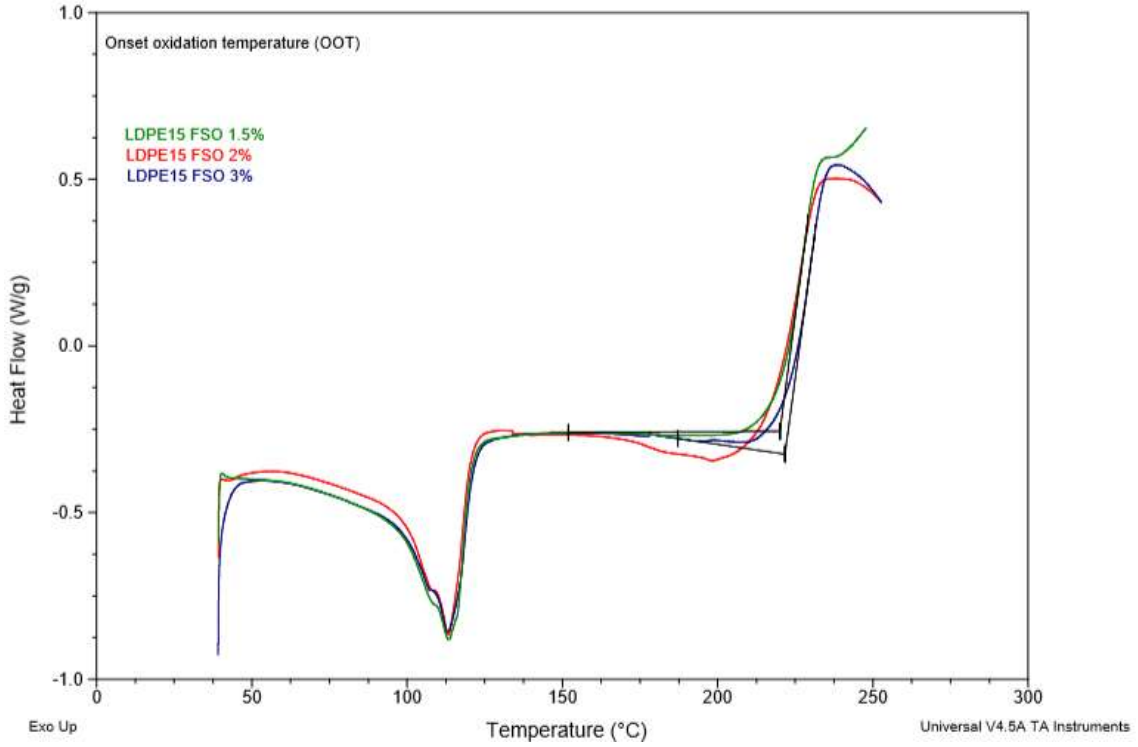

Figure 4.49. DSC curves on the antioxidant system: $LDPE_{15}$ FSO.

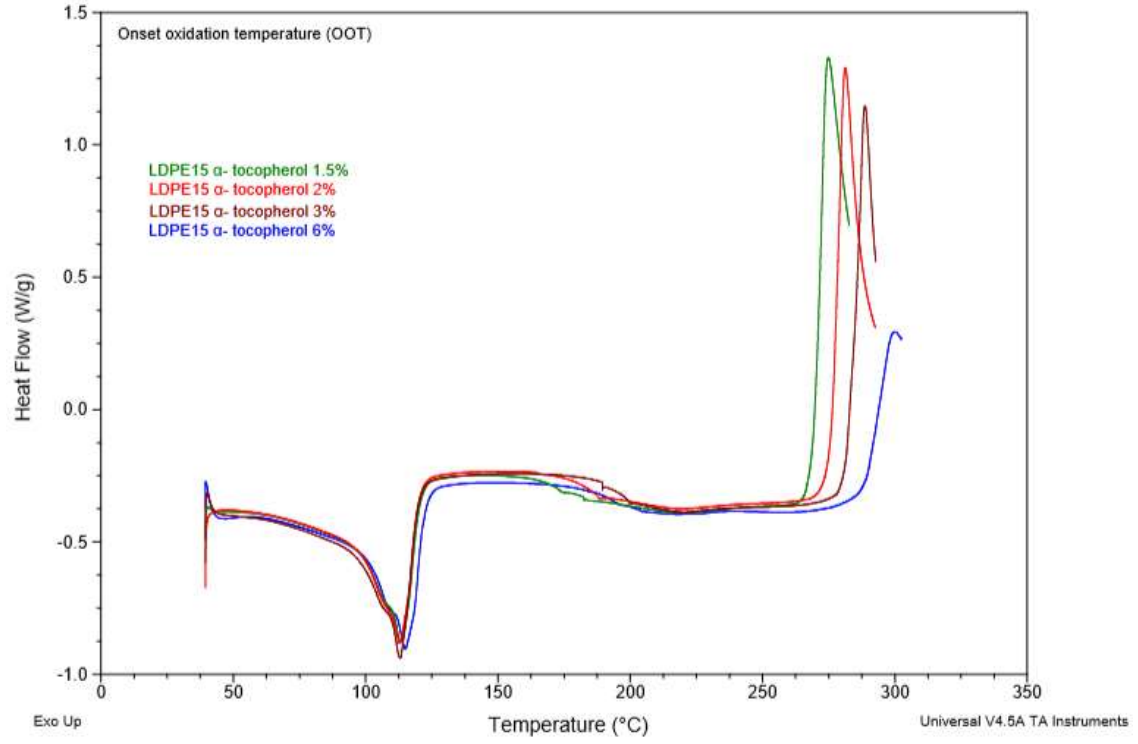

Figure 4.50. DSC curves on the antioxidant system: $LDPE_{15}$ α-tocopherol.

In the case of the antioxidant system $LDPE_{15}$ FSO, there is no significant difference in the observed OOT value as the percentage of antioxidant increased in formulation. The thermo-oxidative stability of $LDPE_{15}$ FSO against un-stabilized $LDPE_{15}$ was approximately 4% higher. Figure 4.51 depicts the observed OOT values.

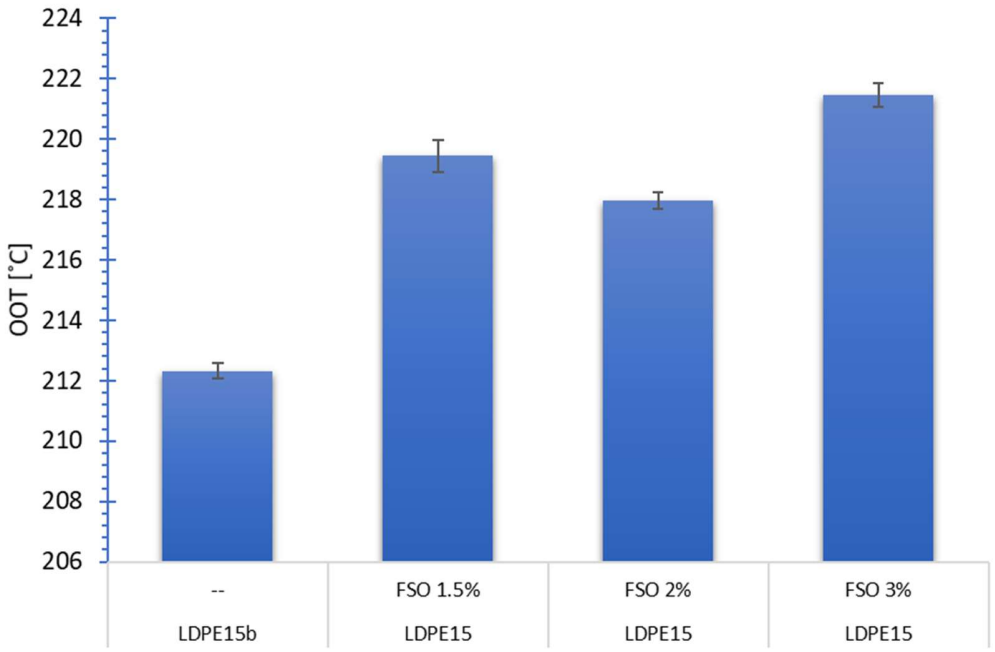

Figure 4.51. OOT results for $LDPE_{15}$ formulated with FSO. $LDPE_{15}^{b}$ (un-stabilized after extrusion).

The antioxidant system $LDPE_{15}$ α-tocopherol showed a higher thermo-oxidative stability with OOT values in the range of 269 °C and 290 °C for a percentage in weight of α-tocopherol of 1.5% and 6% respectively. Figure 4.52 illustrates the observed OOT values.

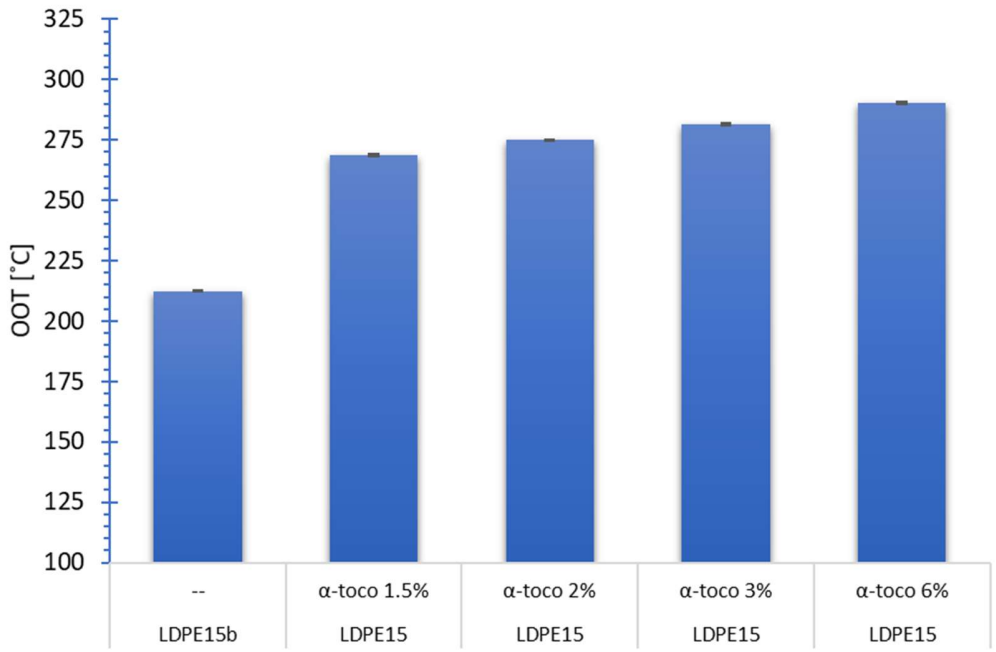

Figure 4.52. OOT results for $LDPE_{15}$ formulated with α-tocopherol. $LDPE_{15}^{b}$ (un-stabilized after extrusion).

The thermo-oxidative stability of FSO and α-tocopherol on LDP_{15} was followed up for a month (Table 4.25). It was observed no significant difference in terms of OOT. Furthermore, representative formulations on α-tocopherol at 1.5, 3, and 6% were assess up to an aging time of 2 months with no significant change on the oxidation onset temperature (OOT).

			Fresh		1 month	2 month
Polymer	Antioxidant	% in formula	OOT [°C]	+/-	OOT [°C]	OOT [°C]
$LDPE_{15}$[a]	--	--	213.3	0.27	---	---
$LDPE_{15}$[b]	--	--	212.3	0.52	216.1	---
$LDPE_{15}$	FSO 1.5%	1.5%	219.4	0.28	221.0	---
$LDPE_{15}$	FSO 2%	2%	218.0	0.38	221.5	---
$LDPE_{15}$	FSO 3%	3%	221.5	0.52	224.2	---
$LDPE_{15}$	α-toco 1.5%	1.5%	268.7	0.75	272.9	274.9
$LDPE_{15}$	α-toco 2%	2%	275.0	1.00	279.2	---
$LDPE_{15}$	α-toco 3%	3%	281.6	2.19	282.2	281.3
$LDPE_{15}$	α-toco 6%	6%	290.4	2.63	---	287.3

Table 4.25. OOT results for $LDPE_{15}$ after extrusion process.

The incorporation of flaxseed oil and α-tocopherol provided thermo-oxidative stability to $LDPE_{15}$ during extrusion process. The observed values in terms of OOT showed that α-tocopherol is a more efficient antioxidant with higher oxidation onset temperatures. It may be possible that the pooled of antioxidants (including lignans) present in the flaxseed oil are lesser in terms of concentration as compared to α-tocopherol nevertheless, flaxseed oil is rich in omega 3 thus, being a potential advantage to incorporate in an antioxidant system for food packaging applications.

Thermal degradation kinetic analysis

The apparent energy of activation at decomposition (Ea_{deg}) was calculated from the TGA thermal curves at a fixed degrees of conversion (α). Figure 4.53 and Figure 4.54 present a schematic representation of the thermal degradation profiles for the antioxidant systems: $LDPE_{15}$ FSO and $LDPE_{15}$ α-tocopherol respectively. Table 4.26 shows the formulations assessed.

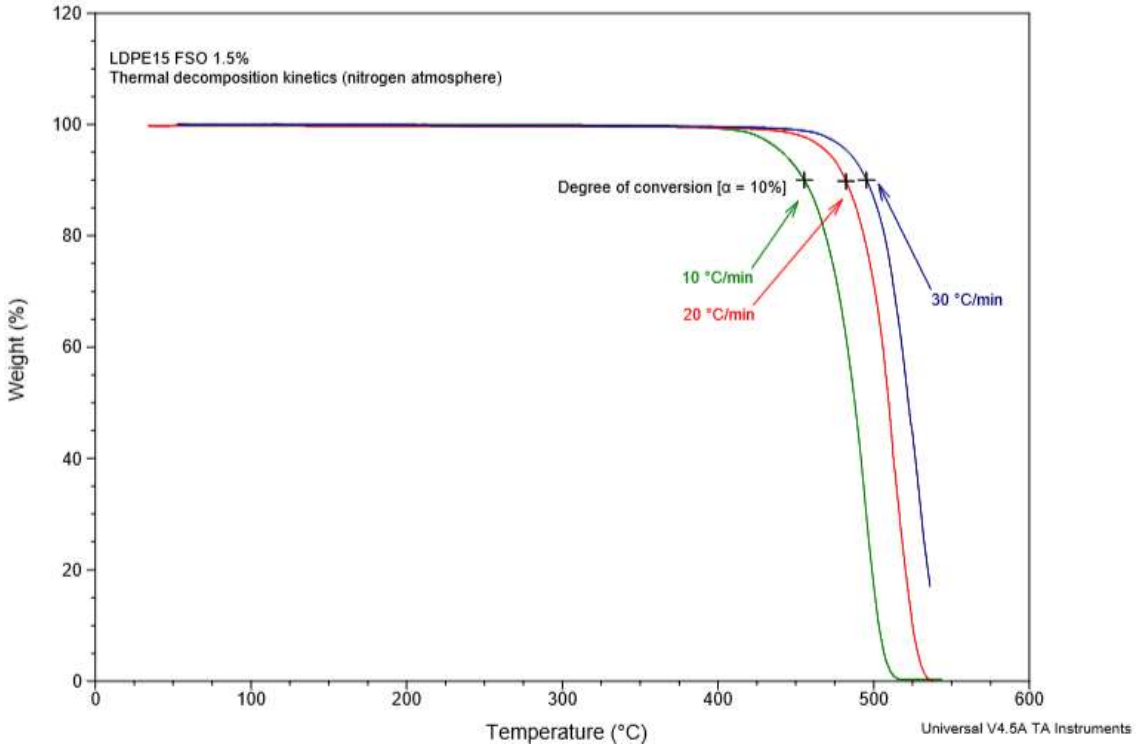

Figure 4.53. Thermal curves of $LDPE_{15}$ FSO (in N_2 atmosphere at 10, 20, and 30 °C/min).

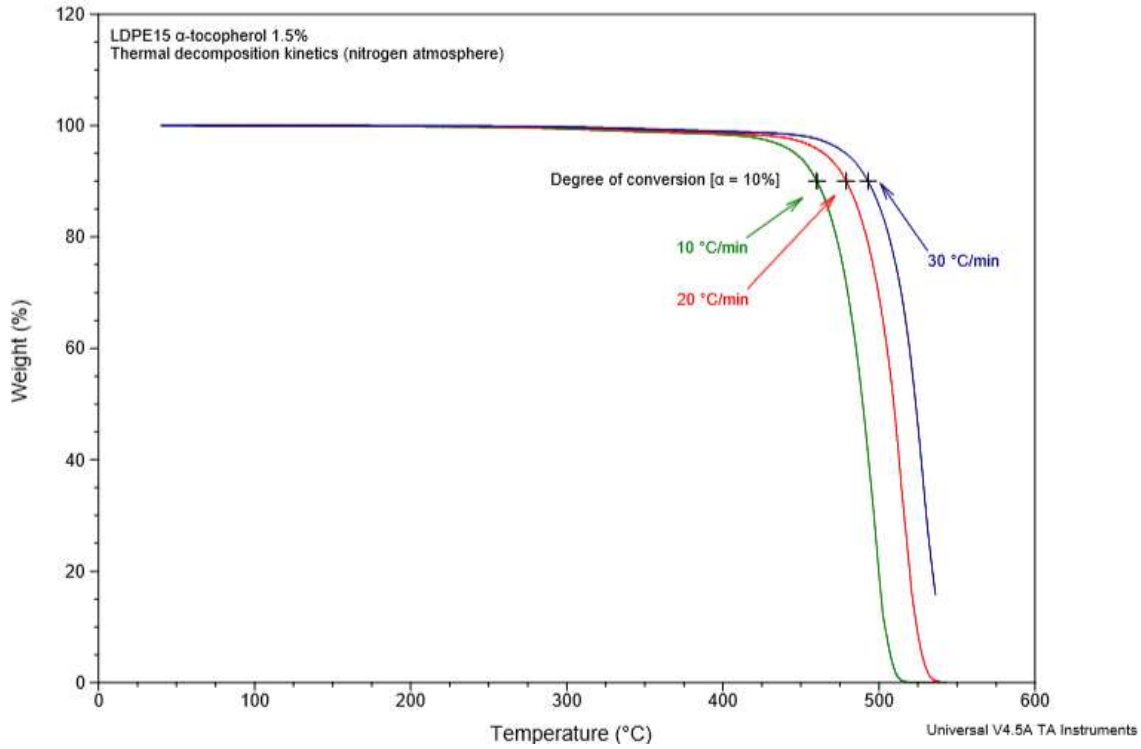

Figure 4.54. Thermal curves of $LDPE_{15}$ α-tocopherol (in N_2 atmosphere at 10, 20, and 30 °C/min).

Polymer	Antioxidant	% in formula
$LDPE_{15}$[a]	--	--
$LDPE_{15}$[b]	--	--
$LDPE_{15}$	FSO 1.5%	1.5%
$LDPE_{15}$	FSO 2%	2%
$LDPE_{15}$	FSO 3%	3%
$LDPE_{15}$	α-toco 1.5%	1.5%
$LDPE_{15}$	α-toco 2%	2%
$LDPE_{15}$	α-toco 3%	3%
$LDPE_{15}$	α-toco 6%	6%

Table 4.26. $LDPE_{15}$ formulations assessed by thermogravimetric kinetic analysis.

Figure 4.55 and Figure 4.56 show the Arrhenius plots based on the ASTM E1641, Kissinger, and Friedman decomposition kinetic methods for $LDPE_{15}$ FSO 1.5% and $LDPE_{15}$ α-tocopherol 1.5% respectively.

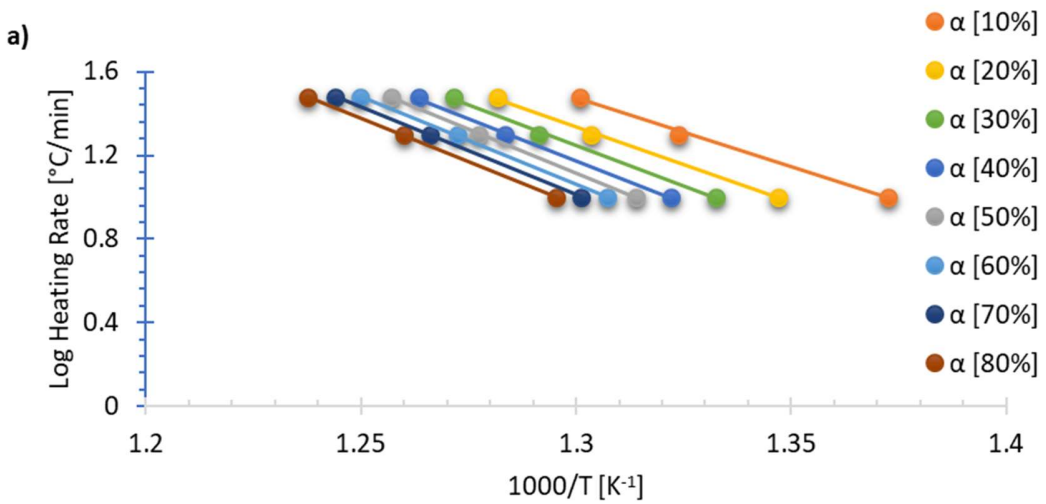

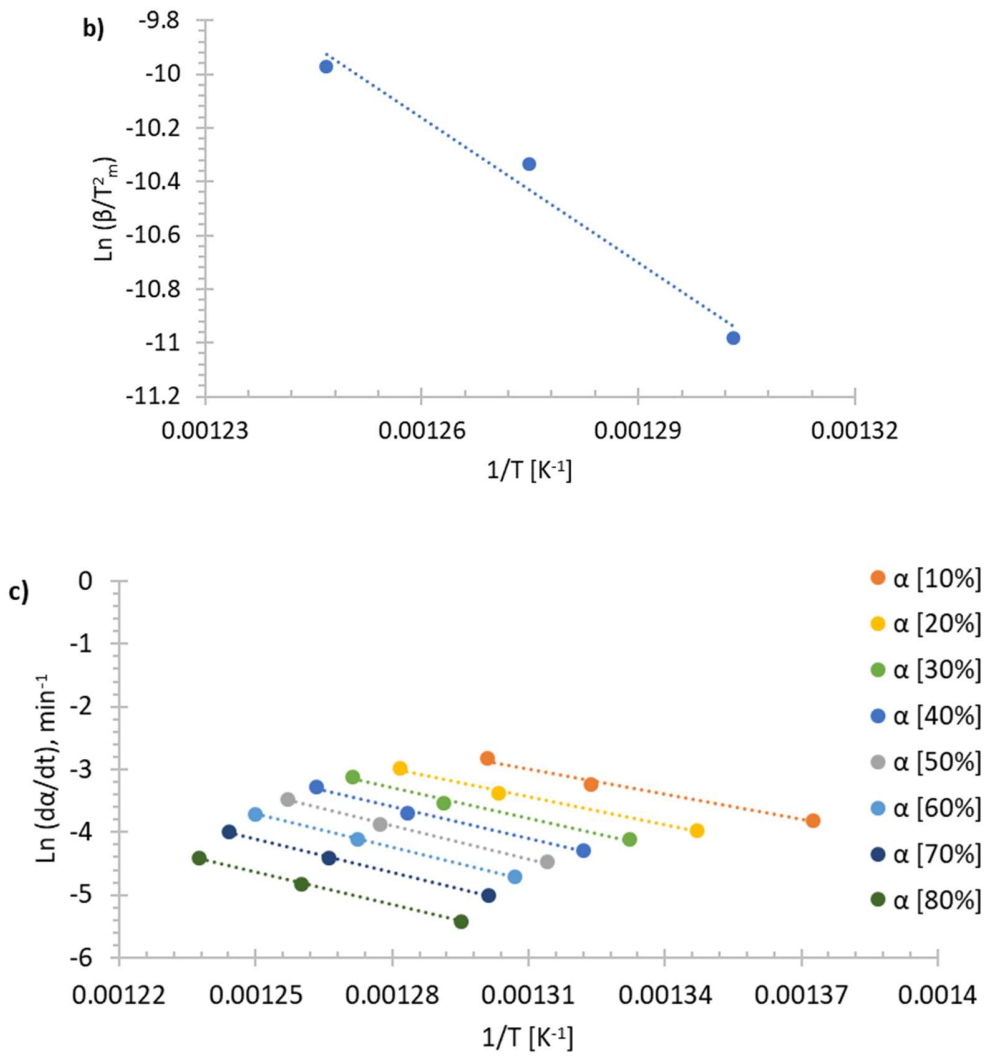

Figure 4.55. Arrhenius plot of isoconversional methods on $LDPE_{15}$ FSO 1.5%. a) ASTM E1641, b) Kissinger, c) Friedman.

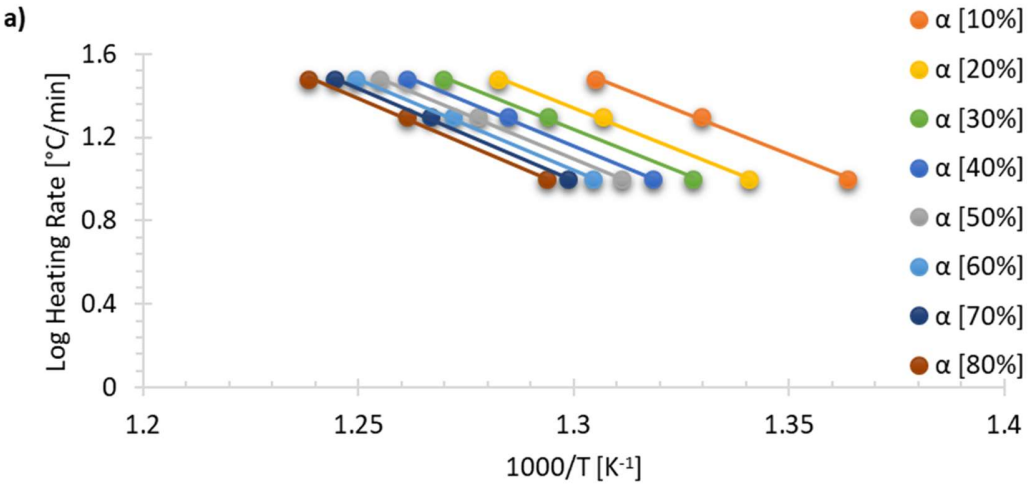
a)
Log Heating Rate [°C/min]
1.6
1.2
0.8
0.4
0
1.2
1.25
1.3
1.35
1.4
1000/T [K-1]
α [10%]
α [20%]
α [30%]
α [40%]
α [50%]
α [60%]
α [70%]
α [80%]

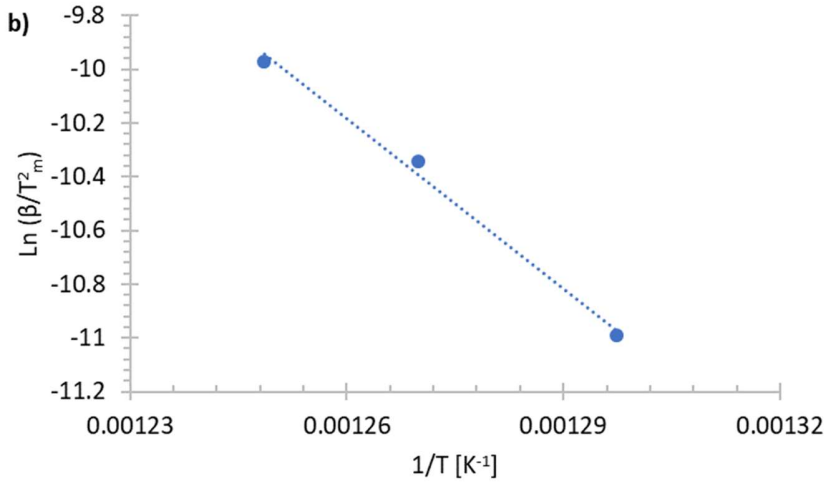
b)
Ln (β/T2m)
-9.8
-10
-10.2
-10.4
-10.6
-10.8
-11
-11.2
0.00123
0.00126
0.00129
0.00132
1/T [K-1]

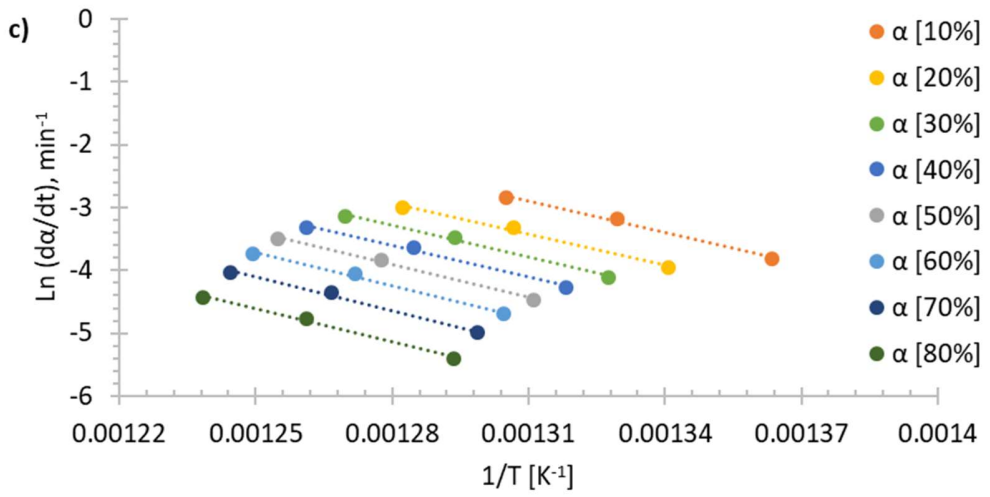

Figure 4.56. Arrhenius plot of isoconversional methods on $LDPE_{15}$ α-tocopherol 1.5%. a) ASTM E1641, b) Kissinger, c) Friedman.

Table 4.27 shows the resultant apparent energy of activation (Ea_{deg}) by the isoconversional methods approach. Following the assumption of the ASTM E1641 test method and the averaged Ea_{deg} calculated from the Friedman method.

			Apparent energy of activation Ea_{deg} [Kj/mol]					
Polymer	Antioxidant	% in formula	ASTM E1641	+/-	Kissinger	+/-	Friedman	+/-
$LDPE_{15}$[b]	--	--	136.5	3.1	136.4	---	138.4	3.0
$LDPE_{15}$	FSO 1.5%	1.5%	136.1	11.8	148.0	---	134.4	11.2
$LDPE_{15}$	FSO 3%	3%	143.4	2.6	170.9	---	148.1	2.6
$LDPE_{15}$	α-toco 1.5%	1.5%	148.9	4.2	151.0	---	141.4	4.1
$LDPE_{15}$	α-toco 3%	3%	137.1	5.8	152.9	---	147.2	5.8
$LDPE_{15}$	α-toco 6%	6%	145.0	3.1	162.7	--	143.2	3.9

Table 4.27. Apparent energies of activation (Ea_{deg}) on un-stabilized extruded $LDPE_{15}$[b] and $LDPE_{15}$ formulation. * Kissinger approach considers the temperature at the maximum rate of decomposition (d2α/d2t).

The resulting averaged apparent energies of activation (Ea_{deg}) of $LDPE_{15}$ formulated with either FSO or α-tocopherol by extrusion process were higher than the Ea_{deg} observed for un-stabilized $LDPE_{15}$. Also, it is observed an increment of Ea_{deg} as the percentage of antioxidant increased (Figure 4.57). Figure 4.58 illustrates the degradation kinetic profile at different degrees of conversion (α).

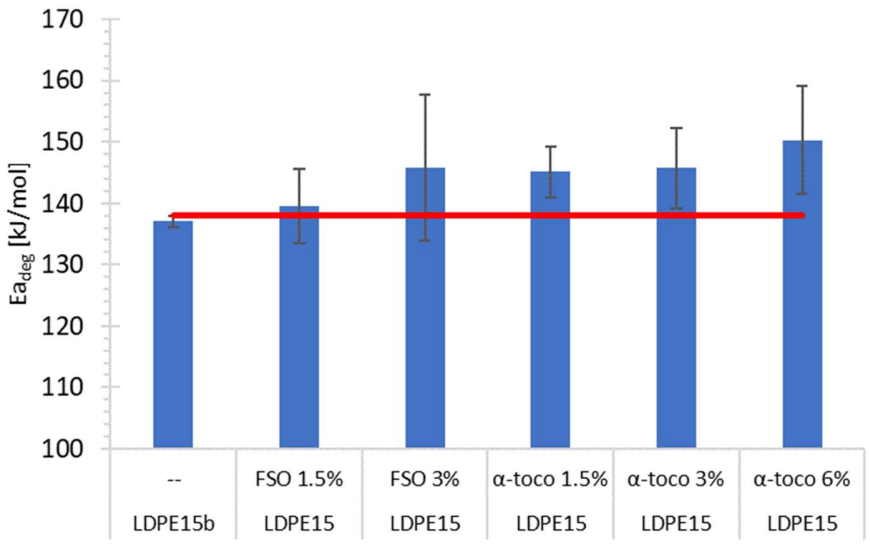

Figure 4.57. Averaged apparent energies of activation (Ea_{deg}) on un-stabilized extruded $LDPE_{15}$[b] and $LDPE_{15}$ formulated with antioxidant within a conversion degree (α) between 10% and 70%.

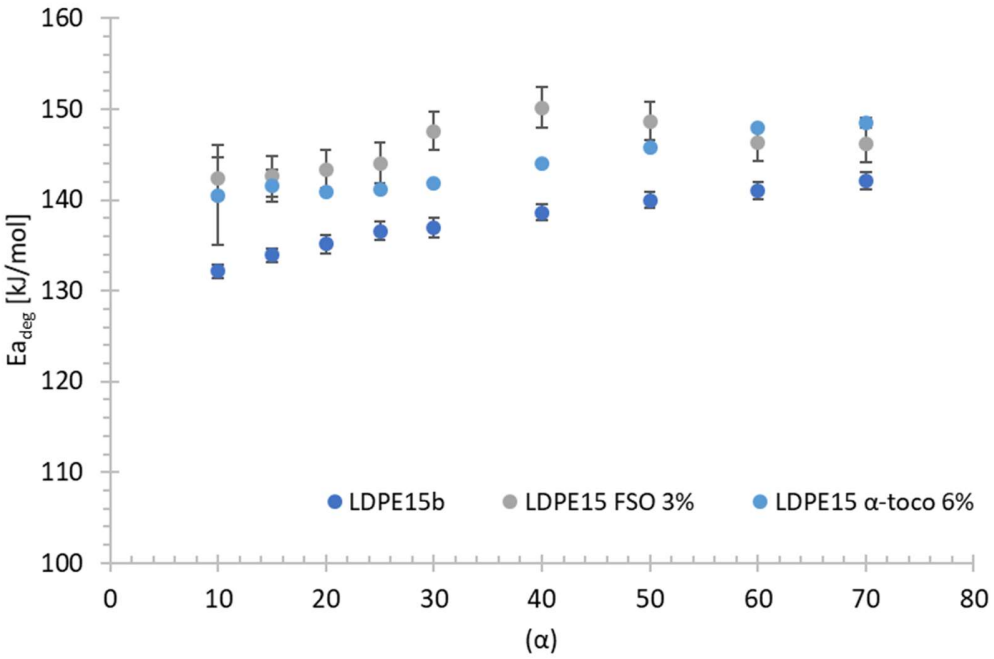

Figure 4.58. Thermal degradation kinetic profile for un-stabilized extruded $LDPE_{15}^{b}$, $LDPE_{15}$ FSO 3%, and $LDPE_{15}$ α-tocopherol 6%.

Results may confirm the stabilization effect of an antioxidant on un-stabilized extruded $LDPE_{15}^{b}$, the two proposed test-methods evaluated by thermal analysis may provide antioxidant screening for polymer formulation by means of the oxidation onset temperature (OOT) and the apparent activation energy (Ea_{deg}).

Oxidation onset temperature

Results confirmed the positive effect of an antioxidant on the thermo-oxidative stability of $LDPE_{15}$, it was observed that OOT value shifted towards higher temperatures (higher thermal stability) as the antioxidant concentration (% w/w) was increased. Thus, under the experimental conditions assessed, it may be concluded that, α-tocopherol presented the highest thermal stability on $LDPE_{15}$ during extrusion process.

Furthermore, it may be correlated the oxidation onset temperature to the general polymer degradation mechanism where polymer in the presence of an energy source may initiate a degradation path to yield alkyl and hydrogen radicals:

$$RH + Energy \rightarrow R^{\bullet} + H^{\bullet} \quad (4.9)$$

And in the case of oxidative conditions, such as the case of the OOT test-method, polymer may undergo oxidation to yield alkyl and hydroperoxyl radicals.

$$RH + O_2 \rightarrow R^{\bullet} + {}^{\bullet}OOH \quad (4.10)$$

During the propagation step, there is an increase in the number of radicals:

$$R^{\bullet} + O_2 \rightarrow ROO^{\bullet} \quad (4.11)$$

$$ROO^{\bullet} + RH \rightarrow ROOH + R^{\bullet} \quad (4.12)$$

The presence of an antioxidant with free radical scavenging activity may inhibit to some extent (upon depletion) the radical formation by quenching peroxy radicals ($ROO^{\bullet}$) yielding an hydroperoxide and an antioxidant radical form which is more stable.

$$ROO^{\bullet} + AH \rightarrow ROOH + A^{\bullet} \quad (4.13)$$

Hence, the reducing action of an antioxidant may be followed by DSC at the onset temperature from the exothermic oxidation reaction which triggers polymer degradation.

Apparent energy of activation (Ea_{deg})

The determination of Ea_{deg} by thermogravimetry showed that it may be possible to estimate the effect of antioxidant on $LDPE_{15}$ during extrusion. The experimental conditions evaluated for the methods implemented (ASTM E1641, Friedman, and Kissinger) followed the temperature dependence of the process reaction rate through the Arrhenius equation.

In all cases, as observed in Figure 4.55 and Figure 4.56, the plots showed a good linear fit ($R^2 > 0.99$) that may be caused by a single reaction rate or a dominant reaction rate within a degree of conversion (α) between 10% and 70%. Furthermore, the derivate TGA curves confirmed a single degradation step for all the experimental conditions assessed.

In the particular case of $LDPE_{15}$ FSO, it is observed that the variation observed in the Ea_{deg} relied within the standard deviation of the corresponding E_{adeg} extruded $LDPE_{15}$ (Figure 4.58). Thus, being a possible threshold at a minimum FSO concentration (%w/w) to achieve thermal stability in $LDPE_{15}$. On the other hand, α-tocopherol reported higher Ea_{deg} values and outside of the standard deviation of the corresponding Ea_{deg} extruded $LDPE_{15}$. Thus, confirming a higher thermal stability for the antioxidant system $LDPE_{15}$ α-tocopherol.

4.9.3.2 Rheological analysis

Dynamic oscillatory test

Frequency sweep dynamic tests were performed at a fixed percentage of strain (2.5%) and within the linear viscoelastic region for all the test temperatures evaluated. Master curves were generated using the TA Orchestrator software at a reference temperature of 140 °C. extruded un-stabilized $LDPE_{15}{}^{b}$ and $LDPE_{15}$ formulated with antioxidant were evaluated to assess complex viscosity (η^*) and the calculated energy of activation (Ea) for each antioxidant system; zero-shear viscosity values (η_0) were calculated from the complex viscosity (η^*) data using the cross model fitting and the TA Orchestrator software. Table 4.28 shows the $LDPE_{15}$ formulations assessed.

Polymer	Extrusion temperature [°C]	Antioxidant	% in formula
$LDPE_{15}^{b}$	150	--	--
$LDPE_{15}$	150	FSO	1.5%
$LDPE_{15}$	150	FSO	2%
$LDPE_{15}$	150	FSO	3%
$LDPE_{15}$	150	α-toco	1.5%
$LDPE_{15}$	150	α-toco	3%
$LDPE_{15}$	150	α-toco	6%

Table 4.28. Extruded $LDPE_{15}^{b}$ and $LDPE_{15}$ formulations assessed by dynamic oscillatory test.

The values of Ea obtained under the experimental conditions assessed are in Table 4.29.

Sample	Ea [kJ/mol]	r^2	Gc [Pa]	ωc [rad/sec]	1/ωc [s]
$LDPE_{15}^{b}$	69.7	1.00	1.94E+04	0.75	1.3
$LDPE_{15}$ FSO^{1}	70.3	1.00	1.92E+04	0.89	1.1
$LDPE_{15}$ FSO^{2}	67.1	1.00	1.48E+04	1.21	0.8
$LDPE_{15}$ FSO^{3}	65.9	1.00	1.29E+04	1.31	0.8
$LDPE_{15}$ α-toco^{1}	66.4	1.00	1.79E+04	1.14	0.9
$LDPE_{15}$ α-toco^{2}	67.2	1.00	1.16E+04	1.27	0.8
$LDPE_{15}$ α-toco^{3}	66.8	1.00	1.87E+04	1.70	0.6

Table 4.29. Summary of rheological properties for extruded $LDPE_{15}^{b}$ and $LDPE_{15}$ formulated with flaxseed oil and α-tocopherol: energy of activation (Ea), modulus at the crossover point (Gc), frequency at the crossover point (ωc), and the reciprocal of ωc which denotes the relaxation time.*FSO^{1,2,3} corresponds to a percentage of 1.5, 2, and 3% (% w/w) and α-toco^{1,2,3} corresponds to a percentage of 1.5, 3, and 6% (% w/w) respectively.

In general, it is observed slight lower Ea values for the $LDPE_{15}$ stabilized with antioxidant as compared to the extruded un-stabilized $LDPE_{15}^{b}$ with an observed Ea value of 69.7 kJ/mol.

The mechanism of degradation for LDPE is by a competition reaction between chain scission and crosslinking. A higher Ea value for extruded $LDPE_{15}^{b}$ as compared to $LDPE_{15}$ formulated with an antioxidant system, may indicate that the predominant degradation reaction is by crosslinking. Hence, it is needed a higher energy to move the polymer chains.

Such a degradation path may be corroborated with a higher zero shear viscosity value (η_0). From results, extruded un-stabilized $LDPE_{15}^{b}$ and $LDPE_{15}$ FSO 1.5% (% w/w), presented η_0 values higher than those observed for the rest of the antioxidant formulations. Possibly, there is a threshold in the percentage of FSO incorporated to suppress or retard degradation.

The antioxidant system $LDPE_{15}$ α-toco 6% reported the lowest η_0 value (8.61×10^4 Pa), a reduction of approximately 51% compared to the extruded un-stabilized $LDPE_{15}$. Also, the crossover point (G'/G'') is shifted toward higher frequencies with an observed difference in the relaxation time of 44% compared to the extruded un-stabilized $LDPE_{15}$. This difference may be possibly attributed to a change in the polymer structure induced by degradation of the un-stabilized $LDPE_{15}^{b}$. Table 4.30 presents the remaining rheological data.

			Slope at low freq.			low frequency		
Sample	η_0 [Pa.s]	r^2	G' [Pa]	G'' [Pa]	η* [Pa.s]	G' [Pa]	G'' [Pa]	η* [Pa.s]
$LDPE_{15}^{b}$	1.70E+05	0.99	1.13	0.76	-0.20	167.63	677.36	1.88E+05
$LDPE_{15}$ FSO[1]	1.62E+05	0.99	1.16	0.77	-0.19	140.95	634.31	1.81E+05
$LDPE_{15}$ FSO[2]	1.13E+05	0.99	1.25	0.81	-0.16	95.06	505.92	1.23E+05
$LDPE_{15}$ FSO[3]	1.06E+05	0.99	1.29	0.83	-0.15	87.14	498.60	1.14E+05
$LDPE_{15}$ α-toco[1]	1.17E+05	0.99	1.29	0.83	-0.14	97.15	530.14	1.24E+05
$LDPE_{15}$ α-toco[2]	1.07E+05	0.99	1.32	0.84	-0.14	79.09	475.36	1.15E+05
$LDPE_{15}$ α-toco[3]	8.61E+04	0.99	1.36	0.85	-0.13	56.60	387.46	9.19E+04

Table 4.30. Summary of rheological properties for extruded $LDPE_{15}^{b}$ and $LDPE_{15}$ formulated with flaxseed oil and α-tocopherol: zero shear viscosity (η_0) and storage modulus (G'), loss modulus (G'') and complex viscosity (η^*) measured at low frequency. *FSO[1,2,3] corresponds to a percentage of 1.5, 2, and 3% (% w/w) and α-toco[1,2,3] corresponds to a percentage of 1.5, 3, and 6% (% w/w) respectively.

It is observed a slight variation in the slopes of G', G'' and η_0 from the rheological data analysis at low frequency (<0.01 rad/s). In all the samples, the resultant slope at the terminal region for the storage modulus was lower than 2 (G'< 2) and lower than 1 for the loss modulus (G'' < 1) confirming a deviation from a linear polymer (Amintowlieh, Tzoganakis, Hatzikiriakos, & Penlidis, 2014).

Perhaps, a single thermo-mechanical event by extrusion process on $LDPE_{15}$ did not change significantly the polymer structure induced by crosslinking. Furthermore, the modulus at the crossover point (ωc) was utilized to theoretically estimate the polydispersity index (PI) according to the following equation (Shroff & Mavridis, 1995):

$$PI = \frac{10^5}{Gc} \tag{4.14}$$

Results listed in Table 4.31 shows the calculated PI indexes for all the $LDPE_{15}$ samples evaluated by dynamic frequency sweep test at a temperature of 180 °C.

Sample	Gc [Pa]	PI
$LDPE_{15}{}^{b}$	1.62E+04	6.18
$LDPE_{15}$ FSO^{1}	1.74E+04	5.74
$LDPE_{15}$ FSO^{2}	1.73E+04	5.79
$LDPE_{15}$ FSO^{3}	1.83E+04	5.48
$LDPE_{15}$ α-toco^{1}	1.76E+04	5.70
$LDPE_{15}$ α-toco^{2}	1.80E+04	5.55
$LDPE_{15}$ α-toco^{3}	1.81E+04	5.52

Table 4.31. Polydispersity Index (PI) results for extruded un-stabilized $LDPE_{15}{}^{b}$ and $LDPE_{15}$ formulated. *FSO^{1,2,3} corresponds to a percentage of 1.5, 2, and 3% (% w/w) and α-toco^{1,2,3} corresponds to a percentage of 1.5, 3, and 6% (% w/w) respectively.

The resulting PI indexes may provide an estimation on the molecular weight distribution (MWD). The higher the PI index the broader the MWD and vice versa. Considering the PI of extruded un-stabilized $LDPE_{15}^{b}$ a reference point, the resulting PI indexes for all the antioxidant formulations showed a reduction of the PI index in the range of 7 and 11%. Being the sample $LDPE_{15}$ α-tocopherol 6% the formulation with the lower PI index obtained.

On the assumption that, under the experimental conditions evaluated, the extruded un-stabilized $LDPE_{15}^{b}$ is degraded by extrusion process (as previously observed in chapter III), the lower PI index observed for all the antioxidant formulations may indicate that there is a lesser extent of degradation.

Figure 4.59 and Figure 4.60 depict the effect of antioxidant incorporation into un-stabilized $LDPE_{15}$ in terms of zero shear viscosity (η_0), energy of activation (Ea), and relaxation time (1/ωc).

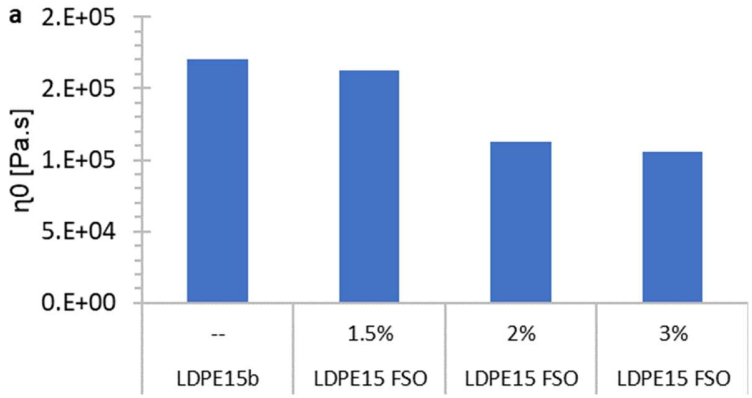

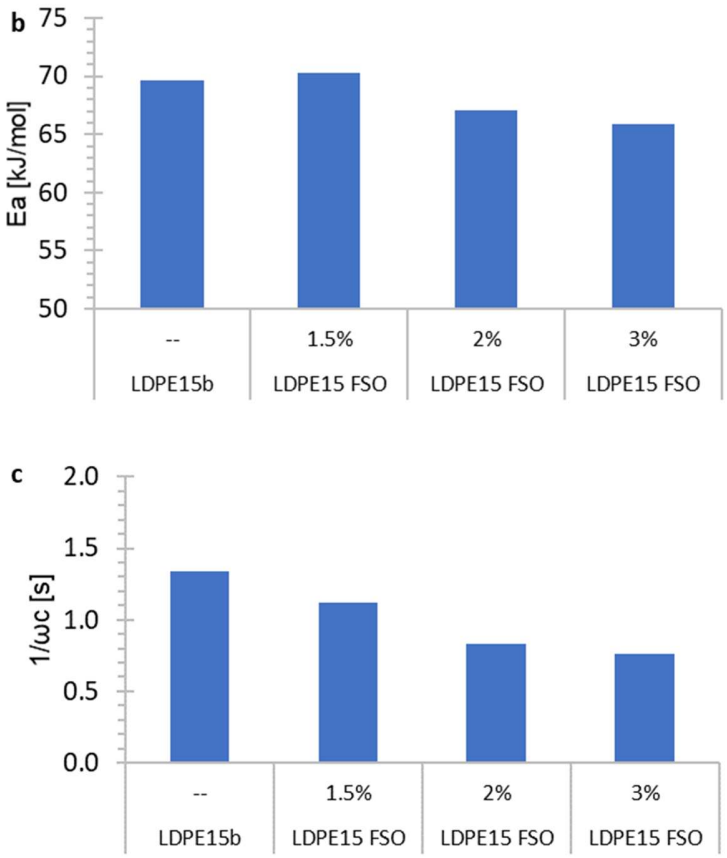

Figure 4.59. Rheological properties of $LDPE_{15}$ with and without (w/o) FSO in formulation. **a**. zero shear viscosity (η_0) **b**. energy of activation (Ea) **c**. relaxation time (1/ωc). *$LDPE_{15}^{b}$ extruded w/o antioxidant).

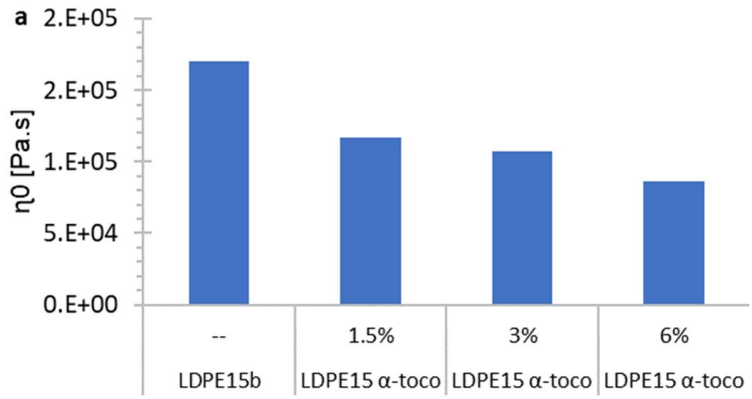

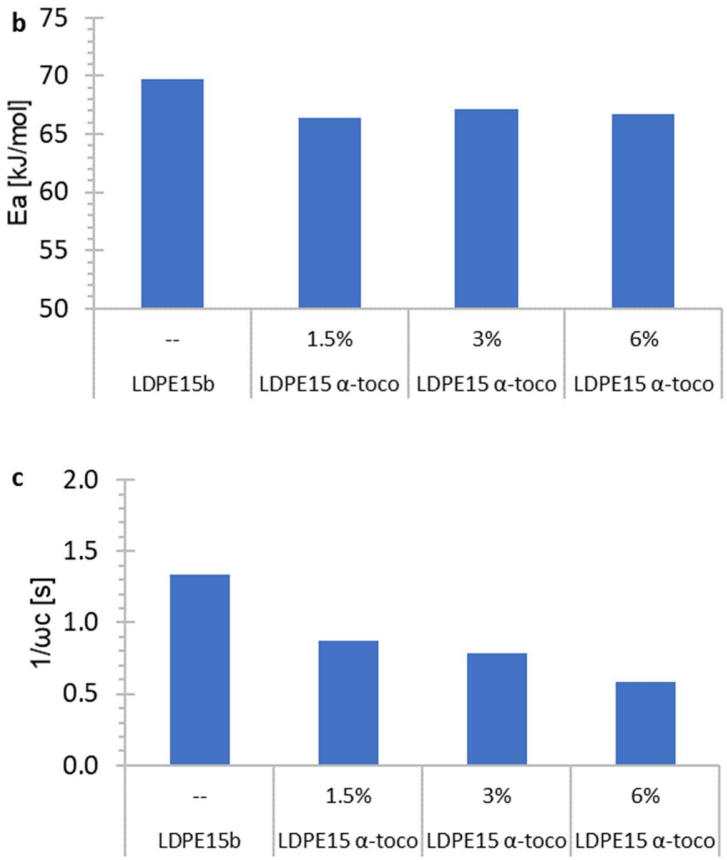

Figure 4.60. Rheological properties of $LDPE_{15}$ with and without (w/o) α-tocopherol in formulation. **a**. zero shear viscosity (η_0) **b**. energy of activation (Ea) **c**. relaxation time (1/ωc). *$LDPE_{15}^{b}$ extruded w/o antioxidant).

4.9.4 Antioxidant system formulation on $LDPE_{15}$

The incorporation of natural antioxidants such as flaxseed oil and α-tocopherol provided thermal stability to $LDPE_{15}$ during extrusion process. Previously, it has been reported the effect of a binary antioxidant mixture on the final antioxidant capacity against $DPPH^{\cdot}$ radical.

It was observed an additive effect on the total percentage of $DPPH^{\cdot}$ radical scavenged when using ascorbic acid and the α-tocopherol analogous, trolox. The combination of α-tocopherol and ascorbic acid in polymer formulation is interesting, ascorbic acid is an antioxidant that

possess different modes of action such as a metal chelator, oxygen scavenger, and reducing agent. Furthermore, it is reported in literature the synergistic effect of ascorbic acid on tocopherol by reducing the tocopheroxyl radical to the parent tocopherol antioxidant. This, may open the possibility for a potential incorporation of a blend of antioxidants into $LDPE_{15}$ such as the tertiary antioxidant system: flaxseed oil / α-tocopherol / ascorbic acid.

The objective is twofold: to provide thermal stability to $LDPE_{15}$ during extrusion and also, evaluate the additive effect of α-tocopherol and ascorbic acid on flaxseed oil on the premise that it may provide thermo-oxidative protection.

4.9.4.1 Binary Antioxidant blend

$LDPE_{15}$ α-tocopherol ascorbic acid ($LDPE_{15}$ α-toco AsA)

Align to the objective of incorporation of a tertiary antioxidant blend including flaxseed oil, as a novel and potential thermal stabilizer natural source, preliminary experimentation was carried out on the binary antioxidant system α-tocopherol – ascorbic acid to study the effect of incorporation by extrusion into $LDPE_{15}$.

4.9.4.1.1 Thermal analysis

Thermal analysis was characterized using DSC on a TA instrument Q100 following the oxidation onset temperature method (OOT).

Oxidation onset temperature (OOT)

Figure 4.61 shows the oxidation onset temperature for the binary antioxidant formulation α-tocopherol – ascorbic acid incorporated into $LDPE_{15}$ and a comparison with an extruded un-stabilized $LDPE_{15}^{b}$ and $LDPE_{15}$ formulated with α-tocopherol.

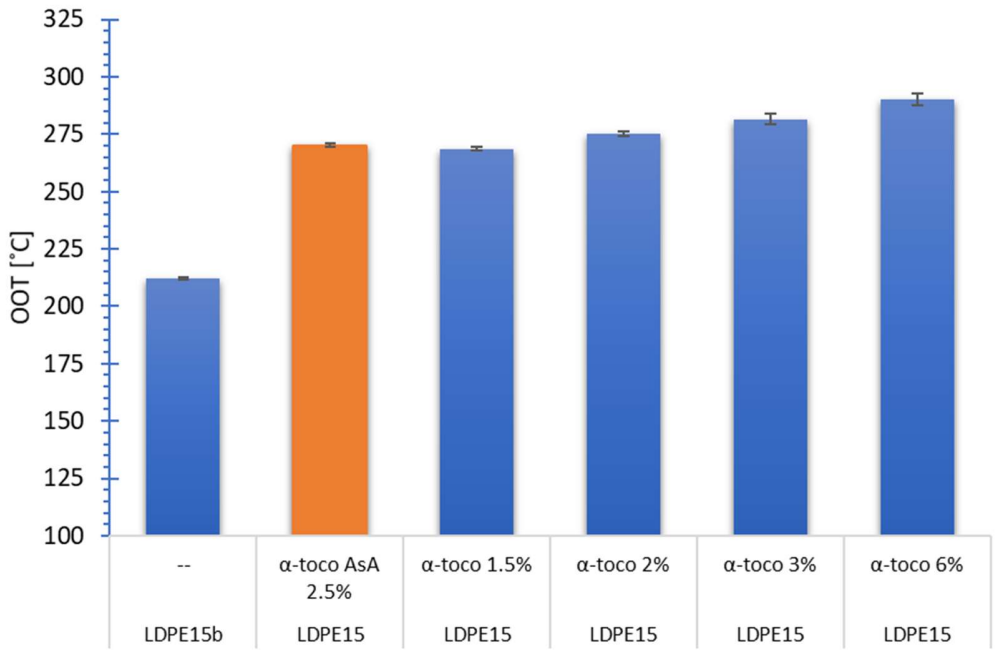

Figure 4.61. OOT results for $LDPE_{15}$ formulated with α-tocopherol at different antioxidant concentrations (% w/w), $LDPE_{15}$ formulated with the binary antioxidant blend: α-tocopherol - ascorbic acid and extruded un-stabilized $LDPE_{15}^{b}$ (control reference).

The resulting value of oxidation onset temperature (270 °C) for the formulation $LDPE_{15}$ α-tocopherol - ascorbic acid is similar to the OOT values observed for the formulation $LDPE_{15}$ α-tocopherol at 1.5% and 2% in weight (269 °C and 275 °C respectively). Results are expressed as the average of at least two replicates. From Figure 4.61 it may be inferred that there is an additive effect of the binary antioxidant blend α-tocopherol and ascorbic acid on the thermal stability of $LDPE_{15}$ during extrusion.

4.9.4.1.2 Rheological analysis

Frequency sweep dynamic test were performed at 2.5% of strain. Master curves were generated using the TA Orchestrator software at a reference temperature of 140 °C. extruded un-stabilized $LDPE_{15}{}^{b}$ and $LDPE_{15}$ formulated with α-tocopherol and α-tocopherol – ascorbic acid were evaluated to assess complex viscosity (η^*) and the calculated energy of activation (Ea) for each antioxidant system; zero-shear viscosity values (η_0) were calculated from the complex viscosity (η^*) data using the cross model fitting and the TA Orchestrator software. Table 4.32 shows the $LDPE_{15}$ formulations assessed.

					reference temp. 180°C			
Sample	η_0 [Pa.s]	r^2	Ea [Kj/mol	r^2	Gc [Pa]	ωc [rad/sec]	1/ωc [s]	PI
$LDPE_{15}{}^{b}$	1.70E+05	0.99	69.7	1.00	1.62E+04	4.33	0.2	6.2
$LDPE_{15}$ α-toco[2]	1.07E+05	0.99	65.1	1.00	1.80E+04	7.22	0.1	5.6
$LDPE_{15}$ α-toco AsA	9.01E+04	1.00	64.7	1.00	1.89E+04	7.24	0.1	5.3

Table 4.32. Summary of rheological properties for extruded $LDPE_{15}{}^{b}$ and $LDPE_{15}$ formulated with antioxidant(s): $LDPE_{15}$ α-toco[2] (3% w/w) and $LDPE_{15}$ α-toco AsA (final percentage in formula 2.5% at the composition in % of weight of 95/5/5 respectively).

As previously observed, the incorporation of α-tocopherol by extrusion process in un-stabilized $LDPE_{15}$ resulted in a reduction of approximately 37% in the zero shear viscosity (η_0) value compared to the extruded un-stabilized $LDPE_{15}$, whereas the binary antioxidant blend α-tocopherol – ascorbic acid had a reduction in η_0 of 47%. This lower η_0 value may be attributed to a higher thermo-oxidative stabilization provided by the binary antioxidant blend during extrusion.

Furthermore, the energy of activation values of $LDPE_{15}$ incorporated with antioxidants were slightly lower than the Ea of the extruded un-stabilized $LDPE_{15}$. Though the Ea values are

close each other, it may be attributed the higher Ea value observed for the extruded un-stabilized $LDPE_{15}$ to an extent of degradation dominated by crosslinking reactions as previously discussed. Figure 4.62 presents the zero shear viscosity (η_0) and energy of activation (Ea) values.

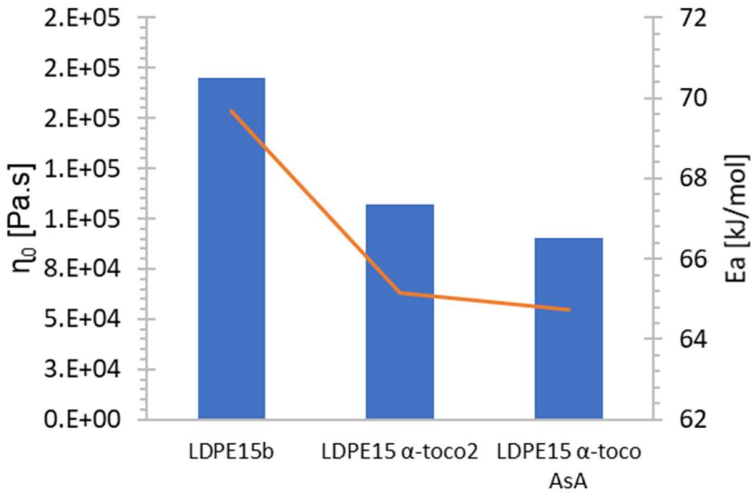

Figure 4.62. Rheological properties of extruded $LDPE_{15}^{b}$ and $LDPE_{15}$ formulated with antioxidant: $LDPE_{15}$ α-toco[2] (3% w/w) and $LDPE_{15}$ α-toco AsA (final percentage in formula 2.5% at the composition in % of weight of 95/5/5 respectively).

From Figure 4.62 it could be observed that the η_0 and Ea values corroborate the assumption proposed on the thermal stability of $LDPE_{15}$ formulated with antioxidant(s) and the effect of the thermo-oxidative degradation on un-stabilized $LDPE_{15}$ by extrusion process. Indeed, it may be concluding that the thermal stability provided by the binary antioxidant blend α-tocopherol – ascorbic acid reported the best results. Also, the polydispersity index (PI) evaluated at a reference temperature of 180 °C showed that, the binary antioxidant blend α-tocopherol – ascorbic acid had the lowest PI index from the antioxidant formulations assessed.

4.9.4.2 Tertiary Antioxidant blend

Plastic processors generally re-processed the scrap material in a controlled and traceable manner by a simple process to re-use the plastic material. The additional thermo-mechanical events during recycling may pose degradation in the polymer backbone hence, the need to use thermal stabilizers and to assess the polymer thermal resistance.

$LDPE_{15}$ α-tocopherol ascorbic acid ($LDPE_{15}$ FSO α-toco AsA)

The effect of incorporation of the tertiary antioxidant blend flaxseed oil – α-tocopherol – ascorbic acid into low-density polyethylene ($LDPE_{15}$) by extrusion process was assessed by thermal and rheological analyses. 9 sequential extrusion cycles were validated in order to study the thermal stability of $LDPE_{15}$ during polymer processing and recycling.

4.9.4.2.1 Thermal analysis

Thermal analysis was characterized using DSC on a TA instrument Q100 following the oxidation onset temperature method (OOT).

Oxidation onset temperature (OOT)

Table 4.33 shows the OOT results for bare and extruded un-stabilized $LDPE_{15}^{a, b}$ and $LDPE_{15}$ formulated with flaxseed oil - α-tocopherol - ascorbic acid.

						1 month	
Polymer	Cycle	Antioxidant	% in formula	OOT [°C]	+/-	OOT [°C]	+/-
$LDPE_{15}^{a}$		--	--	213.3	0.27	---	---
$LDPE_{15}^{b}$		--	--	212.3	0.52	216.1	---
$LDPE_{15}$	1	FSO α-toco AsA	2.5%	239.4	1.48	226.9	1.5
$LDPE_{15}$	3	FSO α-toco AsA	2.5%	236.6	0.59	221.5	1.5
$LDPE_{15}$	6	FSO α-toco AsA	2.5%	231.3	0.74	222.5	0.5
$LDPE_{15}$	9	FSO α-toco AsA	2.5%	229.8	1.50	223.5	0.7

Table 4.33. OOT results for bare and extruded $LDPE_{15}^{a, b}$ un-stabilized as a control reference and $LDPE_{15}$ formulated with FSO α-tocopherol ascorbic acid (final percentage in formula 2.5% at the composition in % of weight of 95/5/5 respectively) during 9 sequential extrusion cycles.

Results from Table 4.33 confirmed that the tertiary antioxidant blend FSO α-tocopherol ascorbic acid provided thermal stability during the 9 sequential extrusion cycles. The observed oxidation onset temperature (OOT) at the first extrusion event (cycle 1) presented a difference of +27 °C between the tertiary antioxidant blend and the extruded un-stabilized $LDPE_{15}^{b}$. Finally, at the last extrusion event (cycle 9), the tertiary antioxidant blend still presented higher thermal stability than the extruded un-stabilized $LDPE_{15}^{b}$ (+17 °C). It is important to remark that all the OOT values reported a low standard deviation.

$LDPE_{15}$ FSO α-toco AsA samples were kept in a dry and dark place for a month and followed-up by the OOT method. It was observed that, within the 9 sequential extrusion cycles, the OOT values remained higher than the extruded un-stabilized $LDPE_{15}^{b}$ thus, it may be possible that remaining antioxidants provided thermo-oxidative stability during the DSC thermal run. On average, there was a decay in the OOT value during the recycling process of 4.5% within a month. Figure 4.63 illustrates the OOT results.

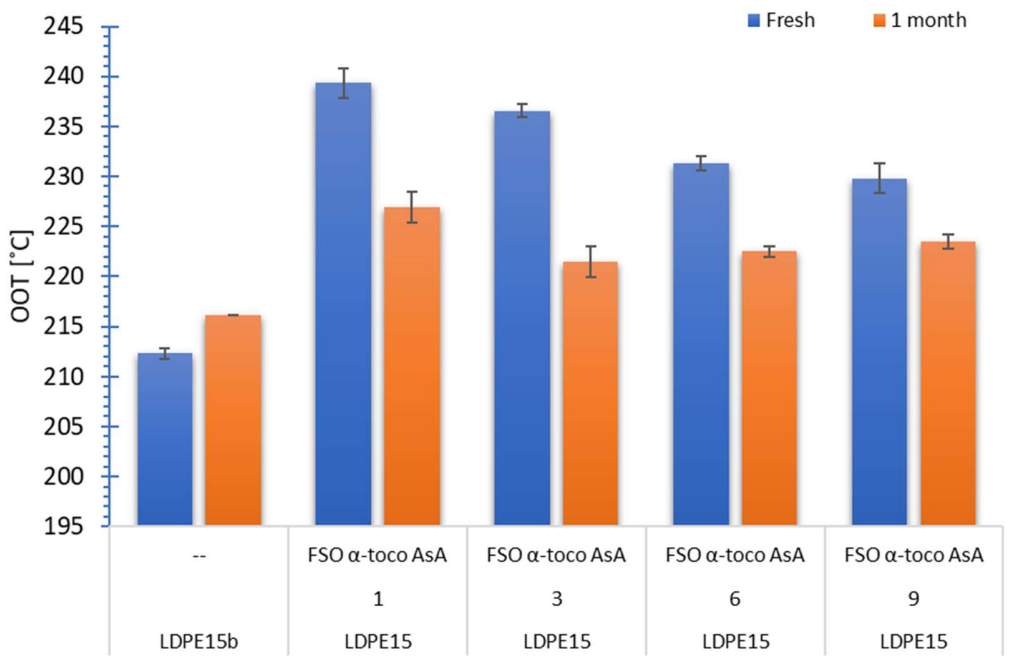

Figure 4.63. OOT results for extruded $LDPE_{15}^{b}$ un-stabilized as a control reference and $LDPE_{15}$ formulated with FSO α-tocopherol - ascorbic acid (final percentage in formula 2.5% at the composition in % of weight of 95/5/5) during 9 sequential extrusion cycles.

In Figure 4.64 it is presented the OOT values for a 9 sequential extrusion cycles on three low-density polyethylene grades: un-stabilized $LDPE_{15}$ (w/o antioxidant), stabilized $LDPE_{33}$ (with antioxidant), and the tertiary antioxidant blend $LDPE_{15}$ FSO - α-tocopherol - ascorbic acid.

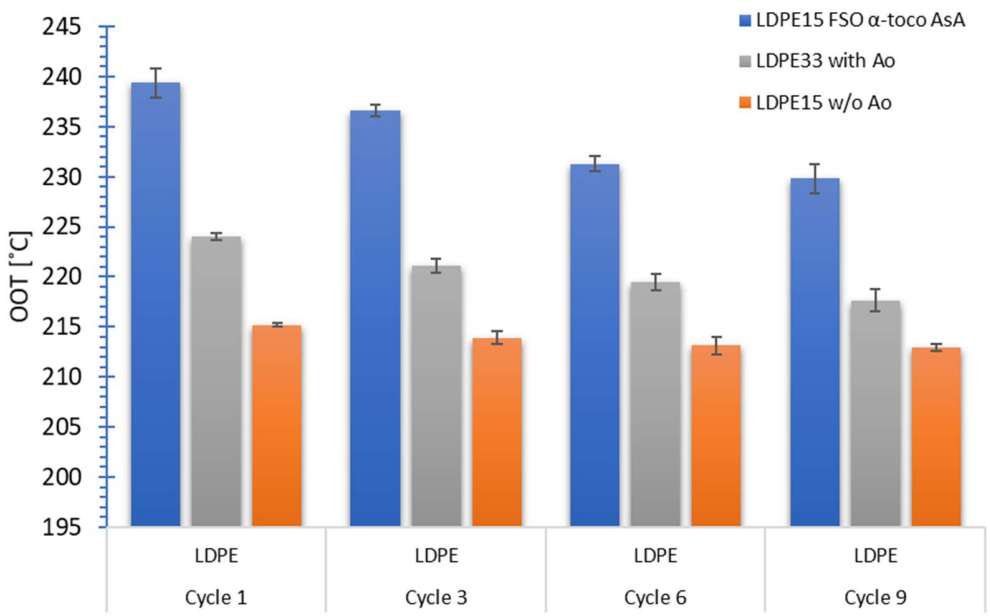

Figure 4.64. OOT results during 9 sequential extrusion cycles for extruded $LDPE_{15}^{b}$, stabilized $LDPE_{33}$, and $LDPE_{15}$ formulated with FSO α-tocopherol - ascorbic acid (final percentage in formula 2.5% at the composition in % of weight of 95/5/5) during 9 sequential extrusion cycles.

As observed in Figure 4.64, it may be possible to conclude that the proposed tertiary antioxidant blend FSO α-tocopherol - ascorbic acid provided the highest thermal resistance on un-stabilized LDPE by means of the oxidation onset temperature (OOT).

4.9.4.2.2 Rheological analysis

Dynamic viscosity (η^*) was assessed as a function of temperature. Dynamic temperature steps test was evaluated at a frequency of 1 rad/s and in a descending temperature interval from 190 °C to 140°C using a ramp temperature step of -2 °C. The effect of temperature on dynamic viscosity (η^*) is shown in Table 4.34.

	140 °C			190 °C		
Sample	G' [Pa]	G'' [Pa]	n* [Pa.s]	G' [Pa]	G'' [Pa]	n* [Pa.s]
$LDPE_{15}$ FSO α-toco AsA^{1st}	11437.7	12676.5	17073.8	3662.5	6070.3	7089.6
$LDPE_{15}$ FSO α-toco AsA^{9th}	11630.6	12446.3	17034.8	4501.6	6730.8	8097.5
$LDPE_{15}^{1st}$	12877.0	13769.1	18852.2	5051.9	7514.6	9054.9
$LDPE_{15}^{9th}$	16974.8	15182.7	22774.1	6754.0	8122.2	10563.4

Table 4.34. Dynamic temperature steps test results for $LDPE_{15}$ formulated with FSO α-tocopherol and ascorbic acid (final percentage in formula 2.5% at the composition in % weight of 95/5/5) and $LDPE_{15}$ un-stabilized.

At the initial test temperature of 190 °C both un-stabilized $LDPE_{15}$ samples, corresponding to extrusion cycle 1 and cycle 9, showed on average an increment of approximately 29% on the dynamic viscosity (η*) compared to the $LDPE_{15}$ formulated with α-tocopherol – ascorbic acid.

The end of the ramp test temperature (140 °C) showed a significant variation in η* between un-stabilized $LDPE_{15}$ sample at cycle 1 and cycle 9 with an observed increment in η* of approximately 46%.

This increment in η* of un-stabilized $LDPE_{15}$ as a function of the number of sequential extrusion cycles may be attributed to the extent of degradation on un-stabilized $LDPE_{15}$ during the multi-extrusion cycle analysis. As it was discussed in chapter 3, based on results it was concluded that the corresponding degradation mechanism of $LDPE_{15}$ was predominantly by crosslinking. Figure 4.65 illustrates the effect of temperature on dynamic viscosity (η*).

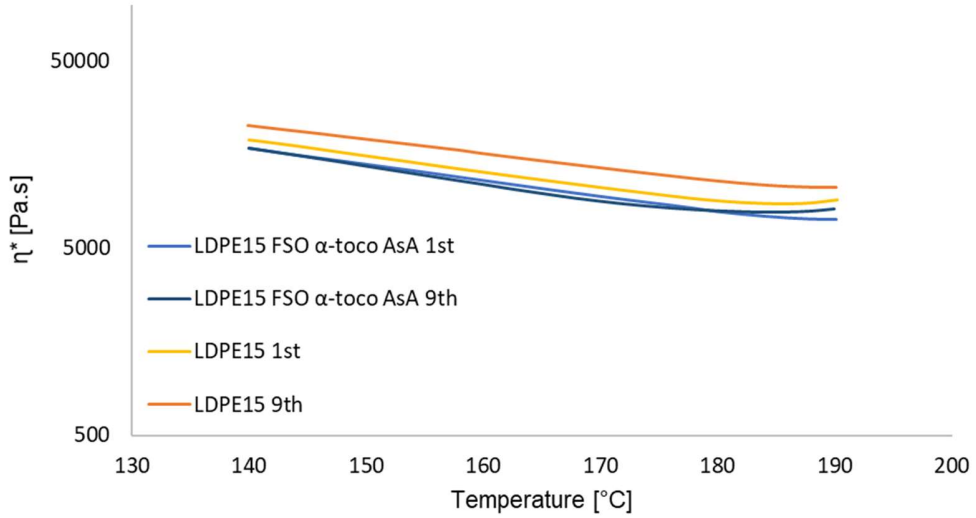

Figure 4.65. Dynamic temperature steps evaluated at a frequency of 1 rad/s and a temperature interval from 190 °C to 140°C.

Based on rheological characterization, it may be possible to conclude that, the tertiary antioxidant blend FSO α-toco AsA provided thermal resistance to $LDPE_{15}$.

4.9.5 Extrusion and formulation of isotactic polypropylene (i-PP)

i-PP Maltodextrin – ascorbic acid in polypropylene (i-PP MDX – AsA)

First incorporation of encapsulated ascorbic acid into polypropylene was performed in a binary antioxidant blend with α-tocopherol. Former formulation α-tocopherol and ascorbic acid was previously evaluated in low-density polyethylene ($LDPE_{15}$) at low extrusion temperatures (150 °C) with good results but, with the constrain that, above an extrusion temperature of 180 °C (condition needed to process i-PP) ascorbic acid starts to degrade.

Former results on thermal analysis of the system maltodextrin – ascorbic acid (MDX – AsA) showed an improvement in thermal stability and opened the possibility to incorporate

ascorbic acid as a potential antioxidant source into polypropylene. Table 4.35 shows the experimental conditions evaluated.

Polymer	Additive 1	% weight	Additive 2	% weight	Extrusion Temp. [°C]
i-PP	---	---	---	---	180
i-PP	α-tocopherol	1.50%	MD - As. Ac.	1%	180
i-PP	α-tocopherol	1.50%	MD - As. Ac.	3%	180
i-PP	α-tocopherol	1.50%	MD - As. Ac.	6%	180
i-PP	α-tocopherol	1.50%	---	---	180
i-PP	---	---	MD - As. Ac.	0.1 g/mL	180

Table 4.35. Experimental runs.

Results for the binary antioxidant blend showed a good antioxidant efficiency by means of an improvement of the oxidation onset temperature as compared to the bare un-stabilized polypropylene. Thus, a higher thermal stability for polypropylene during extrusion was achieved.

The formula i-PP MDX – AsA showed an averaged oxidation onset temperature (OOT) of around 250 °C. Remarks were drawn based on all results highlighting the need of a replicate particularly, for the latter test. A purging time > 15 minutes before the i-PP-MD As. Ac. test was performed to remove all α-tocopherol from the extruder.

A replication of the last test was performed to corroborate the oxidation onset temperature (OOT) and to eliminate the noise of prior antioxidant(s) formulas in the extruder. Two MDX - AsA concentrations were tested: 0.1 g/mL and 0.2 g/mL. Processing conditions were kept constant and bare i-PP ran first as a control reference. Results are summarized in Table 4.36 and represent in all cases, the average of three replicates.

Material	Antioxidant	Dosing [g/mL]	OOT [°C]	
i-PP	MD - As. Ac.[a]	0.1	253.5	+/- 1.82
	MD - As. Ac.[b]	0.1	200.92	+/- 4.32
	MD - As. Ac.	0.2	227.29	+/- 3.56

Table 4.36. OOT results for the system MDX - AsA. [a] First extrusion trials. [b] Replication trial performed on MDX - AsA.

MDX - AsA[b] as the replicate and with the extruder clean (without prior antioxidant(s) formulas) showed that there is no improvement in thermal stability as compared to bare i-PP and additionally, the replicate demonstrates that there is a confounding variable (extruder condition) where the influence of α-tocopherol remained in the barrel provided thermal stability on the extrudate. An additional test was performed: MDX - AsA in a two-fold concentration with an observed OOT of 227 °C.

Experimental results confirmed that, encapsulated ascorbic acid in maltodextrin can be processed at 180°C and provided a higher thermal stability to polypropylene during extrusion with a resulting oxidation onset temperature of 227.29 °C, an improvement of approximately +27 °C as compare to bare i-PP.

4.10 General Overview

In response toward consumer needs (healthy living) and a circular economy model where prosperity is grounded on reutilization, two antioxidant packages were proposed and incorporated into bare un-stabilized isotactic polypropylene (i-PP) and bare un-stabilized low-density polyethylene ($LDPE_{15}$).

The incorporation of flaxseed oil in a tertiary antioxidant blend provided thermal stability to $LDPE_{15}$. It was observed that after 9 sequential extrusion cycles, the thermal stability by means of the OOT value was higher than the corresponding un-stabilized extrudate $LDPE_{15}$.

In the case of isotactic polypropylene (i-PP), the encapsulation of ascorbic acid in maltodextrin provided thermal protection at the processing extrusion temperatures for i-PP. The characterized sample showed a higher thermal stability than its counterpart un-stabilized extrudate i-PP.

Bibliography

Al-Malaika, S., Ashley, H., & Issenhuth, S. (1994). The antioxidant role of α-tocopherol in polymers. I. The nature of transformation products of α-tocopherol formed during melt processing of LDPE. *Journal of Polymer Science Part A: Polymer Chemistry*, *32*(16), 3099–3113. https://doi.org/10.1002/pola.1994.080321610

Amintowlieh, Y., Tzoganakis, C., Hatzikiriakos, S. G., & Penlidis, A. (2014). Effects of processing variables on polypropylene degradation and long chain branching with UV irradiation. *Polymer Degradation and Stability*, *104*(1), 1–10. https://doi.org/10.1016/j.polymdegradstab.2014.03.016

Antolín, I. P., & Meneses, M. M. (2000). Aplicación de la espectrofotometría UV-visible al estudio de la estabilidad térmica de aceites vegetales comestibles. *Grasas y Aceites*, *51*, 424–428.

Bennette, L., Logan, A., Shiferaw-Terefe, N., Singh, T., & Robin, W. (2014). Measuring the Oxidation Potential in Foods. In G. Bartosz (Ed.), *Food Oxidants and Antioxidants Chemical, Biological, and Functional Properties* (pp. 47–79). CRC Press.

Berdhal, D. R., Nahas, R. I., & Barren, J. P. (2010). Synthetic and natural antioxidant additives in food stabilization: current applications and future research. In E. A. Decker, R. J. Elias, & J. D. McClements (Eds.), *Oxidation in foods and beverages and antioxidant applications. Volume 1: Understanding mechanisms of oxidation and antioxidant activity* (pp. 272–313). Woodhead Publishing.

Brewer, M. S. (2011). Natural Antioxidants: Sources, Compounds, Mechanisms of Action, and Potential Applications. *Comprehensive Reviews in Food Science and Food Safety*, *10*(4), 221–247. https://doi.org/10.1111/j.1541-4337.2011.00156.x

Burton, G. W., & Ingold, K. U. (1986). Vitamin E: Application. *Acc .Chem. Res.*, *19*(7), 194–201.

Colon, M., & Nerín, C. (2016). Synergistic, antagonistic and additive interactions of green tea polyphenols. *European Food Research and Technology*, *242*(2), 211–220. https://doi.org/10.1007/s00217-015-2532-9

Daun, J. K., Barthet, V. J., Chornick, T. L., & Duguid, S. (2003). Structure, Composition, and

Variety Development of Flaxseed. In L. U. Thompson & S. C. Cunnane (Eds.), *Flaxseed in Human Nutrition* (2nd ed., pp. 1–40). AOCS Press.

de Britto, D., & Campana-Filho, S. P. (2007). Kinetics of the thermal degradation of chitosan. *Thermochimica Acta*, *465*, 73–82. https://doi.org/10.1016/j.tca.2007.09.008

Decker, E. A., Chen, B., Panya, A., & Elias, R. J. (2010). Understanding antioxidant mechanisms in preventing oxidation in foods. In E. A. Decker, R. J. Elias, & J. D. McClements (Eds.), *Oxidation in foods and beverages and antioxidant applications. Volume 1: Understanding mechanisms of oxidation and antioxidant activity* (First, pp. 225–243). Woodhead Publishing.

Espín, J. C., Soler-Rivas, C., & Wichers, H. J. (2000). Characterization of the total free radical scavenger capacity of vegetable oils and oil fractions using 2,2-diphenyl-1-picrylhydrazyl radical. *Journal of Agricultural and Food Chemistry*, *48*(3), 648–656. https://doi.org/10.1021/jf9908188

Fang, Z., & Bhandari, B. (2010). Encapsulation of polyphenols - A review. *Trends in Food Science and Technology*, *21*(10), 510–523. https://doi.org/10.1016/j.tifs.2010.08.003

Gliszczynska-Swigło, A., & Oszmianski, J. (2014). Antioxidant and Prooxidant Activity of Food Components. In G. Bartosz (Ed.), *Food Oxidants and Antioxidants Chemical, Biological, and Functional Properties* (pp. 375–431). CRC Press.

Hong, P.-Z., Li, S.-D., Ou, C.-Y., Li, C.-P., Yang, L., & Zhang, C.-H. (2007). Thermogravimetric Analysis of Chitosan. *Journal of Applied Polymer Science*, *105*, 547–551. https://doi.org/10.1002/app

Hussain, S. A., Abdelkader, H., Abdullah, N., & Kmaruddin, S. (2018). Review on micro-encapsulation with Chitosan for pharmaceuticals applications. *MOJ Current Research & Reviews*, *1*(2), 77–84. https://doi.org/10.15406/mojcrr.2018.01.00013

Jomova, K., Lawson, M., & Valko, M. (2014). Mechanisms of Antioxidant Activity. In G. Bartosz (Ed.), *Food Oxidants and Antioxidants Chemical, Biological, and Functional Properties* (pp. 325–342). CRC Press.

Kiokias, S., Varzakas, T., & Oreopoulou, V. (2008). In vitro activity of vitamins, flavonoids, and natural phenolic antioxidants against the oxidative deterioration of oil-based systems. *Critical Reviews in Food Science and Nutrition*, *48*(1), 78–93.

https://doi.org/10.1080/10408390601079975

Lazzari, M., & Chiantore, O. (1999). Drying and oxidative degradation of linseed oil. *Polymer Degradation and Stability*, *65*(2), 303–313. https://doi.org/10.1016/S0141-3910(99)00020-8

Mishra, M. (2016). Overview of Encapsulation and Controlled Release. In M. Mishra (Ed.), *Handbook of Encapsulation and Controlled Release* (pp. 4–15). Boca Raton Florida: CRC Press.

Nedovic, V., Kalusevic, A., Manojlovic, V., Levic, S., & Bugarski, B. (2011). An overview of encapsulation technologies for food applications. *Procedia Food Science*, *1*, 1806–1815. https://doi.org/10.1016/j.profoo.2011.09.265

Nieva-Echevarría, B., Manzanos, M. J., Goicoechea, E., & Guillén, M. D. (2015). 2,6-Di-Tert-Butyl-Hydroxytoluene and Its Metabolites in Foods. *Comprehensive Reviews in Food Science and Food Safety*, *14*(1), 67–80. https://doi.org/10.1111/1541-4337.12121

Peniche-Covas, C., Argüelles-Monal, W., & San Román, J. (1993). A kinetic study of the thermal degradation of chitosan and a mercaptan derivative of chitosan. *Polymer Degradation and Stability*, *39*(1), 21–28. https://doi.org/10.1016/0141-3910(93)90120-8

Saavedra-Leos, Z., Leyva-Porras, C., Araujo-Díaz, S. B., Toxqui-Terán, A., & Borrás-Enríquez, A. J. (2015). Technological application of maltodextrins according to the degree of polymerization. *Molecules*, *20*(12), 21067–21081. https://doi.org/10.3390/molecules201219746

Shahidi, F., & Ambigaipalan, P. (2015). Phenolics and polyphenolics in foods, beverages and spices: Antioxidant activity and health effects - A review. *Journal of Functional Foods*, *18*, 820–897. https://doi.org/10.1016/j.jff.2015.06.018

Shroff, R., & Mavridis, H. (1995). New Measures of Polydispersity from Rheological Data. *Journal of Applied Polymer Science*, *57*, 1605–1626.

Wandrey, C., Bartkowiak, A., & Harding, S. E. (2010). Materials for Encapsulaton. In N. J. Zuidam & V. Nedovic (Eds.), *Encapsulation Technologies for Active Food Ingredients and Food Processing* (pp. 31–100). Springer.

CHAPTER V
CONCLUSIONS

Plastic consumption is a continuing reality in the world and society plays a key role as a counterweight. Social awareness towards sustainable practices set the path to the scope of this project dissertation: to deliver a formulation, with natural additives, that provides thermal stability for the two most consumed olefin resins, isotactic polypropylene and low-density polyethylene. We have designed the problem and identified three processes, within the food system, that needs to be addressed.

Natural antioxidants

The antioxidant capacity of single molecules and foodstuff against free radicals was assessed by spectrophotometry. Antioxidants were evaluated by synthetic radicals such as $ABTS^{\cdot+}$ and $DPPH^{\cdot}$ and a bio-sourced radical such as superoxide anion. Based on test-methods standardization, the antioxidants were screened by its antioxidant capacity and among them, ascorbic acid, α-tocopherol, and flaxseed oil were selected. Also, thermal stability analysis by TGA was carried out on antioxidants to assess the degradation profile and evaluate the antioxidant performance during polymer processing. Align to this, we could estimate that, ascorbic acid had poor thermal stability thus, restricting its application only for low-density polyethylene. We concluded that ascorbic acid, α-tocopherol, and flaxseed oil have antioxidant capacity and we provided a solution for ascorbic acid formulated in isotactic polypropylene.

Polymers

Thermal and rheological analyses were performed on both polymer resins to determine the state of the art prior to formulation and processing. Thermal degradation analysis by TGA was performed on isotactic polypropylene and low-density polyethylene to evaluate their apparent energy of activation (Ea_{deg}); the energy of activation in the melt state (Ea) was validated by rheological dynamic test and the oxidation onset temperature (OOT) method, carried out by DSC, was standardized and optimized to assess thermal degradation of polymers. We could conclude that, the methods employed successfully assessed the thermo-mechanicals events during polymer processing on the thermo-oxidative stability of polymer resins.

Formulation and Recyclability

We validated the individual effect of the selected antioxidants during polymer processing to conclude that, the tertiary antioxidant blend of flaxseed oil, α-tocopherol, and ascorbic acid provided thermal stability in low-density-polyethylene for 9 multiple extrusion cycles. The results evaluated by the oxidation onset temperature (OOT) showed a better performance than the commercial low-density polyethylene counterpart.

It has been proven that ascorbic acid has high antioxidant activity. Thus, we presented a solution to incorporate ascorbic acid into isotactic polypropylene for high-processing temperatures. The encapsulation of ascorbic acid using maltodextrin as a food grade matrix carrier was performed. We concluded based on the antioxidant capacity and thermal analysis that, the incorporation of encapsulated ascorbic acid with α-tocopherol provided thermal stability to isotactic polypropylene during extrusion.

Align to the scope of this dissertation, we provided a natural antioxidant package formulation for polymer processing on low-density polyethylene and isotactic polypropylene. The studied formulas fitted into a greener food system, Foodyplast.

$LDPE_{15}$ Technical data sheet

PEBD ALCUDIA® PE015

DESCRIPCIÓN

El grado ALCUDIA® PE015 se fabrica en reactor autoclave. Está indicado para la producción de películas por extrusión tubular y plana. Combina una notable facilidad de procesado con buenas propiedades mecánicas y ópticas. No contiene aditivos.

APLICACIONES

- Película para envasado y embalaje.
- Película retráctil de gran resistencia mecánica.
- Sacos de mediana capacidad.

Se recomienda trabajar con temperaturas de fundido entre 170-190ºC. Las condiciones óptimas de transformación se deben ajustar para cada línea de producción.

PROPIEDADES	VALOR	UNIDAD	MÉTODO
General			
Indice de fluidez (190ºC, 2.16kg)	1	g/10 min	ISO 1133
Densidad a 23°C	921	kg/m^3	ISO 1183
Película [1]			
Resistencia al impacto (F_{50})	150	g	ISO 7765-1
Resistencia al rasgado (Elmendorf) (DM/DT)	175 / 150	cN	ISO 6383-2
Resistencia a la tracción en el punto de rotura (DM/DT)	24 / 22	MPa	ISO 527-3
Resistencia a la tracción en el punto de fluencia (DM/DT)	11 / 10	MPa	ISO 527-3
Alargamiento en el punto de rotura (DM/DT)	300 / 550	%	ISO 527-3
Coeficiente de fricción (Dinámico)	0.9	-	ISO 8295
Brillo (45º)	60	-	ASTM D-2457
Turbidez	11	%	ASTM D-1003
Otras			
Temperatura de reblandecimiento Vicat (carga 10 N)	92	ºC	ISO 306

(1) Película de 50 µm de espesor, relación de soplado 2.25:1, altura de la línea de enfriamiento 50 cm.

El grado ALCUDIA® PE015 cumple la normativa europea de materiales para uso en contacto con alimentos. Para información más detallada, contacten con el Laboratorio de Asistencia Técnica y Desarrollo o con el Servicio de Atención Comercial.

$LDPE_{33}$ Technical data sheet

PEBD ALCUDIA® PE033

DESCRIPCIÓN

El grado ALCUDIA® PE033 se fabrica en reactor autoclave. Está indicado para la producción de películas por extrusión tubular y plana. Combina una notable facilidad de procesado con buenas propiedades mecánicas y ópticas. Contiene antioxidante.

APLICACIONES

- Películas para envasado y embalaje.
- Película retráctil de gran resistencia mecánica.
- Sacos de gran capacidad.

Se recomienda trabajar con temperaturas de fundido entre 190-220ºC. Las condiciones óptimas de transformación se deben ajustar para cada línea de producción.

PROPIEDADES	VALOR	UNIDAD	MÉTODO
General			
Indice de fluidez (190ºC, 2.16kg)	0.3	g/10 min	ISO 1133
Densidad a 23°C	921	kg/m^3	ISO 1183
Película (1)			
Resistencia al impacto (F_{50})	900	g	ISO 7765-1
Resistencia al rasgado (Elmendorf) (DM/DT)	750 / 1100	cN	ISO 6383-2
Resistencia a la tracción en el punto de rotura (DM/DT)	20 / 19	MPa	ISO 527-3
Resistencia a la tracción en el punto de fluencia (DM/DT)	10 / 10	MPa	ISO 527-3
Alargamiento en el punto de rotura (DM/DT)	650 / 730	%	ISO 527-3
Coeficiente de fricción (Dinámico)	>0.4	-	ISO 8295
Brillo (45º)	55	-	ISO 2813
Turbidez	16	%	ASTM D-1003
Otras			
Temperatura de reblandecimiento Vicat (carga 10 N)	93	ºC	ISO 306

(1) Película de 200 µm de espesor, relación de soplado 2.25:1, altura de la línea de enfriamiento 60 cm.

El grado ALCUDIA® PE033 cumple la normativa europea de materiales para uso en contacto con alimentos. Para información más detallada, contacten con el Laboratorio de Asistencia Técnica y Desarrollo o con el Servicio de Atención Comercial.

ANNEX A

Alpha-tocopherol (α-Toc)

Figure 1. Represents the degradation analysis by ASTM E1641 method.

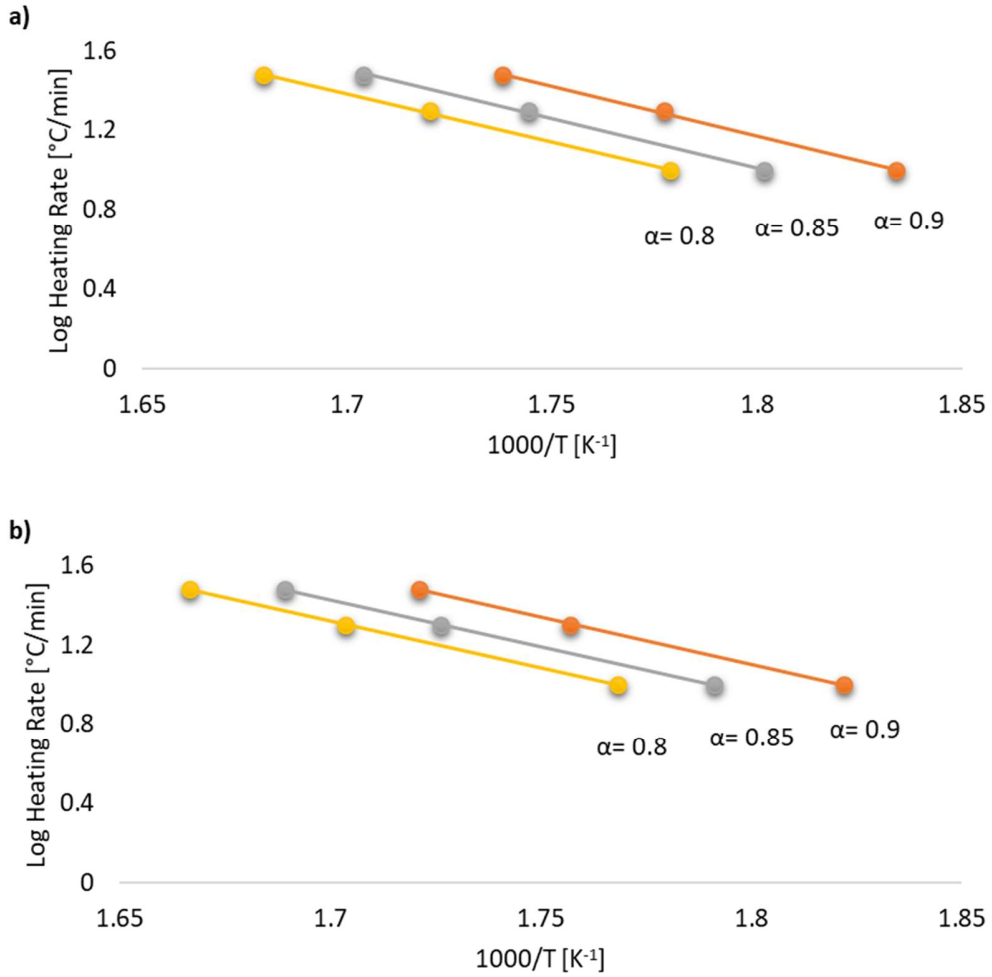

Figure 1. Calculated apparent energy of activation (Ea_{deg}) for α-tocopherol by ASTM E1641 method. a) nitrogen and b) air.

Figure 2. Represents the degradation analysis by Kissinger method.

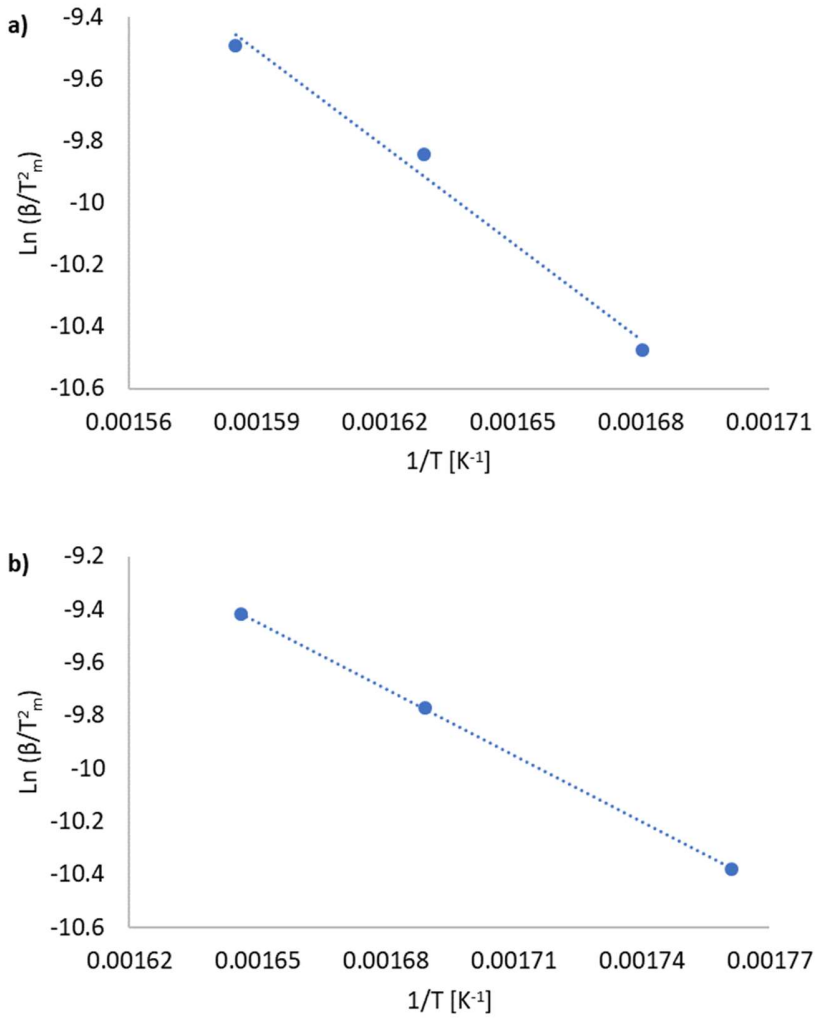

Figure 2. Calculated apparent energy of activation (Ea_{deg}) for α-tocopherol by Kissinger method. a) nitrogen and b) air.

Figure 3. Represents the degradation analysis by Friedman method.

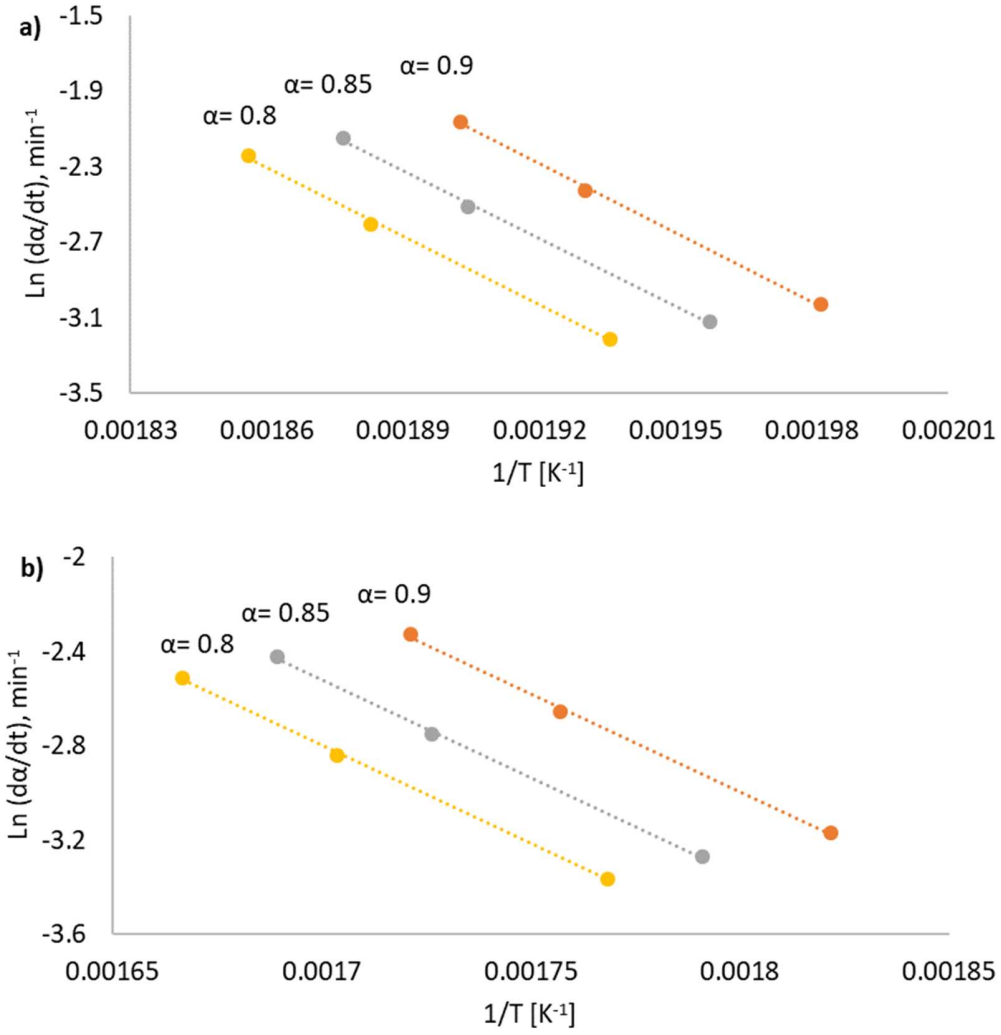

Figure 3. Calculated apparent energy of activation (Ea_{deg}) for α-tocopherol by Friedman method. a) nitrogen and b) air.

Linseed oil (LSO)

Figure 4. Represents the degradation analysis by ASTM E1641 method.

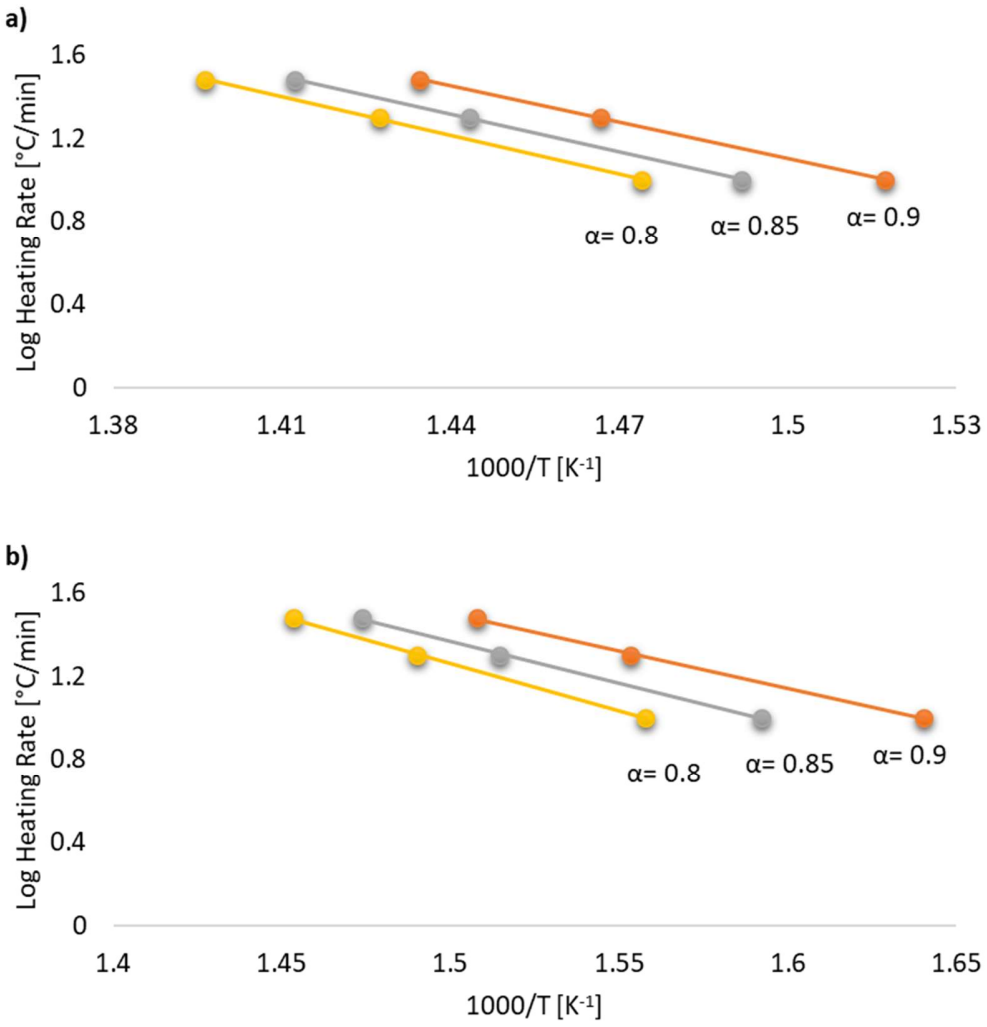

Figure 4. Calculated apparent energy of activation (Ea_{deg}) for linseed oil (LSO) by ASTM E1641 method. a) nitrogen and b) air.

Figure 5. Represents the degradation analysis by Kissinger method.

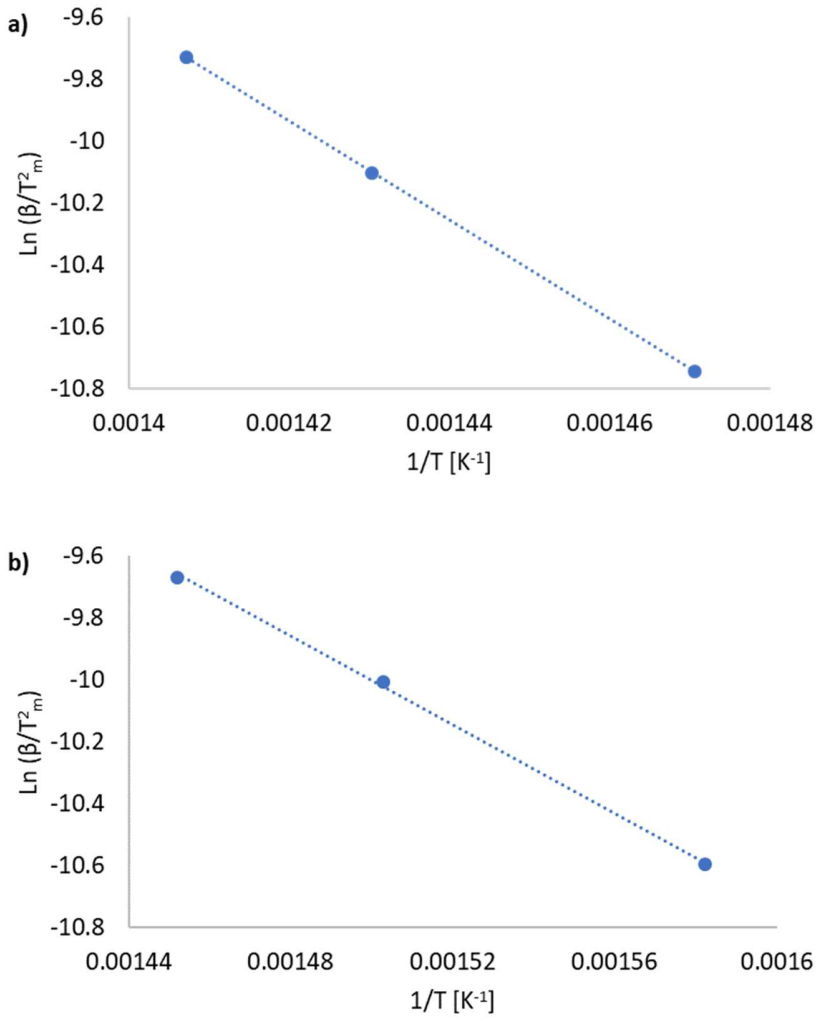

Figure 5. Calculated apparent energy of activation (Ea_{deg}) for linseed oil (LSO) by Kissinger method. a) nitrogen and b) air.

Figure 6. Represents the degradation analysis by Friedman method.

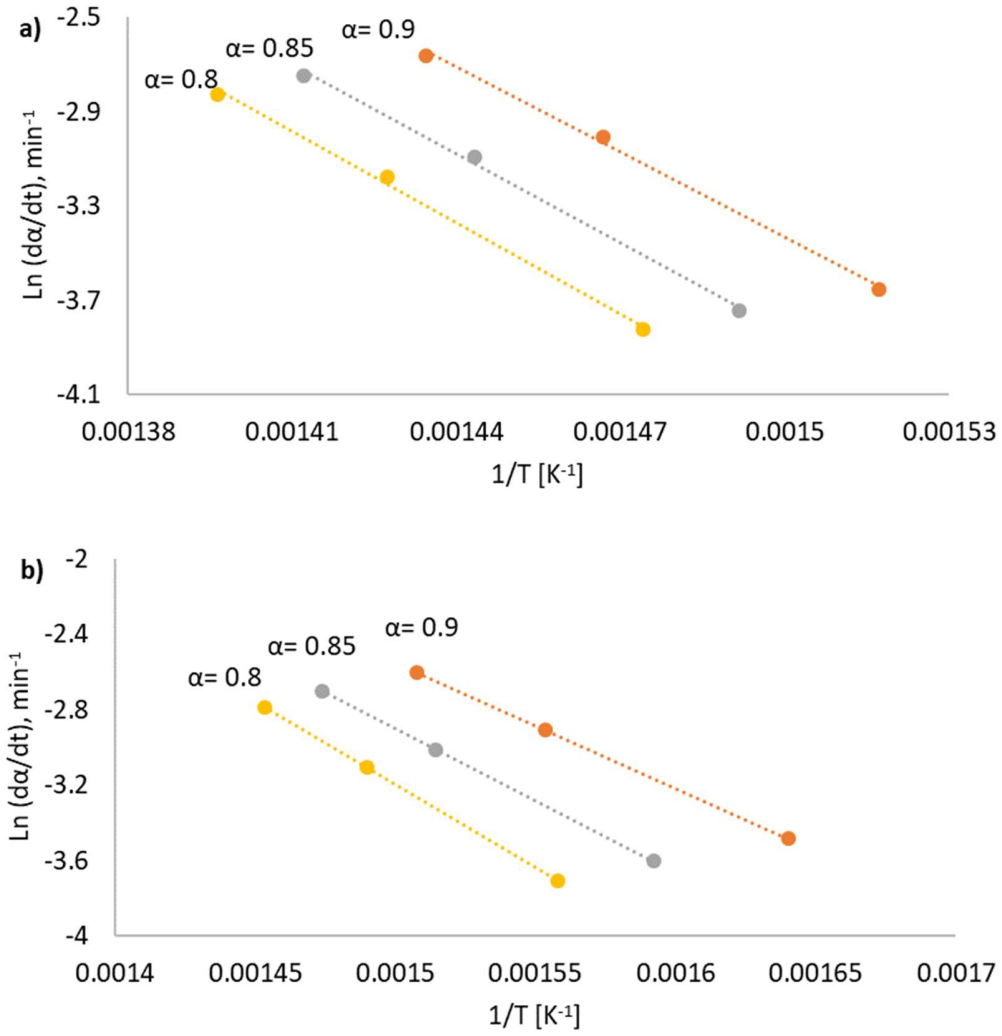

Figure 6. Calculated apparent energy of activation (Ea_{deg}) for linseed oil (LSO) by Friedman method. a) nitrogen and b) air.

Flaxseed oil (FSO)

Figure 7. Represents the degradation analysis by ASTM E1641 method.

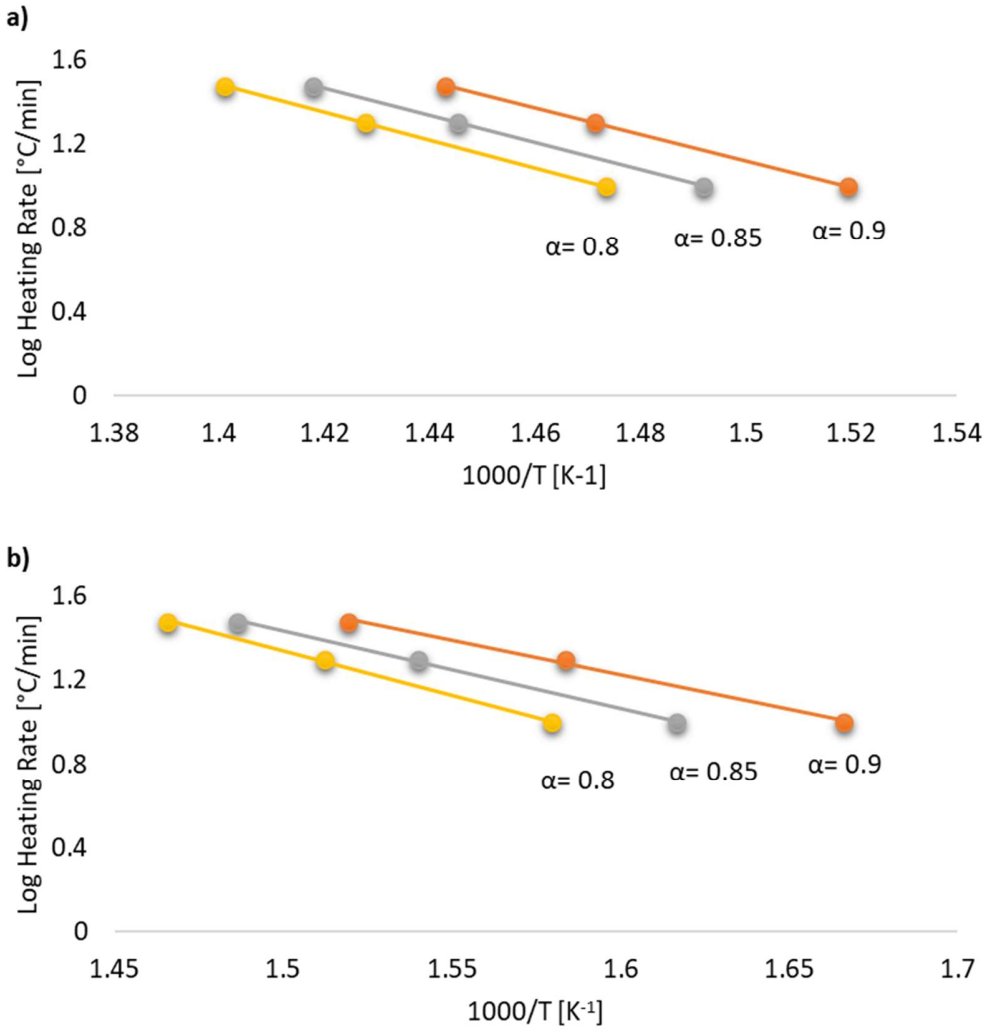

Figure 7. Calculated apparent energy of activation (Ea_{deg}) for flaxseed oil (FSO) by ASTM E1641 method. a) nitrogen and b) air.

Figure 8. Represents the degradation analysis by Kissinger method.

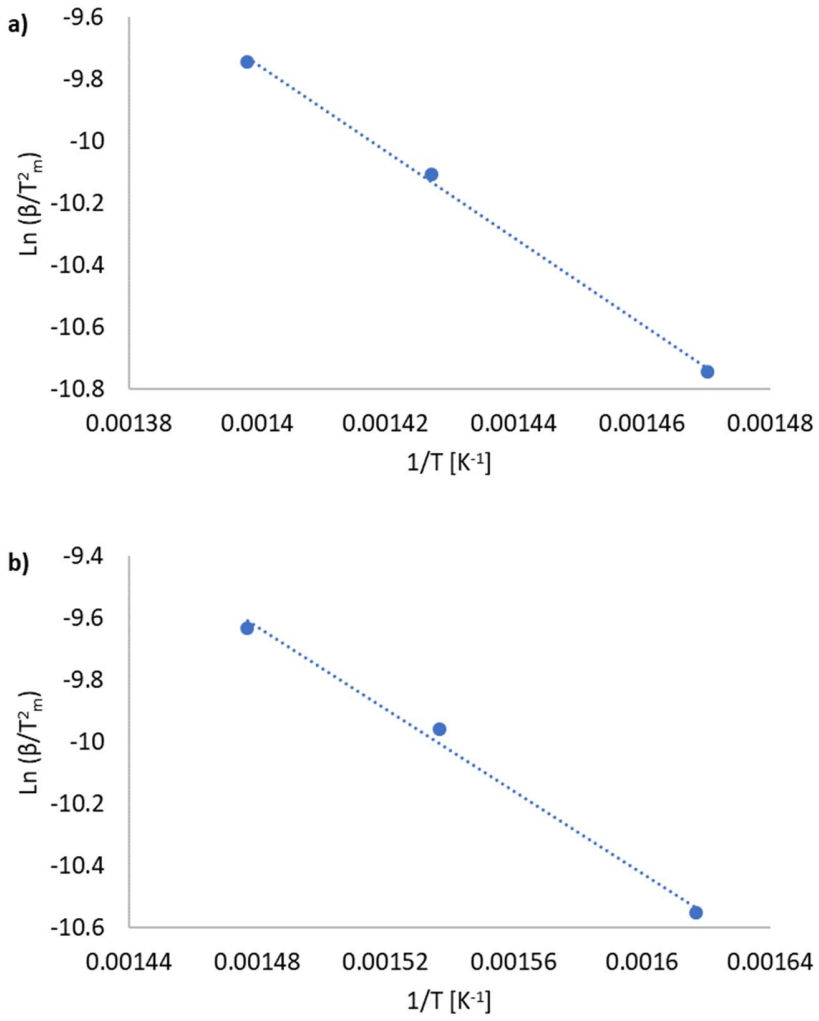

Figure 8. Calculated apparent energy of activation (Ea_{deg}) for flaxseed oil (FSO) by Kissinger method. a) nitrogen and b) air.

Figure 9. Represents the degradation analysis by Friedman method.

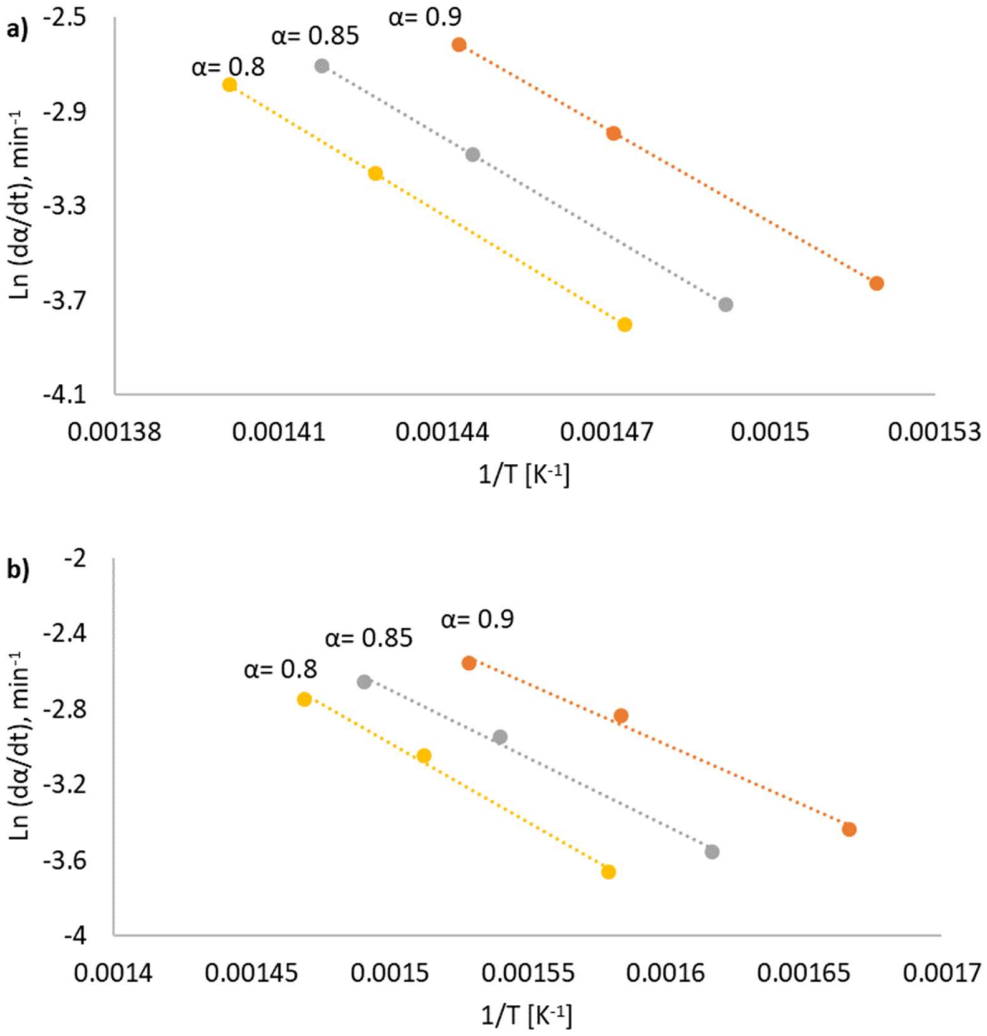

Figure 9. Calculated apparent energy of activation (Ea_{deg}) for flaxseed oil (FSO) by Friedman method. a) nitrogen and b) air.